Linear Flavour-Wave Theory of SU(N) Lattice Models with Arbitrary Irreducible Representations

Thèse N° 9585

Francisco Hyunkyu KIM

ÉCOLE POLYTECHNIQUE
FÉDÉRALE DE LAUSANNE

« Der Vogel kämpft sich aus dem Ei. Das Ei ist die Welt. Wer geboren werden will, muss eine Welt zerstören. Der Vogel fliegt zu Gott. Der Gott heisst Abraxas. »

Hermann Hesse,
Demian

A mes parents,

qui n'ont jamais cessé de me soutenir.

감사합니다.

Remerciements

Abstract

This thesis explores various approaches of studying the long-range colour order of antiferro-magnetic SU(N) Heisenberg models with the linear flavour-wave theory (LFWT). The LFWT is an extension of the well-known SU(2) spin-wave theory to SU(N), and this semi-classical method has been used to study SU(N) models with colour-ordered ground states in the fundamental irreducible representation (irrep). The aim of this thesis is to study various SU(N) Heisenberg models in different irreps and in various colour configurations, in part by extending the LFWT method to different irreps of SU(N).

This will be achieved by using three different methods all using different bosonic representations. First, the LFWT will be performed using the multiboson method that introduces a boson for each state of a given irrep. Then, a different SU(3) bosonic representation first introduced by Mathur & Sen will be presented and used to perform the LFWT calculations. Finally, another way of applying the LFWT will be shown using the bosons first used by Read & Sachdev for SU(N) irreps with rectangular Young tableaux. The specific models that will be treated by these methods are the fully antisymmetric SU(N) models on the square, honeycomb, and triangular lattices with $m > 1$ particles per site, as well as the bipartite SU(3) Heisenberg chain in the adjoint irrep to show how the LFWT can be used for mixed symmetries. The last chapter of the thesis will be dedicated to another problem related to the accidental line of zero modes in the harmonic spectrum of the antiferromagnetic SU(3) Heisenberg model on the square lattice with one particle per site in a three-sublattice order. The objective will be to try to lift the accidental zero modes in the spectrum.

Keywords: condensed matter physics, flavour-wave theory, Heisenberg model, spin-wave theory, SU(N), irreducible representation.

Résumé

Ce travail présente les différentes façons d'étudier l'ordre de couleur à longue distance en utilisant la théorie des ondes de couleur (LFWT) dans les modèles de Heisenberg SU(N) antiferromagnétiques. La LFWT est une généralisation de la théorie semi-classique des ondes de spin SU(2) à la symétrie SU(N). Cette théorie a connu son succès dans les études de systèmes SU(N) avec des configurations de couleurs variées. Toutefois, l'application de cette théorie a été limitée jusqu'ici à la représentation irréductible (irrep) fondamentale de SU(N), et il est souhaitable d'avoir à disposition une méthode qui permettrait d'appliquer la LFWT à d'autres irreps de SU(N). L'objectif de cette thèse est donc d'y remédier en développant une telle méthode, et de l'utiliser afin d'étudier les propriétés de basse énergie des modèles SU(N).

Nous présenterons la LFWT en utilisant trois représentations bosoniques différentes : la représentation multibosonique, la représentation bosonique de Mathur & Sen et la représentation bosonique de Read & Sachdev. Ces méthodes seront ensuite utilisées dans le cadre des modèles SU(N) dans les irreps complètement antisymétriques sur le réseau carré, hexagonal et triangulaire avec $m > 1$ particules par site, puis pour étudier le modèle SU(3) dans l'irrep adjointe ainsi que dans les irreps arbitraires. La dernière partie de cette thèse sera consacrée à la problématique liée aux modes accidentels d'énergie zéro du modèle SU(3) sur le réseau carré avec une particule par site dans une configuration de couleurs à trois sous-réseaux.

Mots-clefs : physique de la matière condensée, théorie des ondes de couleur, modèle de Heisenberg, théorie des ondes de spin, SU(N), représentation irreductible.

Zusammenfassung

In dieser Arbeit wird das antiferromagnetische SU(N) Heisenberg-Modell mithilfe der soge-
nannten linearen Flavourwellentheorie (LFWT) betrachtet. Die LFWT ist eine Erweiterung
der wohlbekannten Spinwellentheorie, die die Untersuchung der Quantenfluktuationen des
geordneten SU(2)-Spins erlaubt. Die LFWT wird benutzt, um die Anordnung der SU(N)-
Teilchen – die hier Farben oder Flavour genannt werden – in der fundamentalen irreduziblen
Darstellung (Irrep) zu erforschen. Es ist aber noch unklar, wie diese Methode auf weitere Irreps
mit verschiedenen Symmetrien angewandt werden kann. Diese Arbeit präsentiert daher die
Ausweitung der LFWT-Methode auf verschiedene Irreps und die Analyse der Quantenfluktua-
tionen in mehreren Gittermodellen mit verschiedenen Farbkonfigurationen.

Dafür werden drei bosonische Darstellungen der SU(N)-Generatoren verwendet. Zuerst wird
die multibosonische Methode vorgestellt, die ein Boson für jeden Zustand der SU(N)-Irrep
einführt. Danach wird eine bosonische Darstellung der SU(3) gezeigt, die zuerst von Ma-
thur & Sen eingeführt wurde, und schliesslich werden die Read & Sachdev Bosonen präsentiert.
Die Modelle, die hier betrachtet werden, sind das quadratische Gitter, das dreieckige Gitter
und das hexagonale Gitter mit $m > 1$ Teilchen pro Gitterstelle in den vollständig antisymmetri-
schen SU(N)-Irreps sowie das eindimensionale Heisenberg-Modell in der adjungierten Irrep
der SU(3) mit einer gemischten Symmetrie. Das letzte Kapitel behandelt eine weitere Fragestel-
lung: Es befasst sich mit den unbeabsichtigten Null-Energie-Moden in dem Energiespektrum
des SU(3)-Modells in der fundamentalen Irrep.

Stichwörter: Physik der kondensierten Materie, Flavourwellentheorie, Heisenberg-Modell,
Spinwellentheorie, SU(N), irreduzible Darstellung.

Contents

Contents

I Introduction

With the development of quantum mechanics in the early 20th century, condensed matter physics has become one of the most active fields of research in modern physics. It is a field of research that deals with systems with large number of constituents and the many-body interactions resulting from them, which makes it particularly appealing for potential technological advancements related to device engineering. This, in part, explains the vast interest in this field of research. However, it is also about answering fundamental questions in physics related to the new phases of matter and emergent phenomena arising from the complexity of the many-body interactions. As Anderson—one of the pioneers of the field—pointed out, "more is different": a new level of fundamental complexity arises from a large collection of elementary particles which needs to be understood [1]. An important subject in this quest is understanding the new phases of matter that emerge at low temperature, and the SU(N)-spin-symmetric models offer an exciting prospect in this matter thanks to the abundance of interesting phases and physical phenomena that they can accommodate.

When discussing spin-magnetic systems, one usually refers to the SU(2) spin-degrees of freedom of the electrons or the ions, and solid-state compounds with such magnetic properties exist in nature. However, one could imagine extending the SU(2) degrees of freedom to a more general SU(N) symmetry even though such systems do not exist naturally in a lattice configuration. The N degrees of freedom are called *colours* or *flavours*, whose nomenclature originates from the SU(3) colour/flavour symmetries in elementary particles. Such quantum SU(N)-spin systems represent an interesting setting in which strong correlations can lead to various exotic ground states due to quantum fluctuations, and have been extensively studied theoretically in various settings. To briefly mention some notable investigations, the one-dimensional system in the fundamental irreducible representation (irrep) of SU(N) has been solved exactly by Sutherland already in the 70s using the Bethe ansatz [2] showing the ground-state energy and the spin-wave-like excitations, and other investigations with field-theoretical methods and abelian bosonisation in 1D has been carried out in the 80s by Affleck [3, 4]. In addition, calculations using the mean-field saddle-point treatment in the large-N limit have been performed for various irreps [5, 6, 7, 8, 9, 10] in the late 80s and early 90s, a type of

valence-bond solid (VBS) ground states have also been investigated for SU(2N) chains [11] and the list goes on. Most of the studies have been performed on the fundamental irrep or the completely symmetric (or antisymmetric) irreps of SU(N), as exemplified by Ref [12], but the field still being active, the irreps with mixed symmetries are also being investigated recently. Recent efforts are also centered around numerical simulations which offer a very powerful way of studying the ground-state properties of the SU(N) systems, ranging from the colour-ordered state to plaquette states, VBS, dimerized states, spin liquids and many more. To name a few, there is the exact diagonalisation (ED) [13, 14] that can be used for small system sizes, whereas Quantum Monte Carlo (QMC) methods [15, 16, 17, 18, 19, 20, 21, 22] can be applied to cases without the sign problem. There are also the variational Monte Carlo method [23, 24, 25, 26, 27] and the tensor network algorithms such as density matrix renormalization group (DMRG) or projected entangled-pair states (PEPS) [28, 29, 30, 31, 32] that can yield remarkable results in 1D or 2D.

The most exciting prospect, however, is that the SU(N)-symmetric models do not remain a purely theoretical exercise anymore thanks to the substantial leap of progress that has been made in recent years in the field of ultracold atom manipulation in optical lattices [33, 34, 35, 36, 37, 38, 39, 40, 41]. Using sufficiently cooled ytterbium atoms or alkaline-earth atoms and by loading this ultracold atomic gas in optical lattices created by orthogonal lasers, it is possible to create a system which then exhibits the SU(N) symmetry. This becomes possible thanks to the near-complete decoupling of the nuclear spin I and the electronic angular momentum in the ground state of these atoms. This then imposes the independence of the scattering parameters of the system from the nuclear spins, after which the Hamiltonian of the system turns out to be SU(N)-symmetric with $N = 2I + 1$ [39]. In addition, different irreps of SU(N) can be realised by using the exchange process between different energy levels and the Hund coupling between the SU(N) colours [42]. As it is reported that up to $N \leq 10$ can be realised with strontium atoms (^{87}Sr) [35], and with potentially several particles per site [38, 39], the SU(N) has recently risen to prominence again, and its fascinating physics in the context of the many-body physics could slowly start being revealed in the near future.

Such experimental realisation can be described by the fermionic SU(N) Hubbard model

$$\mathcal{H} = -t \sum_{\langle i,j \rangle, \mu} \left(f_{i,\mu}^{\dagger} f_{j,\mu} + \text{H.c.} \right) + U \sum_{i, \mu < \nu} n_{i,\mu} n_{i,\nu}, \tag{1.1}$$

with $f_{i,\mu}^{\dagger}$, $f_{i,\mu}$ being fermionic operators with N degrees of freedom μ acting on site i, and $n_{i,\mu} = f_{i,\mu}^{\dagger} f_{i,\mu}$. This is indeed a generalisation of the conventional SU(2) spin Hubbard model to N colours. In the Mott insulating phase with one particle per site, the low-energy physics of this model to second order in t/U is captured by the antiferromagnetic SU(N) Heisenberg models

$$\mathcal{H} = J \sum_{<i,j>} \sum_{\mu, \nu} \hat{S}_{\nu}^{\mu}(i) \hat{S}_{\mu}^{\nu}(j), \tag{1.2}$$

where the operators $\hat{S}^\mu_\nu$ simply exchanges the SU(N) spins μ with ν. When having one particle per site, the spin states are described by the fundamental irrep of SU(N)—denoted by the Young tableau with one box □ as we shall see shortly. By contrast, when multiple particles are present per site, the spin states are described by a different irrep of SU(N) depending on the colour symmetry that the particles form.

This antiferromagnetic (AFM) SU(N) Heisenberg model with $J > 0$ will be the main focus of this thesis, in which the long-range colour-ordered ground states will be investigated. The theoretical tool that will be used for this purpose is the method called the *linear flavour-wave theory* (LFWT). It is essentially a semi-classical method of studying the low-energy excitations of a colour-ordered system, and it is a generalisation of the well-known SU(2) spin-wave (SW) theory (that can be found in many textbooks such as Refs. [43, 44]): the spin wave in SU(2) becomes the flavour wave in SU(N). The theory of antiferromagnetic SU(2) spin waves has been first developed by Anderson and Kubo [45, 46], for which a nice review can be found in Ref. [47]. The aim was to study the Néel ground-state configuration [48] of antiferromagnets with large spin-S. It relies on the assumption that the antiferromagnetically ordered configuration is indeed the ground state and that quantum fluctuations about the ordered state are small. If the quantum fluctuations are small, or if S is large—hence the semi-classical nature of this method—an expansion in powers of $\frac{1}{S}$ can be justified. It is a simple yet powerful method for probing ordered systems, and it surprisingly yields remarkably accurate results even for $S = \frac{1}{2}$ which is not a large number [47]. The LFWT applies the same semi-classical approximation to the SU(N) colours, and it originates from the pioneering works of Papanicolaou[49, 50] in which he was studying the spin-1 bilinear-biquadratic model that has a high SU(3) symmetry point. It was further used and developed by Chubukov [51] and Joshi et al. [52]. More recently, it has been used to assess the possibility a long-range colour order in 2D lattices with SU(3) or SU(4) symmetries with one particle per site, i.e., in the fundamental representation [53, 28, 31]. However, it is not clear how to apply the LFWT with irreps other than the fundamental irrep of SU(N), and it is desirable to have such a simple and powerful method available for other, more complicated irreps. In 2D and 3D, the Mermin-Wagner-Coleman theorem [54, 55] allows for the existence of a long-range order at zero temperature (or at any temperature in 3D), which means that the LFWT can definitely be a very useful tool. However, it can still be beneficial in 1D where the theorem excludes the possibility of having long-range colour order at any temperature, as it can, for instance, give a point of comparison with respect to field-theoretical calculations as in Ref. [12].

This thesis thus aims to address this by developing various ways of dealing with the LFWT in different irreps. Before diving into the heart of the matter, let us first (very) briefly introduce some notions on SU(3) that will be important in the subsequent development.

1.1 The SU(N) **Lie algebra**

1.1.1 The basic concepts

The *Lie algebra* $\mathfrak{su}(N)$ of the Lie group SU(N)—simply referred to as the SU(N) algebra by physicists—has a basis consisting of $N^2 - 1$ generators T_α of SU(N). With the help of the Lie bracket (or the commutator) and the (completely antisymmetric) structure constants $f_{\alpha\beta\gamma}$, the Lie algebra is defined by

$$[T_\alpha, T_\beta] = i f_{\alpha\beta\gamma} T_\gamma, \tag{1.3}$$

where the Einstein summation convention is implied. In the defining representation of SU(N), the SU(N) generators can be given by the $N \times N$ *generalised Gell-Mann matrices* λ_α which are a generalised version of the Gell-Mann matrices of SU(3) that span the SU(3) Lie algebra. They are traceless and hermitian, and they are related to the generators T_α by the relation

$$T_\alpha = \frac{1}{2}\lambda_\alpha. \tag{1.4}$$

The *rank* of this algebra is $N - 1$, which means that there are $N - 1$ independent diagonal matrices among λ_α. This also means that there are $N - 1$ independent generators that we call the *Cartan generators H_i*. The Cartan generators can be simultaneously diagonalised, and the resulting $N - 1$ eigenvalues of a state of a given irrep of SU(N) are called *weights* who can then be plotted on a $N - 1$ dimensional *weight diagram*.

In the basis of Cartan generators, the defining commutation relations of SU(N) (1.3) can be given in terms of the $\frac{N(N-1)}{2}$ pairs of raising and lowering operators $E_{\pm k}$ as with the SU(2) commutation relations with S_z, S_+, S_-. This is called the Cartan-Weyl basis.[1]

There are two important irreps: the defining irrep (that is often called the *fundamental irrep*) and the *adjoint irrep*. For SU(N), there are $N - 1$ fundamental irreps which are $\bigwedge^k \mathbb{C}$ (anti-symmetric tensors with $k \in \{1, \dots, N-1\}$). However, only the defining irrep ($k = 1$) is usually referred to as the fundamental irrep. The adjoint irrep is the representation of the algebra generated by the structure constants themselves. The set of matrices T_α is given by

$$[T_\alpha]_{\beta\gamma} = -i f_{\alpha\beta\gamma} T_\gamma. \tag{1.5}$$

There also is the *conjugate representation* (or the dual representation): we can always define another representation with $\tilde{T}_\alpha := -T_\alpha^*$ such that

$$[\tilde{T}_\alpha, \tilde{T}_\beta] = [T_\alpha, T_\beta]^* = -i f_{\alpha\beta\gamma} T_\gamma^* = i f_{\alpha\beta\gamma} \tilde{T}_\gamma. \tag{1.6}$$

There are of course many other irreps. If we were to form a n-fold tensor product of a $\mathbb{C}^N$

---

[1]Without further details, we note that this Cartan-Weyl basis actually covers the complexification of $\mathfrak{su}(N)$ which is $\mathfrak{sl}(N, \mathbb{C})$.

vector, there would be $n!$ possible permutations related to different irreducible subspaces of the permutation group S_n. Thanks to the formalism developed by Young [56], these irreducible subspaces can be easily visualised by the Young tableaux with n boxes, and they can be used to label the irreps of SU(N).
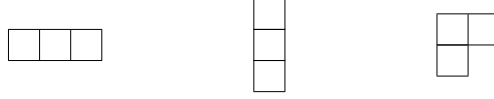
Figure 1.1 – Examples of Young tableaux corresponding to a three-fold tensor product with different symmetries.

The number of boxes of in a row cannot exceed that of the adjacent row above, and the number of boxes in a column cannot exceed that of the adjacent column on the left. A column cannot have more than $N-1$ boxes (because N boxes represents the trivial representation). The boxes placed horizontally denote the symmetrisation, and the boxes placed vertically denote the antisymmetrisation. The Young tableaux such as has a mixed symmetry, whose corresponding irreps are neither completely symmetric nor completely antisymmetric under transpositions.

For instance, let us consider two-particle states with SU(3) particles whose (orthogonal single-particle) colour states are denoted by A, B and C. We then have the symmetriser S_{12} and the antisymmetriser A_{12} defined by

$$S_{12} = \frac{1}{2}\left(e + P_{12}\right) \qquad\qquad A_{12} = \frac{1}{2}\left(e - P_{12}\right), \tag{1.7}$$

where e is the identity operator of S_2 and P_{12} is the transposition operator. For $\psi \equiv A_1 B_2$, we can then have

$$\psi^S \equiv S_{12}\psi = \frac{1}{2}\left(A_1 B_2 + B_1 A_2\right) \tag{1.8}$$

that lives in the irrep , or

$$\psi^A \equiv A_{12}\psi = \frac{1}{2}\left(A_1 B_2 - B_1 A_2\right) \tag{1.9}$$

that lives in the irrep . These states can be denoted in terms of the *Weyl tableau*:

$$\psi^S \quad\longrightarrow\quad \boxed{A\,|\,B}, \qquad\qquad \psi^A \quad\longrightarrow\quad \boxed{\begin{matrix}A\\B\end{matrix}}. \tag{1.10}$$

The labels in the Weyl tableaux are such that they are in alphabetical order in each row and column (the letters can be repeated in each row, but not in each column). The states of a given irrep can be created in a similar fashion with the symmetrisers or antisymmetrisers and by orthonormalising the resulting states.[2]

---

[2] Alternatively, the orthogonal units—also introduced by Young [56]—can be used, which work on the same

The multiplicity of an irrep can be given by the number of the corresponding *standard Young tableaux* which are Young tableaux filled with distinct numbers from 1 to n in increasing order in each row and column. For instance, the Young tableau ⊞ has multiplicity 2 since there are two possible standard Young tableaux for it: $\begin{array}{|c|c|}\hline 1 & 2 \\\hline 3 \\\cline{1-1}\end{array}$ and $\begin{array}{|c|c|}\hline 1 & 3 \\\hline 2 \\\cline{1-1}\end{array}$.

The dimension D (i.e., the number of states) of a given irrep can be easily computed with the help of its Young tableau. For this, we first need the *hook-length* of each box of the Young tableau. The hook length of a box is given by the number of boxes directly to the right and below plus the box itself. What we are interested in here is the product of the hook lengths of all the boxes in a given Young tableau, which we will denote by h. As an example, the hook length of each box of the following Young tableau in shown as follows:

$$\begin{array}{|c|c|c|}\hline 5 & 3 & 1 \\\hline 3 & 1 \\\cline{1-2} 1 \\\cline{1-1}\end{array} \quad \implies \quad h = 5 \cdot 3^2 \cdot 1^3 = 45. \tag{1.11}$$

Next, we attribute another number to each box starting with the upper left box by giving it the number N. Using this as a reference box, one then adds 1 for each box on the right, and one subtracts 1 for each box below. The numbers of each box are then multiplied together to form the number H. The dimension of an irrep is then simply given by $D = \frac{H}{h}$. For instance, the dimension of a SU(4) irrep ⊞⊞ would be calculated as follows:

$$\begin{array}{|c|c|c|}\hline N & N+1 & N+2 \\\hline N-1 & N \\\cline{1-2} N-2 \\\cline{1-1}\end{array} \quad \implies \quad H = (N-2)(N-1)N^2(N+1)(N+2)$$

$$\implies \quad D = \frac{H}{h} = \frac{2 \cdot 3 \cdot 4^2 \cdot 5 \cdot 6}{5 \cdot 3^2 \cdot 1^3} = 64. \tag{1.12}$$

Let us show another example: the irrep ⊞ of SU(3). Its dimension is 8 with a multiplicity of 2. Its states, well-known in particle physics for describing the hadron symmetry [57], are listed in Table 1.1. The states are symmetric in particles 1 and 2 in one case, and the states are antisymmetric in particles 1 and 2 in the other case, showing the double multiplicity of this irrep.

The fundamental irrep of SU(N) is always denoted by the Young tableau □. The conjugate irrep of a given irrep is given by replacing each column containing l boxes by a $N-l$-box column, and then flipping it around the vertical axis in the middle. For example, the conjugate irrep of SU(4) ⊞ is given by

$$\begin{array}{|c|c|}\hline & \\\hline \\\cline{1-1}\end{array} \quad = \quad \begin{array}{|c|c|}\hline & \\\hline & \\\hline & \\\hline\end{array}. \tag{1.13}$$

principle of (anti)symmetrisation. The details can be found in Ref. [13].

Weyl tableau	$\begin{array}{cc}1&2\\3&\end{array}$	$\begin{array}{cc}1&3\\2&\end{array}$
$\begin{array}{cc}A&A\\C&\end{array}$	$\frac{1}{\sqrt{6}}(ACA+CAA-2AAC)$	$\frac{1}{\sqrt{2}}(ACA-CAA)$
$\begin{array}{cc}A&A\\B&\end{array}$	$-\frac{1}{\sqrt{6}}(ABA+BAA-2AAB)$	$\frac{1}{\sqrt{2}}(ABA-BAA)$
$\begin{array}{cc}A&B\\B&\end{array}$	$\frac{1}{\sqrt{6}}(ABB+BAB-2BBA)$	$\frac{1}{\sqrt{2}}(ABB-BAB)$
$\begin{array}{cc}B&B\\C&\end{array}$	$\frac{1}{\sqrt{6}}(CBB+BCB-2BBC)$	$-\frac{1}{\sqrt{2}}(BCB-CBB)$
$\begin{array}{cc}A&C\\C&\end{array}$	$-\frac{1}{\sqrt{6}}(ACC+CAC-2CCA)$	$-\frac{1}{\sqrt{2}}(ACC-CAC)$
$\begin{array}{cc}B&C\\C&\end{array}$	$-\frac{1}{\sqrt{6}}(BCC+CBC-2CCB)$	$-\frac{1}{\sqrt{2}}(BCC-CBC)$
$\begin{array}{cc}A&B\\C&\end{array}$	$-\frac{1}{\sqrt{12}}(2ABC+2BAC-CBA$ $-CAB-ACB-BCA)$	$-\frac{1}{2}(ACB+BCA-CBA-CAB)$
$\begin{array}{cc}A&C\\B&\end{array}$	$\frac{1}{2}(CAB-CBA+ACB-BCA)$	$\frac{1}{\sqrt{12}}(2ABC-2BAC+CBA$ $-CAB+ACB-BCA)$

Table 1.1 – The states of the SU(3) adjoint irrep. The particle index is implicit in the order of the colours. In the first column, the states are symmetric in (12), whereas the states are antisymmetric in (12).

The adjoint irrep of SU(N), on the other hand, is given by the Young tableau containing $N-1$ boxes in the first column and 1 box in the second column, e.g., ⊟ for the SU(4) adjoint irrep.

The irreps of SU(N) can also be labelled by their dimension D, e.g., the SU(3) irrep ⊟ is thus called the irrep **8**. However, there is a nother way of labelling them, which is by using the *Dynkin label*. The Dynkin label is a $N-1$ tuple,[3] and the correspondence between the Young tableaux and the Dynkin labels are given as follows:

Young tableau with row lengths r_i with $i \in \{1,\ldots,N-1\}$

$$\updownarrow \tag{1.14}$$

Dynkin label $[r_1-r_2, r_2-r_3,\ldots,r_{N-1}]$

As an example,

$$\text{SU(3)} \quad \leftrightarrow \quad [1,1], \qquad \text{SU(5)} \quad \leftrightarrow \quad [0,2,1,0]. \tag{1.15}$$

---

[3]The rank of SU(N) being $N-1$, only $N-1$ labels are required to characterise an irrep.

For more details on the Lie algebras and SU(N) groups, we refer the interested readers to Refs. [58, 59, 60] and the references therein. Lastly, let us illustrate an example of a weight diagram by showing that of the SU(2) irrep **S** = 1 and the fundamental irrep of SU(3) in Figure 1.2. Both irreps have three states, but the SU(2) irreps have only one pair of ladder operator
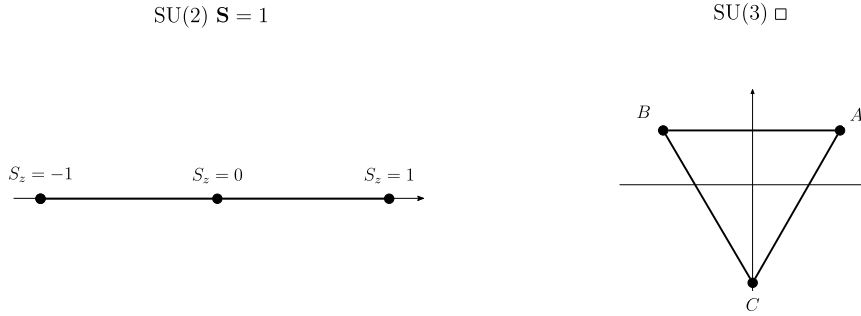
Figure 1.2 – The weight diagram of SU(2) **S** = 1 and the fundamental irrep of SU(3). The weight diagram of SU(3) fundamental irrep is in two dimensions spanned by H_1 and H_2.

($\hat{S}^+$, $\hat{S}^-$) whereas SU(3) irreps have three pairs of ladder operators ($\hat{S}^A_B$, $\hat{S}^B_A$, $\hat{S}^A_C$, $\hat{S}^C_A$, $\hat{S}^B_C$, $\hat{S}^C_B$, $\hat{S}^B_C$). This is shown in its weight diagram by the fact that all the three states are connected by three vertices in three different directions. In the weight diagram of the SU(2) **S** = 1 irrep, there is only one direction along which the states are connected. As N grows, the number of ladder operators grows as well, which makes the structure of the group more complex as well.[4] As we shall see in chapter II, this is the reason why the quantum fluctuations grow as N becomes large.

1.1.2   From the Cartan-Weyl basis to $\hat{S}^\mu_\nu$

As we will be working with the SU(N) colour-operators $\hat{S}^\mu_\nu$, let us see how they can be translated from the Cartan-Weyl basis of SU(N). Let us take the example of SU(3). The Gell-Mann

---

[4]Apart from the algebraic considerations, the group SU(N) becomes more complex in the topological sense as well, as N become large. For instance, SU(2) is diffeomorphic to the three-dimensional sphere S^3—it has three generators—so one could simply think that SU(3) is diffeomorphic to S^8. However, SU(3) has a more complex fibre-bundle structure: it is a S^3-bundle over S^5.

matrices λ_α ($\alpha \in \{1,\dots,8\}$) are given by

$$\lambda_1 := \begin{pmatrix} 0 & 1 & 0 \\ 1 & 0 & 0 \\ 0 & 0 & 0 \end{pmatrix}, \qquad \lambda_2 := \begin{pmatrix} 0 & -i & 0 \\ i & 0 & 0 \\ 0 & 0 & 0 \end{pmatrix}, \qquad \lambda_3 := \begin{pmatrix} 1 & 0 & 0 \\ 0 & -1 & 0 \\ 0 & 0 & 0 \end{pmatrix},$$

$$\lambda_4 := \begin{pmatrix} 0 & 0 & 1 \\ 0 & 0 & 0 \\ 1 & 0 & 0 \end{pmatrix}, \qquad \lambda_5 := \begin{pmatrix} 0 & 0 & -i \\ 0 & 0 & 0 \\ i & 0 & 0 \end{pmatrix}, \tag{1.16}$$

$$\lambda_6 := \begin{pmatrix} 0 & 0 & 0 \\ 0 & 0 & 1 \\ 0 & 1 & 0 \end{pmatrix}, \qquad \lambda_7 := \begin{pmatrix} 0 & 0 & 0 \\ 0 & 0 & -i \\ 0 & i & 0 \end{pmatrix}, \qquad \lambda_8 := \frac{1}{\sqrt{3}} \begin{pmatrix} 1 & 0 & 0 \\ 0 & 1 & 0 \\ 0 & 0 & -2 \end{pmatrix}.$$

There are two Cartan generators H_1, H_2 and three pairs of raising and lowering generators $E_{\pm 1}, E_{\pm 2}, E_{\pm 3}$. They obey the commutation relations

$$[H_i, E_k] = \alpha_{ik} E_k, \qquad [E_k, E_{-k}] = \sum_{i=i}^{2} \gamma_{ki} H_i, \qquad [E_k, E_l] = N_{kl} E_m, \tag{1.17}$$

with $i \in \{1,2\}$ and $k \in \{1,2,3\}$. The coefficients $\alpha_{ik}, \gamma_{ki}, N_{kl}$ can be consulted, e.g., in Ref. [60], and are given by

	α_{ik}	
k	a_{1k}	a_{2k}
1	1	0
2	$\frac{1}{2}$	1
3	$-\frac{1}{2}$	1

	γ_{ki}	
k	γ_{k1}	γ_{k2}
1	2	0
2	2	$\frac{3}{2}$
3	-1	$\frac{3}{2}$

	N_{kl}		
k	l	m	N_{kl}
2	-1	3	-1
3	-2	-1	1
3	1	2	-1

$$\tag{1.18}$$

with the properties that $\alpha_{i\,-k} = -\alpha_{ik}$, $\gamma_{-k\,i} = -\gamma_{ki}$, $N_{lk} = -N_{kl}$ and $N_{-k\,-l} = -N_{kl}$.

These generators can be expressed in terms of the Gell-Mann matrices λ_α:[5]

$$H_1 := \frac{1}{2} \lambda_3 = \frac{1}{2} \begin{pmatrix} 1 & 0 & 0 \\ 0 & -1 & 0 \\ 0 & 0 & 0 \end{pmatrix}, \qquad\qquad H_2 := \frac{1}{\sqrt{3}} \lambda_8 = \frac{1}{3} \begin{pmatrix} 1 & 0 & 0 \\ 0 & 1 & 0 \\ 0 & 0 & -2 \end{pmatrix},$$

$$E_{+1} := \frac{1}{2} (\lambda_1 + i\lambda_2) = \begin{pmatrix} 0 & 1 & 0 \\ 0 & 0 & 0 \\ 0 & 0 & 0 \end{pmatrix}, \qquad E_{-1} := \frac{1}{2} (\lambda_1 - i\lambda_2) = \begin{pmatrix} 0 & 0 & 0 \\ 1 & 0 & 0 \\ 0 & 0 & 0 \end{pmatrix} \left(= E_{+1}^\dagger \right), \tag{1.19}$$

$$E_{\pm 2} := \frac{1}{2} (\lambda_4 \pm i\lambda_5), \qquad\qquad E_{\pm 3} := \frac{1}{2} (\lambda_6 \pm i\lambda_7).$$

---

[5]Note that the coefficients in the definition of H_1 and H_2 can differ depending on the normalisation convention.

The generators $E_{\pm 1}, E_{\pm 2}, E_{\pm 3}$ are indeed ladder operators and we can thus define

$$
\begin{aligned}
\hat{S}_\alpha^\beta &\equiv E_{+1}, & \hat{S}_\alpha^\gamma &\equiv E_{+2}, & \hat{S}_\beta^\gamma &\equiv E_{+3}, \\
\hat{S}_\beta^\alpha &\equiv E_{-1}, & \hat{S}_\gamma^\alpha &\equiv E_{-2}, & \hat{S}_\gamma^\beta &\equiv E_{-3}.
\end{aligned}
\tag{1.20}
$$

To obtain the diagonal operators $\hat{S}_\alpha^\alpha, \hat{S}_\beta^\beta, \hat{S}_\gamma^\gamma$ with H_1, H_2, we can use the tracelessness condition $\sum_{\mu=1}^{N} \hat{S}_\mu^\mu = 0$ as an extra equation. Solving

$$
\begin{cases}
H_1 = \frac{1}{2}\hat{S}_\alpha^\alpha - \frac{1}{2}\hat{S}_\beta^\beta \\
H_2 = \frac{1}{3}\hat{S}_\alpha^\alpha + \frac{1}{3}\hat{S}_\beta^\beta - \frac{2}{3}\hat{S}_\gamma^\gamma \\
\hat{S}_\alpha^\alpha + \hat{S}_\beta^\beta + \hat{S}_\gamma^\gamma = 0
\end{cases}
\tag{1.21}
$$

we finally obtain

$$
\begin{cases}
\hat{S}_\alpha^\alpha = H_1 + \frac{1}{2}H_2 \\
\hat{S}_\beta^\beta = -H_1 + \frac{1}{2}H_2 \\
\hat{S}_\gamma^\gamma = -H_2.
\end{cases}
\tag{1.22}
$$

It can be verified that the commutation relations (1.17) become

$$
\left[\hat{S}_\beta^\alpha, \hat{S}_\nu^\mu \right] = \delta_\nu^\alpha \hat{S}_\beta^\mu - \delta_\beta^\mu \hat{S}_\nu^\alpha.
\tag{1.23}
$$

in terms of the operators $\hat{S}_\nu^\mu$, with $\alpha, \beta, \mu, \nu \in \{A, B, C\}$. This thus defines the SU(3) commutation relations in terms of the operators $\hat{S}_\nu^\mu$. This construction is of course valid for any SU(N).

1.1.3 Natural bosonic representation of the states and of $\hat{S}_\nu^\mu$

We already encountered the states of the adjoint irrep of SU(3) in Table 1.1. Using the second quantisation, we could naturally associate single-particle states to bosons $b_{\mu,a}(i)$, where μ is the colour index $\mu \in \{A, B, C\}$ and a is the particle number index $a \in \{1, 2, 3\}$. This is the most natural bosonic representation of these states. Let us then use the convention

$$
b_{\mu,1}^\dagger(i) b_{\nu,2}^\dagger(i) b_{\xi,3}^\dagger(i) |0\rangle = |\mu_1 \nu_2 \xi_3\rangle \equiv |\mu\nu\xi\rangle,
\tag{1.24}
$$

with $\mu, \nu, \xi \in \{A, B, C\}$. We will simply omit the particle number knowing that it can be implicitly read off from the order of the colours. Then the state $\boxed{\begin{smallmatrix}A&A\\C&\end{smallmatrix}}$ can be written as

$$
\boxed{\begin{smallmatrix}A&A\\C&\end{smallmatrix}} \equiv \frac{1}{\sqrt{2}}(|ACA\rangle - |CAA\rangle) = \frac{1}{2}\left(b_{A,1}^\dagger b_{C,2}^\dagger b_{A,3}^\dagger - b_{C,1}^\dagger b_{A,2}^\dagger b_{A,3}^\dagger \right)|0\rangle.
\tag{1.25}
$$

in terms of these bosons.

Now, what is the expression of the generators $S_\nu^\mu(i)$ in this natural bosonic representation? We know that they permute the colour μ and ν. Since we have joined three particles with tensor products, we simply need to permute the colours of all the three particles. If n is the number of particles per site (here, $n = 3$), we then have

$$\hat{S}_\nu^\mu(i) = \sum_{a=1}^n b_{\nu,a}^\dagger(i) b_{\mu,a}(i) - \frac{1}{N}\delta_\nu^\mu \hat{n}(i), \tag{1.26}$$

where

$$\hat{n}(i) = \sum_{\mu=1}^N \sum_{a=1}^n b_{\mu,a}^\dagger(i) b_{\mu,a}(i). \tag{1.27}$$

The second term in Eq. (1.26) is to satisfy

$$\sum_{\mu=1}^N \hat{S}_\mu^\mu = 0, \tag{1.28}$$

which is related to the tracelessness of the SU(N) generators. However, the essential part in the action of this bosonic representation of $\hat{S}_\nu^\mu$ is the first term, i.e. the permutation of the colours. The SU(N) commutation relations (1.23) is satisfied with this definition of $\hat{S}_\nu^\mu$, whether it is with or without this constant term.

1.2 Linear flavour-wave theory in the fundamental irrep

Let us now show how the LFWT works with a concrete example. We consider the AFM SU(3) Heisenberg model with one particle per site on the square lattice with a three-sublattice colour-order as shown in Figure 1.3. As we consider one SU(3)-colour particle per site, we are
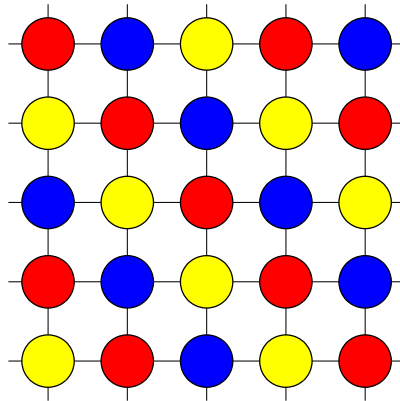
Figure 1.3 – The tripartite order considered for the LFWT calculations shown in this section.

dealing with the fundamental irrep. We will closely follow the calculations performed by Bauer

et al. [31]. The Hamiltonian is given by

$$\mathcal{H} = J \sum_{\langle l,l'' \rangle} \sum_{\mu,\nu} \hat{S}^\mu_\nu(l) \hat{S}^\nu_\mu(l''), \tag{1.29}$$

where μ, ν are the flavours A, B and C. As seen in Eq. (1.1.3), the bosonic representation of the generators S^μ_ν can be given by

$$\hat{S}^\mu_\nu(l) = b^\dagger_\nu(l) b_\mu(l), \tag{1.30}$$

with the constraint that

$$\sum_{\mu \in \{A,B,C\}} b^\dagger_\mu(l) b_\mu(l) = n_c. \tag{1.31}$$

This is in fact a generalisation of the Schwinger bosons in SU(2).

In the large-n_c limit with the assumption of an ordered state, the Holstein-Primakoff bosons can be also used. Let us first consider a site l that belongs to the sublattice of the flavour A ($l \in \Lambda_A$). We then write $\hat{S}^A_A(l)$ as follows:

$$\begin{aligned} \hat{S}^A_A(l) &= n_c - b^{A\dagger}_B(l) b^A_B(l) - b^{A\dagger}_C(l) b^A_C(l) \\ &=: n_c - m_A(l). \end{aligned} \tag{1.32}$$

The superscript A indicates the sublattice we are dealing with, whereas the subscript labels the flavour of the fluctuation. This leads to

$$\hat{S}^A_B(l) = b^{A\dagger}_B(l) b^A_A(l) = b^{A\dagger}_B(l) \sqrt{n_c - m_A(l)} \tag{1.33a}$$

$$\hat{S}^B_A(l) = b^{A\dagger}_A(l) b^A_B(l) = \sqrt{n_c - m_A(l)}\, b^A_B(l), \tag{1.33b}$$

whose square roots can be Taylor-expanded in order to get a $\frac{1}{n_c}$-expansion of the Hamiltonian.

Let us now compute the harmonic spectrum with terms of order n_c. The Hamiltonian (1.29) can be written as follows: $\mathcal{H} = \sum_{\mu < \nu} \mathcal{H}_{\mu\nu}$, where $\mu, \nu \in \{A, B, C\}$. We first look at the sub-Hamiltonian $\mathcal{H}_{AB}$ that involves the bonds between $l \in \Lambda_A$ and $l'' \in \Lambda_B$:

$$\sum_{\mu,\nu} S^\nu_\mu(l) S^\mu_\nu(l') = n_c \left[b^{A\dagger}_B(l) b^A_B(l) + b^{B\dagger}_A(l') b^B_A(l') + b^{A\dagger}_B(l) b^{B\dagger}_A(l') + b^A_B(l) b^B_A(l') \right] \tag{1.34}$$

The Fourier transform with

$$b^A_B(l) = \sqrt{\frac{3}{N_{\text{sites}}}} \sum_{\mathbf{k} \in \text{RBZ}} b^A_B(\mathbf{k}) e^{-i\mathbf{k}\mathbf{r}_l}, \tag{1.35}$$

with N_{sites} being the number of sites, gives rise to

$$\Longrightarrow \mathcal{H}_{AB}^{(2)} = zJn_c \sum_{\mathbf{k}\in\text{RBZ}} \left[b_{A,\mathbf{k}}^{B\dagger} b_{A,\mathbf{k}}^{B} + b_{B,-\mathbf{k}}^{A\dagger} b_{B,-\mathbf{k}}^{A} + \gamma_{\mathbf{k}} b_{B,-\mathbf{k}}^{A\dagger} b_{A,\mathbf{k}}^{B\dagger} + \gamma_{\mathbf{k}}^{*} b_{B,-\mathbf{k}}^{A} b_{A,\mathbf{k}}^{B} \right], \tag{1.36}$$

where $z = 2$ is the coordination number between two sublattices Λ_A and Λ_B, and

$$\gamma_{\mathbf{k}} = \frac{1}{2}\left(e^{ik_x} + e^{ik_y} \right). \tag{1.37}$$

It is important to note here that only the colours A and B are involved in $\mathcal{H}_{AB}$ in this quadratic-order expansion. This is an important fact that will be observed repeatedly throughout this thesis.

The sub-Hamiltonians $\mathcal{H}_{BC}$ and $\mathcal{H}_{AC}$ are also similar, and the Bogoliubov transformation detailed in Appendix A finally yields the diagonalised quadratic Hamiltonian

$$\mathcal{H} = zJn_c \sum_{\mathbf{k}\in\text{RBZ}} \sum_{\mu\in\{A,B\}} \sum_{\nu\neq\mu} \omega_{\mathbf{k}}\left(\tilde{b}_{\mu,\mathbf{k}}^{\nu\dagger} \tilde{b}_{\mu,\mathbf{k}}^{\nu} + \frac{1}{2}\right) - zJn_c \frac{N}{3} \tag{1.38}$$

with

$$\omega_{\mathbf{k}} = \sqrt{1 - \left|\gamma_{\mathbf{k}}\right|^2}. \tag{1.39}$$

We briefly note here that there is an accidental line of zero modes related to an infinitely
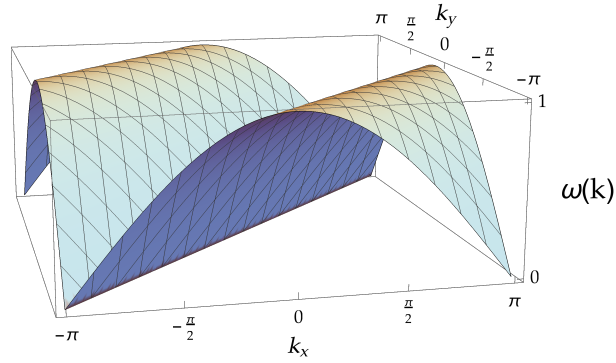
Figure 1.4 – The dispersion relation $\omega_{\mathbf{k}}$ of the AFM SU(3) Heisenberg model in the tripartite configuration.

degenerate classical ground-state manifold in the model. We will come back to this later in chapter VI.

1.3 Outline of the thesis

The essential concepts having all been introduced, we will gradually present different methods of applying the LFWT for different irreps. This will be achieved by using three different bosonic representations of the SU(N) operators $\hat{S}_v^\mu$.

The chapter II will first present the LFWT multiboson method where one boson will be introduced for each state of a given irrep. The completely antisymmetric irreps with multiple particles per site on the square/honeycomb/triangular lattices will be considered, after which the SU(3) adjoint irrep will be considered. We will then revisit the LFWT in the SU(3) adjoint irrep in chapter III by introducing the Mathur & Sen bosonic representation for SU(3). The chapter IV will then present the Read & Sachdev bosonic representation with which the LFWT for completely antisymmetric irreps of SU(N) and the adjoint irrep of SU(3) will be performed. The chapter V is a summary of the differences between the three boson representations. Finally, the chapter VI treats a somewhat different subject, namely our attempt at lifting the accidental zero modes (that we saw in Figure 1.4) in the harmonic spectrum of the SU(3) Heisenberg model on the square lattice with one particle per site. Also, a brief concluding chapter can be found in chapter VII.

We would like to draw the attention of the readers on the fact[6] that

- The N degrees of SU(N) will be called "colours" throughout the thesis, denoted by the capital letters $A, B, C, \ldots$ (or by numbers $1, 2, 3, \ldots$ in some rare cases for better readability or for convenience).

- As is often the case in physics and mathematics, the letter i is used as an index but it can also mean $\sqrt{-1}$ in the same equation.

- Some abbreviations used in this thesis include

  the linear flavour-wave theory (LFWT),
  the irreducible representation (irrep),
  the spin wave (SW),
  the valence bond solid (VBS),
  the quantum Monte Carlo (QMC).

---

[6]We also note that the Mathematica package for symbolic calculations named "SNEG" [61] has been occasionally used, when using Mathematica.

II Multiboson Linear Flavour-Wave Method

Introduction: colour order, or no colour order?

As the first way of performing the LFWT for a SU(N) Heisenberg model in any arbitrary irrep, this Chapter will present the multiboson method, a method set up with Karlo Penc, Pierre Nataf and Frédéric Mila's collaboration [62]. This method is based on the multiboson SW approach that has been used in various SU(2) spin models with $S > \frac{1}{2}$ by Papanicolaou [49, 63, 50], Onufrieva [64], Chubukov [51], Masashige et al. [65], Romhányi and Penc [66], Penc et al. [67] among others and thus rests on a solid foundation. The distinctive feature of this approch in contrast to the conventional SW theory is that it introduces bosonic operators for higher-order spin operators as well, allowing to probe higher-order excitations of the system. Although we are not interested in multipolar transitions, the multiboson approach is still of interest in our case as it allows the LFWT to be applied on irreps other than the fundamental irrep. This generalisation to arbitrary irreps becomes possible because the multiboson method introduces a generalised boson for each of the states of a given irrep, after which we can apply the Holstein-Primakoff transformation as in the traditional SWT or the LFWT in the fundamental irrep with the help of a large parameter that we introduce.

Ultimately, this method will enables us to calculate the low-energy spectra of a given SU(N) system. It also provides us a mean to quantify the quantum fluctuations, hence providing a way to predict the existence (or the absence) of an ordered state. Let us illustrate the method by applying it to different SU(N) irreps with increasing complexity: we will first look at a model in the fully antisymmetric irrep before moving on to the most general case, which is an irrep with mixed symmetry.

The first section of this Chapter will thus mainly involve the SU(4) Heisenberg model on the bipartite square lattice in the fully antisymmetric irrep denoted by the Young tableau ⊟, the simplest model in 2D with a fully antisymmetric irrep void of the frustration problem. Once we have understood how to implement the method, we will be investigating some physically interesting questions: is an ordered state a possible ground-state candidate for a 2D square lattice at zero temperature? Is an ordered ground state also possible in other geometries in 2D

such as the triangular and the honeycomb lattices? If the answer is yes for the square lattice, then what happens when the system goes from a 2D square lattice to a parallel 1D chains by turning off the vertical couplings between the sites, for instance? After settling these questions on the fully antisymmetric case, we will move on to the concluding section of this chapter in which we will show how to apply the multiboson LFWT on the SU(3) Heisenberg chain in 1D in the SU(3) adjoint representation (denoted by the Young tableau ⊞), which has a mixed symmetry. The physical interest here will to discover the low-energy spectra of such a one dimensional system.

2.1 Fully antisymmetric irreps

In this section, we consider the 2D square/honeycomb/triangular lattices with $m > 1$ particles per site whose SU(N) wavefunctions are completely antisymmetric and whose interactions are given by the AFM SU(N) Heisenberg Hamiltonian

$$\mathcal{H} = J \sum_{<i,j>} \sum_{\mu,\nu} \hat{S}^\mu_\nu(i)\hat{S}^\nu_\mu(j). \tag{2.1}$$

Ultimately, we would like to know whether a long-range colour order can exist or not in these systems, and for which values of N and m this is the case. For the square lattice and the honeycomb lattice, we will look at the bipartite configuration ($n_{\text{sub}} = 2$) whereas the triangular lattice will be in the tripartite configuration ($n_{\text{sub}} = 3$). In addition, we will be choosing N and m such that $n_{\text{sub}} = \frac{N}{m}$. This ensures that we can find a simple colour-ordered ground-state configuration without frustration.

The motivation for investigating these models come from Refs [68, 69]. Notably, there is a phase diagram in Ref. [69] that predicts chiral spin liquid and valence cluster states on the square lattice for large N and m. However, for small N and m, the quantum fluctuations are relatively small and long-range colour-order can form, and the question is to discover whether relatively small values of N and m can have a colour order. For $m = 1$ the stabilisation of the antiferromagnetically ordered phase has been already reported up to $N = 5$ for square lattices and up to $N = 3$ for triangular lattices with the LFWT and different numerical methods [70, 71, 53, 28, 13, 72]. But what about $m = 2$? For the SU(4) AFM Heisenberg, the large-N limit calculations at zero temperature have long predicted a degenerate dimerized ground state in one dimension [6, 8], with DMRG and VMC also reaching the same conclusion [73, 23]. In two dimensions on a square lattice, on the other hand, the Néel-ordered configuration has been suggested as a possible ground state by some numerical simulations such as the VMC calculations [23] and QMC carried out with system sizes up to 16×16 [20, 22]. And although Assaad [16] seems to suggest the absence of long-range order with the system size of 24×24, his recent computations on system sizes up to 40×40 suggest a small local moment in the 2D model [74]. We will thus attempt to contribute to this discussion with the LFWT here.
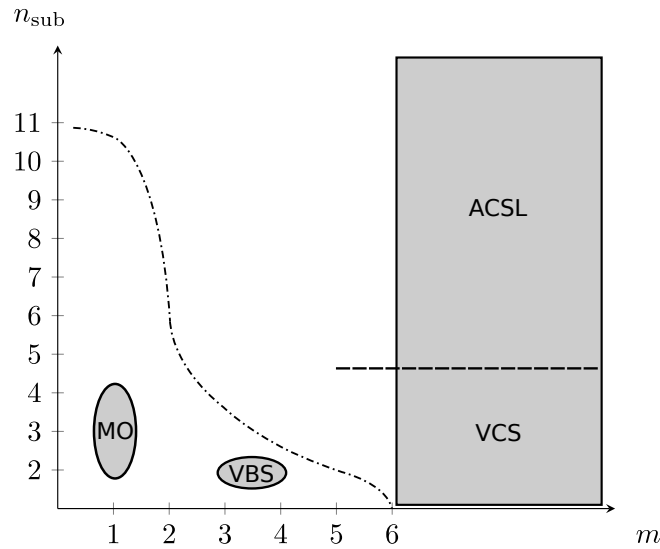
Figure 2.1 – The sketch of the phase diagram for the SU(N) Heisenberg model on the 2D square lattice, shown by Hermele and Gurarie in Ref. [69]. The shaded regions indicate that the ground state is known or that there is a convincing ground-state candidate with substantial evidence. The magnetic order (MO), the valence-bond solid (VBS), the valence cluster state (VCS) and the Abelian chiral spin liquid (ACSL) are present here. The dash-dotted line shows the experimentally realisable parameters. It can be seen that the magnetically ordered region is on $m = 1$ and for small values of $N = n_{\text{sub}} m$. Our aim is to see if the magnetically ordered region can be slightly extended to other small values of m and N.

2.1.1 Two SU(4) particles per site on the square lattice

Let us imagine that we have a square lattice on which we have two ($m = 2$) SU(4) particles per site whose interactions are Heisenberg-like with their nearest neighbours. Furthermore, the particles on each site form a wavefunction that belongs to the fully antisymmetric irrep [0, 1, 0] denoted by the Young tableau ⊟ (it contains m vertical boxes). If we assume that this system has a colour order at zero temperature, we can easily conclude that one of the classical ground state configurations is the one depicted in Figure 2.2, where the square lattice is in a bipartite configuration with two different colors on one sublattice and the two remaining colors sit on the second sublattice. We would like to study the low-energy spectra of the system related to the quantum fluctuations by using the LFWT just as in section 1.2 with the fundamental irrep. Now that we have more than one particle per site with different colours, how do we perform the semi-classical approximation?

One way to proceed is to think in terms of the "composite particles", i.e., in terms of the states of the irrep rather than the individual colours they are composed of. Previously, we had been expressing the SU(N) generators in terms of bosons representing N colours, as it is the natural representation of the N degrees of freedom of SU(N). However, one could also use a different bosonic representation of the SU(N) generators: we could write them in terms of

(a) Two particles per site.

(b) Wavefunction (or composite particle) of each site.
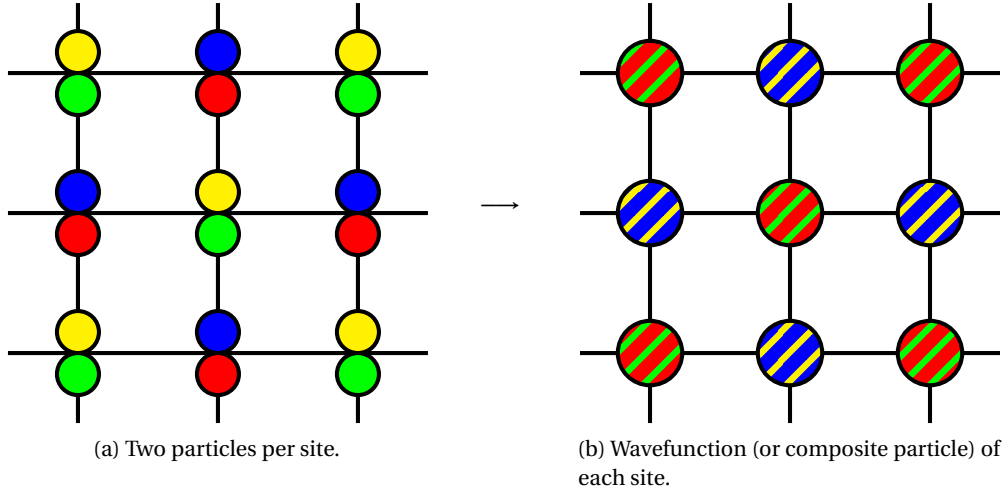
Figure 2.2 – A bipartite 2D square lattice with two particles per site. The flavours A, B, C, D are represented by the colors blue, yellow, red, green respectively. The lattice is in an ordered configuration where two different colours are on one sublattice and the two remaining colours are on the other sublattice.

bosons representing the individual composite states of the irrep ⊟. This effectively amounts to having an anisotropic SU(6) Hamiltonian, in the sense that the Hamiltonian can be written in terms of SU(6) operators without being fully SU(6)-symmetric. As we will shortly see, this will provide us with a natural and easy way of approaching the semi-classical limit with the Holstein-Primakoff bosons.

The linear flavour-wave theory of SU(4) $m = 2$ **square**

Let us label the four degrees of freedom of SU(3) by A, B, C and D. The irrep ⊟ is six-dimensional, and its basis can be given by

$$\left\{ \frac{1}{\sqrt{2}}\big((|A_1 B_2\rangle - |B_1 A_2\rangle\big), \frac{1}{\sqrt{2}}\big((|A_1 C_2\rangle - |C_1 A_2\rangle\big), \frac{1}{\sqrt{2}}\big(|D_1 A_2\rangle - |A_1 D_2\rangle\big) \right.$$
$$\left. \frac{1}{\sqrt{2}}\big(|B_1 C_2\rangle - |C_1 B_2\rangle\big), \frac{1}{\sqrt{2}}\big(|B_1 D_2\rangle - |D_1 B_2\rangle\big), \frac{1}{\sqrt{2}}\big(|C_1 D_2\rangle - |D_1 C_2\rangle\big) \right\}, \tag{2.2}$$

where the states are labelled with the four SU(4) colours and the particle subscripts $_{1,2}$. These states are indeed created with bosons introduced in subsection 1.1.3. The states are antisymmetric in the particle indices. For convenience, let us denote these states by the following elements of the set

$$\Gamma := \{AB, AC, DA, BC, BD, CD\}. \tag{2.3}$$

Let us attribute a boson to each of these states. In other words, the bosons d_{AB}, d_{AC}, d_{DA}, d_{BC},

d_{BD}, d_{CD} and their adjoint counterparts will be used to create and annihilate these six states. The idea now is to express the SU(4) generators $\hat{S}_\nu^\mu$ in terms of these bosons.

We know that the generators $\hat{S}_\nu^\mu$ have the effect of permuting colour μ with colour ν. So if we choose to act $\hat{S}_B^A$ on the state AC, we should obtain the state BC. Furthermore, the action of the generators is closed, which means that the resulting state should still belong to the same irrep. We can thus conclude that $\hat{S}_B^A$ should contain a term such as $d_{BC}^\dagger d_{AC}$. Taking another example, the application of $\hat{S}_C^A$ on the state AB should yield CB. The state CB is not exactly an element of our set Γ in which we defined all the possible states of our irrep, but it does correspond however to BC with a minus sign if we trace back their definitions to Eq. (2.2). This could be shown more rigorously by using the natural bosonic representation of the generators $\hat{S}_\nu^\mu$ (Eq. (1.26) in subsection 1.1.3), and it will be shown for a more general irrep later in section 2.2. Here, we will simply check the validity of our logic by checking the commutation relations of $\hat{S}_\nu^\mu$ in their new bosonic expressions with bosons d. This is sufficient to show that our construction respects the SU(4) symmetry as it should. Following our construction, the generators $\hat{S}_\nu^\mu$ are finally given by

$$
\begin{aligned}
&\hat{S}_B^A := d_{BC}^\dagger d_{AC} - d_{BD}^\dagger d_{DA}, && \hat{S}_A^B := \left(\hat{S}_B^A\right)^\dagger, \\
&\hat{S}_C^A := -d_{BC}^\dagger d_{AB} - d_{CD}^\dagger d_{DA}, && \hat{S}_A^C := \left(\hat{S}_C^A\right)^\dagger, \\
&\hat{S}_D^A := -d_{BD}^\dagger d_{AB} - d_{CD}^\dagger d_{AC}, && \hat{S}_A^D := \left(\hat{S}_D^A\right)^\dagger, \\
&\hat{S}_C^B := d_{CD}^\dagger d_{BD} + d_{AC}^\dagger d_{AB}, && \hat{S}_B^C := \left(\hat{S}_C^B\right)^\dagger, \\
&\hat{S}_D^B := -d_{CD}^\dagger d_{BC} - d_{DA}^\dagger d_{AB}, && \hat{S}_B^D := \left(\hat{S}_D^B\right)^\dagger, \\
&\hat{S}_D^C := d_{BD}^\dagger d_{BC} - d_{DA}^\dagger d_{AC}, && \hat{S}_C^D := \left(\hat{S}_D^C\right)^\dagger, \\
&\hat{S}_A^A := d_{AB}^\dagger d_{AB} + d_{AC}^\dagger d_{AC} + d_{DA}^\dagger d_{DA} - \frac{\hat{N}}{2}, && \hat{S}_B^B := d_{AB}^\dagger d_{AB} + d_{BC}^\dagger d_{BC} + d_{BD}^\dagger d_{BD} - \frac{\hat{N}}{2}, \\
&\hat{S}_C^C := d_{AC}^\dagger d_{AC} + d_{BC}^\dagger d_{BC} + d_{CD}^\dagger d_{CD} - \frac{\hat{N}}{2}, && \hat{S}_D^D := d_{DA}^\dagger d_{DA} + d_{BD}^\dagger d_{BD} + d_{CD}^\dagger d_{CD} - \frac{\hat{N}}{2},
\end{aligned}
\tag{2.4}
$$

where

$$
\hat{N} := d_{AB}^\dagger d_{AB} + d_{AC}^\dagger d_{AC} + d_{DA}^\dagger d_{DA} + d_{BC}^\dagger d_{BC} + d_{BD}^\dagger d_{BD} + d_{CD}^\dagger d_{CD}.
\tag{2.5}
$$

One can check that these definitions satisfy the SU(N) commutation relation

$$
\left[\hat{S}_\beta^\alpha, \hat{S}_\nu^\mu\right] = \delta_\nu^\alpha \hat{S}_\beta^\mu - \delta_\beta^\mu \hat{S}_\nu^\alpha,
\tag{2.6}
$$

thus showing that the suggested bosonic representation of the SU(4) generators is legitimate. Note that the terms $-\frac{\hat{N}}{2}$ in Eq. (2.4) have been introduced solely to satisfy the relation $\sum_{\mu=1}^{N} \hat{S}_\mu^\mu = 0$. which is related to the tracelessness of the SU(N) generators. However, the operator $\hat{N}$ simply counts the number of composite particles per site, and its expectation value should always be equal to 1 if we were to stay within our irrep ☐. Consequently, we can safely ignore these terms

(a) Weight diagram of the irrep $[0, 1, 0]$ of SU(4).

(b) Action of the generators in the weight diagram.
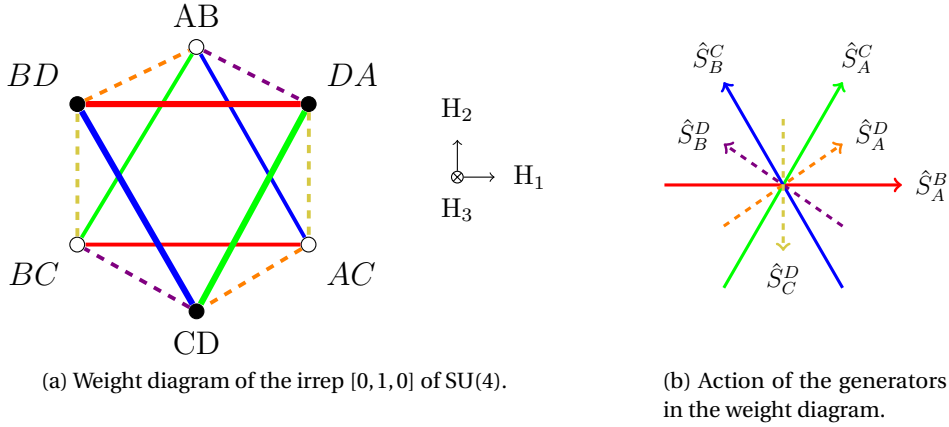
Figure 2.3 – The weight diagram of the six-dimensional antisymmetric SU(4) irrep. The weight diagram is in three dimensions in the Cartan-generator basis $\{H_1, H_2, H_3\}$, as SU(4) is a group of rank 3. The triangle with thicker lines pointing downwards is above the other triangle pointing upwards in the weight diagram. The vertices have been coloured to help recognize the corresponding ladder operators of SU(4) depicted in (b). The red, green and blue (solid) vertices are in the H_1-H_2 plane, whereas the three other (dotted) colours have a H_3 component.

in the following calculations: they do not alter their outcome. It is also worth noting that the SU(N) commutation relations (2.6) remain true even without the terms $-\frac{\hat{N}}{2}$ in Eqs. (2.4).

The transitions between states induced by $\hat{S}_\nu^\mu$, described in the bosonic language in Eqs. (2.4), can be nicely seen in the weight diagram of ⊟ of SU(4) illustrated in Figure 2.3. The filled or unfilled circles represent the weights (or the states in this case). There are $\frac{N(N-1)}{2} = 6$ directions in which the weights are connected, and these directions are associated to the 6 pairs of generators (or ladder operators) of SU(4). For instance, we can see that the transition between the states AC and BC are related to $\hat{S}_B^A$ and $\hat{S}_A^B$.

We can introduce a more compact way of writing Eqs. (2.4). We can write $\hat{S}_\nu^\mu$ as

$$\hat{S}_\nu^\mu = \sum_{\substack{\alpha = A \\ \alpha \neq \mu, \nu}}^{D} d_{\alpha\nu}^\dagger d_{\alpha\mu}, \tag{2.7}$$

where the (antisymmetric) indices $_{\alpha\nu}$ or $_{\alpha\mu}$ of the bosons are ordered in such a way that they correspond to the labels of the states in Γ. When reordering the indices, the sign of the permutations needs to be taken into account, i.e., $d_{\nu\mu}^\dagger = -d_{\mu\nu}^\dagger$, to reflect the antisymmetry of the states of this irrep.

Lastly, it should be noted that the choice of basis in (2.2) is somewhat arbitrary. For instance, we could have chosen the state $\frac{1}{\sqrt{2}}\big(|A_1 D_2\rangle - |D_1 A_2\rangle\big)$ as a basis element instead of the state $\frac{1}{\sqrt{2}}\big(|D_1 A_2\rangle - |A_1 D_2\rangle\big)$ used in (2.2). These two states differ by a minus sign, which would have induced a minus sign in certain terms of the generators $\hat{S}_\nu^\mu$ in (2.4) and give us the label AD instead of the label DA (the generator $\hat{S}_B^A = d_{BC}^\dagger d_{AC} - d_{BD}^\dagger d_{DA}$ would have become

$\hat{S}^A_B = d^\dagger_{BC} d_{AC} + d^\dagger_{BD} d_{AD}$). But the commutation relations (1.23) would still be satisfied, and the subsequent physical conclusions would remain the same.

Without loss of generality, the classical ground-state Néel order can be assumed to be composed of the state AB on sublattice Λ_{AB} and the state CD on sublattice Λ_{CD} as depicted in Figure 2.2. Note that these two states are as far apart as possible from one another in the weight diagram in Figure 2.3.

It is important to remember that there is a constraint imposed by the model on every site i of the lattice, given by

$$\sum_{\eta \in \Gamma} d^\dagger_\eta(i) d_\eta(i) = n_c, \tag{2.8}$$

where $n_c = 1$ for each site. Note that the boson index $\eta \in \Gamma$ now refers to the composite states in Γ. With the assumption of small fluctuations around our presumed colour order, we can use the Holstein-Primakoff prescription by considering the limit $n_c \to \infty$. This is equivalent to the semi-classical approximation in the SU(2) spin-wave theory, where we let $S \to \infty$. In terms of the Young tableaux, this would correspond to having n_c columns $\overbrace{\square \cdots \square}^{n_c}$ and letting n_c go to infinity. Let us introduce the pair of Holstein-Primakoff bosons $a(i)$ for the sites $i \in \Lambda_{AB}$ and $b(j)$ for the sites $j \in \Lambda_{CD}$. The constraint (2.8) then becomes

$$a^\dagger_{AB}(i) a_{AB}(i) = n_c - \sum_{\eta \in \Gamma \setminus \{AB\}} a^\dagger_\eta(i) a_\eta(i),$$
$$b^\dagger_{CD}(j) b_{CD}(j) = n_c - \sum_{\eta \in \Gamma \setminus \{CD\}} b^\dagger_\eta(j) b_\eta(j), \tag{2.9}$$

from which we derive

$$a^\dagger_{AB}(i), a_{AB}(i) \to \sqrt{n_c - \sum_{\eta \in \Gamma \setminus \{AB\}} a^\dagger_\eta(i) a_\eta(i)} \simeq \sqrt{n_c} - \frac{1}{2\sqrt{n_c}} \sum_{\eta \in \Gamma \setminus \{AB\}} a^\dagger_\eta(i) a_\eta(i),$$
$$b^\dagger_{CD}(j), b_{CD}(j) \to \sqrt{n_c - \sum_{\eta \in \Gamma \setminus \{CD\}} b^\dagger_\eta(j) b_\eta(j)} \simeq \sqrt{n_c} - \frac{1}{2\sqrt{n_c}} \sum_{\eta \in \Gamma \setminus \{CD\}} b^\dagger_\eta(j) b_\eta(j), \tag{2.10}$$

in the same way as in the SU(2) spin-wave theory. The beauty of this transformation is that the commutation relations (1.23), $\left[\hat{S}^\alpha_\beta, \hat{S}^\mu_\nu \right] = \delta^\alpha_\nu \hat{S}^\mu_\beta - \delta^\mu_\beta \hat{S}^\alpha_\nu$, stay valid up to order $\mathcal{O}(1)$ in n_c even after this transformation.

Expanding the square roots in $1/n_c$ allows us to a obtain a decomposition of the Hamiltonian in powers of $\sqrt{n_c}$:

$$\mathcal{H} = \mathcal{H}^{(0)} + \mathcal{H}^{(1)} + \mathcal{H}^{(2)} + \mathcal{O}(n_c^{\frac{1}{2}}). \tag{2.11}$$

Here, the term $\mathcal{H}^{(1)}$ is equal to zero since we started the expansion from a classical ground state, and the term $\mathcal{H}^{(0)}$ is a constant. We are thus interested in the quadratic Hamiltonian

$\mathscr{H}^{(2)}$ which is given by

$$
\begin{aligned}
\mathscr{H}^{(2)} = J n_c \sum_{i \in \Lambda_{AB}} \sum_{\langle j \rangle} \Big[& 2 a_{CD}^\dagger(i) \, a_{CD}(i) + 2 b_{AB}^\dagger(j) \, b_{AB}(j) \\
& + a_{AC}^\dagger(i) \, a_{AC}(i) + b_{BD}^\dagger(j) \, b_{BD}(j) + a_{AC}^\dagger(i) \, b_{BD}^\dagger(j) + a_{AC}(i) \, b_{BD}(j) \\
& + a_{BD}^\dagger(i) \, a_{BD}(i) + b_{AC}^\dagger(j) \, b_{AC}(j) + a_{BD}^\dagger(i) \, b_{AC}^\dagger(j) + a_{BD}(i) \, b_{AC}(j) \\
& + a_{DA}^\dagger(i) \, a_{DA}(i) + b_{BC}^\dagger(j) \, b_{BC}(j) + a_{DA}^\dagger(i) \, b_{BC}^\dagger(j) + a_{DA}(i) \, b_{BC}(j) \\
& + a_{BC}^\dagger(i) \, a_{BC}(i) + b_{DA}^\dagger(j) \, b_{DA}(j) + a_{BC}^\dagger(i) \, b_{DA}^\dagger(j) + a_{BC}(i) \, b_{DA}(j) \Big].
\end{aligned}
\tag{2.12}
$$

We observe here that a different choice of basis mentioned above (AD instead of DA) would have induced a minus sign in front of the terms $a_{DA}^\dagger(i) \, b_{BC}^\dagger(j)$, $a_{DA}(i) \, b_{BC}(j)$, $a_{BC}^\dagger(i) \, b_{DA}^\dagger(j)$ and $a_{BC}(i) \, b_{DA}(j)$. However, the result of the subsequent diagonalisation would have remained the same, yielding the same dispersion relations at the end.

We now perform the Fourier transform,

$$
a_\alpha(i) = \sqrt{\frac{2}{N_{\text{sites}}}} \sum_{\mathbf{k} \in \text{RBZ}} a_\alpha(\mathbf{k}) e^{-i\mathbf{k}\mathbf{r}_i}, \qquad b_\alpha(j) = \sqrt{\frac{2}{N_{\text{sites}}}} \sum_{\mathbf{k} \in \text{RBZ}} b_\alpha(\mathbf{k}) e^{-i\mathbf{k}\mathbf{r}_j},
\tag{2.13}
$$

with the state index $\alpha \in \Gamma$ and the number of sites N_{sites}. The sum runs over the reduced Brillouin zone (RBZ). The Hamiltonian in $\mathbf{k}$-space is then given by

$$
\mathscr{H}^{(2)} = \mathscr{H}_0^{(2)} + \mathscr{H}_1^{(2)} + \mathscr{H}_2^{(2)} + \mathscr{H}_3^{(2)} + \mathscr{H}_4^{(2)}
\tag{2.14}
$$

where

$$
\begin{aligned}
\mathscr{H}_0^{(2)} &= J n_c \sum_{\mathbf{k} \in \text{RBZ}} 2 \mathcal{A}_{\text{sq}} \Big[a_{CD,\mathbf{k}}^\dagger a_{CD,\mathbf{k}} + b_{AB,\mathbf{k}}^\dagger b_{AB,\mathbf{k}} \Big], \\
\mathscr{H}_1^{(2)} &= J n_c \sum_{\mathbf{k} \in \text{RBZ}} \Big[\mathcal{A}_{\text{sq}} \big(a_{AC,\mathbf{k}}^\dagger a_{AC,\mathbf{k}} + b_{BD,\mathbf{k}}^\dagger b_{BD} \big) + \mathcal{B}_{\text{sq},\mathbf{k}} \big(a_{AC,\mathbf{k}}^\dagger b_{BD,-\mathbf{k}}^\dagger + a_{AC,\mathbf{k}} b_{BD,-\mathbf{k}} \big) \Big], \\
\mathscr{H}_2^{(2)} &= J n_c \sum_{\mathbf{k} \in \text{RBZ}} \Big[\mathcal{A}_{\text{sq}} \big(a_{BD,\mathbf{k}}^\dagger a_{BD,\mathbf{k}} + b_{AC,\mathbf{k}}^\dagger b_{AC,\mathbf{k}} \big) + \mathcal{B}_{\text{sq},\mathbf{k}} \big(a_{BD,\mathbf{k}}^\dagger b_{AC,-\mathbf{k}}^\dagger + a_{BD,\mathbf{k}} b_{AC,-\mathbf{k}} \big) \Big], \\
\mathscr{H}_3^{(2)} &= J n_c \sum_{\mathbf{k} \in \text{RBZ}} \Big[\mathcal{A}_{\text{sq}} \big(a_{DA,\mathbf{k}}^\dagger a_{DA,\mathbf{k}} + b_{BC,\mathbf{k}}^\dagger b_{BC,\mathbf{k}} \big) + \mathcal{B}_{\text{sq},\mathbf{k}} \big(a_{DA,\mathbf{k}}^\dagger b_{BC,-\mathbf{k}}^\dagger + a_{DA,\mathbf{k}} b_{BC,-\mathbf{k}} \big) \Big], \\
\mathscr{H}_4^{(2)} &= J n_c \sum_{\mathbf{k} \in \text{RBZ}} \Big[\mathcal{A}_{\text{sq}} \big(a_{BC,\mathbf{k}}^\dagger a_{BC,\mathbf{k}} + b_{DA,\mathbf{k}}^\dagger b_{DA,\mathbf{k}} \big) + \mathcal{B}_{\text{sq},\mathbf{k}} \big(a_{BC,\mathbf{k}}^\dagger b_{DA,-\mathbf{k}}^\dagger + a_{BC,\mathbf{k}} b_{DA,-\mathbf{k}} \big) \Big],
\end{aligned}
\tag{2.15}
$$

in which the sums run over the reduced magnetic Brillouin zone and

$$
\mathcal{A}_{\text{sq}} := 4, \qquad \mathcal{B}_{\text{sq},\mathbf{k}} := 4\gamma_{\text{sq},\mathbf{k}}, \qquad \gamma_{\text{sq},\mathbf{k}} := \frac{1}{2} \big(\cos k_x + \cos k_y \big).
\tag{2.16}
$$

$\gamma_{\text{sq},\mathbf{k}}$ is called the geometrical factor as it encodes the geometry of the lattice. Note that the value of $\mathcal{A}_{\text{sq}}$ actually corresponds to the coordination number between two sublattices $z_{\text{sq}} = 4$,

and that $\mathcal{B}_{\mathrm{sq}} = z_{\mathrm{sq}}\gamma_{\mathrm{sq},\mathbf{k}}$. It is also important to note that all the terms in $\mathscr{H}^{(2)}$ are of the same order in our expansion parameter n_c. Now that the expansion has been done, we can reestablish the constraint (2.8) by setting $n_c = 1$ (but we will keep writing the variable n_c in the equations for general considerations). The terms $\mathscr{H}^{(2)}_{1,...,4}$ in Eq. (2.15) can be diagonalized separately with the Bogoliubov transformation described in Appendix section 1.1 in an identical fashion. For instance, the diagonalisation of bosons $a_{AC,\mathbf{k}}, b_{BD,\mathbf{k}}$ in $\mathscr{H}^{(2)}_1$ can be performed with

$$
\begin{pmatrix} \tilde{a}^{\dagger}_{AC,\mathbf{k}} \\ \tilde{b}_{BD,-\mathbf{k}} \end{pmatrix} = \begin{pmatrix} u_{\mathbf{k}} & v_{\mathbf{k}} \\ v_{\mathbf{k}} & u_{\mathbf{k}} \end{pmatrix} \begin{pmatrix} a^{\dagger}_{AC,\mathbf{k}} \\ b_{BD,-\mathbf{k}} \end{pmatrix},
\tag{2.17}
$$

where

$$
u_{\mathbf{k}} = \sqrt{\frac{1}{2}\left(\frac{\mathcal{A}_{\mathrm{sq}}}{\omega_{\mathrm{sq},\mathbf{k}}} + 1\right)}, \qquad v_{\mathbf{k}} = \sqrt{\frac{1}{2}\left(\frac{\mathcal{A}_{\mathrm{sq}}}{\omega_{\mathrm{sq},\mathbf{k}}} - 1\right)},
$$
$$
\omega_{\mathrm{sq},\mathbf{k}} = \sqrt{\mathcal{A}^2_{\mathrm{sq}} - \mathcal{B}^2_{\mathrm{sq},\mathbf{k}}}.
\tag{2.18}
$$

Hence, the diagonalized quadratic Hamiltonian finally reads as

$$
\mathscr{H}^{(2)} = \sum_{\mathbf{k}\in\mathrm{RBZ}}\left\{\sum_{\eta\in\Gamma\backslash\{AB,CD\}}\varepsilon_{\mathrm{sq}}(\mathbf{k})\left[\left(\tilde{a}^{\dagger}_{\eta,\mathbf{k}}\tilde{a}_{\eta,\mathbf{k}} + \frac{1}{2}\right) + \left(\tilde{b}^{\dagger}_{\eta,\mathbf{k}}\tilde{b}_{\eta,\mathbf{k}} + \frac{1}{2}\right)\right]\right.
$$
$$
\left. + 8Jn_c\left(a^{\dagger}_{CD,\mathbf{k}}a_{CD,\mathbf{k}} + b^{\dagger}_{AB,\mathbf{k}}b_{AB,\mathbf{k}}\right)\right\} - 8JN_{\mathrm{sites}}n_c,
\tag{2.19}
$$

where we defined

$$
\begin{aligned}
\varepsilon_{\mathrm{sq}}(\mathbf{k}) &:= Jn_c\omega_{\mathrm{sq}}(\mathbf{k}) \\
&= Jn_c\sqrt{\mathcal{A}^2_{\mathrm{sq}} - \mathcal{B}^2_{\mathrm{sq},\mathbf{k}}} = 4Jn_c\sqrt{1 - \gamma^2_{\mathrm{sq},\mathbf{k}}} \\
&= 4Jn_c\sqrt{1 - \left[\frac{1}{2}\left(\cos k_x + \cos k_y\right)\right]^2}.
\end{aligned}
\tag{2.20}
$$

The dimensionless energy spectrum $\omega_{\mathrm{sq}}(\mathbf{k})$ is shown in Figure 2.4. There are 8 dispersive modes and 2 localised modes of energy $8Jn_c$. We see that the dispersive modes come from the bosons of the Bogoliubov transformation in Eq. (2.17) whereas the flat localised modes originate from the bosons $a_{CD}(i), b_{AB}(j)$.

Let us investigate the flat modes more closely, starting with the mode $8a^{\dagger}_{CD}a_{CD}$. This term stems from $\hat{S}^C_C(i)\hat{S}^C_C(j)$ and $\hat{S}^D_D(i)\hat{S}^D_D(j)$ (i.e., $a^{\dagger}_{CD}(i)a_{CD}(i)b^{\dagger}_{CD}(j)b_{CD}(j)$) of the Hamiltonian before the square-root expansion. The presence of the boson $a_{CD}(i)$ on the site $i \in \Lambda_{AB}$ actually implies that we have the state CD on the site i, which would only be possible had there been two colour exchanges from our initial state AB, by applying two successive ladder operators (see Figure 2.3). The same reasoning also applies to the second flat mode $8b^{\dagger}_{AB}b_{AB}$ from the perspective of the sublattice Λ_{CD}. We see that these flat modes in fact stem from multipolar transitions requiring more than one flavour exchanges. These multipolar excitations do not

(a) Energy spectrum of the dispersive modes.

(b) 2D cut of the energy spectrum.
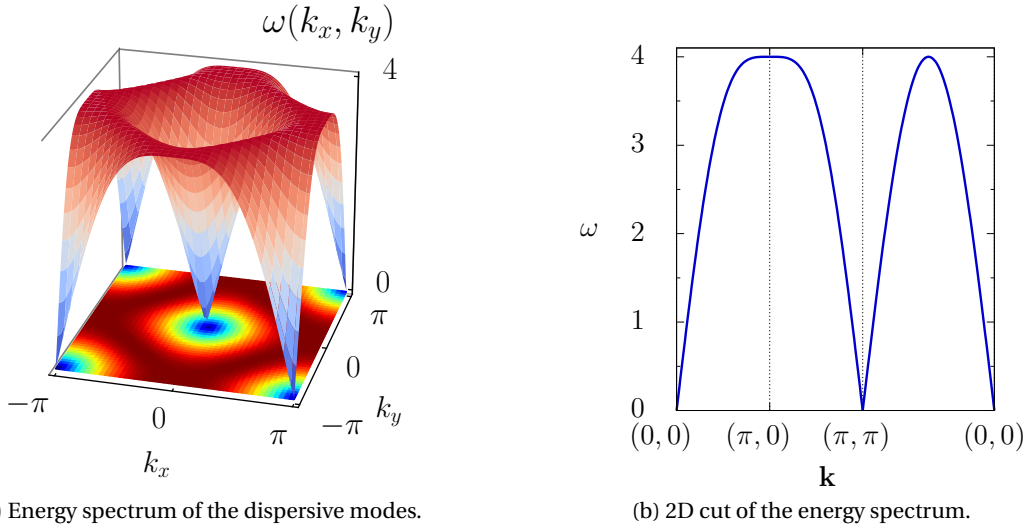
Figure 2.4 – The energy spectrum of the dispersive modes of the SU(4) $m = 2$ square lattice, plotted in the extended Brillouin zone. Figure adapted from Ref [62] with the permission of the APS, © 2017 American Physical Society.

interact in the quadratic order of our expansion in n_c [66, 67, 62], in which only excitations with one colour exchange interact. As these excitations are local and do not propagate, they thus appear as flat modes here.[7]

The 8 dispersive modes given by the dipersion relation (2.57), on the other hand, come from the exchange of one colour from the initial states AB or CD. There are four ways of exchanging one colour from AB, the initial state of the first sublattice: $A \to C$, $A \to D$, $B \to C$ and $B \to D$ (the exchange $A \to B$ is forbidden by antisymmetry). This is illustrated in the weight diagram, Figure 2.3, by the fact that there are four vertices connecting AB to its four adjacent points. Similarly, there are also four ways of achieving this from CD. These $4 + 4 = 8$ transitions are the dynamics described by the 8 dispersive modes in Eq. (2.19). It is worthwhile nothing these (degenerate) dispersive modes are identical to the dispersion relation of the SU(2) spin-wave theory on the square lattice. The only difference is the larger number of modes in our model, which is due to the larger number of possible colour transitions mentioned above.

For future reference, we observe that the Hamiltonian in the extended (structural) Brillouin zone can be given as follows:

$$\mathcal{H}^{(2)} = \sum_{\mathbf{k} \in \mathrm{BZ}} \left\{ \sum_{\zeta=1}^{4} \varepsilon_{\mathrm{sq}}(\mathbf{k}) \left(\tilde{f}_{\zeta,\mathbf{k}}^{\dagger} \tilde{f}_{\zeta,\mathbf{k}} + \frac{1}{2} \right) + 8Jn_c f_{CD,\mathbf{k}}^{\dagger} f_{CD,\mathbf{k}} \right\} - 8JN_{\mathrm{sites}} n_c. \tag{2.21}$$

Here, we introduced bosons $\tilde{f}_\sigma$ for the dispersive modes and f for the flat modes, all defined

---

[7]An example of a physically accessible multipolar mode gaining a dispersion with anisotropy terms in a SU(2) Hamiltonian can be found in Ref. [66].

on the extended Brillouin zone. We then have 4 dispersive modes and 1 flat mode.

As a last side remark, we also note that the energy per site originating from the quantum fluctuations is

$$
\begin{aligned}
\frac{E}{N_{\text{sites}}} &= -8Jn_c + 4 \cdot \left\langle \frac{\varepsilon_{\text{sq}}(\mathbf{k})}{2} \right\rangle \\
&= -1.264Jn_c.
\end{aligned}
\tag{2.22}
$$

Ordered moment of the $SU(4)$ **square lattice**

Now that we have the low-energy spectra of the system, we can think about calculating the ordered moment—the "magnetisation" so to speak—of the system. Since we assume a large condensate of the state AB on sublattice Λ_{AB}, we can define the ordered color moment on it as

$$
\begin{aligned}
m_i &= \frac{1}{n_c} \left\langle a_{AB}^\dagger(i) a_{AB}(i) \right\rangle \\
&= \frac{1}{n_c} \left(n_c - \left\langle \sum_{\eta \in \Gamma \setminus \{AB\}} a_\eta^\dagger(i) a_\eta(i) \right\rangle \right),
\end{aligned}
\tag{2.23}
$$

so that the fully polarised classical Néel state is $m_i = 1$. On the other hand, if there is no colour order, then $m_i = 0$. Note that we can define m_j for the sublattice Λ_{CD} in the same way,

$$
\begin{aligned}
m_j &= \frac{1}{n_c} \left\langle b_{CD}^\dagger(j) b_{CD}(j) \right\rangle \\
&= \frac{1}{n_c} \left(n_c - \left\langle \sum_{\eta \in S \setminus \{CD\}} b_\eta^\dagger(j) b_\eta(j) \right\rangle \right),
\end{aligned}
\tag{2.24}
$$

and that $m_i = m_j$ since the structure of both sublattices is the same. The reduction of the ordered moment due to quantum fluctuations is the second term in Eq. (2.23),

$$
\begin{aligned}
\Delta m_i &= \frac{1}{n_c} \left\langle \sum_{\eta \in S \setminus \{AB\}} a_\eta^\dagger(i) a_\eta(i) \right\rangle \\
&= 4 \left\langle v_{\mathbf{k}}^2 \right\rangle = 4 \left\langle \frac{1}{2} \left(\frac{\mathcal{A}_{\text{sq}}}{\omega_{\text{sq}}} - 1 \right) \right\rangle \\
&= 0.786,
\end{aligned}
\tag{2.25}
$$

where we used the fact that

$$
\left\langle a_\eta^{AB\dagger}(i) a_\eta^{AB}(i) \right\rangle = \left\langle v_{\mathbf{k}}^2 \right\rangle,
\tag{2.26a}
$$

$$
\left\langle a_{CD}^{AB\dagger}(i) a_{CD}^{AB}(i) \right\rangle = 0, \qquad\qquad \left\langle a_{AB}^{CD\dagger}(i) a_{AB}^{CD}(i) \right\rangle = 0
\tag{2.26b}
$$

for $\eta \in S \setminus \{CD\}$ as a consequence of the Bogoliubov transformation. This reflects the impossibility for the state AB to fluctuate into the state CD with the bilinear Heisenberg exchange in the harmonic order, and we see that there is no contribution to the ordered moment calculation from the flat localised modes found in our harmonic-order Hamiltonian. Finally, the ordered moment is given by

$$m_i = 1 - \Delta m_i = 0.214. \tag{2.27}$$

As expected, the quantum fluctuations perturb the colour order, so m_i is smaller than 1, the value of the fully polarised state. However, it is still greater than zero, $m_i > 0$, meaning that the LFWT predicts that our model can potentially retain a long-range colour order. It should be noted though that the correction is rather big—the reduction of the order is close to 80%.

Let us point out that there is an alternative way of defining the ordered moment. Ref. [22], for instance, defines the ordred moment of any site i of a SU(N) bipartite lattice as

$$m_i^{\text{alt}} = \frac{2}{N} \left(\sum_{\mu=1}^{N/2} S_\mu^\mu(i) - \sum_{\mu=\frac{N}{2}+1}^{N} S_\mu^\mu(i) \right), \tag{2.28}$$

yielding an ordered moment of $m_i = \pm 1$ for the fully ordered Néel configuration. Here, the sign of m_i depends on the sublattice. This definition is in fact equivalent to the definition of Eq. (2.23) in the harmonic order, up to a sign that depends on the sublattice:

$$
\begin{aligned}
m_i^{\text{alt}} &= \frac{1}{2} \left(\langle \hat{S}_A^A \rangle + \langle \hat{S}_B^B \rangle - \langle \hat{S}_C^C \rangle - \langle \hat{S}_D^D \rangle \right) \\
&= \frac{1}{2} \Big(\left\langle d_{AB}^\dagger(i) d_{AB}(i) + d_{AC}^\dagger(i) d_{AC}(i) + d_{DA}^\dagger(i) d_{DA}(i) \right\rangle \\
&\quad + \left\langle d_{AB}^\dagger(i) d_{AB}(i) + d_{BC}^\dagger(i) d_{BC}(i) + d_{BD}^\dagger(i) d_{BD}(i) \right\rangle \\
&\quad - \left\langle d_{AC}^\dagger(i) d_{AC}(i) + d_{BC}^\dagger(i) d_{BC}(i) + d_{CD}^\dagger(i) d_{CD}(i) \right\rangle \\
&\quad - \left\langle d_{DA}^\dagger(i) d_{DA}(i) + d_{BD}^\dagger(i) d_{BD}(i) + d_{CD}^\dagger(i) d_{CD}(i) \right\rangle \Big) \\
&\xrightarrow{n_c \to \infty} \left\langle d_{AB}^\dagger(i) d_{AB}(i) \right\rangle = \left\langle a_{AB}^\dagger(i) a_{AB}(i) \right\rangle \\
&= 0.214,
\end{aligned} \tag{2.29}
$$

where the we took into account the fact that the condensate of the site i is formed by the state AB.
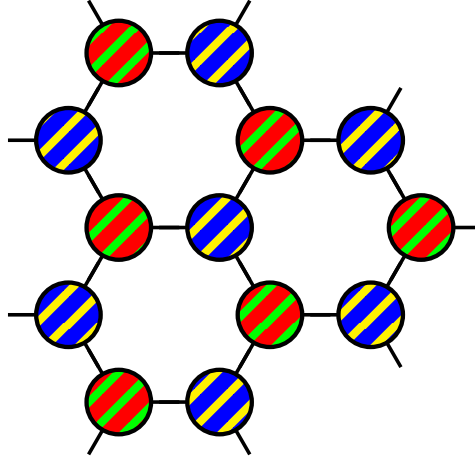
Figure 2.5 – The ordered bipartite hexagonal configuration with two colours per site.

2.1.2 Two $SU(4)$ particles per site on the honeycomb lattice

The linear flavour-wave theory of $SU(4)$ $m = 2$ **honeycomb lattice**

Now that we have sorted out how to apply the LFWT on the square lattice with two particles per site, we can easily perform the same calculations for the honeycomb lattice with two particles $SU(4)$ particles per site by following the method in subsection 2.1.1. The number of colours N and the number of sublattices remain the same, so we assume two sublattices Λ_{AB} and Λ_{CD}, and $\Gamma = \{AB, AC, DA, BC, BD, CD\}$ as before. The only difference will be the factors that depend on the geometry, like the geometrical factor $\gamma_{\text{hon},\mathbf{k}}$. The calculations are otherwise identical. The assumed colour order is illustrated in Fig. 2.5. From this, we can derive the harmonic Hamiltonian for the bipartite honeycomb lattice:

$$
\mathcal{H}^{(2)} = \sum_{\mathbf{k} \in \text{BZ}} \left\{ \sum_{\eta \in \Gamma \setminus \{AB, CD\}} \varepsilon_{\text{hon}}(\mathbf{k}) \left[\left(\tilde{a}_{\eta,\mathbf{k}}^{\dagger} \tilde{a}_{\eta,\mathbf{k}} + \frac{1}{2} \right) + \left(\tilde{b}_{\eta,\mathbf{k}}^{\dagger} \tilde{b}_{\eta,\mathbf{k}} + \frac{1}{2} \right) \right] \right.
$$
$$
\left. + 6Jn_c \left(a_{CD,\mathbf{k}}^{\dagger} a_{CD,\mathbf{k}} + b_{AB,\mathbf{k}}^{\dagger} b_{AB,\mathbf{k}} \right) \right\} - 6JN_{\text{sites}} n_c. \tag{2.30}
$$

The sums with $\mathbf{k}$ run over the structural Brillouin zone of the honeycomb lattice, i.e. we have doubly degenerate modes. The dispersion relation of the dispersive ("magnetic") branch (see Figure 2.6) is given by

$$
\varepsilon_{\text{hon}}(\mathbf{k}) := Jn_c \omega_{\text{hon}}(\mathbf{k})
$$
$$
:= Jn_c \sqrt{\mathcal{A}_{\text{hon}} - |\mathcal{B}_{\text{hon}}(\mathbf{k})|^2} = \mathcal{A}_{\text{hon}} Jn_c \sqrt{1 - |\gamma_{\text{hon}}(\mathbf{k})|^2} \tag{2.31}
$$
$$
= 3Jn_c \sqrt{1 - |\gamma_{\text{hon}}(\mathbf{k})|^2}
$$

(a) Energy spectrum of the dispersive modes.

(b) 2D cut of the energy spectrum.

Figure 2.6 – The energy spectrum of the dispersive modes of the SU(4) $m = 2$ hexagonal lattice. Figure adapted from Ref [62] with the permission of the APS, © 2017 American Physical Society.

with

$$
\mathcal{A}_{hon} := 3, \qquad \mathcal{B}_{hon} := 3\gamma_{\text{hon},\mathbf{k}},
$$
$$
\gamma_{\text{hon}}(\mathbf{k}) := \frac{1}{3}\left(e^{ik_y} + e^{i\left(\frac{\sqrt{3}}{2}k_x - \frac{1}{2}k_y\right)} + e^{i\left(-\frac{\sqrt{3}}{2}k_x - \frac{1}{2}k_y\right)} \right).
$$

(2.32)

The energy contribution of the quantum fluctuations is

$$
E/N_{\text{sites}} = -6Jn_c + 4 \cdot \left\langle \frac{\varepsilon_{\text{hon}}(\mathbf{k})}{2} \right\rangle
$$
$$
= -1.259Jn_c.
$$

Ordered moment of the SU(N) **honeycomb**

The formula for the reduction of the ordered moment is the same as in Eq. (2.25) as we also deal with the bipartite SU(4) configuration with two particles per site:

$$
\Delta m_i = \frac{1}{n_c} \left\langle \sum_{\eta \in S \backslash \{AB\}} a_\eta^\dagger(i) a_\eta(i) \right\rangle
$$
$$
= \left\langle 4 \cdot \frac{1}{2} \left(\frac{\mathcal{A}_{\text{hon}}}{\omega_{\text{hon}}} - 1 \right) \right\rangle
$$
$$
= 1.0328,
$$
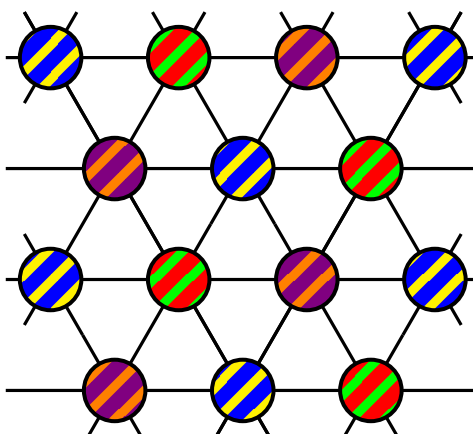
Figure 2.7 – The ordered tripartite triangular configuration with two colours per site.

The reduction is larger than 1, indicating that it is thus unlikely that a colour order exists for this model. We observe, however, that the reduction is only marginally above the full-polarization value (it exceeds it by 3%, to be precise). Hence, it cannot be absolutely excluded that a small ordered moment might survive quantum fluctuations.

2.1.3 Two $SU(6)$ **particles per site on the triangular lattice**

The linear flavour-wave theory of $SU(6)$ $m = 2$ **triangular lattice**

Let us now consider the triangular lattice with an antiferromagnetic coupling. The simplest colour configuration without frustration and with more than one particle per site is the three sublattice order with two different $SU(6)$ colour particles per site, depicted in Figure 2.7. We thus have an AFM $SU(6)$ Hamiltonian in the irrep $\boxed{}$.

Even though the symmetry of the Hamiltonian is $SU(6)$ instead of $SU(4)$, and even though we now have a three-sublattice order rather than the two sublattice order, the physical mechanism of the LFWT and its method remain identical to what we have seen in subsection 2.1.1 and subsection 2.1.2. Following the construction with the $SU(4)$ models, we use the letters A, B, C, D, E and F to label the 6 colours of $SU(6)$. The irrep in question is 15 dimensional, whose basis Γ will be written in the same way as in Eq. (2.3):

$$\Gamma := \{AB, AC, AD, AE, AF, BC, BD, BE, BF, CD, CE, CF, DE, DF, EF\}. \tag{2.33}$$

As in previous $SU(4)$ models, we attribute a bosonic operator d_η for each state $\eta \in \Gamma$. The Hamiltonian of our model is then given by Eq. (2.1) written in terms of these bosons d by using Eq. (2.7).

We now choose the lattice colour configuration such that there is a large condensate of the state AB on the first sublattice Λ_{AB}, the state CD on the second sublattice Λ_{CD} and the state EF on the third sublattice Λ_{EF}. As in section 1.2, we will divide the Hamiltonian

into sub-Hamiltonians containing the bonds between different pairs of sublattices: $\mathcal{H} = \mathcal{H}_{AB,CD} + \mathcal{H}_{CD,EF} + \mathcal{H}_{EF,AB}$. From the constraint $\sum_{\eta \in \Gamma} d_\eta^\dagger(i) d_\eta(i) = n_c$ in (2.8), we obtain the Holstein-Primakoff bosons

$$
\begin{aligned}
a_{AB}^\dagger(i), a_{AB}(i) &\rightarrow \sqrt{n_c - \sum_{\eta \in \Gamma \setminus \{AB\}} a_\eta^\dagger(i) a_\eta(i)}, \\
b_{CD}^\dagger(j), b_{CD}(j) &\rightarrow \sqrt{n_c - \sum_{\eta \in \Gamma \setminus \{CD\}} b_\eta^\dagger(j) b_\eta(j)}, \\
c_{EF}^\dagger(k), c_{EF}(k) &\rightarrow \sqrt{n_c - \sum_{\eta \in \Gamma \setminus \{EF\}} c_\eta^\dagger(k) c_\eta(k)},
\end{aligned}
\tag{2.34}
$$

where $i \in \Lambda_{AB}$, $j \in \Lambda_{CD}$ and $k \in \Lambda_{EF}$. Using the Holstein-Primkoff bosons in the Hamiltonian, the quadratic Hamiltonian $\mathcal{H}^{(2)}$ is obtained. Here, we will show $\mathcal{H}_{AB,CD}^{(2)}$ only, as the structure of the other sub-Hamiltonians is the same. After the Fourier transform,

$$
\begin{aligned}
a_\alpha(i) &= \sqrt{\frac{3}{N_{\text{sites}}}} \sum_{\mathbf{k} \in \text{RBZ}} a_\alpha(\mathbf{k}) e^{-i\mathbf{k}\mathbf{r}_i}, \qquad b_\alpha(j) = \sqrt{\frac{3}{N_{\text{sites}}}} \sum_{\mathbf{k} \in \text{RBZ}} b_\alpha(\mathbf{k}) e^{-i\mathbf{k}\mathbf{r}_j}, \\
c_\alpha(k) &= \sqrt{\frac{3}{N_{\text{sites}}}} \sum_{\mathbf{k} \in \text{RBZ}} c_\alpha(\mathbf{k}) e^{-i\mathbf{k}\mathbf{r}_k},
\end{aligned}
\tag{2.35}
$$

the quadratic Hamiltonian $\mathcal{H}_{AB,CD}^{(2)}$ is given by

$$
\mathcal{H}_{AB,CD}^{(2)} = \sum_{\alpha=0}^{4} \mathcal{H}_{AB,CD;\alpha}^{(2)}
\tag{2.36}
$$

where

$$
\begin{aligned}
\mathcal{H}_{AB,CD;0}^{(2)} &= J n_c \sum_{\mathbf{k} \in \text{RBZ}} \Big[2\mathcal{A}_{\text{tri}} \Big(a_{CD,\mathbf{k}}^\dagger a_{CD,\mathbf{k}} + b_{AB,\mathbf{k}}^\dagger b_{AB,\mathbf{k}} \Big) \\
&\qquad \mathcal{A}_{\text{tri}} \Big(a_{CE,\mathbf{k}}^\dagger a_{CE,\mathbf{k}} + a_{CF,\mathbf{k}}^\dagger a_{CF,\mathbf{k}} + a_{DE,\mathbf{k}}^\dagger a_{DE,\mathbf{k}} + a_{DF,\mathbf{k}}^\dagger a_{DE,\mathbf{k}} \\
&\qquad + b_{AE,\mathbf{k}}^\dagger b_{AE,\mathbf{k}} + b_{AF,\mathbf{k}}^\dagger b_{AF,\mathbf{k}} + b_{BE,\mathbf{k}}^\dagger b_{BE,\mathbf{k}} + b_{BF,\mathbf{k}}^\dagger b_{BF,\mathbf{k}} \Big) \Big] \\
\mathcal{H}_{AB,CD;1}^{(2)} &= J n_c \sum_{\mathbf{k} \in \text{RBZ}} \Big[\mathcal{A}_{\text{tri}} \Big(a_{AC,\mathbf{k}}^\dagger a_{AC,\mathbf{k}} + b_{BD,\mathbf{k}}^\dagger b_{BD} \Big) + \mathcal{B}_{\text{tri},\mathbf{k}} \Big(a_{AC,\mathbf{k}}^\dagger b_{BD,-\mathbf{k}}^\dagger + a_{AC,\mathbf{k}} b_{BD,-\mathbf{k}} \Big) \Big], \\
\mathcal{H}_{AB,CD;2}^{(2)} &= J n_c \sum_{\mathbf{k} \in \text{RBZ}} \Big[\mathcal{A}_{\text{tri}} \Big(a_{BD,\mathbf{k}}^\dagger a_{BD,\mathbf{k}} + b_{AC,\mathbf{k}}^\dagger b_{AC,\mathbf{k}} \Big) + \mathcal{B}_{\text{tri},\mathbf{k}} \Big(a_{BD,\mathbf{k}}^\dagger b_{AC,-\mathbf{k}}^\dagger + a_{BD,\mathbf{k}} b_{AC,-\mathbf{k}} \Big) \Big], \\
\mathcal{H}_{AB,CD;3}^{(2)} &= J n_c \sum_{\mathbf{k} \in \text{RBZ}} \Big[\mathcal{A}_{\text{tri}} \Big(a_{AD,\mathbf{k}}^\dagger a_{AD,\mathbf{k}} + b_{BC,\mathbf{k}}^\dagger b_{BC,\mathbf{k}} \Big) - \mathcal{B}_{\text{tri},\mathbf{k}} \Big(a_{AD,\mathbf{k}}^\dagger b_{BC,-\mathbf{k}}^\dagger + a_{AD,\mathbf{k}} b_{BC,-\mathbf{k}} \Big) \Big], \\
\mathcal{H}_{AB,CD;4}^{(2)} &= J n_c \sum_{\mathbf{k} \in \text{RBZ}} \Big[\mathcal{A}_{\text{tri}} \Big(a_{BC,\mathbf{k}}^\dagger a_{BC,\mathbf{k}} + b_{DA,\mathbf{k}}^\dagger b_{DA,\mathbf{k}} \Big) - \mathcal{B}_{\text{tri},\mathbf{k}} \Big(a_{BC,\mathbf{k}}^\dagger b_{AD,-\mathbf{k}}^\dagger + a_{BC,\mathbf{k}} b_{AD,-\mathbf{k}} \Big) \Big].
\end{aligned}
\tag{2.37}
$$

It is very similar to the SU(4) Hamiltonian in (2.15), albeit with more flat modes in $\mathcal{H}_{AB,CD;0}^{(2)}$. It can be seen that only bosons involving colours A, B, C, D are present. Since the Hamiltonian
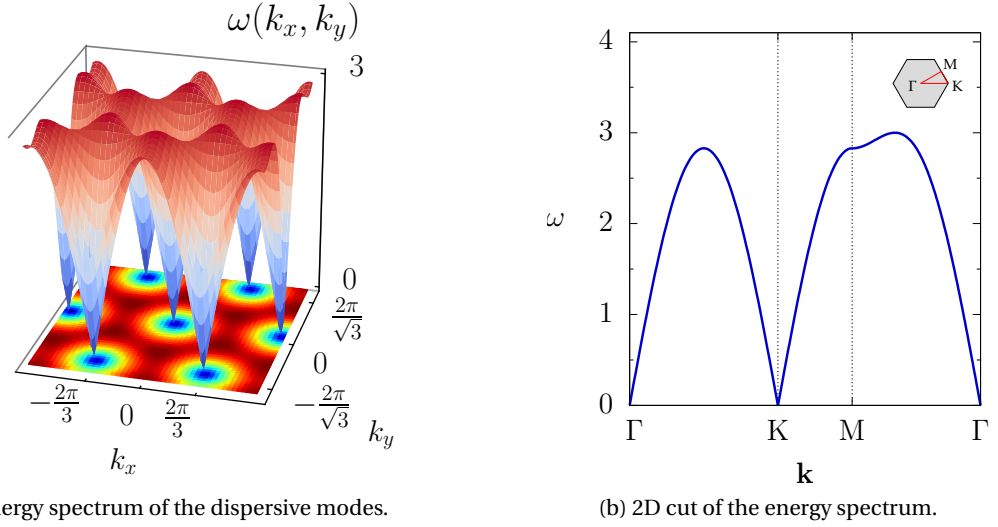
(a) Energy spectrum of the dispersive modes.

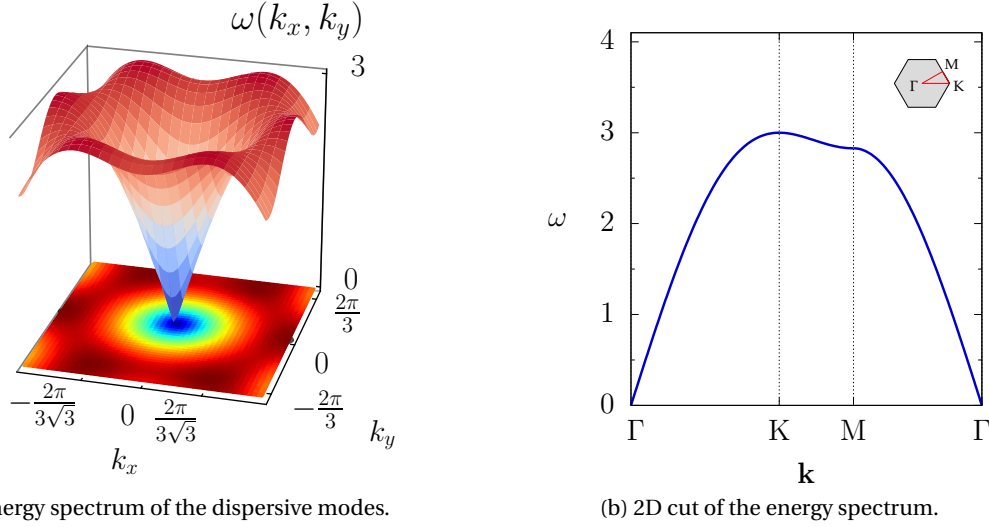(b) 2D cut of the energy spectrum.

Figure 2.8 – The energy spectrum of the dispersive modes of the SU(6) $m = 2$ triangular lattice. Figure adapted from Ref [62] with the permission of the APS, © 2017 American Physical Society.

$\mathcal{H}^{(2)}_{AB,CD}$ only involves the bonds bewteen the sublattices Λ_{AB} and Λ_{CD}, it is not possible to have the colours E, F by exchanging one colour particle between these two sublattices from the fully polarised initial condensate. This would be only possible with higher-order exchange processes, i.e. if we would use the next-order terms in the Hamiltonian expansion.

The sub-Hamiltonians $\mathcal{H}^{(2)}_{AB,CD;\alpha}$, $i \in \{1,\dots,4\}$, need diagonalisation. Since their structure is identical to that of the SU(4) Hamiltonian, we can use the Bogoliubov transformation in (2.17). Each of these $\mathcal{H}^{(2)}_{AB,CD;\alpha}$ yields two diagonalized modes, so we will obtain 8 modes for $\mathcal{H}^{(2)}_{AB,CD}$ from this Bogoliubov transformation. The same applies to $\mathcal{H}^{(2)}_{CD,EF}$ and $\mathcal{H}^{(2)}_{EF,AB}$. Hence, by gathering the flat modes carefully, the full Hamiltonian $\mathcal{H}^{(2)}$ is given by

$$
\begin{aligned}
\mathcal{H}^{(2)} = \sum_{\mathbf{k}\in\text{RBZ}} \Bigg\{ & \varepsilon_{\text{tri}}(\mathbf{k}) \left[\sum_{\eta\in\Gamma_{AB}} \left(\tilde{a}^{\dagger}_{\eta,\mathbf{k}} \tilde{a}_{\eta,\mathbf{k}} + \frac{1}{2} \right) + \sum_{\eta\in\Gamma_{CD}} \left(\tilde{b}^{\dagger}_{\eta,\mathbf{k}} \tilde{b}_{\eta,\mathbf{k}} + \frac{1}{2} \right) + \sum_{\eta\in\Gamma_{EF}} \left(\tilde{c}^{\dagger}_{\eta,\mathbf{k}} \tilde{c}_{\eta,\mathbf{k}} + \frac{1}{2} \right) \right] \\
& + 2\mathcal{A}_{\text{tri}} J n_c \Big(a^{\dagger}_{CD,\mathbf{k}} a_{CD,\mathbf{k}} + a^{\dagger}_{EF,\mathbf{k}} a_{EF,\mathbf{k}} + b^{\dagger}_{AB,\mathbf{k}} b_{AB,\mathbf{k}} + b^{\dagger}_{EF,\mathbf{k}} b_{EF,\mathbf{k}} + c^{\dagger}_{AB,\mathbf{k}} c_{AB,\mathbf{k}} \\
& + c^{\dagger}_{CD,\mathbf{k}} c_{CD,\mathbf{k}} + \sum_{\eta\in\bar{\Gamma}_{AB}} a^{\dagger}_{\eta,\mathbf{k}} a_{\eta,\mathbf{k}} + \sum_{\eta\in\bar{\Gamma}_{CD}} b^{\dagger}_{\eta,\mathbf{k}} b_{\eta,\mathbf{k}} + \sum_{\eta\in\bar{\Gamma}_{EF}} c^{\dagger}_{\eta,\mathbf{k}} c_{\eta,\mathbf{k}} \Big) \Bigg\} - 12 J N_{\text{sites}} n_c,
\end{aligned}
$$

(2.38)

where the dispersion relation (see Fig. 2.8) is given by

$$\varepsilon_{\mathrm{tri}}(\mathbf{k}) := J n_c \omega_{\mathrm{tri}}(\mathbf{k})$$
$$:= J n_c \sqrt{\mathcal{A}_{\mathrm{tri}} - |\mathcal{B}_{\mathrm{tri}}(\mathbf{k})|^2} = \mathcal{A}_{\mathrm{tri}} J n_c \sqrt{1 - |\gamma_{\mathrm{tri}}(\mathbf{k})|^2} \tag{2.39}$$
$$= 3 J n_c \sqrt{1 - |\gamma_{\mathrm{tri}}(\mathbf{k})|^2}$$

with

$$\mathcal{A}_{tri} := 3, \qquad \mathcal{B}_{tri} := 3\gamma_{\mathrm{tri},\mathbf{k}},$$
$$\gamma_{\mathrm{tri}}(\mathbf{k}) := \frac{1}{3}\left(e^{ik_x} + 2e^{-i\frac{1}{2}k_x}\cos\frac{\sqrt{3}}{2}k_y \right). \tag{2.40}$$

Furthermore, the following sets have been used for ease of notation:

$$\bar{\Gamma} := \Gamma \setminus \{AB, CD, EF\},$$
$$\bar{\Gamma}_{AB} := \{CE, CF, DE, DF\}, \qquad \bar{\Gamma}_{CD} := \{AE, AF, BE, BF\}, \qquad \bar{\Gamma}_{EF} := \{AC, AD, BC, BD\},$$
$$\Gamma_{AB} := \bar{\Gamma} \setminus \bar{\Gamma}_{AB} = \{AC, AD, AE, AF, BC, BD, BE, BF\}, \tag{2.41}$$
$$\Gamma_{CD} := \bar{\Gamma} \setminus \bar{\Gamma}_{CD} = \{AC, AD, BC, BD, CE, CF, DE, DF\},$$
$$\Gamma_{EF} := \bar{\Gamma} \setminus \bar{\Gamma}_{EF} = \{AE, AF, BE, BF, CE, CF, DE, DF\}.$$

The similarity between the geometrical factors of the honeycomb lattice and the triangular lattice in (2.32) and (2.40) is due to the fact that the geometric bonds linking two sublattices in both cases have the same angle.

Let us now look at the number of modes that we obtain in this case. As before, we will concentrate on the sublattice Λ_{AB} and thus look at the bosons $a(i)$ in the Hamiltonian (2.38), as the reasoning will be identical for the two remaining sublattices. We obtain 8 dispersive modes, $\tilde{a}^\dagger_{\eta,\mathbf{k}}\tilde{a}_{\eta,\mathbf{k}}$ with $\eta \in \Gamma_{AB}$, that are all associated to permuting one colour in the initial state AB. As we can change either A or B to C, D, E, F without violating the antisymmetry of our irrep, we obtain 8 modes. The 6 states in $\bar{\Gamma}_{AB}$, on the other hand, are obtained by exchanging both A and B (in the initial state AB) with a different colour, and they correspond precisely to the flat modes that we obtain in the Hamiltonian (2.38).

As the structure of the sub-Hamiltonian is the same for Λ_{CD} and Λ_{EF}, we can unfold the modes into the extended (structural) Brillouin zone, as in Hamiltonian (2.21), by introducing the bosons $\tilde{f}_\sigma$ for the dispersive modes and bosons f_ρ for the flat modes. We then have

$$\mathcal{H}^{(2)} = \sum_{\mathbf{k}} \left[\omega_{\mathrm{tri}}(\mathbf{k}) \sum_{\zeta=1}^{8}\left(\tilde{f}^\dagger_\zeta(\mathbf{k})\tilde{f}_\zeta(\mathbf{k}) + \frac{1}{2} \right) + 2\mathcal{A}_{\mathrm{tri}} J n_c \sum_{\rho=1}^{6} f^\dagger_\rho(\mathbf{k}) f_\rho(\mathbf{k}) \right] - 12 J n_c. \tag{2.42}$$

We then have 8 dispersive modes corresponding to the possible colour transitions and 6 flat modes, as explained above.

Lastly, we observe that the energy per site originating from the quantum fluctuations is

$$E/N = Jn_c \left(-12 + 8 \cdot \left\langle \frac{\omega_{\text{tri}}(\mathbf{k})}{2} \right\rangle \right)$$

$$= -2.518 Jn_c. \tag{2.43}$$

Ordered moment of the SU(6) $m = 2$ **triangular lattice**

We compute the ordered moment $m_i = \frac{1}{n_c} \left\langle a_{AB}^\dagger(i) a_{AB}(i) \right\rangle$ as defined in Eq. (2.23). The computation of the reduction of the ordered moment shows that

$$\Delta m_i = \frac{1}{n_c} \left\langle \sum_{\eta=\Gamma\backslash\{AB\}} a_\eta^\dagger(i) a_\eta(i) \right\rangle$$

$$= \frac{1}{n_c} \left\langle 8 \cdot \frac{1}{2} \left(\frac{3Jn_c}{Jn_c \omega_{\text{tri}}(\mathbf{k})} - 1 \right) \right\rangle$$

$$= 2.066, \tag{2.44}$$

where we see again that the flat modes do not contribute to the reduction of the order. As the reduction is far greater than 1, we can thus conclude that the color order is verly likely to be destroyed by quantum fluctuations.

2.1.4 General considerations: m particles per site

Let us briefly wrap up what we have seen until here. At the harmonic level of the Hamiltonian expansion, we have seen that the dispersive modes come from permuting one colour between two neighbouring sites from the initial condensate states. In the weight diagram, this amounts to counting the number of weights connected adjacently to the state of the initial condensate. This is because the only off-diagonal quadratic terms that generate the dispersiveness of the modes come from such exchange terms in the Heisenberg Hamiltonian (2.1). If we are dealing with the geometries considered above (bipartite square/honeycomb and tripartite triangular lattices) with $m = \frac{N}{n_{\text{sub}}}$ particles per site in the fully antisymmetric irrep, then this will always be the case as a consequence of the structure of SU(N) irreps and the Holstein-Primakoff condensate (2.10) and (2.34) from which we only collect terms of the order n_c. At this order, it turns out that the terms that will yield the dispersive modes necessarily come from $S_\nu^\mu(i) S_\mu^\nu(j)$ in which μ and ν will both be one of the colours of the initial condensates.

We have also seen that the exchange processes requiring more that one colour-exchange result in flat modes at the end of the calculations in the quadratic order. The flat modes come from the terms $\hat{S}_\nu^\mu(i) \hat{S}_\mu^\nu(j)$ and $\hat{S}_\mu^\mu(i) \hat{S}_\mu^\mu(j)$ where neither the colour μ nor $\nu \neq \mu$ is present in the initial condensates of the sites i and j. And careful inspection of the Hamiltonian structure allows us to conclude that the energy of the flat band will be at $n_p \mathcal{A} Jn_c$, where $n_p \in \{2, \ldots, m\}$ is the number of colour permutations required from the original condensate ($\mathcal{A}$

is the coordination number between two sublattices that was introduced in Eqs. (2.16), (2.32) and (2.40)).

Hence, the physical picture is very clear here. The states that are attainable by one colour permutation between two neighbouring sites in the initial condensate yield dispersive branches, and all other states requiring n_p number of colour-exchanges from the initial state will produce flat bands in the quadratic Hamiltonian. This behaviour is indeed also observed in the SU(2) spin-S spin-wave calculations using the multiboson method in Ref. [66]. At the harmonic order of the expansion, $2S$ modes emerge in the (extended) Brillouin zone, from which all but one mode are flat. The sole dispersive branch corresponds to the conventional spin-wave mode, and it corresponds to flipping one spin-$\frac{1}{2}$ from the neighboring sites (it corresponds to changing the fully polarised spin state $S_{\max} = \pm S$ by one quantum $\Delta S_z = 1/2$). The rest of the modes (that are all flat) correspond to higher-order transitions requiring more than one spin permutation (reducing the polarisation by more than one quantum).

The origin of the terms of order n_c from the Hamiltonian (2.1) allows us to write the harmonic LFWT Hamiltonian of any SU(N) model of one of the three lattice geometries studied above with the according value of m, by counting the number of possible colour-exchanges. We only need to adapt the number of modes according to the geometry we are considering (we know, for instance, that the honeycomb lattice has twice as many modes as the square lattice due to the difference in the unit cell). Let us now write down explicitly the general expression of a harmonic SU(N) LFWT Hamiltonian for any N in one of the configurations above.

For a given (fully) antisymmetric SU(N) irrep, the generators $\hat{S}_\nu^\mu$ on a given site i can be expressed as

$$\hat{S}_\nu^\mu(i) = \sum_{\substack{\alpha_1,...,\alpha_m \\ \alpha_1,...,\alpha_m \neq \mu,\nu}} \mathrm{sgn}(\sigma_1)\,\mathrm{sgn}(\sigma_2)\, d^\dagger_{\sigma_1\cdot(\alpha_1...\alpha_m\nu)}(i) d_{\sigma_2\cdot(\alpha_1...\alpha_m\mu)}(i), \tag{2.45}$$

where the indices $\alpha_1,\ldots,\alpha_m$ run over the N colors and σ_1,σ_2 are permutation operators that order the letters in alphabetical order. This is of course a direct generalisation of Eq. (2.7). It permutes the color μ with ν while taking care of the sign change in order to respect the antisymmetry of the states.

After following the procedures described in subsection 2.1.1 for the square lattice with $m = \frac{N}{2}$ and subsection 2.1.3 for the triangular lattice with $m = \frac{N}{3}$, the Hamiltonian will be given by

$$\mathcal{H}^{(2)} = \sum_{\mathbf{k}} \left\{ \varepsilon_{\mathrm{sq/tri}}(\mathbf{k}) \sum_{\zeta=1}^{m(N-m)} \left(\tilde{f}_\zeta^\dagger(\mathbf{k})\tilde{f}_\zeta(\mathbf{k}) + \frac{1}{2} \right) + \sum_{n_p=2}^{m} n_p \mathcal{A}_{\mathrm{sq/tri}} J n_c \sum_{\rho=1}^{\binom{m}{n_p}\binom{N-m}{n_p}} f_\rho^\dagger(\mathbf{k}) f_\rho(\mathbf{k}) \right\} \\ - \frac{m(N-m)}{2} \mathcal{A}_{\mathrm{sq/tri}} J n_c N, \tag{2.46}$$

where the sum runs over the extended Brillouin zone. The coordination number between

sublattices are $\mathcal{A}_{\text{sq}} = 4$ for the square lattice and $\mathcal{A}_{\text{tri}} = 3$ for the triangular lattice (see Eqs. (2.16) and (2.40)) and the dispersion relations are given by Eqs. (2.20) and (2.39).

This is simply because there exists $\binom{m}{n_p}\binom{N-m}{n_p}$ accessible states by applying n_p colour permutations from the initial state. So these transitions will be expressed as flat modes at energy $n_p \mathcal{A}_{\text{sq/tri}} J n_c$. As for the dispersive branches, there are $\binom{m}{1}\binom{N-m}{1} = m(N-m)$ of them. When counting these numbers, one should remember that the dimension of the antisymmetric irrep we are considering is $\binom{N}{m}$ and that the use of the Holstein-Primakoff prescription means that one boson will be replaced by a number, resulting in $\binom{N}{m} - 1$ branches in the structural Brillouin zone in total. Since N and m are not independent ($m = \frac{N}{n_{\text{sub}}}$), we can even simplify the numbers further: the square lattice will actually have m^2 (or $\frac{N^2}{4}$) dispersive branches and the triangular lattice will have $2m^2$ (or $\frac{2N^2}{9}$) branches. Knowing this, we can compute the ordered colour moment of the system for a given number of particles per site m, as the reduction of the magnetisation Δm_i only comes from the dispersive modes, i.e., from the permitted fluctuation channels from the initial condensate. The quantity Δm_i is then given by

$$
\begin{aligned}
\Delta m_i^{\text{sq}}(m) &= m^2 \left\langle \frac{1}{2}\left(\frac{\mathcal{A}_{\text{sq}}}{\omega_{\text{sq}}(\mathbf{k})} - 1 \right) \right\rangle \\
&= 0.197 m^2
\end{aligned}
\tag{2.47}
$$

for the square lattice, and

$$
\begin{aligned}
\Delta m_i^{\text{tri}}(m) &= 2m^2 \left\langle \frac{1}{2}\left(\frac{\mathcal{A}_{\text{tri}}}{\omega_{\text{tri}}(\mathbf{k})} - 1 \right) \right\rangle \\
&= 0.516 m^2
\end{aligned}
\tag{2.48}
$$

for the triangular lattice.

The same conclusion also applies for the honeycomb lattice, with the only difference being the number of branches that is doubled in the structural Brillouin zone. Introducing an index χ to account for the doubling of the branches, we obtain

$$
\mathcal{H}^{(2)} = \sum_{\mathbf{k}} \sum_{\chi=1}^{2} \left\{ \varepsilon_{\text{hon}}(\mathbf{k}) \sum_{\zeta=1}^{m(N-m)} \left(\tilde{f}_{\zeta,\chi}^{\dagger}(\mathbf{k}) \tilde{f}_{\zeta,\chi}(\mathbf{k}) + \frac{1}{2} \right) + \sum_{n_p=2}^{m} n_p \mathcal{A}_{\text{hon}} J n_c \sum_{\rho=1}^{\binom{m}{n_p}\binom{N-m}{n_p}} f_{\rho,\chi}^{\dagger}(\mathbf{k}) f_{\rho,\chi}(\mathbf{k}) \right\}
$$
$$
- \frac{m(N-m)}{2} \mathcal{A}_{\text{hon}} J n_c N
\tag{2.49}
$$

for the honeycomb lattice, with $\mathcal{A}_{\text{hon}} = 3$. The reduction of the magnetisation as a function of m is now given by

$$
\begin{aligned}
\Delta m_i^{\text{hon}}(m) &= m^2 \left\langle \frac{1}{2}\left(\frac{\mathcal{A}_{\text{hon}}}{\omega_{\text{hon}}(\mathbf{k})} - 1 \right) \right\rangle \\
&= 0.258 m^2.
\end{aligned}
$$

Since we have seen previously that the reduction of the magnetisation $\Delta m_i^{\text{hon,tri}}$ is already larger than 1 for the smallest non-trivial value $m = 2$ on the honeycomb and triangular lattices, it seems unlikely that such color-ordered states would be the ground state of these systems. For the square lattice, it can be seen from Eq. (2.47) that $\Delta m_i^{\text{sq}} > 1$ for $m \geq 3$. The only configuration that could possibly retain a long-range finite color-order as a ground state according to the multiboson LFWT calculations is the SU(4) $m = 2$ square lattice. This conclusion indeed corresponds to the physical picture that quantum fluctuations grow as N becomes larger (remember that there are $N(N-1)/2$ pairs of ladder operators ($\hat{S}_\nu^\mu$, $\mu \neq \nu$) for a given N, i.e., the potential number of possible colour-permutation grows as N becomes larger). As N becomes greater (and, consequently, m as well), there are more and more colour permutations: the number of possible colour permutations from the initial state grows as $m(N - m)$, so there are more and more fluctuation channels that destroy the potential long-range order.

We can thus conclude that the only candidate for persisting colour long-range order is the bipartite square lattice with two SU(4) particles per site, filling the corresponding point missing in the phase diagram of the SU(N) square lattice in Ref. [69]. In the bipartite honeycomb configuration, the same SU(4)-symmetry particles have stronger quantum fluctuations and destroys the colour order, and this is due to the lower coordination number z of the honeycomb lattice that bolsters the quantum fluctuations. This is a phenomenon also observed with the SU(2) spin-$\frac{1}{2}$ particles in the Néel configuration: the magnetic moment is smaller in the honeycomb lattice than in the square lattice. Taking the values of the reduction of the magnetic moment of these two lattices from Refs. [45, 75], one finds the following ratio of Δm between the square lattice and the honeycomb lattice: $0.1966/0.2582 = 0.7614$. This ratio is the same in our SU(4) $m = 2$ models: $0.7864/1.0328 = 0.7614$. In both cases, the difference of the magnetic moments come from the geometry since the particle symmetry is the same in both cases.

It is interesting to note that the data extracted from a pinning-field QMC study [22] shows that the SU(4) Hubbard model at half-filling on the square lattice indeed seems to retain a finite magnetisation value in the Heisenberg limit ($m = 0.125 \pm 0.044$) [74], although it is smaller than our value in Eq. (2.27). This QMC result is indeed in line with the more recent auxiliary field QMC results with a larger system size in Ref. [74]: $m \simeq 0.11$.

2.1.5 Dimensional crossover of the 2D square lattice to 1D chains

This subsection stems from the collaboration with Fakher Assaad, Karlo Penc and Frédéric Mila [74]. Now that a possible long-range colour order as been established for the SU(4) $m = 2$ square lattice, we can ask ourselves what the LFWT can tell us about the dimensional crossover, i.e., when one starts to weaken the vertical bonds of the square lattice to go from the 2D square lattice to a collection of 1D chains, since it is believed that the ground state of the 1D SU(4) $m = 2$ chain is the valence-bond solid (VBS) state. Fakher Assaad's results of the auxiliary field QMC simulations with system sizes up to 40×40 show a small local moment in the 2D model and supports a continuous transition between the Néel state and the VBS state during

(a) Néel

(b) VBS
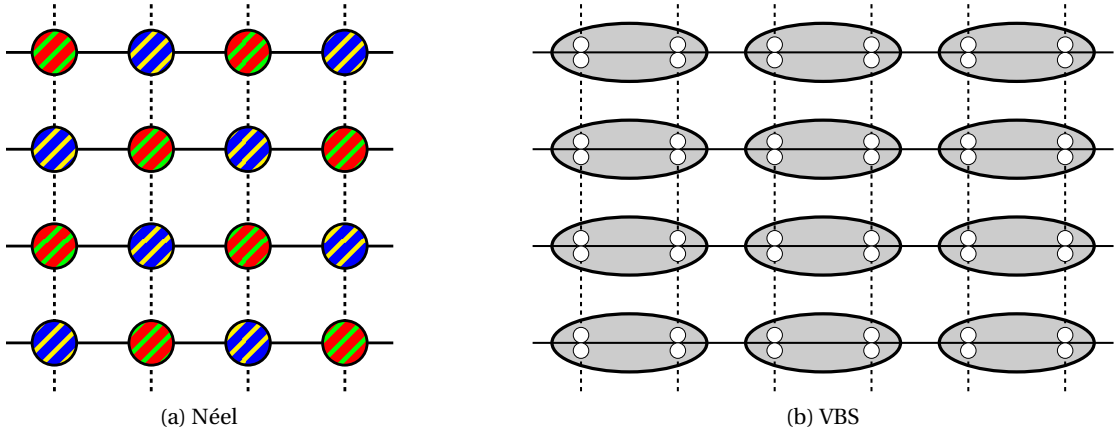
Figure 2.9 – (a) An illustration of the Néel-like configuration with two particles per site with an ordering vector $\mathbf{q} = (\pi, \pi)$. The flavours A, B, C, D are represented by the colors blue, yellow, red, green respectively. (b) A VBS configuration with two particles per site with an ordering vector $\mathbf{q} = (\pi, 0)$. The horizontal lines represent the intra-chain coupling J_x whereas the vertical dashed lines represent the inter-chain coupling J_y that controls the dimensional crossover.

the dimensional transition. The ground-state candidates in 2D and 1D, namely the Néel-like configuration and the VBS configuration, are shown in Fig. 2.9.

We first define the anisotropic SU(4) AFM Heisenberg model in 2D with the intra-chain coupling J_x and the inter-chain coupling J_y,

$$\mathcal{H} = \sum_{\langle \vec{\imath}, \vec{\jmath} \rangle} \sum_{\mu, \nu} J_{\vec{\imath}, \vec{\jmath}} \, \hat{S}_\nu^\mu(\vec{\imath}) \hat{S}_\mu^\nu(\vec{\jmath}). \tag{2.50}$$

The site indices $\langle \vec{\imath}, \vec{\jmath} \rangle$ run over the nearest neighbours, and the indices $\mu, \nu \in \{A, B, C, D\}$ label the flavours. The nearest-neighbour coupling $J_{\vec{\imath}, \vec{\jmath}}$ is given by

$$J_{\vec{\imath}, \vec{\jmath}} = \begin{cases} J_x & \text{for intra-chain bonds (horizontal)}, \\ J_y & \text{for inter-chain bonds (vertical)}. \end{cases} \tag{2.51}$$

At the isotropic point $J_x = J_y$, the model describes the square lattice in subsection 2.1.1 whereas the regime $\frac{J_y}{J_x} = 0$ corresponds to decoupled chains. The rest of the calculations is nearly identical to the LFWT procedure in subsection 2.1.1, so we will only show some important intermediate equations. The harmonic Hamiltonian $\mathcal{H}^{(2)} = \sum_{\alpha=0}^{4} \mathcal{H}_\alpha^{(2)}$ after the

37

Holstein-Primakoff prescription is given by

$$
\begin{aligned}
\mathcal{H}_0^{(2)} &= n_c \sum_{\mathbf{k}\in\text{RBZ}} 2\mathcal{A} \left[a_{CD,\mathbf{k}}^\dagger a_{CD,\mathbf{k}} + b_{AB,\mathbf{k}}^\dagger b_{AB,\mathbf{k}} \right], \\
\mathcal{H}_1^{(2)} &= n_c \sum_{\mathbf{k}\in\text{RBZ}} \left[\mathcal{A} \left(a_{AC,\mathbf{k}}^\dagger a_{AC,\mathbf{k}} + b_{BD,\mathbf{k}}^\dagger b_{BD} \right) + \mathcal{B}_\mathbf{k} \left(a_{AC,\mathbf{k}}^\dagger b_{BD,-\mathbf{k}}^\dagger + a_{AC,\mathbf{k}} b_{BD,-\mathbf{k}} \right) \right], \\
\mathcal{H}_2^{(2)} &= n_c \sum_{\mathbf{k}\in\text{RBZ}} \left[\mathcal{A} \left(a_{BD,\mathbf{k}}^\dagger a_{BD,\mathbf{k}} + b_{AC,\mathbf{k}}^\dagger b_{AC,\mathbf{k}} \right) + \mathcal{B}_\mathbf{k} \left(a_{BD,\mathbf{k}}^\dagger b_{AC,-\mathbf{k}}^\dagger + a_{BD,\mathbf{k}} b_{AC,-\mathbf{k}} \right) \right], \quad (2.52) \\
\mathcal{H}_3^{(2)} &= n_c \sum_{\mathbf{k}\in\text{RBZ}} \left[\mathcal{A} \left(a_{DA,\mathbf{k}}^\dagger a_{DA,\mathbf{k}} + b_{BC,\mathbf{k}}^\dagger b_{BC,\mathbf{k}} \right) + \mathcal{B}_\mathbf{k} \left(a_{DA,\mathbf{k}}^\dagger b_{BC,-\mathbf{k}}^\dagger + a_{DA,\mathbf{k}} b_{BC,-\mathbf{k}} \right) \right], \\
\mathcal{H}_4^{(2)} &= n_c \sum_{\mathbf{k}\in\text{RBZ}} \left[\mathcal{A} \left(a_{BC,\mathbf{k}}^\dagger a_{BC,\mathbf{k}} + b_{DA,\mathbf{k}}^\dagger b_{DA,\mathbf{k}} \right) + \mathcal{B}_\mathbf{k} \left(a_{BC,\mathbf{k}}^\dagger b_{DA,-\mathbf{k}}^\dagger + a_{BC,\mathbf{k}} b_{DA,-\mathbf{k}} \right) \right],
\end{aligned}
$$

with

$$
\begin{aligned}
\mathcal{A} &:= 2J_x + 2J_y, \\
\mathcal{B}_\mathbf{k} &:= 2J_x \cos k_x + 2J_y \cos k_y.
\end{aligned}
\qquad (2.53)
$$

The constraint can now be reset to $n_c = 1$. To diagonalize terms $\mathcal{H}_{1,\dots,4}^{(2)}$, we use the Bogoliubov transformation as follows:

$$
\begin{pmatrix} \tilde{a}_{AC,\mathbf{k}}^\dagger \\ \tilde{b}_{BD,-\mathbf{k}} \end{pmatrix} = \begin{pmatrix} u_\mathbf{k} & v_\mathbf{k} \\ v_\mathbf{k} & u_\mathbf{k} \end{pmatrix} \begin{pmatrix} a_{AC,\mathbf{k}}^\dagger \\ b_{BD,-\mathbf{k}} \end{pmatrix},
\qquad (2.54)
$$

with

$$
\begin{aligned}
u_\mathbf{k} &= \sqrt{\frac{1}{2}\left(\frac{\mathcal{A}}{\omega_\mathbf{k}} + 1\right)}, \qquad v_\mathbf{k} = \sqrt{\frac{1}{2}\left(\frac{\mathcal{A}}{\omega_\mathbf{k}} - 1\right)}, \\
\omega_\mathbf{k} &= \sqrt{\mathcal{A}^2 - \mathcal{B}_\mathbf{k}^2}.
\end{aligned}
\qquad (2.55)
$$

Hence, the diagonalized quadratic Hamiltonian finally reads as

$$
\boxed{
\begin{aligned}
\mathcal{H}^{(2)} = \sum_{\mathbf{k}\in\text{RBZ}} \Bigg\{ & \sum_{\eta\in\Gamma\setminus\{AB,CD\}} \varepsilon_\mathbf{k} \left[\left(\tilde{a}_{\eta,\mathbf{k}}^\dagger \tilde{a}_{\eta,\mathbf{k}} + \frac{1}{2} \right) + \left(\tilde{b}_{\eta,\mathbf{k}}^\dagger \tilde{b}_{\eta,\mathbf{k}} + \frac{1}{2} \right) \right] \\
& + 8 \left(a_{CD,\mathbf{k}}^\dagger a_{CD,\mathbf{k}} + b_{AB,\mathbf{k}}^\dagger b_{AB,\mathbf{k}} \right) \Bigg\} + \text{const.},
\end{aligned}
}
\qquad (2.56)
$$

with

$$
\begin{aligned}
\omega_\mathbf{k} &= \sqrt{\mathcal{A}^2 - \mathcal{B}_\mathbf{k}^2} \\
&= (2J_x + 2J_y)\sqrt{1 - \left(\frac{2J_x \cos k_x + 2J_y \cos k_y}{2J_x + 2J_y}\right)^2}.
\end{aligned}
\qquad (2.57)
$$

The spectrum of the isotropic ($J_x = J_y = 1$) case is plotted in Figure 2.4.
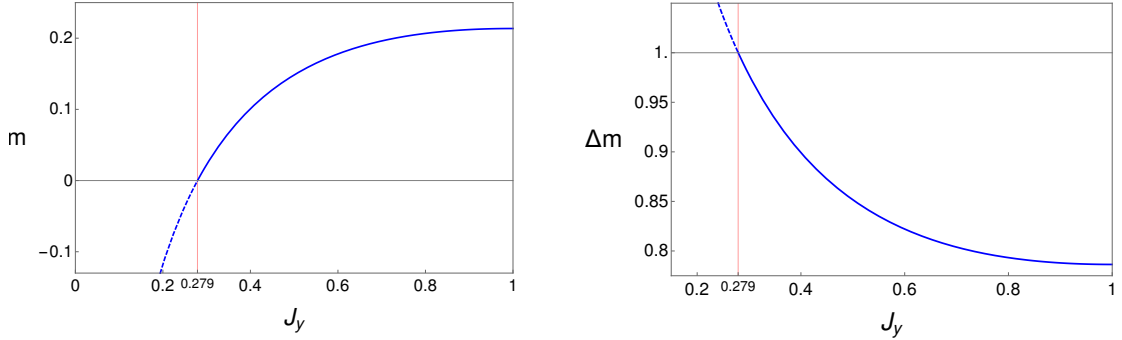
(a) The ordered moment as a function of J_y.

(b) The reduction of the order as a function of J_y.

Figure 2.10 – The magnetisation and the reduction of it as a function of J_y. The magnetisation below $J_y^c = 0.279$ is negative, suggesting that the order is completely destroyed below this value.

Let us now study the magnetisation and the dimensional crossover of the system. Using the definition of the ordered moment in Eq. (2.23), we obtain

$$
\begin{aligned}
m_1(J_x, J_y) &= \frac{1}{2}\left(\sum_{\mu=A}^{B} S_\mu^\mu(i) - \sum_{\mu=C}^{D} S_\mu^\mu(i)\right)\\
&= 1 - \sum_{\eta \in \Gamma \setminus \{AB\}} \left\langle a_\eta^\dagger(i) a_\eta(i) \right\rangle\\
&= 1 - 4\left\langle v_{\mathbf{k}}^2 \right\rangle,
\end{aligned}
\tag{2.58}
$$

where we used the fact that $\left\langle a_{CD}^\dagger(i) a_{CD}(i) \right\rangle = 0$, i.e. the localised band does not contribute to the reduction of the magnetisation. Let us now fix the value of the intra-chain coupling $J_x = 1$ for simplicity. In the isotropic case, $J_y = 1$, it has already been concluded in subsection 2.1.1 that the magnetic moment retains a finite value, $m = 0.214$, and that this would suggest a potential flavour order of the system. From this isotropic point, we can now investigate the dimensional crossover by searching for the value of J_y^c such that $m = 0$. The magnetisation m vanishes when

$$
J_y^c = 0.279.
\tag{2.59}
$$

as shown in Figure 2.9, in which the ordered moment and its reduction are plotted. Below this value of J_y, quantum fluctuations completely destroy the flavour order, indicating a possible phase transition. Hence, the LFWT indeed predicts a phase transition from the Néel ordered state when sliding into a 1D system, in line with the auxiliary field QMC results in Ref. [74]. However, the Néel-like phase appears to be much more robust within the LFWT calculations, as the value of $J_y^c = 0.279$ is much lower than the QMC prediction $J_y^c = 0.74 - 0.78$ [74].

2.2   SU(3) **adjoint irreducible representation**

We have seen how to use the LFWT with the multiboson approach in the fully antisymmetric irreps. The nice aspect we did not mention about these antisymmetric irreps is that the weights are not degenerate, i.e., the states of these irreps do not belong to a multi-dimensional space in the weight space. These made things "easy" when we were trying to figure out the transitions between the states induced by the generators $\hat{S}_\nu^\mu$ in Eq (2.4). However, for a general irrep with a potentially mixed symmetry, there exists degenerate weights—some states share the same weight in the weight diagram. This makes the process of deriving the multibosonic expression of $\hat{S}_\nu^\mu$ as in Eq (2.4) less straightforward. In this section, we will apply the steps in section 2.1 to the SU(3) adjoint irrep which has a degenerate zero-weight. The SU(3) adjoint irrep has a mixed symmetry, and in a way, can be considered a "minimal model" in the SU(N) world: it contains all the particular and distinctive features of SU(N) irreps. Once we know how to apply the multiboson LFWT with this irrep, we will hold a general recipe for the multiboson LFWT theory for any arbitrary irrep.

For this, we need a plausible theoretical model involving a colour-order. We thus consider the antiferromagnetic bipartite chain on which we put three SU(3) particles per site whose wavefunction lives in ▭. The Hamiltonian of this model is given by

$$\mathcal{H} = J \sum_{<i,j>} \sum_{\mu,\nu} \hat{S}_\nu^\mu(i) \hat{S}_\mu^\nu(j) \tag{2.60}$$

with the colour indices $\mu, \nu \in \{A, B, C\}$, and we assume a classical ground-state configuration such that we have $\boxed{\begin{smallmatrix}A&A\\C\end{smallmatrix}}$ on one sublattice and $\boxed{\begin{smallmatrix}B&B\\C\end{smallmatrix}}$ on the other sublattice.[8]

The choice of this model is not fortuitous as there is a physical motivation behind it, but we will come to this in the next chapter and focus on the methodology of the multiboson LFWT here.

---

[8]It is indeed shown in Ref. [76], using the coherent states that Mathur & Sen introduces in Ref. [77], that this configuration is indeed a ground state. For a given SU(3) irrep of $[p, q]$, the coherent states are given by

$$|\vec{z}, \vec{w}\rangle_{[p,q]} \equiv \frac{1}{\sqrt{p!q!}} (\vec{z} \cdot \vec{a}^\dagger)^p (\vec{w} \cdot \vec{b}^\dagger)^q |0\rangle$$

with the tracelessness condition $\vec{z} \cdot \vec{w} = 0$ and the normalisation condition $|\vec{z}|^2 = |\vec{w}|^2 = 1$. In the case of the adjoint irrep $p = q = 1$, the expectation of the generators are given by $\langle \vec{z}, \vec{w} | \hat{S}_\beta^\alpha | \vec{z}, \vec{w} \rangle = p(z^{\alpha*} z_\beta - w^\alpha w_\beta^*)$, and our Hamiltonian using these coherent states are then given by

$$\mathcal{H} = Jp^2 \sum_i \left[|\vec{z}_i^* \cdot \vec{z}_{i+1}|^2 + |\vec{w}_i^* \cdot \vec{w}_{i+1}|^2 - |\vec{z}_i \cdot \vec{w}_{i+1}|^2 - |\vec{w}_i \cdot \vec{z}_{i+1}|^2 \right].$$

The classical ground state would then be given by $\vec{z}_{2n} = \vec{w}_{2n+1}^* = \vec{\phi^1}$ and $\vec{w}_{2n}^* = \vec{z}_{2n+1} = \vec{\phi^2}$ such that $\vec{\phi^1}$ and $\vec{\phi^2}$ are two (normalised) orthogonal fields. In terms of the SU(3) fundamental irrep basis $\{\boxed{A}, \boxed{B}, \boxed{C}\}$ and its conjugate irrep basis $\left\{ \boxed{\begin{smallmatrix}B\\C\end{smallmatrix}}, \boxed{\begin{smallmatrix}A\\C\end{smallmatrix}}, \boxed{\begin{smallmatrix}A\\B\end{smallmatrix}} \right\} \equiv \{\bar{A}, \bar{B}, \bar{C}\}$, the bipartite configuration of $\boxed{\begin{smallmatrix}A&A\\C\end{smallmatrix}}$ and $\boxed{\begin{smallmatrix}B&B\\C\end{smallmatrix}}$ indeed satisfies these conditions.

2.2.1 General method for deriving the action of the generators

First things first: let us quickly show again the states of the eight-dimensional SU(3) adjoint irrep $\tiny\young(13,2)$ that we saw in Table 1.1 in section 1.1. Since there are two such eight-dimensional irreps, $\tiny\young(12,3)$ and $\tiny\young(13,2)$, we will use $\tiny\young(13,2)$ that is antisymmetric in (12). The specific choice of the equivalent irreps does not matter, as they all obey the same SU(N) transformation rules.

The states of the SU(3) adjoint irrep $\tiny\young(13,2)$ in Table 1.1 are presented here once more in Table 2.1 (in the bosonic language) as follows:

$$
\young(AA,C) \;\equiv\; \tfrac{1}{\sqrt{2}}\big(|ACA\rangle - |CAA\rangle\big) \qquad\qquad \young(AA,B) \;\equiv\; \tfrac{1}{\sqrt{2}}\big(|ABA\rangle - |BAA\rangle\big)
$$

$$
\young(AB,B) \;\equiv\; \tfrac{1}{\sqrt{2}}\big(|ABB\rangle - |BAB\rangle\big) \qquad\qquad \young(BB,C) \;\equiv\; -\tfrac{1}{\sqrt{2}}\big(|BCB\rangle - |CBB\rangle\big)
$$

$$
\young(BC,C) \;\equiv\; -\tfrac{1}{\sqrt{2}}\big(|BCC\rangle - |CBC\rangle\big) \qquad\qquad \young(AC,C) \;\equiv\; -\tfrac{1}{\sqrt{2}}\big(|ACC\rangle - |CAC\rangle\big)
$$

$$
\young(AB,C) \;\equiv\; -\tfrac{1}{2}\big(|ACB\rangle + |BCA\rangle \qquad\qquad \young(AC,B) \;\equiv\; \tfrac{1}{\sqrt{12}}\big(2|ABC\rangle - 2|BAC\rangle + |CBA\rangle
$$

$$
-\,|CBA\rangle - |CAB\rangle\big) \qquad\qquad\qquad\qquad -\,|CAB\rangle + |ACB\rangle - |BCA\rangle\big)
$$

Table 2.1 – The states of the SU(3) adjoint irrep.

Now, let us recall the expression of the generators $S_\nu^\mu(i) = \sum\limits_{a=1}^{3} b_{\nu,a}^\dagger(i) b_{\mu,a}(i) - \tfrac{1}{3}\delta_\nu^\mu \hat{n}$ in Eq. (1.26), and see what happens when we apply $\hat{S}_A^B$ to the state $\young(AB,B)$:

$$
\hat{S}_A^B \,\young(AB,B) = \sum_{a=1}^{3} b_{A,a}^\dagger b_{B,a} \left[\frac{1}{\sqrt{2}}\big(|ABB\rangle - |BAB\rangle\big) \right] = \frac{1}{\sqrt{2}}\big(|ABA\rangle - |BAA\rangle\big)
$$
$$
= \young(AA,B).
$$
$$(2.61)$$

This is similar to what we have seen in subsection 2.1.1 with the antisymmetric SU(4) states, and this is somehow natural and expected when looking at the weight diagram in Figure 2.11. However, there is a situation that we have not encountered yet: what happens when there are potentially two states that can be obtained by applying a ladder operator, as is the case with the two zero-weight states in the middle of the weight diagram in Figure 2.11 ? Let us first observe what happens when we apply $\hat{S}_B^A$ onto $\young(AA,C)$:

$$
\hat{S}_B^A \,\young(AA,C) = \sum_{a=1}^{3} b_{B,a}^\dagger b_{A,a} \left[\frac{1}{\sqrt{2}}\big(|ACA\rangle - |CAA\rangle\big) \right]
$$
$$
= \frac{1}{\sqrt{2}}\big(|BCA\rangle + |ACB\rangle - |CBA\rangle - |CAB\rangle\big)
$$
$$
= -\sqrt{2}\,\young(AB,C).
$$
$$(2.62)$$

In this case, the colour permutation yields only one of the two states in the zero-weight, i.e.,
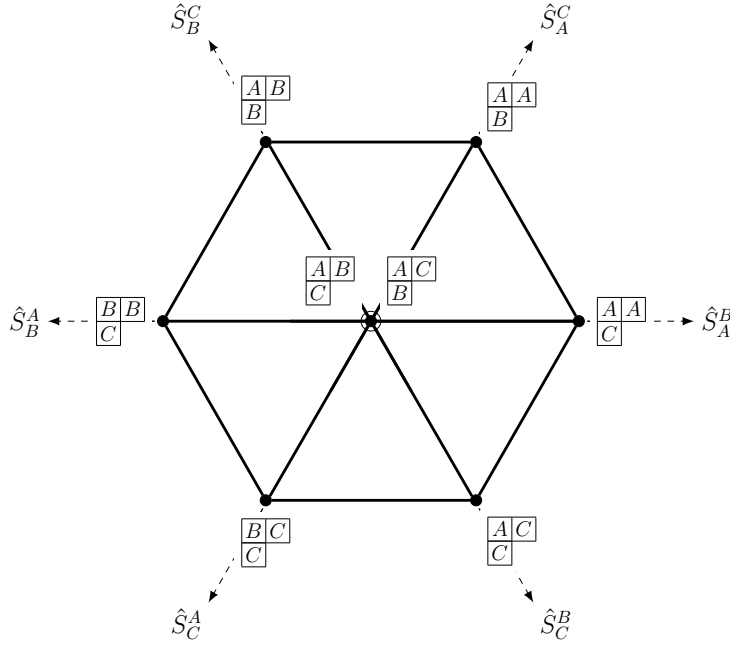
Figure 2.11 – Weight diagram of the irrep **8** of SU(3) and the direction in which the three pairs of ladder operators ($\hat{S}^\mu_\nu$ with $\mu \neq \nu$) operate.

the matrix element of the other state is zero:

$$\left\langle \begin{smallmatrix} A & C \\ B \end{smallmatrix} \big| \hat{S}^A_B \big| \begin{smallmatrix} A & A \\ C \end{smallmatrix} \right\rangle = 0. \tag{2.63}$$

Furthermore, it is interesting to observe that we have the factor $-\sqrt{2}$ popping out (which we did not have in the antisymmetric case), thus yielding a state whose norm is equal to $\sqrt{2}$. In the opposite direction, the results are similar:

$$\hat{S}^A_B \begin{smallmatrix} A & B \\ C \end{smallmatrix} = -\sqrt{2} \begin{smallmatrix} B & B \\ C \end{smallmatrix}, \qquad \hat{S}^A_B \begin{smallmatrix} A & C \\ B \end{smallmatrix} = 0. \tag{2.64}$$

The opposite transition in the other direction from the opposite state in the weight diagram is also similar:

$$\hat{S}^B_A \begin{smallmatrix} B & B \\ C \end{smallmatrix} = \sqrt{2} \begin{smallmatrix} A & B \\ C \end{smallmatrix},$$
$$\hat{S}^B_A \begin{smallmatrix} A & B \\ C \end{smallmatrix} = \sqrt{2} \begin{smallmatrix} A & A \\ C \end{smallmatrix}, \qquad \hat{S}^B_A \begin{smallmatrix} A & C \\ B \end{smallmatrix} = 0. \tag{2.65}$$

So far, we have looked at one of the three pairs of ladder operators, so let us now look at the two other directions:

$$\hat{S}^C_A \begin{smallmatrix} B & C \\ C \end{smallmatrix} = \frac{1}{\sqrt{2}} \begin{smallmatrix} A & B \\ C \end{smallmatrix} + \sqrt{\frac{3}{2}} \begin{smallmatrix} A & C \\ B \end{smallmatrix}, \qquad \hat{S}^A_C \begin{smallmatrix} A & A \\ B \end{smallmatrix} = \frac{1}{\sqrt{2}} \begin{smallmatrix} A & B \\ C \end{smallmatrix} + \sqrt{\frac{3}{2}} \begin{smallmatrix} A & C \\ B \end{smallmatrix},$$
$$\hat{S}^C_B \begin{smallmatrix} A & C \\ C \end{smallmatrix} = \frac{1}{\sqrt{2}} \begin{smallmatrix} A & B \\ C \end{smallmatrix} - \sqrt{\frac{3}{2}} \begin{smallmatrix} A & C \\ B \end{smallmatrix}, \qquad \hat{S}^B_C \begin{smallmatrix} A & B \\ B \end{smallmatrix} = -\frac{1}{\sqrt{2}} \begin{smallmatrix} A & B \\ C \end{smallmatrix} + \sqrt{\frac{3}{2}} \begin{smallmatrix} A & C \\ B \end{smallmatrix}. \tag{2.66}$$

So we see that there is a difference with respect to $\hat{S}^A_B, \hat{S}^B_A$: here, we obtain a superposition of both zero-weight states. But the norm of the resulting superposition state is also equal to $\sqrt{2}$. Note that the pair of ladder operators that generate only one of the two zero-weight states (as in Eq. (2.64)) can change if we use different basis states for the irrep than the ones used in Table 2.1. However, the two other pairs of ladder operators will always generate a linear superposition of both states with the same coefficients as in Eq. (2.66). This is simply the consequence of the symmetry of SU(3).

The rest of the relations involving the rest of the generators and states are more trivial and can be derived similarly, together with the fact that $\hat{S}^\nu_\mu = \left(\hat{S}^\mu_\nu\right)^\dagger$. Now that we know how the generators act on the states, let us assign a boson to each state of our irrep as done in chapter I. We will then express the SU(3) Hamiltonian in terms of these bosons. For convenience, we first label the eight states of the irrep by colors of their normal product state or by numbers:

$$
\begin{array}{llll}
\boxed{\begin{smallmatrix}A & A\\C\end{smallmatrix}} & \longrightarrow & \text{state } ACA & \text{or } 1 \\[2mm]
\boxed{\begin{smallmatrix}A & B\\B\end{smallmatrix}} & \longrightarrow & \text{state } ABB & \text{or } 3 \\[2mm]
\boxed{\begin{smallmatrix}B & C\\C\end{smallmatrix}} & \longrightarrow & \text{state } BCC & \text{or } 5 \\[2mm]
\boxed{\begin{smallmatrix}A & B\\C\end{smallmatrix}} & \longrightarrow & \text{state } ACB & \text{or } 7
\end{array}
\qquad
\begin{array}{llll}
\boxed{\begin{smallmatrix}A & A\\B\end{smallmatrix}} & \longrightarrow & \text{state } ABA & \text{or } 2 \\[2mm]
\boxed{\begin{smallmatrix}B & B\\C\end{smallmatrix}} & \longrightarrow & \text{state } BCB & \text{or } 4 \\[2mm]
\boxed{\begin{smallmatrix}A & C\\C\end{smallmatrix}} & \longrightarrow & \text{state } ACC & \text{or } 6 \\[2mm]
\boxed{\begin{smallmatrix}A & C\\B\end{smallmatrix}} & \longrightarrow & \text{state } ABC & \text{or } 8
\end{array}
\tag{2.67}
$$

The labels are antisymmetric in the first two letters. We associate a boson to each of these (composite) states, which yields eight pairs of bosons $d^\dagger_\alpha, d_\alpha$ with $\alpha \in \{1,\dots,8\}$.

We can start defining the SU(3) operators $\hat{S}^\mu_\nu$ in terms of these bosons d with the help of Eqs. (2.61) to (2.66). For instance, we can infer from Eq. (2.61), $\hat{S}^B_A \boxed{\begin{smallmatrix}A & B\\B\end{smallmatrix}} = \boxed{\begin{smallmatrix}A & A\\B\end{smallmatrix}}$, that $\hat{S}^B_A$ has to

contain the term $d^\dagger_{ABA} d_{ABB}$. All things considered, we obtain

$$
\begin{cases}
\hat{S}^B_A := d^\dagger_{ABA} d_{ABB} + d^\dagger_{ACC} d_{BCC} - \sqrt{2} d^\dagger_{ACA} d_{ACB} + \sqrt{2} d^\dagger_{ACB} d_{BCB} \\
\hat{S}^A_B := \left(\hat{S}^B_A \right)^\dagger \\
\hat{S}^C_A := -d^\dagger_{ACA} d_{ACC} + d^\dagger_{ABB} d_{BCB} + d^\dagger_{ABA} \left(\sqrt{\tfrac{1}{2}} d_{ACB} + \sqrt{\tfrac{3}{2}} d_{ABC} \right) + \left(\sqrt{\tfrac{1}{2}} d^\dagger_{ACB} + \sqrt{\tfrac{3}{2}} d^\dagger_{ABC} \right) d_{BCC} \\
\hat{S}^A_C := \left(\hat{S}^C_A \right)^\dagger \\
\hat{S}^C_B := d^\dagger_{ABA} d_{ACA} + d^\dagger_{BCB} d_{BCC} + d^\dagger_{ABB} \left(-\sqrt{\tfrac{1}{2}} d_{ACB} + \sqrt{\tfrac{3}{2}} d_{ABC} \right) + \left(\sqrt{\tfrac{1}{2}} d^\dagger_{ACB} - \sqrt{\tfrac{3}{2}} d^\dagger_{ABC} \right) d_{ACC} \\
\hat{S}^B_C := \left(\hat{S}^C_B \right)^\dagger \\
\hat{S}^A_A := 2 d^\dagger_{ABA} d_{ABA} + 2 d^\dagger_{ACA} d_{ACA} + d^\dagger_{ABB} d_{ABB} + d^\dagger_{ACC} d_{ACC} + d^\dagger_{ACB} d_{ACB} + d^\dagger_{ABC} d_{ABC} - \hat{n} \\
\quad = d^\dagger_{ABA} d_{ABA} + d^\dagger_{ACA} d_{ACA} - d^\dagger_{BCC} d_{BCC} - d^\dagger_{BCB} d_{BCB} \\
\hat{S}^B_B := 2 d^\dagger_{ABB} d_{ABB} + 2 d^\dagger_{BCB} d_{BCB} + d^\dagger_{ABA} d_{ABA} + d^\dagger_{BCC} d_{BCC} + d^\dagger_{ACB} d_{ACB} + d^\dagger_{ABC} d_{ABC} - \hat{n} \\
\quad = d^\dagger_{ABB} d_{ABB} + d^\dagger_{BCB} d_{BCB} - d^\dagger_{ACA} d_{ACA} - d^\dagger_{ACC} d_{ACC} \\
\hat{S}^C_C := 2 d^\dagger_{ACC} d_{ACC} + 2 d^\dagger_{BCC} d_{BCC} + d^\dagger_{ACA} d_{ACA} + d^\dagger_{BCB} d_{BCB} + d^\dagger_{ACB} d_{ACB} + d^\dagger_{ABC} d_{ABC} - \hat{n} \\
\quad = d^\dagger_{ACC} d_{ACC} + d^\dagger_{BCC} d_{BCC} - d^\dagger_{ABA} d_{ABA} - d^\dagger_{ABB} d_{ABB}
\end{cases}
$$

$$(2.68)$$

where

$$
\begin{aligned}
\hat{n} = & d^\dagger_{ABA} d_{ABA} + d^\dagger_{ABB} d_{ABB} + d^\dagger_{BCB} d_{BCB} + d^\dagger_{BCC} d_{BCC} \\
& + d^\dagger_{ACC} d_{ACC} + d^\dagger_{ACA} d_{ACA} + d^\dagger_{ACB} d_{ACB} + d^\dagger_{ABC} d_{ABC},
\end{aligned}
$$

$$(2.69)$$

i.e., the sum of the number operators of each state. This is to satisfy the tracelessness condition $\sum_\mu S^\mu_\mu = 0$. Without the number operator $\hat{n}$, we see that the diagonal generators $\hat{S}^\mu_\mu$ simply count the number of the colour μ of each state in the irrep.

The definitions in Eqs. (2.68) obey all the SU(3) commutation relations (1.23). The Hamiltonian (2.60) can now be written in terms of the bosons d using Eqs. (2.68) straightaway.

Before continuing, there are two important remarks to be made here. The first is that this construction, although tedious, gives a general method of writing $\hat{S}^\mu_\nu$ in terms of bosons representing each state of an irrep, whatever the irrep that is considered. The second remark is that since we are working with the adjoint irrep, there is another way of figuring out the expressions of $\hat{S}^\mu_\nu$ in terms of the bosons d.

2.2.2 Derive the action of $\hat{S}^\mu_\nu$ for the adjoint irrep

The $N^2 - 1$ states of the adjoint irrep correspond to the $N^2 - 1$ generators T_a ($a \in \{1, \dots, N^2 - 1\}$) because the weights of the SU(N) adjoint irrep correspond to the roots of SU(N), and a state that corresponds to a generator T_a is given by the generator itself, $|T_a\rangle$. For more details, references on Lie algebras or group theory such as Refs. [58, 59, 60] can be consulted. The only
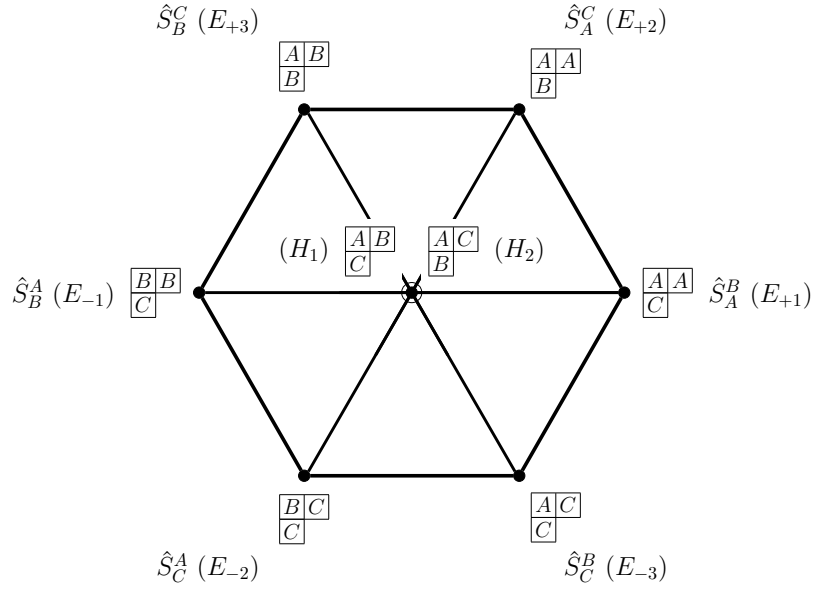
Figure 2.12 – Roots of the irrep **8** of SU(3). The name of the states and the corresponding generators $\hat{S}_\nu^\mu$ are indicated. The generators in the Cartan-Weyl basis are also given in parenthesis. Note that $\hat{S}_A^A = H_1 + \frac{1}{2}H_2$, $\hat{S}_B^B = -H_1 + \frac{1}{2}H_2$ and $\hat{S}_C^C = -H_2$, see subsection 1.1.2.

properties that matter in this case are as follows:

$$\alpha|T_a\rangle + \beta|T_b\rangle = |\alpha T_a + \beta T_b\rangle, \qquad T_a|T_b\rangle = |[T_a, T_b]\rangle, \tag{2.70}$$

with $\alpha, \beta \in \mathbb{C}$ and $a, b \in \{1,\dots,8\}$. So a generator can be associated to a state. This means that the expressions of $\hat{S}_\nu^\mu$ that we want can be read off directly from the commutation relations of SU(3). Here is how.

Let us first associate each of the eight generators in the Cartan-Weyl basis to each of the eight state of our irrep. Since the expression we want for the generators are in terms of the spherical generators $\hat{S}_\nu^\mu$, we need to translate the Cartan-Weyl basis elements to the states $|S_\nu^\mu\rangle$ (which are our reference states and which are normalized per definition) using Eqs. (1.21) and (1.22). We thus get the following correspondence between the states and the generators:

$$
\begin{aligned}
E_{+1} &\sim \boxed{\tfrac{A\,A}{C}} = \big|S_A^B\big\rangle, \quad (\equiv|E_{+1}\rangle) & E_{-1} &\sim \boxed{\tfrac{B\,B}{C}} = \big|S_B^A\big\rangle, \\
E_{+2} &\sim \boxed{\tfrac{A\,A}{B}} = \big|S_B^C\big\rangle, & E_{-2} &\sim \boxed{\tfrac{B\,C}{C}} = \big|S_C^A\big\rangle, \\
E_{+3} &\sim \boxed{\tfrac{A\,B}{B}} = \big|S_B^A\big\rangle, & E_{-3} &\sim \boxed{\tfrac{A\,C}{C}} = \big|S_C^B\big\rangle, \\
H_1 &\sim \boxed{\tfrac{A\,B}{C}} = \sqrt{2}\cdot\tfrac{1}{2}\big(\big|S_A^A\big\rangle - \big|S_B^B\big\rangle\big) & H_2 &\sim \boxed{\tfrac{A\,C}{B}} = \sqrt{\tfrac{3}{2}}\cdot\tfrac{1}{3}\big(\big|S_A^A\big\rangle + \big|S_B^B\big\rangle - 2\big|S_C^C\big\rangle\big) \\
&\qquad\big(\equiv \sqrt{2}|H_1\rangle\big) & &\qquad\Big(\equiv \sqrt{\tfrac{3}{2}}|H_2\rangle\Big)
\end{aligned}
\tag{2.71}
$$

Note that there is a normalization factor in front of $|H_1\rangle$ and $|H_2\rangle$ in contrast to the other states

of the Cartan-Weyl basis $|E_{\pm N}\rangle$, because they are not normalised (remember that the basis states $\left|S_\nu^\mu\right\rangle$ are the ones that are normalised). From this, all we have to do is derive $\hat{S}_\nu^\mu$ in terms of the bosons d with the help of the defining commutation relations of SU(3) and Eq. (2.71). For instance,

$$\hat{S}_A^C \,\boxed{\begin{smallmatrix}B&C\\C&\end{smallmatrix}} = S_A^C \left|S_C^A\right\rangle = \left[S_A^C, S_C^A\right] = [E_{+2}, E_{-2}]$$
$$= H_1 + \frac{3}{2}H_2 = \frac{1}{\sqrt{2}}\left(\sqrt{2}|H_1\rangle\right) + \sqrt{\frac{3}{2}}\left(\sqrt{\frac{3}{2}}|H_2\rangle\right) \tag{2.72a}$$
$$= \frac{1}{\sqrt{2}}\,\boxed{\begin{smallmatrix}A&B\\C&\end{smallmatrix}} + \sqrt{\frac{3}{2}}\,\boxed{\begin{smallmatrix}A&C\\B&\end{smallmatrix}},$$

$$\hat{S}_A^C \,\boxed{\begin{smallmatrix}A&B\\C&\end{smallmatrix}} = S_A^C \left|\sqrt{2}\cdot\frac{1}{2}\left(S_A^A + S_B^B\right)\right\rangle = \left[E_{+2}, \sqrt{2}H_1\right] = -\frac{\sqrt{2}}{2}E_{+2}$$
$$= -\frac{1}{\sqrt{2}}\,\boxed{\begin{smallmatrix}B&C\\C&\end{smallmatrix}}, \tag{2.72b}$$

$$\hat{S}_A^A \,\boxed{\begin{smallmatrix}B&C\\C&\end{smallmatrix}} = \left(H_1 + \frac{1}{2}H_2\right)\left|S_C^A\right\rangle = [H_1, E_{-2}] + \frac{1}{2}[H_2, E_{-2}] = -E_{-2}$$
$$= -\,\boxed{\begin{smallmatrix}B&C\\C&\end{smallmatrix}}. \tag{2.72c}$$

These expressions correspond to what we have derived in Eqs. (2.66) and (2.68).

2.2.3 The Holstein-Primakoff prescription with the SU(3) adjoint irrep

We now assume that we have a large condensate of state 1 ($\boxed{\begin{smallmatrix}A&A\\C&\end{smallmatrix}}$) on the first sublattice Λ_{ACA} and a large condensate of state 4 ($\boxed{\begin{smallmatrix}B&B\\C&\end{smallmatrix}}$) on the second sublattice Λ_{BCB}. We now introduce the expansion parameter n_c that will allow us to perform the semiclassical limit $n_c \to \infty$.[9] Physically, it corresponds to the number of composite particles per site, and since we have one composite particle per site, it will be set back to 1 at the end of the calculations. Since we have n_c particles per site, we can write

$$\sum_{\eta=1}^{8} d_\eta^\dagger(i)d_\eta(i) = n_c, \qquad \sum_{\eta=1}^{8} d_\eta^\dagger(j)d_\eta(j) = n_c, \tag{2.73}$$

for $\forall i \in \Lambda_{ACA}$ and $\forall j \in \Lambda_{BCB}$. We now replace the bosons d_α introduce the Holstein-Primakoff bosons $a(i)$ and $b(j)$ for the sublattices Λ_{ACA} and Λ_{BCB} respectively. The assumption of a large condensate of state 1 on Λ_{ACA} and state 4 on Λ_{BCB} means that the equations above can

---

[9]In terms of the Young tableaux, having the number $n_c = 2$ would correspond to $\boxed{\ \ }$, and having the number $n_c = 3$ would correspond to $\boxed{\ \ \ }$ etc. As a consequence, an example of the condensates in the limit $n_c \to \infty$ would be $\overbrace{\boxed{\begin{smallmatrix}A\\C\end{smallmatrix}}\cdots\boxed{\begin{smallmatrix}A\\C\end{smallmatrix}}}^{n_c}\overbrace{\boxed{\begin{smallmatrix}A\\\end{smallmatrix}}\cdots\boxed{\begin{smallmatrix}A\\\end{smallmatrix}}}^{n_c}$ and $\overbrace{\boxed{\begin{smallmatrix}B\\C\end{smallmatrix}}\cdots\boxed{\begin{smallmatrix}B\\C\end{smallmatrix}}}^{n_c}\overbrace{\boxed{\begin{smallmatrix}B\\\end{smallmatrix}}\cdots\boxed{\begin{smallmatrix}B\\\end{smallmatrix}}}^{n_c}$.

be written as

$$a_1^\dagger(i)a_1(i) = n_c - \sum_{\eta \neq 1} a_\eta^\dagger(i)a_\eta(i), \qquad b_4^\dagger(j)b_4(j) = n_c - \sum_{\eta \neq 4} b_\eta^\dagger(j)b_\eta(j), \tag{2.74}$$

and in the limit where $n_c \to \infty$, we can use the Holstein-Primakoff prescription:

$$a_1^\dagger(i), a_1(i) \longrightarrow \sqrt{n_c - \sum_{\eta \neq 1} a_\eta^\dagger(i)a_\eta(i)} \simeq \sqrt{n_c} - \frac{1}{2\sqrt{n_c}} \sum_{\eta \neq 1} a_\eta^\dagger(i)a_\eta(i),$$

$$b_4^\dagger(j), b_4(j) \longrightarrow \sqrt{n_c - \sum_{\eta \neq 4} b_\eta^\dagger(j)b_\eta(j)} \simeq \sqrt{n_c} - \frac{1}{2\sqrt{n_c}} \sum_{\eta \neq 4} b_\eta^\dagger(j)b_\eta(j). \tag{2.75}$$

The truncation of the Taylor series at this order is sufficient to obtain all the terms of the quadratic Hamiltonian of the order n_c. It is also worthwhile noting that the commutation relations (1.23) stay valid up to order $\mathcal{O}(1)$ even after this transformation. Gathering all the terms of the order n_c, we obtain the quadratic Hamiltonian $\mathcal{H}^{(2)} = \sum_{\alpha=0}^{3} \mathcal{H}_\alpha^{(2)}$:

$$\mathcal{H}^{(2)} = \mathcal{H}_0^{(2)} + \mathcal{H}_1^{(2)} + \mathcal{H}_2^{(2)} + \mathcal{H}_3^{(2)} \qquad \text{where}$$

$$\begin{aligned}
\mathcal{H}_0^{(2)} = Jn_c \sum_{i \in \Lambda_{ACA}} \sum_{<j>} \Big[&2a_8^\dagger(i)a_8(i) + 2b_8^\dagger(j)b_8(j) + 3a_3^\dagger(i)a_3(i) + 3a_5^\dagger(i)a_5(i) \\
&+ 3b_2^\dagger(j)b_2(j) + 3b_6^\dagger(j)b_6(j) + 4a_4^\dagger(i)a_4(i) + 4b_1^\dagger(j)b_1(j) \Big] \\
\mathcal{H}_1^{(2)} = Jn_c \sum_{i \in \Lambda_{ACA}} \sum_{<j>} &\Big[a_2^\dagger(i)a_2(i) + b_5^\dagger(j)b_5(j) + a_2^\dagger(i)b_5^\dagger(j) + a_2(i)b_5(j) \Big] \\
\mathcal{H}_2^{(2)} = Jn_c \sum_{i \in \Lambda_{ACA}} \sum_{<j>} &\Big[a_6^\dagger(i)a_6(i) + b_3^\dagger(j)b_3(j) - a_6^\dagger(i)b_3^\dagger(j) - a_6(i)b_3(j) \Big] \\
\mathcal{H}_3^{(2)} = Jn_c \sum_{i \in \Lambda_{ACA}} \sum_{<j>} &\Big[2a_7^\dagger(i)a_7(i) + 2b_7^\dagger(j)b_7(j) - 2a_7^\dagger(i)b_7^\dagger(j) - 2a_7(i)b_7(j) \Big].
\end{aligned} \tag{2.76}$$

After Fourier-transforming,

$$a_\eta(i) = \sqrt{\frac{2}{N_{\text{sites}}}} \sum_{k \in \text{RBZ}} a_\eta(k)e^{-ikr_i}, \qquad b_\eta(j) = \sqrt{\frac{2}{N_{\text{sites}}}} \sum_{k \in \text{RBZ}} b_\eta(k)e^{-ikr_j}, \tag{2.77}$$

with the state index $\eta \in \{1, \ldots, 8\}$ and the number of sites N_{sites}, the harmonic Hamiltonian in

Fourier space is then given by

$$
\mathcal{H}_0^{(2)} = J n_c \sum_{k \in \text{RBZ}} \Big[4 a_8^\dagger(k) a_8(k) + 4 b_8^\dagger(k) b_8(k) + 6 a_3^\dagger(k) a_3(k) + 6 a_5^\dagger(k) a_5(k)
$$
$$
+ 6 b_2^\dagger(k) b_2(k) + 6 b_6^\dagger(k) b_6(k) + 8 a_4^\dagger(k) a_4(k) + 8 b_1^\dagger(k) b_1(k) \Big]
$$
$$
\mathcal{H}_1^{(2)} = J n_c \sum_{k \in \text{RBZ}} \left(\mathbf{u}_{1,k}^\dagger, \mathbf{u}_{1,-k} \right) M_k \begin{pmatrix} {}^{\text{t}}\mathbf{u}_{1,k} \\ {}^{\text{t}}\mathbf{u}_{1,-k}^\dagger \end{pmatrix},
$$
$$
\mathcal{H}_2^{(2)} = J n_c \sum_{k \in \text{RBZ}} \left(\mathbf{u}_{2,k}^\dagger, \mathbf{u}_{2,-k} \right) M_k \begin{pmatrix} {}^{\text{t}}\mathbf{u}_{2k} \\ {}^{\text{t}}\mathbf{u}_{2,-k}^\dagger \end{pmatrix}, \tag{2.78}
$$
$$
\mathcal{H}_3^{(2)} = J n_c \sum_{k \in \text{RBZ}} \left(\mathbf{u}_{3,k}^\dagger, \mathbf{u}_{3-k} \right) 2 M_k \begin{pmatrix} {}^{\text{t}}\mathbf{u}_{3,k} \\ {}^{\text{t}}\mathbf{u}_{3,-k}^\dagger \end{pmatrix},
$$

where

$$
\mathbf{u}_{1,k}^\dagger := \left(a_2^\dagger(k), b_5^\dagger(k) \right), \qquad \mathbf{u}_{1,-k} := \left(a_2(-k), b_5(-k) \right),
$$
$$
\mathbf{u}_{2,k}^\dagger := \left(a_6^\dagger(k), b_3^\dagger(k) \right), \qquad \mathbf{u}_{2,-k} := \left(a_6(-k), b_3(-k) \right), \tag{2.79a}
$$
$$
\mathbf{u}_{3,k}^\dagger := \left(a_7^\dagger(k), b_7^\dagger(k) \right), \qquad \mathbf{u}_{3,-k} := \left(a_7(-k), b_7(-k) \right),
$$

$$
M_k := \begin{pmatrix} \mathscr{A} & \mathscr{B}_k \\ \mathscr{B}_k & \mathscr{A} \end{pmatrix}, \qquad \mathscr{A} := \begin{pmatrix} 1 & 0 \\ 0 & 1 \end{pmatrix}, \qquad \mathscr{B}_k := \begin{pmatrix} 0 & \gamma_k \\ \gamma_k & 0 \end{pmatrix}, \tag{2.79b}
$$

with the geometrical factor

$$
\gamma_k := \cos k. \tag{2.80}
$$

As the structure of the sub-Hamiltonians in subsection 2.1.1 are the same, we can use the Bogoliubov transformation (2.17). By introducing the new Bogoliubov bosons f_ζ with $\zeta \in \{1, \dots, 6\}$, the diagonalized quadratic Hamiltonian is finally given by to simplify

$$
\boxed{
\begin{aligned}
\mathcal{H}_0^{(2)} = J n_c \sum_{k \in \text{RBZ}} \Big[& \sum_{\zeta=1}^{6} \omega_\zeta(k) \left(f_\zeta^\dagger(k) f_\zeta(k) + \frac{1}{2} \right) \\
& + 4 a_8^\dagger(k) a_8(k) + 4 b_8^\dagger(k) b_8(k) + 6 a_3^\dagger(k) a_3(k) + 6 a_5^\dagger(k) a_5(k) \\
& + 6 b_2^\dagger(k) b_2(k) + 6 b_6^\dagger(k) b_6(k) + 8 a_4^\dagger(k) a_4(k) + 8 b_1^\dagger(k) b_1(k) \Big] + \text{const.}
\end{aligned}
}
\tag{2.81}
$$

up to a constant, where

$$
\begin{aligned}
\omega_{1,2,3,4}(k) &= 2 \sqrt{1 - \cos^2(k)}, \\
\omega_{5,6}(k) &= 4 \sqrt{1 - \cos^2(k)}.
\end{aligned}
\tag{2.82}
$$

These dispersion relations are plotted in Figure 2.13.
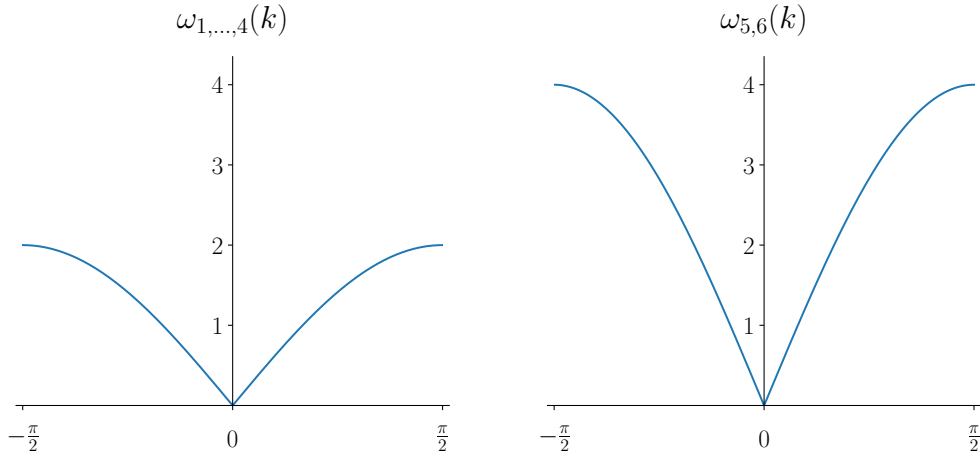
Figure 2.13 – The dispersion relations $\omega_{1,...,6}$ of the bipartite chain.

Let us now look at the modes more closely. There are in total six dispersive modes, $f_1, \ldots, f_6$, four of which have the same dispersion relation $\omega_{1,2,3,4}(k) = 2\sqrt{1 - \cos^2(k)}$. These modes come from the sub-Hamiltonians $\mathcal{H}_1^{(2)}$ and $\mathcal{H}_2^{(2)}$ involving the state 2 ($\boxed{\begin{smallmatrix}A & A\\B\end{smallmatrix}}$), state 3 ($\boxed{\begin{smallmatrix}A & B\\B\end{smallmatrix}}$), state 4 ($\boxed{\begin{smallmatrix}B & B\\C\end{smallmatrix}}$), and state 5 ($\boxed{\begin{smallmatrix}B & C\\C\end{smallmatrix}}$). These states are the ones that can be obtained by one colour permutation between neighbours of the initial condensates, and they lead to dispersive modes as in models with the antisymmetric irreps in 2.1. There is one more state that can be attained with one colour permutation from both sublattices, however, and that is the state 7 ($\boxed{\begin{smallmatrix}A & B\\C\end{smallmatrix}}$). The transition to this state yields the modes $\omega_{5,6}(k)$ stemming from the sub-Hamiltonian $\mathcal{H}_3^{(2)}$, and these modes have a factor 2 compared to the other modes $\omega_{1,2,3,4}(k)$. This is related to Eq. (2.62), where we have seen that such a transition yields a state whose norm is equal to $sqrt2$.

We had also seen in Eq. (2.63) that we cannnot reach the state 8 ($\boxed{\begin{smallmatrix}A & C\\B\end{smallmatrix}}$) by one colour permutation starting from the state 1 or 4 that we are condensing, although it looks possible in principle according to the weight diagram in Figure 2.11. It acutally turns out that

$$\frac{1}{\sqrt{6}}\left(2S_B^C S_C^A - S_B^A\right) \boxed{\begin{smallmatrix}A & A\\C\end{smallmatrix}} = \boxed{\begin{smallmatrix}A & C\\B\end{smallmatrix}}, \tag{2.83}$$

so getting the state 8 requires two colour permutations. Hence, in our harmonic-order Hamiltonian in the n_c-expansion, the modes $a_8^\dagger a_8$ and $b_8^\dagger b_8$ related to the state 8 are flat. The value of this flat energy mode is 4, just like the maximum value of the modes $\omega_{5,6}$ of the state 7.

Equally, the other transitions requiring more than one coulour permutation yield flat modes. The values of these flat modes are larger when more colour permutations are needed. For example, from the perspective of the state 1 of the sublattice Λ_{ACA}, the state 4 is further away than the state 5. This translates into the terms $8a_4^\dagger a_4$ and $6a_5^\dagger a_5$ in the final harmonic Hamiltonian.

In conclusion, the states attainable with one colour permutation from the initial condensates yield the six dispersive modes (with two different velocities), all of whom are linear in k for small values of k.

2.2.4 Considering different states as condensates

If we decide to use a condensate of the state 2 ($\boxed{\frac{A\,A}{B}}$) on the first sublattice and a condensate of the state 5 ($\boxed{\frac{B\,C}{C}}$) on the second sublattice, the resulting quadratic Hamiltonian right after the expansion in n_c has a different structure than Eq. (2.76). However, after the diagonalisation, the resulting dispersion relations will be identical to Eq. (2.82). This is what we show in the following.

Using the same recipe as above, we use the Holstein-Primakoff bosons a and b on the sites of the sublattices Λ_{ABA} and Λ_{BCC}, respectively,

$$
\begin{aligned}
a_2^\dagger(i), a_2(i) &\longrightarrow \sqrt{n_c - \sum_{\eta\neq 2} a_\eta^\dagger(i) a_\eta(i)} \simeq \sqrt{n_c} - \frac{1}{2\sqrt{n_c}} \sum_{\eta\neq 1} a_\eta^\dagger(i) a_\eta(i), \\
b_5^\dagger(j), b_5(j) &\longrightarrow \sqrt{n_c - \sum_{\eta\neq 5} b_\eta^\dagger(j) b_\eta(j)} \simeq \sqrt{n_c} - \frac{1}{2\sqrt{n_c}} \sum_{\eta\neq 4} b_\eta^\dagger(j) b_\eta(j),
\end{aligned}
\tag{2.84}
$$

after which we obtain the quadratic Hamiltonian by gathering all the terms of the order n_c:

$$
\mathcal{H}^{(2)} = \mathcal{H}_0^{(2)} + \mathcal{H}_1^{(2)} + \mathcal{H}_2^{(2)} + \mathcal{H}_3^{(2)} \qquad \text{where}
$$

$$
\begin{aligned}
\mathcal{H}_0^{(2)} &= J n_c \sum_{i\in\Lambda_{ABA}} \sum_{<j>} \Big[3 a_4^\dagger(i) a_4(i) + 3 a_6^\dagger(i) a_6(i) + 4 a_5^\dagger(i) a_5(i) \\
&\qquad\qquad\qquad + 3 b_1^\dagger(j) b_1(j) + 3 b_3^\dagger(j) b_3(j) + 4 b_2^\dagger(j) b_2(j) \Big], \\
\mathcal{H}_1^{(2)} &= J n_c \sum_{i\in\Lambda_{ABA}} \sum_{<j>} \Big[a_1^\dagger(i) a_1(i) + b_4^\dagger(j) b_4(j) + a_1^\dagger(i) b_4^\dagger(j) + a_1(i) b_4(j) \Big], \\
\mathcal{H}_2^{(2)} &= J n_c \sum_{i\in\Lambda_{ABA}} \sum_{<j>} \Big[a_3^\dagger(i) a_3(i) + b_6^\dagger(j) b_6(j) - a_3^\dagger(i) b_6^\dagger(j) - a_3(i) b_6(j) \Big], \\
\mathcal{H}_3^{(2)} &= J n_c \sum_{i\in\Lambda_{ABA}} \sum_{<j>} \Big[2 a_7^\dagger(i) a_7(i) + 2 a_8^\dagger(i) a_8(i) + 2 b_7^\dagger(j) b_7(j) + 2 b_8^\dagger(j) b_8(j) \\
&\qquad + \frac{1}{2} a_7^\dagger(i) b_7^\dagger(j) + \frac{1}{2} a_7(i) b_7(j) + \frac{3}{2} a_8^\dagger(i) b_8^\dagger(j) + \frac{3}{2} a_8(i) b_8(j) \\
&\qquad + \frac{\sqrt{3}}{2} a_7^\dagger(i) b_8^\dagger(j) + \frac{\sqrt{3}}{2} a_7(i) b_8(j) + \frac{\sqrt{3}}{2} a_8^\dagger(i) b_7^\dagger(j) + \frac{\sqrt{3}}{2} a_8(i) b_7(j) \Big].
\end{aligned}
\tag{2.85}
$$

After the Fourier transform, we obtain

$$
\mathcal{H}_0^{(2)} = J n_c \sum_{k \in \text{RBZ}} \Big[6 a_4^\dagger(k) a_4(k) + 6 a_6^\dagger(k) a_6(k) + 8 a_5^\dagger(k) a_5(k)
$$
$$
+ 6 b_1^\dagger(k) b_1(k) + 6 b_3^\dagger(k) b_3(k) + 8 b_2^\dagger(k) b_2(k) \Big],
$$

$$
\mathcal{H}_1^{(2)} = J n_c \sum_{k \in \text{RBZ}} \left(\mathbf{u}_{1,k}^\dagger, \mathbf{u}_{1,-k} \right) M_{1,k} \begin{pmatrix} {}^t\mathbf{u}_{1,k} \\ {}^t\mathbf{u}_{1,-k}^\dagger \end{pmatrix},
$$

$$
\mathcal{H}_2^{(2)} = J n_c \sum_{k \in \text{RBZ}} \left(\mathbf{u}_{2,k}^\dagger, \mathbf{u}_{2-k} \right) M_{2,k} \begin{pmatrix} {}^t\mathbf{u}_{2,k} \\ {}^t\mathbf{u}_{2,-k}^\dagger \end{pmatrix},
$$

$$
\mathcal{H}_3^{(2)} = J n_c \sum_{k \in \text{RBZ}} \left(\mathbf{u}_{3,k}^\dagger, \mathbf{u}_{3,-k} \right) M_{3,k} \begin{pmatrix} {}^t\mathbf{u}_{3,k} \\ {}^t\mathbf{u}_{3,-k}^\dagger \end{pmatrix},
$$

(2.86)

where

$$
\mathbf{u}_{1,k}^\dagger := \left(a_1^\dagger(k), b_4^\dagger(k) \right), \qquad\qquad \mathbf{u}_{1,-k} := \left(a_1(-k), b_4(-k) \right),
$$
$$
\mathbf{u}_{2,k}^\dagger := \left(a_3^\dagger(k), b_6^\dagger(k) \right), \qquad\qquad \mathbf{u}_{2,-k} := \left(a_3(-k), b_6(-k) \right),
$$
$$
\mathbf{u}_{3,k}^\dagger := \left(a_7^\dagger(k), a_8^\dagger(k), b_7^\dagger(k), b_8^\dagger(k) \right), \qquad \mathbf{u}_{3,-k} := \left(a_7(-k), a_8(-k), b_7(-k), b_8(-k) \right),
$$

(2.87a)

$$
M_{1,k} := \begin{pmatrix} \mathscr{A}_1 & \mathscr{B}_{1,k} \\ \mathscr{B}_{1,k} & \mathscr{A}_1 \end{pmatrix}, \qquad \mathscr{A}_1 := \begin{pmatrix} 1 & 0 \\ 0 & 1 \end{pmatrix}, \qquad \mathscr{B}_{1,k} := \gamma_k \begin{pmatrix} 0 & 1 \\ 1 & 0 \end{pmatrix},
$$

$$
M_{2,k} := M_{1,k},
$$

$$
M_{3,k} = \begin{pmatrix} \mathscr{A}_3 & \mathscr{B}_{3,k} \\ \mathscr{B}_{3,k} & \mathscr{A}_3 \end{pmatrix}, \qquad \mathscr{A}_3 := \begin{pmatrix} 2 & 0 & 0 & 0 \\ 0 & 2 & 0 & 0 \\ 0 & 0 & 2 & 0 \\ 0 & 0 & 0 & 2 \end{pmatrix}, \qquad \mathscr{B}_{3,k} := \gamma_k \begin{pmatrix} 0 & 0 & \frac{1}{2} & \frac{\sqrt{3}}{2} \\ 0 & 0 & \frac{\sqrt{3}}{2} & \frac{3}{2} \\ \frac{1}{2} & \frac{\sqrt{3}}{2} & 0 & 0 \\ \frac{\sqrt{3}}{2} & \frac{3}{2} & 0 & 0 \end{pmatrix},
$$

(2.87b)

with the geometrical factor

$$
\gamma_k := \cos k.
$$

(2.88)

The generalised Bogoliubov transformation can be used to diagonalize the system, and the matrix that has to be diagonalized is then

$$
M_{a,k}^{'} := \begin{pmatrix} \mathscr{A}_a & \mathscr{B}_{a,k} \\ -\mathscr{B}_{a,k} & -\mathscr{A}_a \end{pmatrix}, \qquad a \in \{1, 2, 3\}
$$

(2.89)

Its positive eigenvalues yield the frequencies ω_μ of the diagonalized Hamiltonian. More details on the generalised Bogoliubov transformation can be found in Appendix A. All in all, we obtain

$$\mathcal{H}^{(2)} = Jn_c \sum_{k \in \mathrm{RBZ}} \left\{ \sum_{\zeta=1}^{8} \omega_\zeta(k) \left(f_\zeta^\dagger(k) f_\zeta(k) + \frac{1}{2} \right) \right.$$
$$+ 6a_4^\dagger(k) a_4(k) + 6a_6^\dagger(k) a_6(k) + 8a_5^\dagger(k) a_5(k)$$
$$\left. + 6b_1^\dagger(k) b_1(k) + 6b_3^\dagger(k) b_3(k) + 8b_2^\dagger(k) b_2(k) \right\} + \mathrm{const.,}$$

(2.90)

with

$$\omega_{1,2,3,4}(k) = 2\sqrt{1 - \cos^2(k)},$$
$$\omega_{5,6}(k) = 4\sqrt{1 - \cos^2(k)},$$
$$\omega_{7,8} = 4,$$

(2.91)

that are plotted in Figure 2.14.

We indeed see that this Hamiltonian has the same dispersion relations as the Hamiltonian (2.81). As in the previous case with a different condensate, the transition to the zero-weight states (see Eq. (2.66)) from the sub-Hamiltonian $\mathcal{H}_3^{(2)}$ yields the dispersive mode with the higher velocity, $\omega_{4,5}$. This is seen clearly if we re-express the Hamiltonian (2.76) a bit by redefining the bosons a bit. Let us define the bosons f and g as follows,

$$f(i) = \frac{1}{\sqrt{4}} a_7(i) + \sqrt{\frac{3}{4}} a_8(i), \qquad f(j) = \frac{1}{\sqrt{4}} a_7(j) + \sqrt{\frac{3}{4}} a_8(j),$$

$$g(i) = \sqrt{\frac{3}{4}} a_7(i) - \frac{1}{\sqrt{4}} a_8(i), \qquad g(j) = \sqrt{\frac{3}{4}} a_7(j) - \frac{1}{\sqrt{4}} a_8(j),$$

(2.92)

such that they satisfy the bosonic commutation relations $[f, f^\dagger] = 1, [g, g^\dagger] = 1, [f^{(\dagger)}, g^{(\dagger)}] = 0$. We then see that the harmonic Hamiltonian in (2.76) can be written as

$$\mathcal{H}_3^{(2)} = Jn_c \sum_{i \in \Lambda_{ABA}} \sum_{<j>} \left\{ 2g^\dagger(i) g(i) + 2g^\dagger(j) g(j) \right.$$
$$\left. + 2 \left[f^\dagger(i) f(i) + f^\dagger(j) f(j) + f^\dagger(i) f^\dagger(j) + f(i) f(j) \right] \right\}.$$

(2.93)

The terms involving the new bosons $f(i), f(j)$ have the same structure as $\mathcal{H}_1^{(2)}$ and $\mathcal{H}_2^{(2)}$ with a factor 2, and they evidently give the dispersive modes with twice the velocity of the other dispersive modes. From the definition of the boson f in Eq. (2.92), we see that it corresponds to the transition to the zero-weight states $\hat{S}_C^A \boxed{\begin{smallmatrix} A & A \\ B & \end{smallmatrix}}$ or $\hat{S}_A^C \boxed{\begin{smallmatrix} B & C \\ C & \end{smallmatrix}}$ described in Eq. (2.66). The new bosons $g(i), g(j)$ correspond to the states orthogonal to those represented by the bosons $f(i), f(j)$, and they generate flat modes.
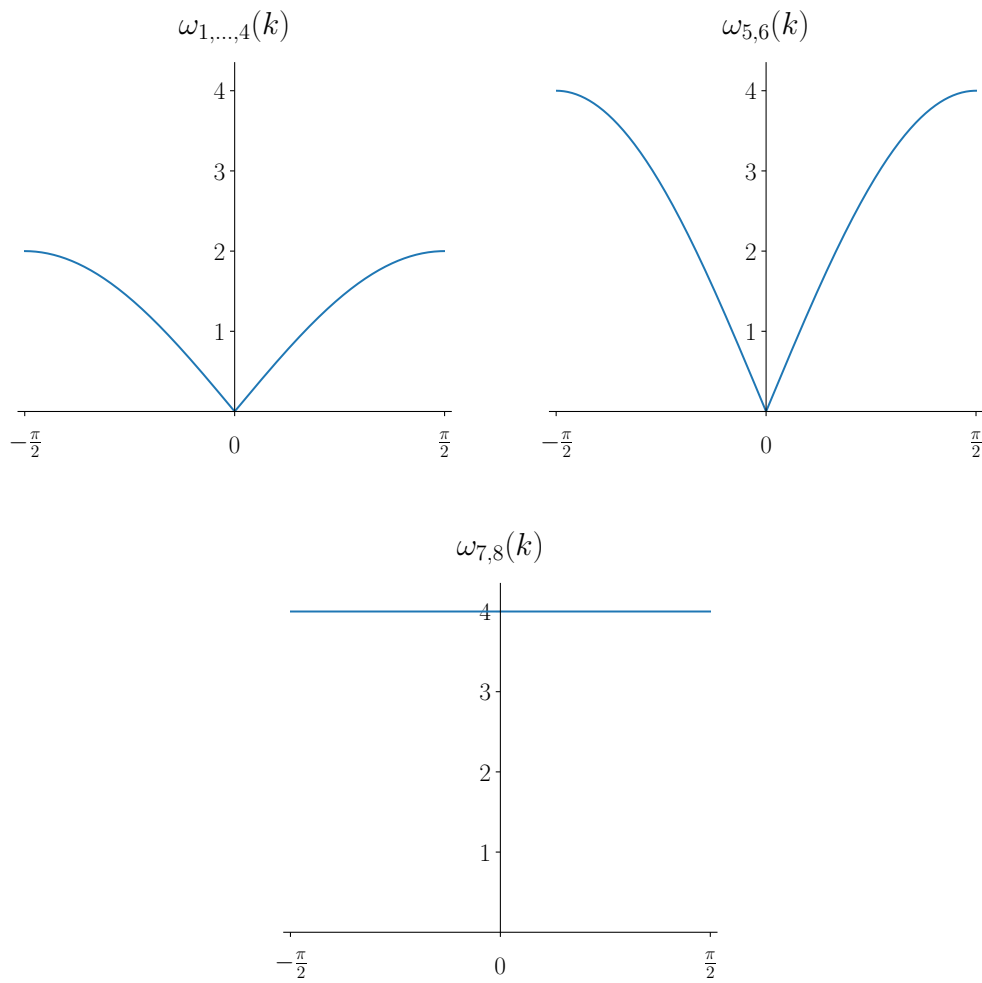
Figure 2.14 – The dispersion relations $\omega_{1,\dots,8}$.

III | Linear Flavour-Wave with Mathur and Sen Bosons

Introduction: low-energy spectra of the $SU(3)$ models

A general prescription for applying the LFWT for any $SU(N)$ irrep has been described (2.2.1). However, it can be a bit tedious to derive the representation of the operators, especially if we are only interested in the dispersive low-energy modes related to the Goldstone modes. Could there be a different possibility of performing the LFWT? A different bosonic representation for the generators $\hat{S}_\nu^\mu$ paves a different way, and this is what we will explore further in this chapter. We will use the bosons introduced by Mathur and Sen [77] for $SU(3)$ and further used and developed by others [78, 79, 80]. We will subsequently name these bosons the "Mathur & Sen" bosons.

The model we will first look at is the bipartite $SU(3)$ chain in the self-conjugate irreps, in particular the adjoint irrep model introduced in section 2.2. It is a model for which we are interested in the low-energy spectrum for investigating interesting physical properties, and it will also allow us to develop a method for performing the LFW expansion using the Mathur & Sen bosons. It will be shown that the spectra yielded by this bosonic representation are the same as those derived previously in section 2.2. Once we know how to deal with the self-conjugate irreps, we will then try to study the low-energy behaviour of the bipartite $SU(3)$ chain in an arbitrary $SU(3)$ irrep. Although we treat the one-dimensional case only, we note that it is easily generalisable to any dimensions.

3.1 The $SU(3)$ chain in the self-conjugate irreducible representations

This chapter is the fruit of the collaboration with Kyle Warmer, Miklós Lajkó, Frédéric Mila and Ian Affleck [76]. The reason why we are particularly interested in the self-conjugate $SU(3)$ irreps is because of the Lieb-Schulz-Mattis-Affleck theorem. The theorem states that a one-dimensional chain with half-integer $SU(2)$ spin per unit cell is either gapless or has a ground state degeneracy, and there exists a generalised version of it for the $SU(N)$ symmetry. In the case of $SU(3)$ chains in the symmetric irrep $[p,0]$ that was studied in Ref. [12], it implies that

this model must either be gapless or have spontaneously broken translation symmetry for all values of p that are not a multiple of 3. The case of the self-conjugate irreps $[p,p]$, however, had not been studied. Consequently, Wamer et al. [76] started working on the self-conjugate SU(3) irrep chains with field-theoretical calculations to show that the Lieb-Schulz-Mattis-Affleck theorem fails in this case as the number of boxes is always a multiple of 3, and the system is always gapped for any $[p,p]$ with an additional feature that the $\mathscr{P}$-symmetry (parity) is broken for odd values of p only. Some AKLT-type ground states are presented in Ref. [76].

The long-range colour order is thus obviously not a ground state of the SU(3) $[p,p]$ 1D chain—the Mermin-Wagner-Coleman theorem [54, 55] would forbid it anyway. But it is a useful assumption to make, as it gives a starting point for field-theoretical calculations. As a consequence, the LFWT calculations were used in the first part of this project to provide an alternative way of obtaining the low-energy spectra of the system. With this, it was shown that the model posesses six Goldstone modes and that they have unequal velocities, all of them being in complete agreement with the results of the field theory.

3.1.1 Mathur & Sen's bosonic representation

Let us introduce another bosonic representation for the SU(3) irreps which is described in [77, 79]. We will closely follow the notation in these articles.

The group SU(3) has rank 2, which means that the states in SU(3) can be written by using two triplets of bosonic operators

$$\left[a_\mu, a_\nu^\dagger\right] = \delta_{\mu\nu}, \qquad \left[b_\mu, b_\nu^\dagger\right] = \delta_{\mu\nu}, \qquad \left[a_\mu, b_\nu\right] = \left[a_\mu, b_\nu^\dagger\right] = 0, \tag{3.1}$$

where $\mu, \nu \in \{A, B, C\}$ are the color degrees of freedom. The vacuum state can then be denoted by $|\vec{0}_a, \vec{0}_b\rangle \equiv |0\rangle$, and we can define the following number operators

$$\hat{N}_a := \sum_{\mu=A}^{C} \hat{N}_{a,\mu} = \sum_{\mu=A}^{C} a_\mu^\dagger a_\mu, \qquad \hat{N}_b := \sum_{\mu=A}^{C} \hat{N}_{b,\mu} = \sum_{\mu=A}^{C} b_\mu^\dagger b_\mu, \tag{3.2}$$

whose eigenvalues will be denoted by $n_a = \sum_{\mu=A}^{C} n_{a,\mu}$ and $n_b = \sum_{\mu=A}^{C} n_{b,\mu}$.

With the help of these bosons and the Gell-Mann matrices λ_k ($k \in \{1, \dots, 8\}$), we can now define the following operators

$$Q_k = \sum_{\mu,\nu=A}^{C} a_\mu^\dagger T_k{}^{\mu\nu} a_\nu - b_\mu^\dagger T_k^{*\mu\nu} b_\nu, \tag{3.3}$$

where T_k are the generators of SU(3) given by $T_k := \frac{1}{2}\lambda_k$. As they are constructed from the Gell-Mann matrices, they automatically satisfy the tracelessness condition. Since λ_k and λ_k^* are being used, it is clear that the three states $a_\mu^\dagger|0\rangle = |\mu\rangle \equiv |_\mu\rangle$ represent the states of the

fundamental irrep ($\square$ or **3**) and that the three states $b_\nu^\dagger |0\rangle = |\bar\nu\rangle \equiv |^\nu\rangle$ represent the states of its conjugate irrep ($\boxminus$ or $\bar{\mathbf{3}}$), with $\mu, \nu \{A, B, C\}$. From this, it is possible to build states in any other irrep. For instance, the states in the irrep $\boxminus$ (or **8**) will satisfy $n_a = 1$ and $n_b = 1$. This construction is related to the tensor method that is well explained in Ref. [59]. It is based on the fact that a representation T_k of the generators of a Lie algebra that satisfies $[T_k, T_l] = i f_{kl}{}^m T_m$ admits a representation $\tilde{T}_k := -T_k^*$ such that

$$\left[\tilde{T}_k, \tilde{T}_l\right] = [T_k, T_l]^* = -i f_{kl}{}^m T_m^* = i f_{kl}{}^m \tilde{T}_m, \tag{3.4}$$

and that a state from the fundamental irrep of SU(3) can form a singlet with the state from its conjugate irrep. We can then write the states of any SU(3) irreps using the tensorial notations with covariant and contravariant indices and use the contraction of indices like in general relativity. In this construction, these indices are translated into the bosons a_μ and b_μ. One important aspect is that it has to satisfy the tracelessness condition related to the tracelessness of the SU(3) generators. If we write a generic SU(3) state using the Einstein summation convention,

$$v^{\mu_1\dots\mu_p}_{\nu_1\dots\nu_q} a_{\mu_1}^\dagger \cdots a_{\mu_p}^\dagger b_{\nu_1}^\dagger \cdots b_{\nu_q}^\dagger |0\rangle = v^{\mu_1\dots\mu_p}_{\nu_1\dots\nu_q} \left|^{\nu_1\dots\nu_q}_{\mu_1\dots\mu_p}\right\rangle, \tag{3.5}$$

then the coefficients v of a state belonging to the irrep $[p, q]$ have to satisfy

$$\delta^{\mu_a}_{\nu_a} v^{\mu_1\dots\mu_p}_{\nu_1\dots\nu_q} = 0, \tag{3.6}$$

where $a \in \{1, \dots, \min(p, q)\}$.

Let us see what this concretely means by taking the example of the adjoint irrep. The states of the adjoint irrep have to satisfy $n_a = n_b = 1$, so we could naively use one boson $a_\mu^\dagger$ and one boson $b_\nu^\dagger$ to create the states of the adjoint irrep. This yields nine states:

$$\left|A\bar{B}\right\rangle, \left|A\bar{C}\right\rangle, \left|B\bar{C}\right\rangle, \left|B\bar{A}\right\rangle, \left|C\bar{A}\right\rangle, \left|C\bar{B}\right\rangle, \left|A\bar{A}\right\rangle, \left|B\bar{B}\right\rangle, \left|C\bar{C}\right\rangle. \tag{3.7}$$

This actually corresponds to $\square \otimes \boxminus$ (or $\mathbf{3} \times \bar{\mathbf{3}}$) as we are using one bosons a and one boson b. However, we know that this tensor product contains not only the adjoint irrep, but also the trivial irrep:

$$\square \otimes \boxminus = \boxminus \oplus \cdot \tag{3.8}$$

The traceless condition (3.6) precisely corresponds to excluding the singlet of the trivial irrep $\left|A\bar{A}\right\rangle + \left|B\bar{B}\right\rangle + \left|C\bar{C}\right\rangle$ (up to a normalisation constant). Linear combinations of states in Eq. (3.7) (namely $\left|A\bar{A}\right\rangle, \left|B\bar{B}\right\rangle, \left|C\bar{C}\right\rangle$) yield either the singlet or the two zero-weight states of the adjoint irrep: the states $\frac{1}{\sqrt{2}}\left(\left|A\bar{A}\right\rangle - \left|B\bar{B}\right\rangle\right)$ and $\frac{1}{\sqrt{6}}\left(\left|A\bar{A}\right\rangle + \left|B\bar{B}\right\rangle - 2\left|C\bar{C}\right\rangle\right)$, see Figure 3.1. They indeed belong to the adjoint irrep as they are orthogonal to the singlet $\frac{1}{\sqrt{6}}\left(\left|A\bar{A}\right\rangle + \left|B\bar{B}\right\rangle + \left|C\bar{C}\right\rangle\right)$.

For our purposes, it is more convenient to express the generators in terms of the raising and
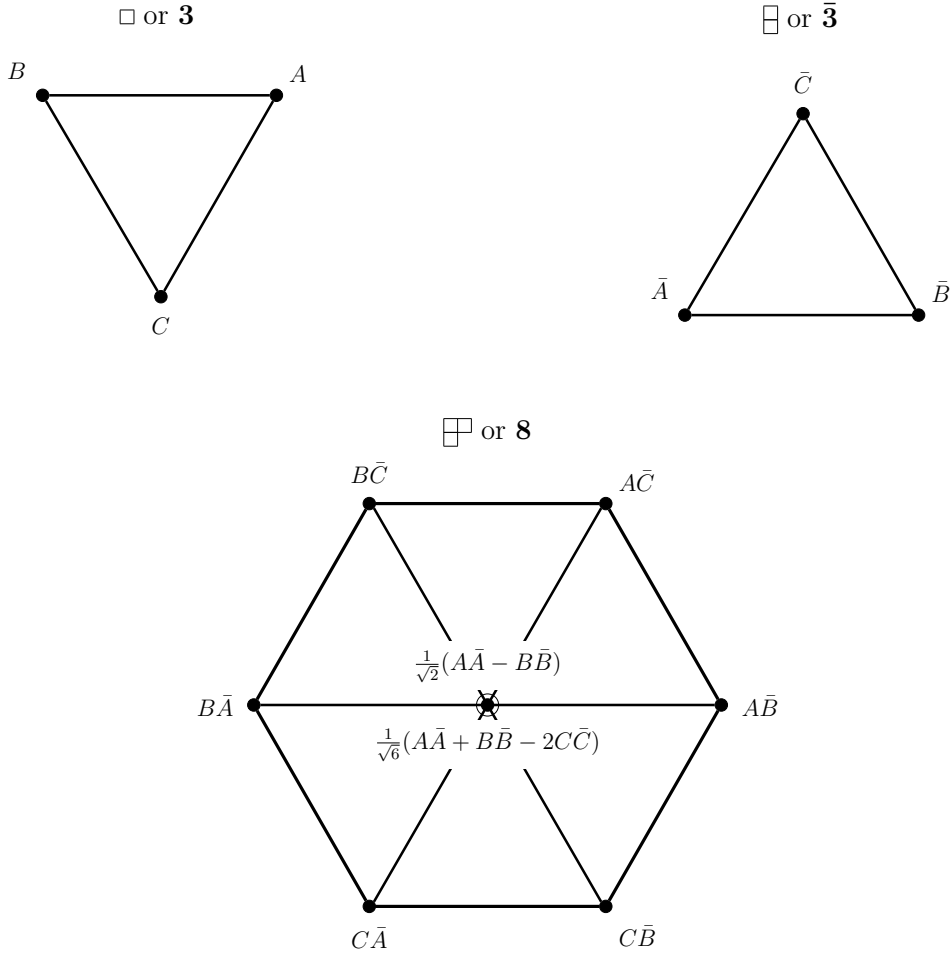
Figure 3.1 – Weight diagram of the irreps **3**, **3̄** and **8**. Out of the nine states from $\mathbf{3} \otimes \mathbf{\bar{3}}$, the singlet $\frac{1}{\sqrt{6}}(A\bar{A} + B\bar{B} + C\bar{C})$ can be constructed, which is a state annihilated by all the raising operators. The eight states in **8** can be obtained by enforcing the tracelessness condition, or by acting the lowering operators on the highest-weight state of **8** which is $A\bar{C}$.

lowering operators $\hat{S}_\nu^\mu$. Following the construction in subsection 1.1.2, we define

$$
\begin{aligned}
\hat{S}_A^B &:= Q_1 + iQ_2, & \hat{S}_B^A &:= Q_1 - iQ_2 \\
\hat{S}_A^C &:= Q_4 + iQ_5, & \hat{S}_C^A &:= Q_4 - iQ_5 \\
\hat{S}_B^C &:= Q_6 + iQ_7, & \hat{S}_C^B &:= Q_6 - iQ_7 \\
\hat{S}_A^A &:= Q_3 + \frac{1}{\sqrt{3}}Q_8, & \hat{S}_B^B &:= -Q_3 + \frac{1}{\sqrt{3}}Q_8, & \hat{S}_C^C &:= -\frac{2}{\sqrt{3}}Q_8,
\end{aligned}
$$

(3.9)

which, after simplification of the expressions, lead to

$$
\hat{S}_\nu^\mu = \left(a_\nu^\dagger a_\mu - b_\mu^\dagger b_\nu\right) - \delta_\nu^\mu \frac{1}{3}(\hat{N}_a - \hat{N}_b),
$$

(3.10)

with $\mu, \nu \in \{1, 2, 3\} (= \{A, B, C\})$. This construction naturally satisfies all the commutation rela-

Figure 3.2 – An example of the states involved in the ground state configuration for $p = 2$. (a) The state of sublattice Λ_1 with p times $\bar{B}$ and p times A. (b) The state of sublattice Λ_2 with p times $\bar{A}$ and p times B.

tions $\left[S_\beta^\alpha, S_\nu^\mu \right] = \delta_\nu^\alpha S_\beta^\mu - \delta_\beta^\mu S_\nu^\alpha$ and the tracelessness condition $\sum_\mu S_\mu^\mu = 0$.

Henceforth, the bosons a_1, a_2, a_3 will be associated to the colors A, B, C, and the bosons b_1, b_2, b_3 will be associated to the colors $\bar{A}$, $\bar{B}$, and $\bar{C}$ (or $\boxed{\begin{smallmatrix}B\\C\end{smallmatrix}}$, $\boxed{\begin{smallmatrix}A\\C\end{smallmatrix}}$ and $\boxed{\begin{smallmatrix}A\\B\end{smallmatrix}}$).

3.1.2 The LFWT with Mathur & Sen bosons

We are now ready to apply the LFWT on the SU(3) antiferromagnetic Heisenberg chain whose Hamiltonian reads as

$$\mathcal{H} = J \sum_{<i,j>} \sum_{\mu,\nu=A}^{C} \hat{S}_\nu^\mu(i) \hat{S}_\mu^\nu(j), \tag{3.11}$$

The states on each site will be in the self-conjugate irreps represented by the Young tableaux with p two-box columns and p one-box columns, i.e., irreps given by the Dynkin label $[p, p]$.

As in subsection 2.2.3, we can choose the classical Néel ground state configuration that is given by p times A and p times $\bar{B}$ on the sites i in the sublattice Λ_{ACA},

$$\left| gs \right\rangle_i := \frac{1}{p!} \left(a_A^\dagger(i) b_B^\dagger(i) \right)^p |0\rangle \equiv (A\bar{B})^{\otimes p}, \tag{3.12}$$

and p times B and p times $\bar{A}$ on sites j in the other sublattice Λ_{BCB}:

$$\left| gs \right\rangle_j := \frac{1}{p!} \left(a_B^\dagger b_A^\dagger \right)^p |0\rangle \equiv (B\bar{A})^{\otimes p}. \tag{3.13}$$

These two states are depicted in terms of the Weyl tableaux in Figure 3.2.

These states satisfy the following constraints

$$\sum_{\mu=A}^{C} a_\mu^\dagger a_\mu = p, \qquad \sum_{\mu=A}^{C} b_\mu^\dagger b_\mu = p, \tag{3.14}$$

where $p = 1$. By taking the semi-classical limit $p \to \infty$ according to our aforementioned assumption of condensates $(A\bar{B})^{\otimes p}$ on $i \in \Lambda_{ACA}$ and $(B\bar{A})^{\otimes p}$ on $j \in \Lambda_{BCB}$, these constraints

become

$$
\begin{aligned}
a_A^\dagger(i)\,a_A(i) &= p - [a_B^\dagger(i)\,a_B(i) + a_C^\dagger(i)\,a_C(i)], \\
b_B^\dagger(i)\,b_B(i) &= p - [b_A^\dagger(i)\,b_A(i) + b_C^\dagger(i)\,b_C(i)], \\
a_B^\dagger(j)\,a_B(j) &= p - [a_A^\dagger(j)\,a_A(j) + a_C^\dagger(j)\,a_C(j)], \\
b_A^\dagger(j)\,b_A(j) &= p - [b_B^\dagger(j)\,b_B(j) + b_C^\dagger(j)\,b_C(j)].
\end{aligned}
\tag{3.15}
$$

From this, we can perform the Holstein-Primakoff transformation

$$
\begin{aligned}
a_A^\dagger(i), a_A(i) &\longrightarrow \sqrt{p - \sum_{\mu \neq A} a_\mu^\dagger(i)\,a_\mu(i)} \approx \sqrt{p} - \frac{1}{2\sqrt{p}} \sum_{\mu \neq A} a_\mu^\dagger(i)\,a_\mu(i), \\
b_B^\dagger(i), b_B(i) &\longrightarrow \sqrt{p - \sum_{\mu \neq B} b_\mu^\dagger(i)\,b_\mu(i)} \approx \sqrt{p} - \frac{1}{2\sqrt{p}} \sum_{\mu \neq B} b_\mu^\dagger(i)\,b_\mu(i), \\
a_B^\dagger(j), a_B(j) &\longrightarrow \sqrt{p - \sum_{\mu \neq B} a_\mu^\dagger(j)\,a_\mu(j)} \approx \sqrt{p} - \frac{1}{2\sqrt{p}} \sum_{\mu \neq B} a_\mu^\dagger(j)\,a_\mu(j), \\
b_A^\dagger(j), b_A(j) &\longrightarrow \sqrt{p - \sum_{\mu \neq A} b_\mu^\dagger(j)\,b_\mu(j)} \approx \sqrt{p} - \frac{1}{2\sqrt{p}} \sum_{\mu \neq A} b_\mu^\dagger(j)\,b_\mu(j).
\end{aligned}
\tag{3.16}
$$

This approximation is justified by the expectation values of the coherent states shown in Eq. (57) in Ref. [77], namely that

$$
{}_{(n_a, n_b)}\left\langle \vec{z}, \vec{w} \left| Q^k \right| \vec{z}, \vec{w} \right\rangle_{(n_a, n_b)} = n_a z_\mu^* \lambda_{\mu\nu}^k z_\nu - n_b w_\mu^* \lambda_{\mu\nu}^{*k} w_\nu,
\tag{3.17}
$$

i.e. the expectation value of the $a_\mu^\dagger a_\mu$ and $b_\mu^\dagger b_\mu$ with respect to the coherent states are given by $n_{a,\mu}$ and $n_{b,\mu}$, respectively.

The truncation of the Taylor series at this order is sufficient to obtain all the terms of the quadratic Hamiltonian of the order p. It is also worthwhile noting that the SU(3) commutation relations (1.23) stay valid up to order $\mathcal{O}(1)$ in p even after this tranformation.

We can now apply this transformation on the Hamiltonian (3.11) written with the bosonic

operators (3.10), which gives the quadratic Hamiltonian $\mathscr{H}^{(2)}$ of the order $\mathscr{O}(p)$:

$$\mathscr{H}^{(2)} = \mathscr{H}_1^{(2)} + \mathscr{H}_2^{(2)} + \mathscr{H}_3^{(2)} \qquad \text{where}$$

$$
\begin{aligned}
\mathscr{H}_1^{(2)} &= J \sum_{i \in \Lambda_{ACA}} \sum_{\langle j \rangle} p \left[a_C^\dagger(j) a_C(j) + b_C^\dagger(i) b_C(i) - b_C^\dagger(i) a_C^\dagger(j) - b_C(i) a_C(j) \right], \\
\mathscr{H}_2^{(2)} &= J \sum_{i \in \Lambda_{ACA}} \sum_{\langle j \rangle} p \left[a_C^\dagger(i) a_C(i) + b_C^\dagger(j) b_C(j) - a_C^\dagger(i) b_C^\dagger(j) - a_C(i) b_C(j) \right], \\
\mathscr{H}_3^{(2)} &= J \sum_{i \in \Lambda_{ACA}} \sum_{\langle j \rangle} p \Big[2 a_B^\dagger(i) a_B(i) + 2 a_A^\dagger(j) a_A(j) + 2 b_A^\dagger(i) b_A(i) + 2 b_B^\dagger(j) b_B(j) \\
&\quad + a_B^\dagger(i) a_A^\dagger(j) - a_B^\dagger(i) b_B^\dagger(j) - b_A^\dagger(i) a_A^\dagger(j) + b_A^\dagger(i) b_B^\dagger(j) \\
&\quad + a_B(i) a_A(j) - a_B(i) b_B(j) - b_A(i) a_A(j) + b_A(i) b_B(j) \Big].
\end{aligned}
\tag{3.18}
$$

The Fourier transform can be applied with

$$
\begin{aligned}
a_\mu(i) &= \sqrt{\frac{2}{N_{\text{sites}}}} \sum_{k \in \text{RBZ}} a_\mu^1(k) e^{-ikr_i}, \qquad a_\mu(j) = \sqrt{\frac{2}{N_{\text{sites}}}} \sum_{k \in \text{RBZ}} a_\mu^2(k) e^{-ikr_j}, \\
b_\mu(i) &= \sqrt{\frac{2}{N_{\text{sites}}}} \sum_{k \in \text{RBZ}} b_\mu^1(k) e^{-ikr_i}, \qquad b_\mu(j) = \sqrt{\frac{2}{N_{\text{sites}}}} \sum_{k \in \text{RBZ}} b_\mu^2(k) e^{-ikr_j}
\end{aligned}
\tag{3.19}
$$

where **k** runs over the reduced Brillouin zone, N_{sites} is the number of sites and the superscripts [1] and [2] keep track of the sublattices Λ_{ACA} and Λ_{BCB} respectively. The quadratric Hamiltonian (3.18) is then given by

$$\mathscr{H}^{(2)} = \sum_{a=1}^{3} \mathscr{H}_a^{(2)} = p \sum_{a=1}^{3} \left[J \sum_{k \in \text{RBZ}} \left(\mathbf{u}_{a,k}^\dagger, \mathbf{u}_{a,-k} \right) M_{a,k} \begin{pmatrix} {}^t\mathbf{u}_{a,k} \\ {}^t\mathbf{u}_{a,-k}^\dagger \end{pmatrix} \right] \tag{3.20}$$

where

$$
\begin{aligned}
\mathbf{u}_{1,k}^\dagger &:= \left(a_C^{1\dagger}(k), b_C^{2\dagger}(k) \right), & \mathbf{u}_{1,-k} &:= \left(a_C^1(-k), b_C^2(-k) \right), \\
\mathbf{u}_{2,k}^\dagger &:= \left(a_C^{2\dagger}(k), b_C^{1\dagger}(k) \right), & \mathbf{u}_{2,-k} &:= \left(a_C^2(-k), b_C^1(-k) \right), \\
\mathbf{u}_{3,k}^\dagger &:= \left(a_B^{1\dagger}(k), b_A^{1\dagger}(k), a_A^{2\dagger}(k), b_B^{2\dagger}(k) \right), & \mathbf{u}_{3,-k} &:= \left(a_B^1(-k), b_A^1(-k), a_A^2(-k), b_B^2(-k) \right),
\end{aligned}
\tag{3.21}
$$

and

$$
M_{1,k} := \begin{pmatrix} \mathscr{A}_1 & \mathscr{B}_{1,k} \\ \mathscr{B}_{1,k} & \mathscr{A}_1 \end{pmatrix}, \qquad \mathscr{A}_1 := \mathbb{1}_2, \qquad \mathscr{B}_{1,k} := \gamma_k \begin{pmatrix} 0 & -1 \\ -1 & 0 \end{pmatrix},
$$

$$
M_{2,k} := M_{1,k}
$$

$$
M_{3,k} := \begin{pmatrix} \mathscr{A}_3 & \mathscr{B}_{3,k} \\ \mathscr{B}_{3,k}^\dagger & \mathscr{A}_3 \end{pmatrix}, \qquad \mathscr{A}_3 := 2 \cdot \mathbb{1}_4, \qquad \mathscr{B}_{3,k} := \gamma_k \begin{pmatrix} 0 & 0 & 1 & -1 \\ 0 & 0 & -1 & 1 \\ 1 & -1 & 0 & 0 \\ -1 & 1 & 0 & 0 \end{pmatrix},
$$

$$\tag{3.22}$$

where the geometrical factor

$$
\gamma_k := \cos k \tag{3.23}
$$

has been introduced. The Hamiltonian can then be diagonalised by using the generalised Bogoliubov transformation, after which the diagonalised Hamiltonian is given by

$$
\boxed{\mathcal{H}^{(2)} = J \sum_{k \in \mathrm{RBZ}} \left\{ \sum_{\zeta=1}^{8} \omega_\zeta(k) \left(f_\zeta^\dagger(k) f_\zeta(k) + \frac{1}{2} \right) \right\} + \mathrm{const.}} \tag{3.24}
$$

up to a constant, where the bosons f_μ are the new Bogoliubov bosons, and

$$
\omega_{1,2,3,4}(k) = 2p \, |\sin k|, \qquad \omega_{5,6}(k) = 4p \, |\sin k|,
$$
$$
\omega_{7,8}(k) = 4p. \tag{3.25}
$$

We obtain 6 dispersive Goldstone modes with two different velocities, and 2 flat modes. The plots of the dispersion relations for $p = 1$ can be found in Figure 3.3.

It can be seen that the dispersion relations here are identical to those obtained with the multiboson method in section 2.2. The physical process of these modes is a bit less obvious here, so let us look at what is happening more closely.

The six Goldstone modes $\omega_{1,\dots,6}$ can each be associated to one of the six off-diagonal generators acting on the initial condensate. For instance, the modes $\omega_{1,2}$ stemming from the sub-Hamiltonian $\mathcal{H}_1^{(2)}$ arise from the Holstein-Primakoff bosons $a_C^{1\dagger}$ and $b_C^{2\dagger}$. These bosons correspond to the action of the generator $\hat{S}_C^A$ on $|\mathrm{gs}\rangle_i$ on sublattice Λ_{ACA} or the action of S_A^C on $|\mathrm{gs}\rangle_j$ on sublattice Λ_{BCB}. This yields another state of the irrep which differs from the original condensate by one color. Similarly, the modes $\omega_{3,4}$ from the sub-Hamiltonian $\mathcal{H}_2^{(2)}$ come from bosons $a_3^{2\dagger}$ and $b_3^{1\dagger}$ that correspond to acting S_B^C on $|\mathrm{gs}\rangle_i$ and acting $\hat{S}_C^B$ on $|\mathrm{gs}\rangle_j$. These modes are thus of the same nature as the dispersive modes we had found in the fully antisymmetric models in section 2.1.

The case of bosons $a_B^{1\dagger}, b_A^{1\dagger}, a_A^{2\dagger}, b_B^{2\dagger}$ in the sub-Hamiltonian $\mathcal{H}_2^{(2)}$ is, however, a bit different. For a better understanding, let us formally rewrite $\mathcal{H}_3^{(2)}$ using the new bosons f and g defined
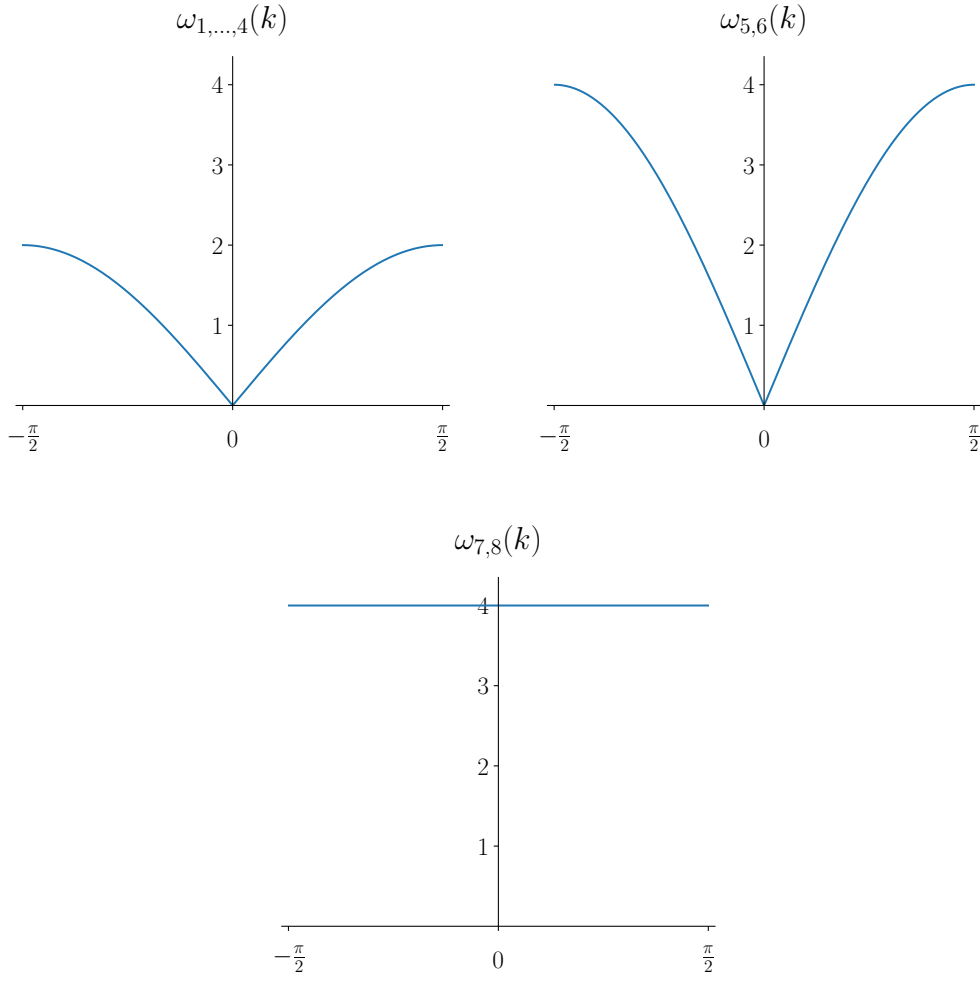
Figure 3.3 – The dispersion relations $\omega_{1,\dots,8}$ for $p = 1$ (adjoint irrep).

as

$$f^1(i) = \frac{1}{\sqrt{2}}\left[a_B^1(i) - b_A^1(i)\right], \qquad f^2(j) = \frac{1}{\sqrt{2}}\left[a_A^2(j) - b_B^2(j)\right],$$
$$g^1(i) = \frac{1}{\sqrt{2}}\left[a_B^1(i) + b_A^1(i)\right], \qquad g^2(j) = \frac{1}{\sqrt{2}}\left[a_A^2(j) + b_B^2(j)\right].$$

(3.26)

The sub-Hamiltonian $\mathcal{H}_3^{(2)}$ in (3.18) can then be written as

$$\mathcal{H}_3^{(2)} = J \sum_{i \in \Lambda_{ACA}} \sum_{\langle j \rangle} p\Big\{2g^{1\dagger}(i)g^1(i) + 2g^{2\dagger}(j)g^2(j)$$
$$+ 2\left[f^{1\dagger}(i)f^1(i) + f^{2\dagger}(j)f^2(j) + f^{1\dagger}(i)f^{2\dagger}(j) + f^1(i)f^2(j)\right]\Big\},$$

(3.27)

where the new g^1, g^2 bosons clearly give non-dispersive flat modes.

63

Let us set $p = 1$ for a second and consider the adjoint irrep with the help of the weight diagram in Figure 3.1. The generators $\hat{S}_B^A$ and $\hat{S}_A^B$ applied on our initial condensates $|\text{gs}\rangle_i$ or $|\text{gs}\rangle_j$ create the state $A\bar{A} - B\bar{B}$ that belongs to a two-dimensional subspace in the weight diagram with zero weights. In terms of the Holstein-Primakoff bosons—remember that we are gathering the terms linear in p only—this state corresponds to $f^{1\dagger}$ on sublattice Λ_{ACA} and $f^{2\dagger}$ on sublattice Λ_{BCB} up to a factor:

$$
\begin{aligned}
\hat{S}_B^A(i)\left|A\bar{B}\right\rangle_i &= \left|B\bar{B}\right\rangle_i - \left|A\bar{A}\right\rangle_i \\
&= \left(a_B^\dagger(i)b_B^\dagger(i) - a_A^\dagger(i)b_A^\dagger(i)\right)|0\rangle \;\xrightarrow{\text{H-P}}\; p\left(a_B^\dagger(i) - b_A^\dagger(i)\right)|0\rangle + \mathcal{O}(p^0) \quad \text{(3.28a)} \\
&\sim \sqrt{2}\,p f^1(i)\,|0\rangle,
\end{aligned}
$$

$$
\begin{aligned}
\hat{S}_A^B(j)\left|B\bar{A}\right\rangle_j &= \left|A\bar{A}\right\rangle_j - \left|B\bar{B}\right\rangle_j \\
&= \left(a_A^\dagger(j)b_A^\dagger(j) - a_B^\dagger(j)b_B^\dagger(j)\right)|0\rangle \;\xrightarrow{\text{H-P}}\; p\left(a_A^\dagger(j) - b_B^\dagger(j)\right)|0\rangle + \mathcal{O}(p^0) \quad \text{(3.28b)} \\
&\sim \sqrt{2}\,p f^2(j)\,|0\rangle.
\end{aligned}
$$

This corresponds precisely to Eqs. (2.62) and (2.65) in the multiboson representation. These will give the remaining two propagating Goldstone modes $\omega_{1,2}$ that come from the sub-Hamiltonian $\mathcal{H}_3^{(2)}$. The reason why these modes have a velocity two times larger than the others is because the states created by $\hat{S}_1^2$ and $\hat{S}_2^1$ from our initial condensate have a squared norm twice as large as the states created by the other generators, an aspect we already encountered again Eqs. (2.62) and (2.65). This is also seen in the factor $\sqrt{2}$ in Eqs. (3.28).

The two remaining (flat) modes $\omega_{7,8}$ come from the bosons g^1 and g^2 who simply generate the states orthogonal to those corresponding to f^1 and f^2 in the matrix M_3 as the result of the diagonalisation of the matrix. The states related to the bosons g^1 and g^2 are $\left|A\bar{A}\right\rangle_i + \left|B\bar{B}\right\rangle_i$ and $\left|A\bar{A}\right\rangle_j + \left|B\bar{B}\right\rangle_j$ respectively, and they are a mixture of the state $\boxed{\begin{smallmatrix} A & C \\ B & \end{smallmatrix}}$ of the irrep $[1,1]$ and of the singlet of the trivial irrep of SU(3). This happens partly because the Hilbert space is enlarged with the Mathur & Sen bosons—there are 9 bosons although there are only 8 states in our irrep in question—and also because of the truncation of our Hamiltonian in the expansion. When applying the generator $\hat{S}_\nu^\mu$ on a state of the irrep $[1,1]$, the resulting state always remains in the same irrep as it should (even though the Mathur & Sen bosons enlarges the Hilbert space). However, the truncation of these generators to a certain order results in some states having an overlap with the trivial irrep.

We would like to point out, however, that these flat-mode bosons g^1 and g^2 obtained from $\mathcal{H}_3^{(2)}$ could also be related to the other remaining zero-weight state $\frac{1}{\sqrt{6}}\left(A\bar{A} + B\bar{B} - 2C\bar{C}\right)$ of the irrep $[1,1]$ that cannot be obtained by a single colour flip from $|\text{gs}\rangle_i$ or $|\text{gs}\rangle_j$ (see Eq. (2.63)). As already mentioned in Eq. (2.83), what we need is at least two colour permutations:

$$
\begin{aligned}
\left(2S_B^C S_C^A - S_B^A\right)\left|A\bar{B}\right\rangle_i &= \left(a_B^\dagger a_A + b_A^\dagger b_B - 2b_C^\dagger b_B a_C^\dagger a_A\right)\left|A\bar{B}\right\rangle_i \\
&= \left|A\bar{A}\right\rangle_i + \left|B\bar{B}\right\rangle_i - 2\left|C\bar{C}\right\rangle_i.
\end{aligned} \quad \text{(3.29)}
$$

Hence, it could be that this state (that is orthogonal to $A\bar{A} - B\bar{B}$) appears as flat modes, just as in subsection 2.2.3, and the modes $\omega_{7,8}$ do not correspond to Goldstone modes. In terms of the Holstein-Primakoff bosons, this state corresponds to the boson $g^1(i)$ if we gather the terms with one colour permutation only:

$$
\begin{aligned}
\left|A\bar{A}\right\rangle_i + \left|B\bar{B}\right\rangle_i - 2\left|C\bar{C}\right\rangle_i &= \left(a_B^\dagger(i)a_A(i) + b_A^\dagger(i)b_B(i) - 2b_C^\dagger(i)b_B(i)a_C^\dagger(i)a_A(i)\right)\left|A\bar{B}\right\rangle_i \\
&\longrightarrow \quad \sqrt{p}\left(a_B^\dagger(i) - b_A^\dagger(i)\right)|0\rangle \\
&\sim \quad \sqrt{p}g^1(i)|0\rangle.
\end{aligned}
\tag{3.30}
$$

Note that we need two colour permutations to obtain $\left|C\bar{C}\right\rangle_i$ from $\left|\text{gs}\right\rangle_i$ or $\left|\text{gs}\right\rangle_j$. Then, what we obtain here is exactly what we see in Eq. (3.27).

For $p > 1$, the logic is the same. The states we obtain by applying the generators S_B^A and S_A^B applied on our initial condensates $\left|\text{gs}(i)\right\rangle$ or $\left|\text{gs}(j)\right\rangle$ is the state $(A\bar{A} - B\bar{B})(A\bar{B})^{\otimes(p-1)}$ up to a factor, and it belongs to a two-dimensional subspace in the weight diagram,[10] just like in the adjoint irrep. The other state that lives in this two-dimensional subspace, i.e., $(A\bar{A} + B\bar{B} - 2C\bar{C})(A\bar{B})^{\otimes(p-1)}$, requires at least two colour permutations and manifests itself as flat modes. All in all, the degenerate points in the weight diagram will always yield flat modes after the diagonalisation of the Hamiltonian. It is to be noted, however, that there are less flat (localised) multipolar modes here than with the multiboson method.

Hence, it can be finally concluded that the dispersion relations related to the Goldstone modes are $\omega_{1,\dots,6}$ for any p, and the velocities of these six Goldstone modes are given by

$$
c_1 := c_2 := c_3 := c_4 := 2pJ, \quad c_5 := c_6 := 4pJ.
\tag{3.31}
$$

These velocities are in complete agreement with the field-theoretical calculations in Ref.[76].

It should be noted here that the dispersive modes are obtained more easily than with the multiboson method as we did not need to derive the expressions of $\hat{S}_\nu^\mu$ separately for the adjoint irrep. As we will see in the next section, we can easily extend this calculation to a generic SU(3) irrep $[p, q]$ with the Mathur & Sen bosons. With the multiboson method, however, it would be very cumbersome to carry out the calculations for a generic irrep $[p, q]$ as the number of bosons become large.

---

[10]For p>1, these states indeed belong to a two-dimensional subspace in the weight diagram, but are not zero-weight states anymore: the weight is $\neq 0$ for these states.

3.2 The $SU(3)$ model in irreducible representation $[p, q]$ on the bipartite d-dimensional lattice

Let us now consider a general d-dimensional bipartite system (1D chain, 2D square, 3D cubic, etc.) with states in any SU(3) irrep $[p, q]$, whose Hamiltonian is given by

$$\mathcal{H} = J \sum_{<i,j>} \sum_{\mu,\nu=A}^{C} \hat{S}^{\mu}_{\nu}(i) \hat{S}^{\nu}_{\mu}(j). \tag{3.32}$$

If we assume a bipartite configuration in d dimensions with the coordination number $2d$, we want to condense two opposite states in the weight diagram. Without loss of generality, we can choose to have a condensate of p times A and q times $\bar{B}$ (e.g. $\boxed{\frac{A\,A\,A}{C}}$ for $p = 2, q = 1$) on the sublattice Λ_1 and p times B and q times $\bar{A}$ (e.g. $\boxed{\frac{B\,B\,B}{C}}$ for $p = 2, q = 1$) on the other sublattice Λ_2, as we did for the adjoint irrep (see footnote 8 on page 40).

These states satisfy the following constraits

$$\sum_{\mu=A}^{C} a^{\dagger}_{\mu} a_{\mu} = p, \qquad \sum_{\mu=A}^{C} b^{\dagger}_{\mu} b_{\mu} = q. \tag{3.33}$$

The semi-classical limit can then be taken to be $p, q \to \infty$ according to our aforementioned assumption of condensates $A, \bar{B}$ on $i \in \Lambda_1$ and $B, \bar{A}$ on $j \in \Lambda_2$. The constraints thus become

$$
\begin{aligned}
a^{\dagger}_A(i) a_A(i) &= p - [a^{\dagger}_B(i) a_B(i) + a^{\dagger}_C(i) a_C(i)], \\
b^{\dagger}_B(i) b_B(i) &= q - [b^{\dagger}_A(i) b_A(i) + b^{\dagger}_C(i) b_C(i)], \\
a^{\dagger}_B(j) a_B(j) &= p - [a^{\dagger}_A(j) a_A(j) + b^{\dagger}_C(j) a_C(j)], \\
b^{\dagger}_A(j) b_A(j) &= q - [b^{\dagger}_B(j) b_B(j) + b^{\dagger}_C(j) b_C(j)].
\end{aligned}
\tag{3.34}
$$

From this, we can perform the Holstein-Primakoff transformation

$$
\begin{aligned}
a^{\dagger}_A(i), a_A(i) &\longrightarrow \sqrt{p - \sum_{\mu \neq A} a^{\dagger}_{\mu}(i) a_{\mu}(i)} \approx \sqrt{p} - \frac{1}{2\sqrt{p}} \sum_{\mu \neq A} a^{\dagger}_{\mu}(i) a_{\mu}(i), \\
b^{\dagger}_B(i), b_B(i) &\longrightarrow \sqrt{q - \sum_{\mu \neq B} b^{\dagger}_{\mu}(i) b_{\mu}(i)} \approx \sqrt{q} - \frac{1}{2\sqrt{q}} \sum_{\mu \neq B} b^{\dagger}_{\mu}(i) b_{\mu}(i), \\
a^{\dagger}_B(j), a_B(j) &\longrightarrow \sqrt{p - \sum_{\mu \neq B} a^{\dagger}_{\mu}(j) a_{\mu}(j)} \approx \sqrt{p} - \frac{1}{2\sqrt{p}} \sum_{\mu \neq B} a^{\dagger}_{\mu}(j) a_{\mu}(j), \\
b^{\dagger}_A(j), b_A(j) &\longrightarrow \sqrt{q - \sum_{\mu \neq A} b^{\dagger}_{\mu}(j) b_{\mu}(j)} \approx \sqrt{q} - \frac{1}{2\sqrt{q}} \sum_{\mu \neq A} b^{\dagger}_{\mu}(j) b_{\mu}(j).
\end{aligned}
\tag{3.35}
$$

The truncation of the Taylor series at this order is sufficient to obtain all the terms of the quadratic Hamiltonian of the order p and of the order q.

3.2. The $SU(3)$ model in irreducible representation $[p, q]$ on the bipartite d-dimensional lattice

We can now apply this transformation to the SU(3) AFM Hamiltonian (3.36) which yields the quadratic Hamiltonian of the order $\mathcal{O}(n_c)$:

$$\mathcal{H}^{(2)} = \mathcal{H}_1^{(2)} + \mathcal{H}_2^{(2)} + \mathcal{H}_3^{(2)} \qquad \text{where}$$

$$\mathcal{H}_1^{(2)} = J \sum_{i \in \Lambda_1} \sum_{\langle j \rangle} \left[q a_C^\dagger(j) a_C(j) + p b_C^\dagger(i) b_C(i) - \sqrt{pq} b_C^\dagger(i) a_C^\dagger(j) - \sqrt{pq} b_C(i) a_C(j) \right],$$

$$\mathcal{H}_2^{(2)} = J \sum_{i \in \Lambda_1} \sum_{\langle j \rangle} \left[q a_C^\dagger(i) a_C(i) + p b_C^\dagger(j) b_C(j) - \sqrt{pq} a_C^\dagger(i) b_C^\dagger(j) - \sqrt{pq} a_C(i) b_C(j) \right],$$

$$\mathcal{H}_3^{(2)} = J \sum_{i \in \Lambda_1} \sum_{\langle j \rangle} p \Big[(p+q) a_B^\dagger(i) a_B(i) + (p+q) a_A^\dagger(j) a_A(j) + (p+q) b_A^\dagger(i) b_A(i) + (p+q) b_B^\dagger(j) b_B(j)$$

$$+ p a_B^\dagger(i) a_A^\dagger(j) - \sqrt{pq} a_B^\dagger(i) b_B^\dagger(j) - \sqrt{pq} b_A^\dagger(i) a_A^\dagger(j) + q b_A^\dagger(i) b_B^\dagger(j)$$

$$+ p a_B(i) a_A(j) - \sqrt{pq} a_B(i) b_B(j) - \sqrt{pq} b_A(i) a_A(j) + q b_A(i) b_B(j) \Big]. \tag{3.36}$$

After Fourier-transforming,

$$a_\mu(i) = \sqrt{\frac{2}{N_{\text{sites}}}} \sum_{\mathbf{k} \in \text{RBZ}} a_\mu^1(\mathbf{k}) e^{-i \mathbf{k} \cdot \mathbf{r}_i}, \qquad a_\mu(j) = \sqrt{\frac{2}{N_{\text{sites}}}} \sum_{\mathbf{k} \in \text{RBZ}} a_\mu^2(\mathbf{k}) e^{-i \mathbf{k} \cdot \mathbf{r}_j},$$

$$b_\mu(i) = \sqrt{\frac{2}{N_{\text{sites}}}} \sum_{\mathbf{k} \in \text{RBZ}} b_\mu^1(\mathbf{k}) e^{-i \mathbf{k} \cdot \mathbf{r}_i}, \qquad b_\mu(j) = \sqrt{\frac{2}{N_{\text{sites}}}} \sum_{\mathbf{k} \in \text{RBZ}} b_\mu^2(\mathbf{k}) e^{-i \mathbf{k} \cdot \mathbf{r}_j}, \tag{3.37}$$

with the sublattice index $^1, ^2$ keeping track of the sublattices Λ_1, Λ_2, we obtain

$$\mathcal{H}^{(2)} = J \sum_{\mathbf{k} \in \text{RBZ}} \sum_{a=1}^{3} \left(\mathbf{u}_{a,\mathbf{k}}^\dagger, \mathbf{u}_{a,-\mathbf{k}} \right) M_{a,\mathbf{k}} \begin{pmatrix} {}^t \mathbf{u}_{a,\mathbf{k}} \\ {}^t \mathbf{u}_{a,-\mathbf{k}}^\dagger \end{pmatrix} \tag{3.38}$$

where

$$\mathbf{u}_{1,\mathbf{k}}^\dagger := \left(a_B^{1\dagger}(\mathbf{k}), a_A^{2\dagger}(\mathbf{k}), b_B^{2\dagger}(\mathbf{k}), b_A^{1\dagger}(\mathbf{k}) \right), \qquad \mathbf{u}_{1,-\mathbf{k}} := \left(a_B^1(-\mathbf{k}), a_A^2(-\mathbf{k}), b_B^2(-\mathbf{k}), b_A^1(-\mathbf{k}) \right),$$

$$\mathbf{u}_{2,\mathbf{k}}^\dagger := \left(a_C^{1\dagger}(\mathbf{k}), b_C^{2\dagger}(\mathbf{k}) \right), \qquad \mathbf{u}_{2,-\mathbf{k}} := \left(a_C^1(-\mathbf{k}), b_C^2(-\mathbf{k}) \right), \tag{3.39}$$

$$\mathbf{u}_{3,\mathbf{k}}^\dagger := \left(a_C^{2\dagger}(\mathbf{k}), b_C^{1\dagger}(\mathbf{k}) \right), \qquad \mathbf{u}_{3,-\mathbf{k}} := \left(a_C^2(-\mathbf{k}), b_C^1(-\mathbf{k}) \right),$$

$$M_{1,\mathbf{k}} := \begin{pmatrix} \mathscr{A}_1 & \mathscr{B}_{1,\mathbf{k}} \\ \mathscr{B}_{1,\mathbf{k}} & \mathscr{A}_1 \end{pmatrix}, \qquad \mathscr{A}_1 := 2d \begin{pmatrix} q & 0 \\ 0 & p \end{pmatrix}, \qquad \mathscr{B}_{1,\mathbf{k}} := 2d\gamma_{\mathbf{k}} \begin{pmatrix} 0 & -\sqrt{pq} \\ -\sqrt{pq} & 0 \end{pmatrix},$$

$$M_{2,\mathbf{k}} := M_{1,\mathbf{k}},$$

$$M_{\mathbf{k}}^3 := \begin{pmatrix} \mathscr{A}_{3,\mathbf{k}} & \mathscr{B}_{3,\mathbf{k}} \\ \mathscr{B}_{3,\mathbf{k}}^\dagger & \mathscr{A}_{3,-\mathbf{k}} \end{pmatrix}, \tag{3.40}$$

$$\mathscr{A}_{3,\mathbf{k}} := 2d(p+q)\mathbb{1}_4, \qquad \mathscr{B}_{3,\mathbf{k}} := 2d\gamma_{\mathbf{k}} \begin{pmatrix} 0 & p & -\sqrt{pq} & 0 \\ p & 0 & 0 & -\sqrt{pq} \\ -\sqrt{pq} & 0 & 0 & q \\ 0 & -\sqrt{pq} & q & 0 \end{pmatrix},$$

with the geometrical factor

$$\gamma_{\mathbf{k}} := \begin{cases} \cos k_x, & d = 1 \\ \frac{1}{2}(\cos k_x + \cos k_y), & d = 2 \\ \frac{1}{3}(\cos k_x + \cos k_y + \cos k_z), & d = 3 \\ \dots \end{cases} \tag{3.41}$$

for the 1D chain, the 2D square lattice, the 3D cubic lattice etc. The generalised Bogoliubov transformation can be used to diagonalise the system, after which the diagonalised Hamiltonian is given by

$$\boxed{\mathscr{H}^{(2)} = J \sum_{\mathbf{k}\in\text{RBZ}} \left\{ \sum_{\zeta=1}^{8} \omega_\zeta(\mathbf{k}) \left(f_\zeta^\dagger(\mathbf{k}) f_\zeta(\mathbf{k}) + \frac{1}{2} \right) \right\} + \text{const.}} \tag{3.42}$$

up to a constant, where the bosons f_μ are the new Bogoliubov bosons, and

$$\begin{aligned} \omega_{1,2}(\mathbf{k}) &= d\left(\sqrt{(p+q)^2 - 4pq\gamma_{\mathbf{k}}^2} - p + q \right), \\ \omega_{3,4}(\mathbf{k}) &= d\left(\sqrt{(p+q)^2 - 4pq\gamma_{\mathbf{k}}^2} + p - q \right), \\ \omega_{5,6}(\mathbf{k}) &= 2d(p+q)\sqrt{1 - \gamma_{\mathbf{k}}^2}, \\ \omega_{7,8}(\mathbf{k}) &= 2d(p+q). \end{aligned} \tag{3.43}$$

Note that $\omega_{3,4,5,6}(\mathbf{k}) \geq 0$, since

$$\begin{aligned} \sqrt{(p-q)^2} &= \sqrt{(p+q)^2 - 4pq} \\ \implies (p-q) &\leq \sqrt{(p+q)^2 - 4pq\gamma_{\mathbf{k}}^2}. \end{aligned} \tag{3.44}$$

Let us now concentrate on the 1D case ($d = 1$) in order to compare the results with the self-
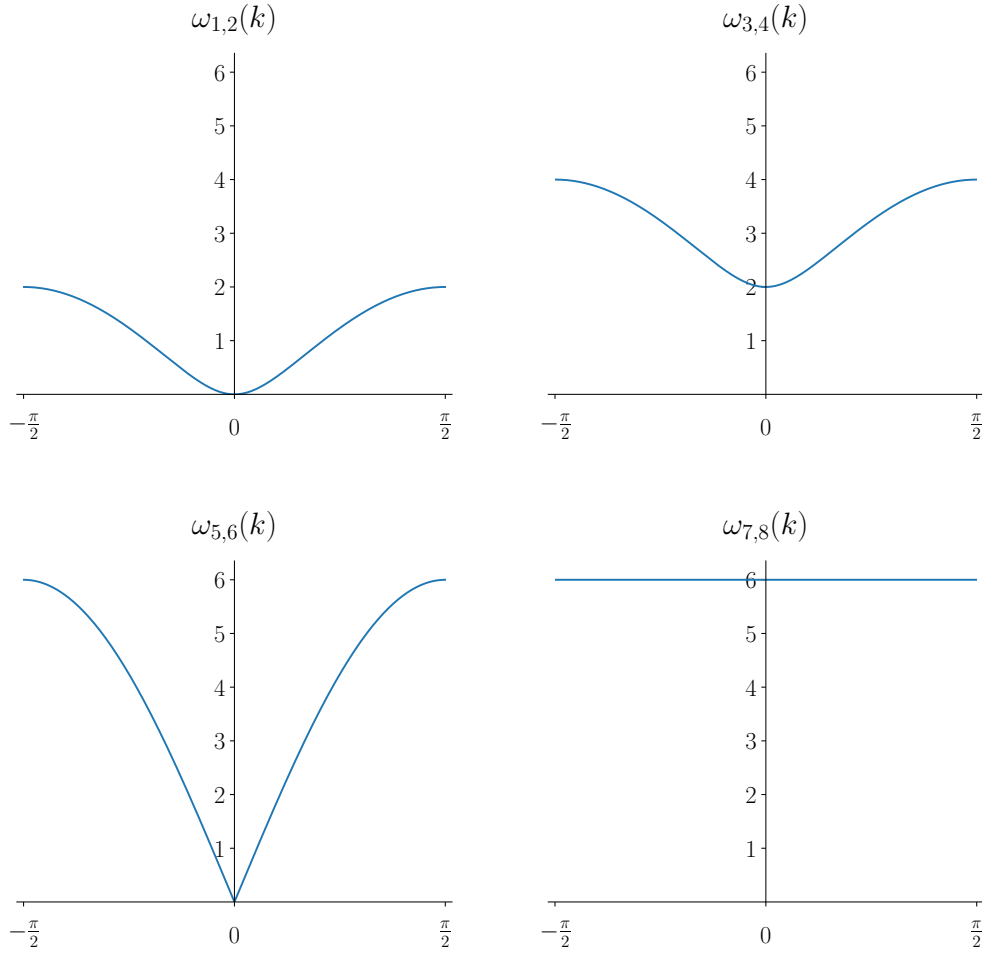
Figure 3.4 – The dispersion relations of the bipartite chain for $p = 2$, $q = 1$.

conjugate irrep calculations done in subsection 3.1.2. For the self-conjugate irreps $p = q$, the dispersive spectra become

$$\omega_{1,2}(\mathbf{k}) = 2p|\sin k|, \qquad \omega_{3,4}(\mathbf{k}) = 2p|\sin k|.$$
$$\omega_{5,6}(\mathbf{k}) = 4p|\sin k|, \qquad \omega_{7,8}(\mathbf{k}) = 4p,$$

(3.45)

matching the dispersion relations we had in Eq. (3.25). However, for general p and q, that is not the case. In general, it is possible to have linear dispersion and quadratic dispersion simultaneously. The Figure 3.4 shows the dispersion relations for $p = 2$, $q = 1$ as an example.

We see that there are two dispersive modes $\omega_{5,6}$ linear in k for small values of k, and four quadratic modes $\omega_{1,2,3,4}$. Two of them, $\omega_{1,2}$, are gapless whereas $\omega_{3,4}$ are gapped. The behaviour of these quadratic modes is reminiscent of the ferrimagnetic models like the antiferromagnetic Heisenberg alternating-spin chains with two different spins, S and s. More details

on these can be found, for example, in Refs. [81, 82, 83]. These models exhibit one gapless quadratic mode exactly like $\omega_{1,2}$ and one gapped quadratic mode exactly like $\omega_{3,4}$, where p, q take the role of S, s. The gapless branch is called the ferromagnetic branch as it reduces the magnetisation of the system, and the gapped branch is called the antiferromagnetic branch has it enhances the magnetisation. These ferrimagnetic systems thus show both ferromagnetic and antiferromagnetic characteristics. Our SU(3) $[p, q]$ model is physically similar to the ferrimagnetic models: the modes $\omega_{3,4,5,6}$ coming from the generators $\hat{S}_C^B, \hat{S}_B^C, \hat{S}_C^A, \hat{S}_A^C$ exhibit a ferrimagnetic behaviour, because the asymmetry of p, q is similar to having two different spins S, s. In addition, the generators $\hat{S}_B^A, \hat{S}_A^B$ show a purely antiferromagnetic behaviour by yielding linearly dispersive modes: exchanging one colour A in the initial condensate $\tiny\begin{array}{|c|c|c|}\hline A & A & A \\\hline C \\\cline{1-1}\end{array}$ with a colour B of a neighbouring site is purely antisymmetric in nature as there is no colour B initially in the condensate.

This model thus has a very unique property of possessing both a ferrimagnetic and an antiferromagnetic behaviour. These characteristics have also been confirmed by Kyle Warmer and Ian Affleck by obtaining the low-energy behaviour of this model using field-theoretical calculations. It would be worth investigating this model further as there are lots of interesting physical questions arising from the mixture of ferrimagnetic and antiferromagnetic characteristics.

This concludes the use of the Mathur & Sen bosons for the application of LFWT for arbitrary SU(3) irreps $[p, q]$. With this bosonic representation, the process of obtaining the dispersion relations seems a little easier than with the multiboson method and it yields significantly less flat modes in which we are not interested in our physical models. However, we have only discussed the case $N = 3$ so far. How would things work for $N > 3$?

3.3   What about $N > 3$?

The construction of Mathur & Sen rely on the fact that $\square$ and $\begin{array}{|c|}\hline\\\hline\\\hline\end{array}$ are conjugate to each other and that their tensor products can form any other irrep of SU(3). For SU(3), this is great as one can build states of any irrep easily by using more products of bosons a and b representing the Young diagrams $\square$ and $\begin{array}{|c|}\hline\\\hline\\\hline\end{array}$, i.e., by "gluing" both types of boxes together next to each other, as the SU(3) Young tableaux can only have two rows of boxes at most. If we were to consider SU(4), however, the fundamental irrep $\square$ and its conjugate irrep $\begin{array}{|c|}\hline\\\hline\\\hline\end{array}$ are not enough to cover all the irreps of SU(4), in this logic of putting the Young tableaux together one next to each other: the self-conjugate antisymmetric irrep $\begin{array}{|c|}\hline\\\hline\end{array}$ would also be needed, which is completely antisymmetric like $\begin{array}{|c|}\hline\\\hline\end{array}$.

In fact, there are $N-1$ completely antisymmetric irreps (with one column in the Young tableau) in SU(N) in general, and we thus need $N - 1$ families of bosons $a_\mu, b_\nu, \ldots$ who represent the states of each of the $N - 1$ completely antisymmetric irrep, as explained in a subsequent article by Mathur and Mani [78] and in Georgi [59]'s book as well. Hence, the construction we used for SU(3) can be generalised for any N by introducing more boson families, but the bosonic

representation of $\hat{S}_\nu^\mu$ has to be found for the irreps ⊟, ⊟ etc. unlike the irrep □ and its conjugate irrep for which the generators $\hat{S}_\nu^\mu$ are easily expressed.

Coming back to the example of $N = 4$, we would have the bosons a for □ and the bosons b for ⊟, similarly to the SU(3) case. In addition, if we were to generalise Eq. (3.3) for SU(4), the representation of the generators T_k ($k \in \{1, \ldots, N^2 - 1\}$) in the irrep ⊟ would be needed to be found for the new boson family $c_1, \ldots, c_6$ describing the six states of ⊟ as well. This is, however, nothing else than the multiboson approach we used in subsection 2.1.1: this is exactly what we did in (2.4). The conclusion is that the LFWT expansion using the Mathur & Sen bosons differ from the multiboson approach in general, e.g., with mixed irreps. But if we were to apply the LFWT with Mathur & Sen bosons for SU(4) ⊟ model in in subsection 2.1.1, it would be identical to the multiboson method.

We have now seen the multiboson method and the Mathur & Sen boson method. They deliver a robust way of performing LFWT, but the calculations can be cumbersome for SU(N) irreps with many boxes in the Young tableau. One can then ask the following question: is there a better-suited bosonic representation for performing the LFWT in general SU(N) irreps? Luckily, Mathur and his collaborators have already thought of a bosonic representation that is more adequate to our need in Ref. [80], and this will be the subject of the next chapter.

IV Linear Flavour-Wave with Read and Sachdev Bosons

Introduction: yet another bosonic representation

This chapter is the result of the collaboration with Karlo Penc, Pierre Nataf and Frédéric Mila [62], along with some useful discussions with Ian Affleck. This time, the harmonic quantum fluctuations will be considered using a different bosonic representation to express the $SU(N)$ generators. This bosonic representation is briefly mentioned by Read and Sachdev in Ref. [8] for $SU(N)$ irreps corresponding to rectangular Young diagrams (e.g. ⊞) with m rows and n_c columns. It is also mentioned in a different mathematical context by Mathur and his collaborators in Ref. [80] in a more general way for any general $SU(N)$ irrep. It is a bosonic representation that extends the well-known Schwinger bosons in $SU(2)$, and it incorporates the symmetry of the Young tableaux.

In this chapter, we will name the new bosons the Read & Sachdev bosons. As we shall see, the computation of the dispersive modes are easier with these bosons for N in general, the way in which we implement the condensate has to be adapted for different irreps.

4.1 Read and Sachdev bosonic representation for rectangular Young tableaux

Before proceeding to the general case, let us first settle with $SU(N)$ irreps with rectangular Young diagram containing m lines and n_c columns. The method will be nearly identical for arbitrary irreps as well, but this will allow for a clearer presentation.

In this bosonic representation, we attribute a boson to each colour and each line of the Young tableau.[11] Which means that in our rectangular case, we will have bosons $d_{\mu a}$ with the colour index $\mu \in \{A, B, \ldots\} \equiv 1 \ldots, N$ and the row index $a \in \{1, \ldots, m\}$. The $SU(N)$ generators $\hat{S}^\mu_\nu$ can

---

[11] Note that this is different from the boson representation introduced in subsection 1.1.3. In that case, the bosons had a colour index and a particle index (related to the number of particles per site).

then be written as

$$\hat{S}_\nu^\mu = \sum_{a=1}^{m} d_{\nu a}^\dagger d_{\mu a} - \frac{\hat{n}}{N}\delta_{\mu\nu}, \tag{4.1}$$

where

$$\hat{n} = \sum_{a=1}^{m} \hat{n}_a = \sum_{a=1}^{m}\sum_{\mu=1}^{N} d_{\mu a}^\dagger d_{\mu a} \tag{4.2}$$

is the total number operator, the Greek letters μ, ν are the color indices and the Latin letters $a, b \in \{1, \ldots, m\}$ are the row indices. The second term in Eq. (4.1) is to satisfy $\sum_\mu S_\mu^\mu = 0$ and can be dropped for the subsequent discussion. This construction naturally satisfy the SU(N) commutation relations (1.23).

If we are working in a given irrep, a set of constraints have to be imposed to ensure that the states indeed belong to the irrep in question:

$$\sum_{\mu=1}^{N} d_{\mu a}^\dagger d_{\mu b} = n_c \delta_{ab}, \tag{4.3}$$

These constraints are a generalisation of the constraints of the SU(2) Schwinger bosons. Here, the constraints involving different rows enforce the antisymmetry of the irrep.

Finally, the Heisenberg Hamiltonian in this bosonic representation can be given by

$$\begin{aligned}
\mathcal{H} &= J \sum_{<i,j>} \sum_{\mu,\nu=1}^{N} \hat{S}_\nu^\mu(i)\hat{S}_\mu^\nu(j) \\
&= J \sum_{<i,j>} \sum_{\mu,\nu=1}^{N} \sum_{a,b=1}^{m} d_{\nu a}^\dagger(i) d_{\mu a}(i) d_{\mu b}^\dagger(j) d_{\nu b}(j).
\end{aligned} \tag{4.4}$$

4.1.1 SU(4) $m = 2$ **on the square lattice**

Let us now reconsider the SU(4) $m = 2, n_c = 1$ square lattice model that we already explored in subsection 2.1.1, with the Read & Sachdev bosons this time. It would be instructive to see how the states of the irrep with m vertical boxes can be created. Let us define the antisymmetric tensor operator

$$A_{\mu_1\mu_2\cdots\mu_m}^\dagger = \frac{1}{\sqrt{m!}}\sum_{a_1=1}^{m}\sum_{a_2=2}^{m}\cdots\sum_{a_m=1}^{m} \epsilon^{a_1,a_2,\cdots a_m} d_{\mu_1 a_1}^\dagger d_{\mu_2 a_2}^\dagger \cdots d_{\mu_m a_m}^\dagger \tag{4.5}$$

in which the fully antisymmetrical Levi-Civita tensor $\epsilon^{a_1,a_2,\cdots a_m}$ is used. This tensor operator contains a sum of m bosonic creation operators. This tensor thus creates a state defined in the

antisymmetric irrep with m rows when applied on the vacuum, e.g.

$$A^\dagger_{\mu\nu\dots}\,|0\rangle = \frac{1}{\sqrt{2}}\left(|\mu\nu\rangle - |\nu\mu\rangle\right). \tag{4.6}$$

Coincidentally, the Read & Sachdev bosons for such a fully antisymmetric irrep are identical to the defining bosons in subsection 1.1.3.

Moving on to the colour order configuration, we consider, as before, the ordered bipartite configuration on the square lattice with the colours A and B on the sublattice Λ_{AB} and the colours C and D on the sublattice Λ_{CD}. Our expansion parameter here is n_c, and we go to the semi-classical limit $n_c \to \infty$ in which there is the assumption of a condensate composed of colors A, B on the sites $i \in \Lambda_{AB}$ and a condensate of colors C, D on the sites $j \in \Lambda_{CD}$. To apply the Holstein-Primakoff in this setting of condensates is, however, somewhat tricky because there are four condensates which are not independent of one another: for Λ_{AB}, there is the condensate related to the boson b_{A1}, but also those who are related to the bosons b_{B1}, b_{A2} and b_{B2}. This is because number operators $\langle \hat{n}_{A1}\rangle$, $\langle \hat{n}_{B1}\rangle$, $\langle \hat{n}_{A2}\rangle$ and $\langle \hat{n}_{B2}\rangle$ are all equally dominant in the limit of $n_c \to \infty$, see Appendix B for more details. If we were to apply the Holstein-Primakoff prescription with these, one would need to take the constraints involving the same row indices in Eq. (4.3),

$$\sum_{\mu=1}^{N} d^\dagger_{\mu 1} d_{\mu 1} = n_c, \qquad\qquad \sum_{\mu=1}^{N} d^\dagger_{\mu 2} d_{\mu 2} = n_c, \tag{4.7}$$

and gather somehow the terms that are large for the square-root expansion to be well-defined. In addition, in order to apply the Holstein-Primakoff prescription consistently, the commutation relations (1.23) should ideally be satisfied up to order $\mathcal{O}(1)$ (this has always been true in the previous cases). Unfortunately, there is no consistent way of choosing one Holstein-Primakoff expansion satisfying all the aforementioned requirements, and they all lead to different results at the end. We hence turn to the Bogoliubov substitution, namely the substitution of the condensed bosons with c-numbers, in the spirit of Bogoliubov's calculations of superfluidity [84]. Since the expectation of $\langle \hat{n}_{A1}\rangle$, $\langle \hat{n}_{A2}\rangle$, $\langle \hat{n}_{B1}\rangle$, $\langle \hat{n}_{B1}\rangle$ are large with respect to the others for Λ_{AB} (and $\langle \hat{n}_{C1}\rangle$, $\langle \hat{n}_{C2}\rangle$, $\langle \hat{n}_{D1}\rangle$, $\langle \hat{n}_{D2}\rangle$ for Λ_{CD}), the c-number substitution in our model is then

$$\begin{aligned}
d^\dagger_{Aa}(i) &\to z^*_{Aa}, & d^\dagger_{Ba}(i) &\to z^*_{Ba}, \\
d^\dagger_{Ca}(j) &\to z^*_{Ca}, & d^\dagger_{Da}(j) &\to z^*_{Da},
\end{aligned} \tag{4.8}$$

for any $i \in \Lambda_{AB}$, $j \in \Lambda_{CD}$, and $a \in \{1,\dots,2\}$. It is worthwhile noting that the conventional spin-wave calculations of SU(2) using the Holstein-Primakoff bosons in the harmonic order amounts to using the c-number replacement for condensed bosons.

With this, the constraints (4.3) for the sublattice Λ_{AB} to order $\mathcal{O}(n_c)$ are reduced to

$$\begin{cases} z_{A1}^* z_{A1} + z_{B1}^* z_{B1} = n_c \\ z_{A2}^* z_{A2} + z_{B2}^* z_{B2} = n_c \\ z_{A1}^* z_{A2} + z_{B1}^* z_{B2} = 0. \end{cases} \tag{4.9}$$

It is to be noted that the complex-conjugate counterpart of the third equation has been dropped as both are equivalent. These constraints can be neatly written in a matrix form U_{AB} by defining

$$z_{\mu a} =: \sqrt{n_c}\, [U_{AB}]_{\mu a} \tag{4.10}$$

with $\mu \in \{A, B\}$ (i.e., the first $\frac{N}{2}$ colors) and $a \in \{1, \ldots, m\}$. What is nice about this is that the constraints (4.9) is translated into a unitarity condition on the matrix U_{AB}. One side remark here: optionally, it is possible to parametrise the matrix elements of U_{AB} as vectors on the Bloch sphere. We can write the constraints (4.3) as

$$\begin{cases} \sum_{a,b} z_{Aa}^* \delta_{a,b} z_{Ab} + \sum_{a,b} z_{Ba}^* \delta_{a,b} z_{Bb} = 2n_c, \\ \sum_{a,b} z_{Aa}^* \sigma_{a,b}^{(\alpha)} z_{Ab} + \sum_{a,b} z_{Ba}^* \sigma_{a,b}^{(\alpha)} z_{Bb} = 0, \end{cases} \tag{4.11}$$

with the Pauli matrices $\sigma_{a,b}^{(\alpha)}$ ($\alpha = x, y, z$), or equivalently,

$$\begin{cases} \mathbf{z}_A^* \cdot \mathbf{z}_A + \mathbf{z}_B^* \cdot \mathbf{z}_B = 2n_c, \\ \mathbf{z}_A^* \cdot \sigma^{(\alpha)} \cdot \mathbf{z}_A + \mathbf{z}_B^* \cdot \sigma^{(\alpha)} \cdot \mathbf{z}_B = 0. \end{cases} \tag{4.12}$$

We can then consider (z_{A1}^*, z_{A2}^*) and (z_{B1}^*, z_{B2}^*) as two SU(2) spinors, and they can be parametrized as

$$z_{A1} = \sqrt{n_c}\, e^{i\chi_{AB}} \cos\frac{\vartheta_{AB}}{2}, \qquad z_{A2} = \sqrt{n_c}\, e^{i\chi_{AB}} \sin\frac{\vartheta_{AB}}{2} e^{-i\varphi_{AB}},$$
$$z_{B1} = \sqrt{n_c}\, \sin\frac{\vartheta_{AB}}{2}, \qquad\qquad z_{B2} = -\sqrt{n_c}\, \cos\frac{\vartheta_{AB}}{2} e^{-i\varphi_{AB}}. \tag{4.13}$$

This ends the consideration of the constraints for the sublattice Λ_{AB}. The same consideration naturally applies to the remaining sublattice Λ_{CD}. In the limit of large n_c, we again start from the constraints (4.3) to obtain

$$\begin{cases} z_{C1}^* z_{C1} + z_{D1}^* z_{D1} = n_c \\ z_{C2}^* z_{C2} + z_{D2}^* z_{D2} = n_c \\ z_{C1}^* z_{C2} + z_{D1}^* z_{D2} = 0, \end{cases} \tag{4.14}$$

which can be rewritten further in a (unitary) matrix form U_{CD},

$$z_{\mu a} =: \sqrt{n_c}\, [U_{CD}]_{\mu a} \tag{4.15}$$

with $\mu \in \{C, D\}$ (i.e., the remaining $\frac{N}{2}$ colors) and $a \in \{1,2\} \equiv \{1,\ldots,m\}$. Alternately, the $z_{\mu a}$ can be parametrised as

$$z_{C1} = \sqrt{n_c}\, e^{i\chi_{CD}} \cos\frac{\vartheta_{CD}}{2}, \qquad z_{C2} = \sqrt{n_c}\, e^{i\chi_{CD}} \sin\frac{\vartheta_{CD}}{2} e^{-i\varphi_{CD}},$$
$$z_{D1} = \sqrt{n_c} \sin\frac{\vartheta_{CD}}{2}, \qquad z_{D2} = -\sqrt{n_c} \cos\frac{\vartheta_{CD}}{2} e^{-i\varphi_{CD}}. \tag{4.16}$$

We are finally ready to replace the bosons $d_{Aa}(i), d_{Ba}(i), d_{Ca}(j), d_{Da}(j)$ (with $a \in \{1,2\}$) and their adjoint counterparts in the Hamiltonian Eq. (4.4) by the corresponding c-numbers above. This yields the harmonic Hamiltonian $\mathscr{H}^{(2)}$ of the order $\mathcal{O}(n_c)$. We can first apply the Fourier transform by introducing the bosons $a_{\mu a}(\mathbf{k})$ for the sublattice Λ_{ACA} and $b_{\mu a}(\mathbf{k})$ for the sublattice Λ_{BCB},

$$d_{\mu a}(i) = \sqrt{\frac{2}{N_{\text{sites}}}} \sum_{\mathbf{k}\in\text{RBZ}} a_{\mu a}(\mathbf{k}) e^{-i\mathbf{k r}_i}, \qquad b_{\mu a}(j) = \sqrt{\frac{2}{N_{\text{sites}}}} \sum_{\mathbf{k}\in\text{RBZ}} b_{\mu a}(\mathbf{k}) e^{-i\mathbf{k r}_j}, \tag{4.17}$$

with N_{sites} being the number of sites. The quadratic Hamiltonian $\mathscr{H}^{(2)}$ is then given by

$$\mathscr{H} = \frac{z_{\text{sq}} J n_c}{2} \sum_{\mathbf{k}\in\text{RBZ}} \left(\mathbf{u}_{\mathbf{k}}^\dagger, \mathbf{u}_{-\mathbf{k}}\right) M_{\mathbf{k}} \begin{pmatrix} {}^{\mathsf{t}}\mathbf{u}_{\mathbf{k}} \\ {}^{\mathsf{t}}\mathbf{u}_{-\mathbf{k}}^\dagger \end{pmatrix} - 2 z_{\text{sq}} J n_c N, \tag{4.18}$$

with $z_{\text{sq}} = 4$ the coordination number and

$$\mathbf{u}_{\mathbf{k}}^\dagger = \left(a_{C1}^\dagger(\mathbf{k}), a_{C2}^\dagger(\mathbf{k}), a_{D1}^\dagger(\mathbf{k}), a_{D2}^\dagger(\mathbf{k}), b_{A1}^\dagger(\mathbf{k}), b_{A2}^\dagger(\mathbf{k}), b_{B1}^\dagger(\mathbf{k}), b_{B2}^\dagger(\mathbf{k})\right),$$
$$\mathbf{u}_{-\mathbf{k}} = \left(a_{C1}(-\mathbf{k}), a_{C2}(-\mathbf{k}), a_{D1}(-\mathbf{k}), a_{D2}(-\mathbf{k}), b_{A1}(-\mathbf{k}), b_{A2}(-\mathbf{k}), b_{B1}(-\mathbf{k}), b_{B2}(-\mathbf{k})\right),$$
$$M_{\mathbf{k}} = \frac{1}{2}\begin{pmatrix} \mathbb{1}_8 & \mathscr{B}_{\mathbf{k}} \\ \mathscr{B}_{\mathbf{k}}^\dagger & \mathbb{1}_8 \end{pmatrix}, \tag{4.19}$$
$$\mathscr{B}_{\mathbf{k}} = \begin{pmatrix} 0 & \gamma_{\text{sq},\mathbf{k}} U^\mathsf{T} \\ \gamma_{\text{sq},\mathbf{k}} U & 0 \end{pmatrix}.$$

The geometrical factor $\gamma_{\text{sq},\mathbf{k}} = \frac{1}{2}(\cos k_x + \cos k_y)$ is the one defined in Eq. (2.16). The matrix U comes from U_{AB} and U_{CD}, i.e., $U_{AB} \otimes U_{CD}^\mathsf{T}$ with permuted columns, and is thus also unitary:

$$U = \begin{pmatrix} z_{A1}z_{C1} & z_{A2}z_{C1} & z_{A1}z_{D1} & z_{A2}z_{D1} \\ z_{A1}z_{C2} & z_{A2}z_{C2} & z_{A1}z_{D2} & z_{A2}z_{D2} \\ z_{B1}z_{C1} & z_{B2}z_{C1} & z_{B1}z_{D1} & z_{B2}z_{D1} \\ z_{B1}z_{C2} & z_{B2}z_{C2} & z_{B1}z_{D2} & z_{B2}z_{D2} \end{pmatrix}. \tag{4.20}$$

It is important to note that this structure of U and of $M_{\mathbf{k}}$ is a consequence of the structure of the Hamiltonian in Eq. (4.18) inherited from the Bogoliubov prescription and the constraints (4.9) and (4.14), and it remains true in general for any values of N and corresponding m. For example, the diagonal entries in M_k being proportional to 1 is a direct consequence of the

constraints involving the same row indices. For a different value of m, the only change will be the size of the matrices U_{AB} and U_{CD}, but the unitarity condition will still remain, and this general structure of $M_{\mathbf{k}}$ will not change.

We can now diagonalize the matrix by using the generalised Bogoliubov transformation. As explained in section 1.2, the matrix $Y = \sigma_z \otimes \mathbb{1}_8$ is used in the Bogoliubov transformation, and the eigenvalues of the matrix $Y M_{\mathbf{k}}$ yield the dispersion relations $\omega_{\mathbf{k}}$. The eigenvalues λ_ζ in this case can be found easily thanks to the simple block structure of $Y M_{\mathbf{k}}$ and by observing that

$$\mathscr{B}_{\mathbf{k}}^\dagger \mathscr{B}_{\mathbf{k}} = \begin{pmatrix} \left|\gamma_{\mathrm{sq},\mathbf{k}}\right|^2 \mathbb{1}_8 & 0 \\ 0 & \left|\gamma_{\mathrm{sq},\mathbf{k}}\right|^2 \mathbb{1}_8 \end{pmatrix} \tag{4.21}$$

for any unitary matrix U. From this, it follows that

$$\begin{aligned} Y M_{\mathbf{k}} Y M_{\mathbf{k}} &= \frac{1}{4}\left(1 - \left|\gamma_{\mathbf{k}}\right|^2\right) \mathbb{1}_{16} \\ &= \lambda^2 \mathbb{1}_{16}, \end{aligned} \tag{4.22}$$

from which we can conclude that the eigenvalues λ_ζ

$$\lambda_\zeta = \pm \frac{1}{2}\sqrt{1 - \left|\gamma_{\mathrm{sq},\mathbf{k}}\right|^2}. \tag{4.23}$$

By regrouping all the terms and by labelling the new Bogoliubov bosons f_ζ, diagonalized quadratic Hamiltonian can be finally given by

$$\mathscr{H} = J n_c \sum_{\mathbf{k} \in \mathrm{RBZ}} \omega_{\mathrm{sq}}(\mathbf{k}) \sum_{\zeta=1}^{8} \left(f_\zeta^\dagger(\mathbf{k}) f_\zeta(\mathbf{k}) + \frac{1}{2}\right) - 2zJn_c N, \tag{4.24}$$

where the eight-fold degenerate dispersion relation $\omega_{\mathrm{sq},\mathbf{k}}$ is given by

$$\omega_{\mathrm{sq}}(\mathbf{k}) = z_{\mathrm{sq}}\sqrt{1 - \left|\gamma_{\mathrm{sq},\mathbf{k}}\right|^2}. \tag{4.25}$$

The dispersion relation obtained here is identical to the dispersion relation (2.20) obtained with the multiboson method in 2.1.1, which is reassuring. Since we started from $mN = \frac{N^2}{2}$ bosons for each sublattice and condensed half of the bosons in each sublattice afterwards, we end up with $\frac{N^2}{2} \cdot 2/2 = \frac{N^2}{2} = 8$ modes in the reduced Brillouin zone (or $\frac{N^2}{4}$ in the extended Brillouin zone), which also corresponds to the number of modes obtained with the multiboson method. Furthermore, there is an added bonus that the multipolar flat modes (in which we were not interested for our physical problem) are absent when using this method.

Let us briefly draw the reader's attention to the fact the derivation of the dispersion relation (4.25) above shows that the dispersion relation does not depend on the choice of the values of $z_{\mu a}$ as long as they satisfy the constraints (4.9) and (4.14) of the semi-classical limit. The constraints here, as we have seen, is equivalent to the unitarity condition of the matrices

U_{AB} and U_{CD}. If we use the parametrisation (4.13) and (4.16) for simplicity, this means that the dispersion relation will be the same whatever the choice of values for the set of parameters $\vartheta_{AB}, \varphi_{AB}, \chi_{AB}$ or $\vartheta_{CD}, \varphi_{CD}, \chi_{CD}$: there exists a gauge degree of freedom for each sublattice.

4.1.2 SU(6) $m = 2$ on the triangular lattice

We know from previous considerations that the structure of the Hamiltonian does not fundamentally change with the geometry of the lattices considered in section 2.1, since we always regroup the bonds between two different pairs of sublattices. Hence, this method can be identically used for the square, honeycomb and triangular lattices in the two-sublattice or three-sublattice configuration. To briefly illustrate this, let us come back to the the SU(6) $m = 2$ Heisenberg model on the tripartite triangular lattice subsection 2.1.3. With colours A, B on the sublattice Λ_{AB}, C, D on Λ_{CD} and E, F on Λ_{EF}, let us decompose the Hamiltonian $\mathcal{H}$ into three sub-Hamiltonians, namely,

$$\mathcal{H} = \mathcal{H}_{AB-CD} + \mathcal{H}_{CD-EF} + \mathcal{H}_{EF-AB}, \tag{4.26}$$

where H_{AB} contains the bonds between Λ_{AB} and Λ_{CD} etc. If we now concentrate on $\mathcal{H}_{AB-CD}$, we arrive to the conclusion that the semi-classical approximation and the Bogoliubov prescription leads to the constraints

$$\begin{cases} z_{A1}^*(i)z_{A1}(i) + z_{B1}^*(i)z_{B1}(i) = n_c \\ z_{A2}^*(i)z_{A2}(i) + z_{B2}^*(i)z_{B2}(i) = n_c \\ z_{A1}^*(i)z_{A2}(i) + z_{B1}^*(i)z_{B2}(i) = 0 \end{cases} \tag{4.27}$$

for $i \in \Lambda_{AB}$, and

$$\begin{cases} z_{C1}^*(j)z_{C1}(j) + z_{D1}^*(j)z_{D1}(j) = n_c \\ z_{C2}^*(j)z_{C2}(j) + z_{D2}^*(j)z_{D2}(j) = n_c \\ z_{C1}^*(j)z_{C2}(j) + z_{D1}^*(j)z_{D2}(j) = 0, \end{cases} \tag{4.28}$$

for $j \in \Lambda_{CD}$, which are identical to Eqs. (4.27) and (4.28). Following the same procedure in subsection 4.1.1, one can replace the condensate bosons by c-numbers satisfying the constraints above. In this case with the three-sublattice order, higher-order terms are generated in the Hamiltonian, unlike in the two-sublattice order calculations where the resulting Hamiltonian is purely quadratic. In other words, the c-number replacement will generate

$$\mathcal{H} = \mathcal{H}^{(2)} + \mathcal{H}^{(3)} + \mathcal{H}^{(4)}, \tag{4.29}$$

where $\mathcal{H}^{(2)} \propto \mathcal{O}(n_c)$, $\mathcal{H}^{(1)} \propto \mathcal{O}(n_c^{\frac{1}{2}})$ and $\mathcal{H}^{(1)} \propto \mathcal{O}(1)$. However, once we truncate the Hamiltonian to keep the dominant term of the order $\mathcal{O}(n_c)$ only, the rest of the calculations are, in fact, identical. The only differences are the factors that depend on the geometry of the lattice

such as $z_{\mathrm{tri}} = 3$ and $\gamma_{\mathrm{tri},\mathbf{k}} = \frac{1}{3}\left(e^{ik_x} + 2e^{-i\frac{1}{2}k_x}\cos\frac{\sqrt{3}}{2}k_y\right)$. Using the Fourier transform,

$$d_{\mu a}(i) = \sqrt{\frac{2}{N_{\mathrm{sites}}}}\sum_{\mathbf{k}\in\mathrm{RBZ}} a_{\mu a}(\mathbf{k})e^{-i\mathbf{k}\mathbf{r}_i}, \qquad d_{\mu a}(j) = \sqrt{\frac{2}{N_{\mathrm{sites}}}}\sum_{\mathbf{k}\in\mathrm{RBZ}} b_{\mu a}(\mathbf{k})e^{-i\mathbf{k}\mathbf{r}_j}, \qquad (4.30)$$

as before with bosons a and b defined on two different sublattices. All in all we obtain an identical sub-Hamiltonian up to geometrical factors:

$$\mathcal{H}_{AB-CD} = Jn_c\sum_{\mathbf{k}\in\mathrm{RBZ}}\omega_{\mathrm{tri}}(\mathbf{k})\sum_{\zeta=1}^{8}\left(f_\zeta^\dagger(\mathbf{k})f_\zeta(\mathbf{k}) + \frac{1}{2}\right) + \mathrm{const.}. \qquad (4.31)$$

with

$$\omega_{\mathrm{tri}}(\mathbf{k}) = z_{\mathrm{tri}}\sqrt{1 - \left|\gamma_{\mathrm{tri},\mathbf{k}}\right|^2}. \qquad (4.32)$$

As for the calculations of $\mathcal{H}_{CD-EF}$ and $\mathcal{H}_{EF-AB}$ involving the sites $l \in \Lambda_{EF}$, we need the constraints,

$$\begin{cases} z_{E1}^*(l)z_{E1}(l) + z_{F1}^*(l)z_{F1}(l) = n_c \\ z_{E2}^*(l)z_{E2} + z_{F2}^*(l)z_{F2}(l) = n_c \\ z_{E1}^*(l)z_{E2} + z_{F1}^*(l)z_{F2}(l) = 0, \end{cases} \qquad (4.33)$$

and the Fourier transform

$$d_{\mu a}(l) = \sqrt{\frac{2}{N_{\mathrm{sites}}}}\sum_{\mathbf{k}\in\mathrm{RBZ}} c_{\mu a}(\mathbf{k})e^{-i\mathbf{k}\mathbf{r}_l}. \qquad (4.34)$$

We see that the calculations will also be identical as in 4.1.1, but with different bosons. Finally, the sum of all the sub-Hamiltonians yields

$$\mathcal{H} = \sum_{\mathbf{k}}\left[\omega_{\mathrm{tri}}(\mathbf{k})\sum_{\zeta=1}^{8}\left(f_\zeta^\dagger(\mathbf{k})f_\zeta(\mathbf{k}) + \frac{1}{2}\right)\right] + \mathrm{const.} \qquad (4.35)$$

in the extended Brillouin zone. As in the multiboson method, we obtain 8 modes in the extended Brillouin zone with the same dispersion relation, again without the flat multipolar modes. The terms that contribute in the order $\mathcal{O}(n_c)$ from this sub-Hamiltonian $\mathcal{H}_{AB-CD}$ are the terms that involve the color permutations $A, B \leftrightarrow C, D$, i.e., the permutation of the colours that are present in the initial condensate—this is also the case in the multiboson approach. As we see here, the lattice geometry just needs to be adapted once we have the method established.

In the next subsection, we briefly present the explicit solutions of the constraints for an arbitrary m and the corresponding value N.

4.1.3 Arbitrary m

As explained in the derivation of the dispersion relation of the SU(4) $m = 2$ square lattice model, the analysis in subsection 4.1.1 can be straightforwardly applied to any arbitrary m (and to the corresponding N) for a given lattice, thanks to the preservation of the structure of the Hamiltonian (4.18). It has also been pointed out that the resulting dispersion relation is identical whatever the values of the c-numbers $z_{\mu a}$ as long as they satisfy the generalized Schwinger constraints. For practical purposes, however, we can also simply use a definite value for $z_{\mu a}$ when calculating the dispersion relation. We thus present here a possible general solution for the constraints for any value of m and show that it indeed yields the dispersion relation obtained above in a general way.

For a given m (or corresponding N), let us assume that we have the color-ordered ground states we considered in the previous cases (square/honeycomb/triangular lattices). We will designate the number of the sublattices by n_{sub}, and each sublattice will be denoted by $l \in \{1, \dots, n_{\text{sub}}\}$. The colours of the condensate on the sublattice l will be indexed by μ. Since there are m particles per site, they will take a value between 1 and m. There will also be row indices $a, b \in \{1, \dots, m\}$. After the Bogoliubov prescription in the limit $n_c \to \infty$, the generalised Schwinger constraints become

$$\sum_{\mu^l = 1}^{m} z_{\mu a}^{l*} z_{\mu b}^{l} = \delta_{ab} n_c. \tag{4.36}$$

for each sublattice l with corresponding condensate colors μ.

Using the identity $\sum_{n_{\text{sub}}=0}^{n-1} e^{q \frac{2\pi i}{n} n_{\text{sub}}} = 0$, where $n \in \mathbb{N}_{>2}$ and $q \in \{1, \dots, n-1\}$, it can be easily verified that

$$z_{\mu a}^{l} \to \varphi_{\mu a}^{l}(m) \sqrt{\frac{n_c}{m}} := \sqrt{n_c} U_{\mu a}^{l}, \tag{4.37}$$

with the phase $\varphi_{\mu a}^{l}(m)$ defined by

$$\varphi_{\mu a}^{l}(m) := e^{-i(a-1)\frac{2\pi}{m}\mu}. \tag{4.38}$$

is a particular solution of the constraints (4.36). An example of the phases for four condensed bosons per site ($m = 4$) is shown in Table 4.1. This corresponds to the SU(8) model on the square/honeycomb lattice or the SU(12) model on the triangular lattice. If we take the values of Table 4.1 for the square lattice model as an example, we can easily perform the generalised Bogoliubov transformation and obtain

$$\mathcal{H} = \sum_{\mathbf{k}} \left[\omega_{\text{sq}}(\mathbf{k}) \sum_{\zeta=1}^{16} \left(f_{\zeta}^{\dagger}(\mathbf{k}) f_{\zeta}(\mathbf{k}) + \frac{1}{2} \right) \right] + \text{const.}, \tag{4.39}$$

i.e. 16 modes in the extended Brillouin zone with the same dispersion relation as in Eq. (4.25).

$\mu \in \{A, B, C, D\}$	$a = 1$	$a = 2$	$a = 3$	$a = 4$
A	0	e^{-ix}	e^{-2ix}	e^{-3ix}
B	0	e^{-2ix}	e^{-4ix}	e^{-6ix}
C	0	e^{-3ix}	e^{-6ix}	e^{-9ix}
D	0	e^{-4ix}	e^{-8ix}	e^{-12ix}

Table 4.1 – Phases $\varphi_{\mu a}(m)$ of the numbers replacing the condensed bosons that satisfy the antisymmetry constraints for $m = 4$. The phase $\varphi_{\mu a}$ for a given μ and a can be read from the Table, in which $x := \frac{2\pi}{m}$.

This, again, agrees with the results of the multiboson calculations (2.46) without the flat modes.

In general, there are Nm bosons per site with the Read & Sachdev bosons, from which $\frac{N}{n_{\text{sub}}} m = m^2$ bosons are replaced by complex numbers. After the Bogoliubov transformation to diagonalise the Hamiltonian, this procedure yields $Nm - m^2 = m(N - m)$ modes in the extended Brillouin zone: this corresponds to the number of dispersive modes we have found with the multiboson approach, see. Eq. (2.46) and subsection 2.1.4.

4.1.4   The magnetisation

We have figured out how to derive the low-energy spectra of these models using the Read & Sachdev bosons, but it would be neat to be able to compute the ordered colour moment as well. Let us take the SU(4) model with $m = 2$ on the square lattice, and try to calculate the ordered moment by using the definition in Eq. (2.28):

$$
\begin{aligned}
m_i &= \frac{1}{2}\left(\sum_{\mu=A}^{B} S_\mu^\mu(i) - \sum_{\mu=C}^{D} S_\mu^\mu(i)\right), \\
&= \frac{1}{2}\Big(\langle \hat{n}_{A1} + \hat{n}_{A2}\rangle + \langle \hat{n}_{B1} + \hat{n}_{B2}\rangle - \langle \hat{n}_{C1} + \hat{n}_{C2}\rangle - \langle \hat{n}_{D1} + \hat{n}_{D2}\rangle\Big) \\
&= \frac{1}{2}\Big(\langle \hat{n}_{A1} + \hat{n}_{B1}\rangle + \langle \hat{n}_{A2} + \hat{n}_{B2}\rangle - \langle \hat{n}_{C1} + \hat{n}_{C2}\rangle - \langle \hat{n}_{D1} + \hat{n}_{D2}\rangle\Big) \\
&= \frac{1}{2}\big[\big(1 - \langle \hat{n}_{C1}\rangle - \langle \hat{n}_{D1}\rangle\big) + \big(1 - \langle \hat{n}_{C2}\rangle - \langle \hat{n}_{D2}\rangle\big) \\
&\qquad - \langle \hat{n}_{C1} + \hat{n}_{C2}\rangle - \langle \hat{n}_{D1} + \hat{n}_{D2}\rangle\big] \\
&= 1 - \Big(\langle \hat{n}_{C1}\rangle + \langle \hat{n}_{D1}\rangle + \langle \hat{n}_{C2}\rangle + \langle \hat{n}_{D2}\rangle\Big).
\end{aligned}
\tag{4.40}
$$

Here, the constraints (4.3) and the assumption of a large condensate of $\langle \hat{n}_{A1}\rangle, \langle \hat{n}_{B1}\rangle, \langle \hat{n}_{A2}\rangle, \langle \hat{n}_{B2}\rangle$ have been used in the forth line. The expectation values in the last line depend on the result of the Bogoliubov transformation which depends on the initial values of $z_{\mu a}$.

If we choose the values

$$z_{A1}^{(*)}(i), z_{B2}^{(*)}(i) \to \sqrt{n_c}, \qquad\qquad z_{C1}^{(*)}(j), z_{D2}^{(*)}(j) \to \sqrt{n_c},$$
$$z_{A2}^{(*)}(i), z_{B1}^{(*)}(i) \to 0, \qquad\qquad z_{C2}^{(*)}(j), z_{D1}^{(*)}(j) \to 0 \tag{4.41}$$

that satisfy our constraints and that correspond to having A on the first row and B on the second row for $i \in \Lambda_{AB}$ (and similarly with C and D for Λ_{CD}), then the Hamiltonian we obtain $\mathcal{H} = \sum_{\alpha=1}^{4} \mathcal{H}_\alpha$ is given by

$$\mathcal{H}_1 = n_c \sum_{\mathbf{k} \in \text{RBZ}} \left[z_{\text{sq}} \left(d_{C1,\mathbf{k}}^\dagger d_{C1,\mathbf{k}} + d_{A1,\mathbf{k}}^\dagger d_{A1,\mathbf{k}} \right) + z_{\text{sq}} \gamma_{\text{sq},\mathbf{k}} \left(d_{C1,\mathbf{k}}^\dagger b_{A1,-\mathbf{k}}^\dagger + d_{C1,\mathbf{k}} d_{A1,-\mathbf{k}} \right) \right],$$

$$\mathcal{H}_2 = n_c \sum_{\mathbf{k} \in \text{RBZ}} \left[z_{\text{sq}} \left(d_{C2,\mathbf{k}}^\dagger d_{C2,\mathbf{k}} + d_{B1,\mathbf{k}}^\dagger d_{B1,\mathbf{k}} \right) + z_{\text{sq}} \gamma_{\text{sq},\mathbf{k}} \left(d_{C2,\mathbf{k}}^\dagger d_{B1,-\mathbf{k}}^\dagger + d_{C2,\mathbf{k}} d_{B1,-\mathbf{k}} \right) \right],$$

$$\mathcal{H}_3 = n_c \sum_{\mathbf{k} \in \text{RBZ}} \left[z_{\text{sq}} \left(d_{D1,\mathbf{k}}^\dagger d_{D1,\mathbf{k}} + d_{A2,\mathbf{k}}^\dagger d_{A2,\mathbf{k}} \right) + z_{\text{sq}} \gamma_{\text{sq},\mathbf{k}} \left(d_{D1,\mathbf{k}}^\dagger d_{A2,-\mathbf{k}}^\dagger + d_{D1,\mathbf{k}} d_{A2,-\mathbf{k}} \right) \right], \tag{4.42}$$

$$\mathcal{H}_4 = n_c \sum_{\mathbf{k} \in \text{RBZ}} \left[z_{\text{sq}} \left(d_{D2,\mathbf{k}}^\dagger d_{D2,\mathbf{k}} + d_{B2,\mathbf{k}}^\dagger d_{B2,\mathbf{k}} \right) + z_{\text{sq}} \gamma_{\text{sq},\mathbf{k}} \left(d_{D2,\mathbf{k}}^\dagger d_{B2,-\mathbf{k}}^\dagger + d_{D2,\mathbf{k}} d_{B2,-\mathbf{k}} \right) \right].$$

The structure of the Hamiltonian is identical to the one obtained with the multiboson method, Eq. (2.15), without the flat modes. Then we can use the same Bogoliubov transformation as in Eq. (2.17) for each of the sub-Hamiltonians. For instance, we define the new Bogoliubov bosons $\tilde{d}$ for $\mathcal{H}_1$ as

$$\begin{pmatrix} \tilde{d}_{C1,\mathbf{k}}^\dagger \\ \tilde{d}_{A1,-\mathbf{k}} \end{pmatrix} = \begin{pmatrix} u_{\mathbf{k}} & v_{\mathbf{k}} \\ v_{\mathbf{k}} & u_{\mathbf{k}} \end{pmatrix} \begin{pmatrix} d_{C1,\mathbf{k}}^\dagger \\ d_{A1,-\mathbf{k}} \end{pmatrix}, \tag{4.43}$$

where

$$u_{\mathbf{k}} = \sqrt{\frac{1}{2}\left(\frac{z_{\text{sq}}}{\omega_{\text{sq},\mathbf{k}}} + 1\right)}, \qquad v_{\mathbf{k}} = \sqrt{\frac{1}{2}\left(\frac{z_{\text{sq}}}{\omega_{\text{sq},\mathbf{k}}} - 1\right)},$$
$$\omega_{\text{sq}}(\mathbf{k}) = z_{\text{sq}} \sqrt{1 - \left|\gamma_{\text{sq},\mathbf{k}}\right|^2}. \tag{4.44}$$

The expectation values in Eq. (4.40) can then be computed:

$$\langle \hat{n}_{C1} \rangle = \langle \hat{n}_{D1} \rangle = \langle \hat{n}_{C2} \rangle = \langle \hat{n}_{D2} \rangle = \left\langle v_{\mathbf{k}}^2 \right\rangle. \tag{4.45}$$

This is identical to what we had found in Eq. (2.26) with the multiboson method. We can then conclude that

$$m_i = 1 - 4\left\langle v_{\mathbf{k}}^2 \right\rangle$$
$$= 0.214, \tag{4.46}$$

which is consistent with the multiboson approach, see Eq. (2.27).

We can thus conclude that the choice of values for $z_{\mu a}$ in Eq. (4.41) indeed yields the colour

magnetisation value that is identical to the value found with the multiboson approach. Such choice of condensates (putting different colours on different rows) works for the other cases as well, e.g., the SU(6) $m = 3$ model on the square lattice, and the calculations are again the same as in the multiboson method. It should be checked whether this is the case for any solutions of the constraints (4.36), but we believe that this is true for any solutions.

This wraps up our discussion on the fully antisymmetric irreps using the Read & Sachdev bosons. Let us now investigate how these bosons could be used in irreps with mixed symmetries by taking the SU(3) adjoint model once again.

4.2 The SU(3) adjoint irrep

As an example of the use of the bosonic representation of Read & Sachdev on non-rectangular irreps, let us come back to the irrep ⊞ of SU(3) from section 2.2 and chapter III, which is of dimension 8. To describe the states of this irrep, we will thus need bosons $d_{\mu a}$ where $\mu \in \{A, B, C\}$ and $a \in \{1, 2\}$ since there are maximum two rows in ⊞. We will denote the maximal row-length of the Young diagram of a given irrep by m, so $m = 2$ in our case. As before, the states of this irrep have to satisfy the generalized Schwinger constraints

$$
\begin{cases}
d_{A1}^\dagger d_{A1} + d_{B1}^\dagger d_{B1} + d_{C1}^\dagger d_{C1} = 2 \\
d_{A2}^\dagger d_{A2} + d_{B2}^\dagger d_{B2} + d_{C2}^\dagger d_{C2} = 1 \\
d_{A1}^\dagger d_{A2} + d_{B1}^\dagger d_{B2} + d_{C1}^\dagger d_{C2} = 0,
\end{cases}
\tag{4.47}
$$

The antisymmetry of the rows 1 and 2 is implemented through the last equation of (4.47). Note that the conjugate of the last equation is not part of the constraints anymore, in contrast to the irreps with rectangular Young tableaux. The expression of the generators $\hat{S}_\nu^\mu$ remains the same as in Eq. (4.2),

$$
\hat{S}_\nu^\mu = \sum_{a=1}^m d_{\nu a}^\dagger d_{\mu a} - \frac{\hat{n}}{N} \delta_{\mu\nu},
\tag{4.48}
$$

even though the Young diagram of the irrep is not rectangular. We will, once again, drop the second term that does not influence the rest of our calculations.

4.2.1 Constructing the states with the Read & Sachdev Bosons

Although it is not necessary to have an explicit expression of the states of our irrep in terms of the Read & Sachdev bosons to perform the LFWT expansion, it is still instructive to look at the construction of the states.

Following the footsteps in subsection 4.1.1, we could try something similar to Eqs. (4.5)

and (4.6). To construct the state $\boxed{\begin{smallmatrix} A & A \\ C \end{smallmatrix}} \equiv ACA$, we could do

$$\boxed{\begin{smallmatrix} A & A \\ C \end{smallmatrix}} = A_{AC}^\dagger b_{A1}^\dagger = \epsilon^{ab} d_{Aa}^\dagger d_{Cb}^\dagger d_{A1}^\dagger |0\rangle. \tag{4.49}$$

in which we used the Einstein summation convention. As with the other bosonic representations we have seen in this thesis, such a construction works well for the states that have no degeneracy in the weight diagram, but there is a freedom in the choice of the states of the doubly degenerate zero-weight states (the two states involving three colours $\boxed{\begin{smallmatrix} A & B \\ C \end{smallmatrix}}$ and $\boxed{\begin{smallmatrix} A & C \\ B \end{smallmatrix}}$). To use the same choice of basis as in the rest of the thesis (and this also presents a systematic way of creating these states with this Read & Sachdev bosonic language), we can take the basis we had in Table 1.1, and translate it into the Read & Sachdev bosons. For example, let us recall from Eq. (1.25) that

$$\boxed{\begin{smallmatrix} A & A \\ C \end{smallmatrix}} \equiv \frac{1}{\sqrt{2}}(|ACA\rangle - |CAA\rangle) = \left(b_{A,1}^\dagger b_{C,2}^\dagger - b_{C,1}^\dagger b_{A,2}^\dagger\right) b_{A,3}^\dagger |0\rangle \tag{4.50}$$

if we use the natural bosonic representation in subsection 1.1.3. The first two colour particles are antisymmetric, and the third colour comes with the particle index $_3$ indicating that it is the third particle. In the Weyl diagram, the third particle sits in the second column that contains one row only. In the Read & Sachdev language, this means that this third colour particle A should be represented by d_{A1}, i.e., with the row index $_1$. Proceeding this way and by adapting the normalisation constant, we can translate all the states in Table 2.1 into the bosonic representation of Read & Sachdev, the result of which is given as follows in Table 4.2:

$$
\begin{array}{lcllcl}
\boxed{\begin{smallmatrix} A & A \\ C \end{smallmatrix}} & \equiv & \frac{1}{\sqrt{3}}\epsilon^{ab} d_{Aa}^\dagger d_{Cb}^\dagger d_{A1}^\dagger |0\rangle &
\boxed{\begin{smallmatrix} A & A \\ B \end{smallmatrix}} & \equiv & \frac{1}{\sqrt{3}}\epsilon^{ab} d_{Aa}^\dagger d_{Bb}^\dagger d_{A1}^\dagger |0\rangle \\[2mm]
\boxed{\begin{smallmatrix} A & B \\ B \end{smallmatrix}} & \equiv & \frac{1}{\sqrt{3}}\epsilon^{ab} d_{Aa}^\dagger d_{Bb}^\dagger d_{B1}^\dagger |0\rangle &
\boxed{\begin{smallmatrix} B & B \\ C \end{smallmatrix}} & \equiv & -\frac{1}{\sqrt{3}}\epsilon^{ab} d_{Ba}^\dagger d_{Cb}^\dagger d_{B1}^\dagger |0\rangle \\[2mm]
\boxed{\begin{smallmatrix} B & C \\ C \end{smallmatrix}} & \equiv & -\frac{1}{\sqrt{3}}\epsilon^{ab} d_{Ba}^\dagger d_{Cb}^\dagger d_{C1}^\dagger |0\rangle &
\boxed{\begin{smallmatrix} A & C \\ C \end{smallmatrix}} & \equiv & -\frac{1}{\sqrt{3}}\epsilon^{ab} d_{Aa}^\dagger d_{Cb}^\dagger d_{C1}^\dagger |0\rangle \\[2mm]
\boxed{\begin{smallmatrix} A & B \\ C \end{smallmatrix}} & \equiv & -\frac{1}{\sqrt{6}}\left(\epsilon^{ab} d_{Ba}^\dagger d_{Cb}^\dagger d_{A1}^\dagger\right. &
\boxed{\begin{smallmatrix} A & C \\ B \end{smallmatrix}} & \equiv & \frac{1}{\sqrt{2}}\epsilon^{ab} d_{Aa}^\dagger d_{Bb}^\dagger d_{C1}^\dagger |0\rangle \\[2mm]
& & \left.+\epsilon^{ab} d_{Aa}^\dagger d_{Cb}^\dagger d_{B1}^\dagger\right)|0\rangle & & &
\end{array}
$$

Table 4.2 – The states of the SU(3) adjoint irrep.

These states obey the constraints (4.47) as it should, and it can be verified that the action of the generators on one of these states generate the states of this adjoint irrep only, thus showing that the action of the generators is closed as it should. Also, all the transitions and their coefficients are identical to those found in subsection 2.2.1 as it should.

4.2.2 LFWT on a bipartite 1D chain

We now proceed to the computation of the spectrum using the LFWT. Using the SU(3) operators in the Read & Sachdev bosonic representation (4.48), we obtain the Heisenberg Hamiltonian in this representation

$$
\begin{aligned}
\mathcal{H} &= J \sum_{<i,j>} \sum_{\mu,\nu=1}^{3} \hat{S}_{\nu}^{\mu}(i) \hat{S}_{\mu}^{\nu}(j) \\
&= J \sum_{<i,j>} \sum_{\mu,\nu=1}^{3} \sum_{a,b=1}^{m} d_{\nu a}^{\dagger}(i) d_{\mu a}(i) d_{\mu b}^{\dagger}(j) d_{\nu b}(j)
\end{aligned}
\tag{4.51}
$$

up to a constant.

The constraints of this irrep are given by

$$
\begin{cases}
\sum_{\mu=1}^{3} d_{\mu 1}^{\dagger} d_{\mu 1} = 2 n_c \\
\sum_{\mu=1}^{3} d_{\mu 2}^{\dagger} d_{\mu 2} = n_c \\
\sum_{\mu=1}^{3} d_{\mu 1}^{\dagger} d_{\mu 2} = 0,
\end{cases}
\tag{4.52}
$$

where μ is the color index, and n_c is our expansion parameter as before, which will be set to 1 at the end.

As before, we assume a bipartite system with $\boxed{\begin{smallmatrix} A & A \\ \hline C \end{smallmatrix}}$ on the sublattice Λ_{ACA} and $\boxed{\begin{smallmatrix} B & B \\ \hline C \end{smallmatrix}}$ on the other sublattice Λ_{BCB}, i.e. we consider

$$
\begin{aligned}
\left| \mathrm{gs}(i) \right\rangle &:= \tilde{C} \left[\epsilon^{ab} d_{Aa}^{\dagger}(i) d_{Cb}^{\dagger}(i) d_{A1}^{\dagger}(i) \right]^{n_c} |0\rangle, \\
\left| \mathrm{gs}(j) \right\rangle &:= \tilde{C} \left[\epsilon^{ab} d_{Ba}^{\dagger}(j) d_{Cb}^{\dagger}(j) d_{B1}^{\dagger}(j) \right]^{n_c} |0\rangle,
\end{aligned}
\tag{4.53}
$$

for any $i \in \Lambda_{ACA}$, $j \in \Lambda_{BCB}$ and $a \in \{1, 2\}$, with $\tilde{C}$ being the normalisation constant. In the limit $n_c \to \infty$, the dominant numbers are

$$
\begin{aligned}
\left\langle d_{A1}^{\dagger}(i) d_{A1}(i) \right\rangle &= 2 n_c, & \left\langle b_{C2}^{\dagger}(i) d_{C2}(i) \right\rangle &= n_c, \\
\left\langle d_{B1}^{\dagger}(j) d_{B1}(j) \right\rangle &= 2 n_c, & \left\langle d_{C2}^{\dagger}(j) d_{C2}(j) \right\rangle &= n_c,
\end{aligned}
\tag{4.54}
$$

and other quadratic combinations of bosons are small compared to these values, see sec-

tion 2.2. Hence, we can use the Holstein-Primakoff approach:

$$
\begin{aligned}
d_{A1}^\dagger(i), d_{A1}(i) &\longrightarrow \sqrt{2n_c - \sum_{\mu \neq A} b_{\mu 1}^\dagger(i) d_{\mu 1}(i)} \approx \sqrt{2n_c} - \frac{1}{2\sqrt{2n_c}} \sum_{\mu \neq A} d_{\mu 1}^\dagger(i) d_{\mu 1}(i), \\
d_{C2}^\dagger(i), d_{C2}(i) &\longrightarrow \sqrt{n_c - \sum_{\mu \neq C} d_{\mu 2}^\dagger(i) d_{\mu 2}(i)} \approx \sqrt{n_c} - \frac{1}{2\sqrt{n_c}} \sum_{\mu \neq C} d_{\mu 2}^\dagger(i) d_{\mu 2}(i), \\
d_{B1}^\dagger(j), d_{B1}(j) &\longrightarrow \sqrt{2n_c - \sum_{\mu \neq B} d_{\mu 1}^\dagger(j) d_{\mu 1}(j)} \approx \sqrt{2n_c} - \frac{1}{2\sqrt{2n_c}} \sum_{\mu \neq B} d_{\mu 1}^\dagger(j) d_{\mu 1}(j), \\
d_{C2}^\dagger(j), d_{C2}(j) &\longrightarrow \sqrt{n_c - \sum_{\mu \neq C} d_{\mu 2}^\dagger(j) d_{\mu 2}(j)} \approx \sqrt{n_c} - \frac{1}{2\sqrt{n_c}} \sum_{\mu \neq C} d_{\mu 2}^\dagger(j) d_{\mu 2}(j).
\end{aligned}
\tag{4.55}
$$

The truncation of the Taylor series at this order is sufficient to obtain all the terms of the quadratic Hamiltonian of the order n_c. As in the other cases where we have used the Holstein-Primakoff bosons, the commutation relations (1.23) stay valid up to order $\mathcal{O}(1)$ even after this transformation.

Note that the ground states (4.53) (trivially) satisfy the constraints (4.47) in the limit $n_c \to \infty$:

$$
\begin{cases}
\sum_{\alpha=1}^{3} d_{\alpha 1}^\dagger(l) d_{\alpha 1}(l) \big| \mathrm{gs}(l) \big\rangle = 2n_c \big| \mathrm{gs}(l) \big\rangle, \\
\sum_{\alpha=1}^{3} d_{\alpha 2}^\dagger(l) d_{\alpha 2}(l) \big| \mathrm{gs}(l) \big\rangle = n_c \big| \mathrm{gs}(l) \big\rangle, \\
\sum_{\alpha=1}^{3} d_{\alpha 1}^\dagger(l) d_{\alpha 2}(l) \big| \mathrm{gs}(l) \big\rangle = 0,
\end{cases}
\tag{4.56}
$$

for any site l.

By using the Holstein-Primakoff bosons, we finally obtain the quadratic Hamiltonian

$$
\mathcal{H}^{(2)} = \mathcal{H}_1^{(2)} + \mathcal{H}_2^{(2)} + \mathcal{H}_3^{(2)} \qquad \text{where}
$$

$$
\begin{aligned}
\mathcal{H}_1^{(2)} &= Jn_c \sum_{i \in \Lambda_{ACA}} \sum_{\langle j \rangle} \Big[2d_{B1}^\dagger(i) d_{B1}(i) + 2d_{A1}^\dagger(j) d_{A1}(j) + 2d_{B1}(i) d_{A1}(j) + 2d_{B1}^\dagger(i) d_{A1}^\dagger(j) \Big], \\
\mathcal{H}_2^{(2)} &= Jn_c \sum_{i \in \Lambda_{ACA}} \sum_{\langle j \rangle} \Big[-d_{A2}^\dagger(i) d_{A2}(i) + d_{A2}^\dagger(j) d_{A2}(j) + d_{C1}^\dagger(i) d_{C1}(i) \\
&\qquad + d_{A2}^\dagger(i) d_{A2}(j) + d_{A2}^\dagger(j) d_{A2}(i) + \sqrt{2} d_{C1}^\dagger(i) d_{A2}^\dagger(j) + \sqrt{2} d_{C1}(i) d_{A2}(j) \Big], \\
\mathcal{H}_3^{(2)} &= Jn_c \sum_{i \in \Lambda_{ACA}} \sum_{\langle j \rangle} \Big[-d_{B2}^\dagger(j) d_{B2}(j) + d_{B2}^\dagger(i) d_{B2}(i) + d_{C1}^\dagger(j) d_{C1}(j) \\
&\qquad + d_{B2}^\dagger(i) d_{B2}(j) + d_{B2}^\dagger(j) d_{B2}(i) + \sqrt{2} d_{B2}^\dagger(i) d_{C1}^\dagger(j) + \sqrt{2} d_{B2}(i) d_{C1}(j) \Big].
\end{aligned}
\tag{4.57}
$$

After Fourier-transforming,

$$d_{\mu a}(i) = \sqrt{\frac{2}{N_{\text{sites}}}} \sum_{k \in \text{RBZ}} a_{\mu a}(k) e^{-ikr_i}, \qquad d_{\mu a}(j) = \sqrt{\frac{2}{N_{\text{sites}}}} \sum_{k \in \text{RBZ}} b_{\mu a}(k) e^{-ikr_j}, \quad (4.58)$$

with the k-space bosons a and b for sublattices Λ_{ACA} and Λ_{BCB}, respectively, and N_{sites} being the number of sites, the Hamiltonian is then given by

$$\mathcal{H}^{(2)} = Jn_c \sum_{k \in \text{RBZ}} \sum_{a=1}^{3} \left(\mathbf{u}_{a,k}^{\dagger}, \mathbf{u}_{a,-k} \right) M_{a,k} \begin{pmatrix} {}^{\text{t}}\mathbf{u}_{a,k} \\ {}^{\text{t}}\mathbf{u}_{a,-k}^{\dagger} \end{pmatrix} \tag{4.59}$$

where

$$\begin{aligned}
\mathbf{u}_{1,k}^{\dagger} &:= \left(a_{B1}^{\dagger}(k), b_{A1}^{\dagger}(k) \right), & \mathbf{u}_{1,-k} &:= \left(a_{B1}(-k), b_{A1}(-k) \right), \\
\mathbf{u}_{2,k}^{\dagger} &:= \left(a_{A2}^{\dagger}(k), b_{A2}^{\dagger}(k), a_{C1}^{\dagger}(k) \right), & \mathbf{u}_{2,-k} &:= \left(a_{A2}(-k), b_{A2}(-k), a_{C1}(-k) \right), \\
\mathbf{u}_{3,k}^{\dagger} &:= \left(b_{B2}^{\dagger}(k), a_{B2}^{\dagger}(k), b_{C1}^{\dagger}(k) \right), & \mathbf{u}_{3,-k} &:= \left(b_{B2}(-k), a_{B2}(-k), b_{C1}(-k) \right),
\end{aligned} \tag{4.60a}$$

$$\begin{aligned}
M_{1,k} &:= \begin{pmatrix} \mathcal{A}_1 & \mathcal{B}_{1,k} \\ \mathcal{B}_{1,k} & \mathcal{A}_1 \end{pmatrix}, & \mathcal{A}_1 &:= 2 \cdot \mathbb{1}_2 & \mathcal{B}_{1,k} &:= 2 \begin{pmatrix} 0 & \gamma_k \\ \gamma_k & 0 \end{pmatrix}, \\[2mm]
M_{2,k} &:= \begin{pmatrix} \mathcal{A}_2 & \mathcal{B}_{2,k} \\ \mathcal{B}_{2,k} & \mathcal{A}_2 \end{pmatrix}, & \mathcal{A}_2 &:= \begin{pmatrix} -1 & \gamma_k & 0 \\ \gamma_k & 1 & 0 \\ 0 & 0 & 1 \end{pmatrix}, & \mathcal{B}_{2,k} &:= \begin{pmatrix} 0 & 0 & 0 \\ 0 & 0 & \sqrt{2}\gamma_k \\ 0 & \sqrt{2}\gamma_k & 0 \end{pmatrix}, \quad (4.60b) \\[2mm]
M_{3,k} &:= M_{2,k},
\end{aligned}$$

with the geometrical factor of a bipartite chain

$$\gamma_k := \cos k. \tag{4.61}$$

Using the generalized Bogoliubov transformation, i.e. by calculating the positive eigenvalues of

$$M_k' := \begin{pmatrix} \mathcal{A} & \mathcal{B}_k \\ -\mathcal{B}_k & -\mathcal{A} \end{pmatrix}, \tag{4.62}$$

we finally obtain the diagonalised Hamiltonian

$$\boxed{\mathcal{H}^{(2)} = Jn_c \sum_{k \in \text{RBZ}} \left\{ \sum_{\mu=1}^{6} \omega_\mu(k) \left(f_\mu^{\dagger}(k) f_\mu(k) + \frac{1}{2} \right) + \omega_7 f_7^{\dagger}(k) f_7(k) + \omega_8 f_8^{\dagger}(k) f_8(k) \right\} + \text{const.}}$$
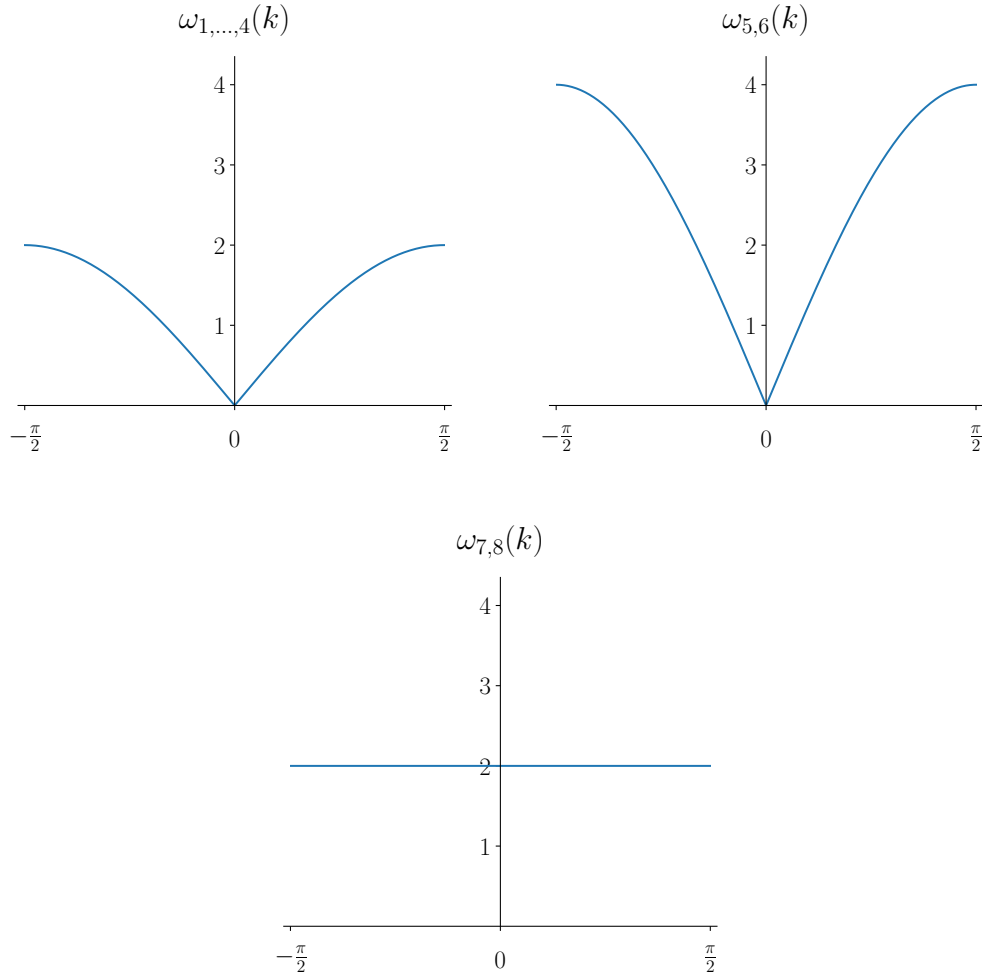
$$\tag{4.63}$$

Figure 4.1 – The dispersion relations $\omega_{1,...,8}$ for $p = 1$ (adjoint irrep).

where the bosons f_μ are the new Bogoliubov bosons, and

$$
\begin{aligned}
\omega_{1,2,3,4}(k) &= 2\sqrt{1 - \cos^2(k)}, \\
\omega_{5,6}(k) &= 4\sqrt{1 - \cos^2(k)}, \\
\omega_{7,8} &= 2.
\end{aligned}
\tag{4.64}
$$

The dispersion relations are plotted in Figure 4.1. The dispersive modes $\omega_{1,...,6}$ are identical to the dispersive modes obtained with the multiboson method in Eq. (2.82) and with the Mathur & Sen bosons in Eq. (3.25).

The matrix M_1 in the Hamiltonian (4.59) that yields the dispersives modes with higher velocity comes from the exchange terms $\hat{S}_B^A(i)\hat{S}_A^B(j)$, $\hat{S}_A^B(i)\hat{S}_B^A(j)$, $\hat{S}_A^A(i)\hat{S}_A^A(j)$ and $\hat{S}_B^B(i)\hat{S}_B^B(j)$ in the Hamiltonian, just as in the two other methods used in this thesis. This also indicates that this

dispersive mode with higher velocity is related to the transition from the condensate states $\boxed{\begin{smallmatrix}A&A\\C&\end{smallmatrix}}$ to $\boxed{\begin{smallmatrix}A&B\\C&\end{smallmatrix}}$ (or from $\boxed{\begin{smallmatrix}B&B\\C&\end{smallmatrix}}$ to $\boxed{\begin{smallmatrix}A&B\\C&\end{smallmatrix}}$), as explained in subsection 2.2.3 with the multiboson method.

The matrices M_2 that yield half of the remaining dispersive modes come from $\hat{S}_C^A(i)\hat{S}_A^C(j)$, $\hat{S}_A^C(i)\hat{S}_C^A(j)$, $\hat{S}_A^A(i)\hat{S}_A^A(j)$ and $\hat{S}_C^C(i)\hat{S}_C^C(j)$, again in line with the two other methods. This corresponds to the transition to the other adjacent states in the weight diagram. The same can be said about M_3. The remaining subspaces of M_2 and M_3 after the diagonalisation are revealed as flat modes as with the Mathur & Sen bosons. The Read & Sachdev bosons also seem to yield flat modes after the diagonalisation of the Hamiltonian when degenerate points are present in the weight diagram, due to the expression of the states (in terms of Read & Sachdev bosons) in these degenerate points. However, the exact nature of the flat modes is difficult to extract here in terms of the Read & Sachdev bosons. We know, though, that these flat modes come from the colour permutation of $A \leftrightarrow C$ and $B \leftrightarrow C$, whereas the flat modes obtained with the Mathur & Sen bosons came from $A \leftrightarrow B$. They thus correspond to different multipolar transitions, and this would explain why the energy of the flat modes differ by a factor 2 in both methods, see Eq. (4.64).

4.3 The $\mathrm{SU}(3)$ model in irreducible representation $[p,q]$ on the bipartite d-dimensional lattice

Now that the calculation method is known for the adjoint irrep $\boxed{}\!\!\boxed{}$ of SU(3), it is easy to extend the calculations to the irrep $[p,q]$ in a d-dimensional bipartite system. We admit the same ground state as in section 3.2. As an example, for $p=2, q=1$, it would be $\boxed{\begin{smallmatrix}A&A&A\\C&&\end{smallmatrix}}$ on the sublattice Λ_1 and $\boxed{\begin{smallmatrix}B&B&B\\C&&\end{smallmatrix}}$ on the other sublattice Λ_2. The coordinate number z here is given by $z = 2d$.

The following steps are nearly identical to the calculations of the adjoint irrep. First, the constraints of this irrep are given by

$$
\begin{cases}
\sum\limits_{\mu=A}^{C} d_{\mu 1}^\dagger d_{\mu 1} = (p+q) \\
\sum\limits_{\mu=A}^{C} d_{\mu 2}^\dagger d_{\mu 2} = q \\
\sum\limits_{\mu=A}^{C} d_{\mu 1}^\dagger d_{\mu 2} = 0,
\end{cases}
\tag{4.65}
$$

where μ is the color index. Then, the semi-classical limit of the bosons of the first row (namely $d_{A1}^{(\dagger)}(i), d_{B1}^{(\dagger)}(j)$) can be taken to be $(p+q) \to \infty$, and the bosons of the second row (namely

$d_{C2}^{(\dagger)}(i), d_{C2}^{(\dagger)}(j))$ can be taken to be $q \to \infty$. The Holstein-Primakoff approach can then be used:

$$
\begin{aligned}
d_{A1}^{\dagger}(i), d_{A1}(i) \quad &\longrightarrow \quad \sqrt{(p+q) - \sum_{\mu \neq A} d_{\mu 1}^{\dagger}(i) d_{\mu 1}(i)} \approx \sqrt{(p+q)} - \frac{1}{2\sqrt{(p+q)}} \sum_{\mu \neq A} d_{\mu 1}^{\dagger}(i) d_{\mu 1}(i), \\
d_{C2}^{\dagger}(i), d_{C2}(i) \quad &\longrightarrow \quad \sqrt{q - \sum_{\mu \neq C} d_{\mu 2}^{\dagger}(i) d_{\mu 2}(i)} \approx \sqrt{q} - \frac{1}{2\sqrt{q}} \sum_{\mu \neq C} d_{\mu 2}^{\dagger}(i) d_{\mu 2}(i), \\
d_{B1}^{\dagger}(j), d_{B1}(j) \quad &\longrightarrow \quad \sqrt{(p+q) - \sum_{\mu \neq B} d_{\mu 1}^{\dagger}(j) d_{\mu 1}(j)} \approx \sqrt{(p+q)} - \frac{1}{2\sqrt{(p+q)}} \sum_{\mu \neq B} d_{\mu 1}^{\dagger}(j) d_{\mu 1}(j), \\
d_{C2}^{\dagger}(j), d_{C2}(j) \quad &\longrightarrow \quad \sqrt{q - \sum_{\mu \neq C} d_{\mu 2}^{\dagger}(j) d_{\mu 2}(j)} \approx \sqrt{q} - \frac{1}{2\sqrt{q}} \sum_{\mu \neq C} d_{\mu 2}^{\dagger}(j) d_{\mu 2}(j).
\end{aligned}
\tag{4.66}
$$

By using the Holstein-Primkaoff bosons, we finally obtain the quadratic Hamiltonian of the order $\mathcal{O}(n_c)$

$$
\mathcal{H}^{(2)} = \mathcal{H}_1^{(2)} + \mathcal{H}_2^{(2)} + \mathcal{H}_3^{(2)} \qquad \text{where}
$$

$$
\begin{aligned}
\mathcal{H}_1^{(2)} = J \sum_{i \in \Lambda_1} \sum_{\langle j \rangle} \Big[&-q d_{A2}^{\dagger}(i) d_{A2}(i) + p d_{A2}^{\dagger}(j) d_{A2}(j) + q d_{C1}^{\dagger}(i) d_{C1}(i) \\
&+ q d_{A2}^{\dagger}(i) d_{A2}(j) + q d_{A2}^{\dagger}(j) d_{A2}(i) \\
&+ \sqrt{q(p+q)} d_{C1}^{\dagger}(i) d_{A2}^{\dagger}(j) + \sqrt{q(p+q)} d_{C1}(i) d_{A2}(j) \Big], \\
\mathcal{H}_2^{(2)} = J \sum_{i \in \Lambda_1} \sum_{\langle j \rangle} \Big[&-q d_{B2}^{\dagger}(j) d_{B2}(j) + p d_{B2}^{\dagger}(i) d_{B2}(i) + q d_{C1}^{\dagger}(j) d_{C1}(j) \\
&+ q d_{B2}^{\dagger}(i) d_{B2}(j) + q d_{B2}^{\dagger}(j) d_{B2}(i) \\
&+ \sqrt{q(p+q)} d_{B2}^{\dagger}(i) d_{C1}^{\dagger}(j) + \sqrt{q(p+q)} d_{B2}(i) d_{C1}(j) \Big], \\
\mathcal{H}_3^{(2)} = J \sum_{i \in \Lambda_1} \sum_{\langle j \rangle} \Big[&(p+q) d_{B1}^{\dagger}(i) d_{B1}(i) + (p+q) d_{A1}^{\dagger}(j) d_{A1}(j) \\
&+ (p+q) d_{B1}(i) d_{A1}(j) + (p+q) d_{B1}^{\dagger}(i) d_{A1}^{\dagger}(j) \Big].
\end{aligned}
\tag{4.67}
$$

After Fourier-transforming,

$$
d_{\mu a}(i) = \sqrt{\frac{2}{N_{\text{sites}}}} \sum_{\mathbf{k} \in \text{RBZ}} a_{\mu a}(k) e^{-i\mathbf{k} \cdot \mathbf{r}_i}, \qquad\qquad d_{\mu a}(j) = \sqrt{\frac{2}{N_{\text{sites}}}} \sum_{\mathbf{k} \in \text{RBZ}} b_{\mu a}(k) e^{-i\mathbf{k} \cdot \mathbf{r}_j}, \tag{4.68}
$$

by introducing two different bosons a and b for sublattices Λ_1 and Λ_2, respectively, the Hamiltonian is then given by

$$
\mathcal{H}^{(2)} = J d \sum_{\mathbf{k} \in \text{RBZ}} \sum_{a=1}^{3} \left(\mathbf{u}_{a,\mathbf{k}}^{\dagger}, \mathbf{u}_{a,-\mathbf{k}} \right) M_{a,\mathbf{k}} \begin{pmatrix} {}^{\text{t}}\mathbf{u}_{a,\mathbf{k}} \\ {}^{\text{t}}\mathbf{u}_{a,-\mathbf{k}}^{\dagger} \end{pmatrix} \tag{4.69}
$$

91

where

$$\mathbf{u}_{1,\mathbf{k}}^{\dagger} := \left(a_{A2}^{\dagger}(\mathbf{k}), b_{A2}^{\dagger}(\mathbf{k}), a_{C1}^{\dagger}(\mathbf{k})\right), \qquad \mathbf{u}_{1,-\mathbf{k}} := \left(a_{A2}(-\mathbf{k}), b_{A2}(-\mathbf{k}), a_{C2}(-\mathbf{k})\right),$$

$$\mathbf{u}_{2,\mathbf{k}}^{\dagger} := \left(b_{B2}^{\dagger}(\mathbf{k}), a_{B2}^{\dagger}(\mathbf{k}), b_{C1}^{\dagger}(\mathbf{k})\right), \qquad \mathbf{u}_{2,-\mathbf{k}} := \left(b_{B2}(-\mathbf{k}), a_{B2}(-\mathbf{k}), b_{C2}(-\mathbf{k})\right), \qquad (4.70)$$

$$\mathbf{u}_{3,\mathbf{k}}^{\dagger} := \left(a_{B1}^{\dagger}(\mathbf{k}), b_{A1}^{\dagger}(\mathbf{k})\right), \qquad \mathbf{u}_{3,-\mathbf{k}} := \left(a_{B1}(-\mathbf{k}), b_{A1}(-\mathbf{k})\right),$$

$$M_{1,\mathbf{k}} := \begin{pmatrix} \mathcal{A}_{1,\mathbf{k}} & \mathcal{B}_{1,\mathbf{k}} \\ \mathcal{B}_{1,\mathbf{k}}^{\dagger} & \mathcal{A}_{1,-\mathbf{k}}^{\mathsf{T}} \end{pmatrix}, \quad \mathcal{A}_{1,\mathbf{k}} := \begin{pmatrix} -q & q\gamma_{\mathbf{k}} & 0 \\ q\gamma_{\mathbf{k}} & p & 0 \\ 0 & 0 & q \end{pmatrix}, \quad \mathcal{B}_{1,\mathbf{k}} := \begin{pmatrix} 0 & 0 & 0 \\ 0 & 0 & \sqrt{q(p+q)}\gamma_{\mathbf{k}} \\ 0 & \sqrt{q(p+q)}\gamma_{\mathbf{k}} & 0 \end{pmatrix},$$

$$M_{2,\mathbf{k}} := M_{1,\mathbf{k}},$$

$$M_{3,\mathbf{k}} := \begin{pmatrix} \mathcal{A}_3 & \mathcal{B}_{3,\mathbf{k}} \\ \mathcal{B}_{3,\mathbf{k}}^{\dagger} & \mathcal{A}_3^{\mathsf{T}} \end{pmatrix}, \quad \mathcal{A}_{3,\mathbf{k}} := \begin{pmatrix} p+q & 0 \\ 0 & p+q \end{pmatrix}, \quad \mathcal{B}_{3,\mathbf{k}} := \begin{pmatrix} 0 & (p+q)\gamma_{\mathbf{k}} \\ (p+q)\gamma_{\mathbf{k}} & 0 \end{pmatrix},$$

$$(4.71)$$

with the geometrical factor

$$\gamma_{\mathbf{k}} := \begin{cases} \cos k_x, & d = 1 \\ \frac{1}{2}(\cos k_x + \cos k_y), & d = 2 \\ \frac{1}{3}(\cos k_x + \cos k_y + \cos k_z), & d = 3 \\ \dots \end{cases} \qquad (4.72)$$

The generalized Bogoliubov transformation then yields the diagonalized Hamiltonian

$$\mathcal{H}^{(2)} = J \sum_{\mathbf{k} \in \mathrm{RBZ}} \left\{ \sum_{\mu=1}^{8} \omega_{\mu}(\mathbf{k}) \left(f_{\mu}^{\dagger}(\mathbf{k}) f_{\mu}(\mathbf{k}) + \frac{1}{2} \right) \right\} + \mathrm{const.} \qquad (4.73)$$

where the bosons f_{μ} are the new Bogoliubov bosons, and

$$\omega_{1,2}(\mathbf{k}) = d \left(\sqrt{(p+q)^2 - 4pq\gamma_{\mathbf{k}}^2} - p + q \right),$$

$$\omega_{3,4}(\mathbf{k}) = d \left(\sqrt{(p+q)^2 - 4pq\gamma_{\mathbf{k}}^2} + p - q \right),$$

$$\omega_{5,6}(\mathbf{k}) = 2d(p+q)\sqrt{1 - \gamma_{\mathbf{k}}^2}, \qquad (4.74)$$

$$\omega_{7,8}(\mathbf{k}) = 2dq.$$

As noted with the help of Eq. (3.44), $\omega_{1,2,3,4}(\mathbf{k})$ are always positive as it should. Encouragingly, the dispersive spectra $\omega_{1,\dots,6}$ are identical to those obtained with the method using the Mathur & Sen bosonic representation. However, the localised $\omega_{7,8}$, again, do not match exactly.

In 1D ($d = 1$), if the parameters are again set to be $p = 2$, $q = 1$ to take an example of a non-self-conjugate irrep, we again find linear dispersion relations and quadratic dispersion relations simultaneously, see Figure 3.4.

This concludes this chapter on the use of Read & Sachdev bosons in the LFWT. The dispersive spectra obtained with this method are identical to the the ones obtained with the other methods we used in this thesis. However, the flat modes obtained here do not match exactly with the other methods, and the way of translating the condensate to a number differs from one irrep to another in this method.

We have now explored three different boson representations that leading to different schemes of applying the LFWT. Let us now present a summary of the differences between the boson representations in the next chapter.

V Recapitulation of the Boson Representations

The three different boson representations of SU(N) that we have encountered in this work—the multiboson representation, the Mathur & Sen representation and the Read & Sachdev representation—all present different advantages and inconveniences when performing the LFWT with them. We will briefly discuss them in this Chapter.

Let us look at the number of bosons of each of the boson representation first. With the multiboson method, in a given irrep, there is a one-to-one correspondence between a boson species and a state of the irrep. Hence, new bosons are introduced each time one considers a different irrep, as the bosons are tied to the states of each irrep. For instance, the bosons used for SU(3) ⊞ will not be the same as those for SU(3) ⊞⊞⊞. For an SU(N) irrep of dimension D, the number of boson species will be D. This means that the number of bosons can be very large if D is large (even for a small N). For obtaining the dispersion relations, the method is straightforward to apply for any irrep of SU(N), and the colour transition corresponding to a mode is clear to see since a boson is directly related to a state in this multiboson representation. However, the caveat is that it generates many flat modes corresponding to multipolar transitions. As the dimension of the irrep D increases, the number of flat modes increases as well. For instance, in the model with the SU(3) adjoint irrep in section 2.2, this method yielded 8 flat modes in the reduced Brillouin zone although we are only interested in the low-energy Goldstone modes. The calculations with this method can also be cumbersome as the bosonic representation of $\hat{S}_\nu^\mu$ must be found each time that one considers a different irrep.

In terms of the Young tableau, the Mathur & Sen representation introduces a boson for each state of the fully antisymmetric irreps with one column such as □, ⊟, etc. In a way, we think in terms of the columns of the Young tableaux in this boson representation. For instance, in the model with the SU(3) adjoint irrep ⊞ that we considered, we used 3 bosons a_μ corresponding to the 3 states of □ and 3 bosons b_ν corresponding to the 3 states of ⊟, with the constraint that $n_a = 1$ and $n_b = 1$ in addition to the tracelessness condition, see Eq. (3.6). The bosons a_μ and b_ν then allow us to construct the states of any generic irrep $[p, q]$ of SU(3) for arbitrary values of p and q with the corresponding constraints ($n_a = p$ and $n_b = q$) and the tracelessness condition. If one would extend this logic to SU(4), the states of any given irrep of SU(4) could

then be described with the 4 bosons a_μ of the fundamental irrep $\square$, the 4 bosons b_ν of its conjugate irrep $\begin{array}{c}\square\\\square\\\square\end{array}$ and the 6 bosons c_ρ of the self-conjugate irrep $\begin{array}{c}\square\\\square\end{array}$. For a general N, we would need $\sum_{m=1}^{N-1} \binom{N}{m} = 2^N - 2$ boson species at most, since a fully antisymmetric irrep with m boxes in the Young tableau with one column has a dimension of $\binom{N}{m}$. Depending on the irrep that is considered, the span of these bosons can be larger than the Hilbert space of the irrep, as it was the case with the SU(3) adjoint irrep we treated in previous chapters: the irrep $\begin{array}{cc}\square&\square\\\square&\end{array}$ has dimension $D = 8$, but the use of one boson a_μ and one boson b_ν together yields 9 states in total. This is thus the reason why the tracelessness condition has to be enforced. We also saw that there is a certain degree of freedom in the choice of the states that are degenerate in the weight diagram, see Figure 3.1. For generic models with SU(3) irreps $[p, q]$, the Mathur & Sen bosons are, in most cases, the best choice to work with, because the calculations are much more efficient than the multiboson method and it involves only the bosons of the fundamental irrep and of its conjugate irrep which are simple to deal with. In addition, the number of flat modes obtained with this method is smaller than in the multiboson method: for the SU(3) model with the adjoint irrep in subsection 3.1.2, we only had 2 flat modes (that came from the colour transition to the state that belongs to the degenerate weight in the weight diagram of $\begin{array}{cc}\square&\square\\\square&\end{array}$). In fact, we saw in section 3.2 that the number of flat modes stays constant (2) for any SU(3) irrep $[p, q]$.

For $N > 4$, however, the calculations of the dispersion relations can be performed much more efficiently with the Read & Sachdev bosons. In this formalism, for a given SU(N) irrep, a boson $d_{\mu a}$ is introduced for each colour μ and for each row a of the Young tableau. Since an irrep of SU(N) can have a maximum of $N - 1$ rows in the Young tableau, it is possible to describe the states of any given irrep using $N(N - 1)$ boson species at most in conjunction with the adequate constraints enforcing the symmetry of the irrep (see below). For instance, for the SU(3) model in the adjoint irrep $\begin{array}{cc}\square&\square\\\square&\end{array}$, the bosons d_{A1}, d_{B1}, d_{C1} and d_{A2}, d_{B2}, d_{C2} were used for the three colours of SU(3) and the two rows of the Young tableau. Hence, there is no one-to-one correspondence between a boson species and a state as it was the case with the multiboson method, and there is a certain degree of freedom in the choice of the states that are degenerate in the weight diagram with this boson representation. For any irrep and any N, the calculations of the dispersion relations are very efficient with this method, and it yields less flat modes than the multiboson method: for fully antisymmetric models in section 4.1 that contained no degenerate point in the weight diagram, it yielded no flat modes, and it yielded 2 flat modes only (due to the degenerate point in the weight diagram) for the SU(3) model in the adjoint irrep, see section 4.2. However, there is a certain ambiguity in the treatment of the condensate, depending on the irrep. As an example, the conventional Holstein-Primakoff could not be used for fully antisymmetric irreps, so the constraints of the irrep had to be implemented differently into the calculations of the LFWT. But the Holstein-Primakoff could be used for the SU(3) adjoint irrep. Another caveat of this method is that the nature of the flat modes are not clear within this framework.

Here is a listed summary of the characteristics of each method:

1. Multiboson method

- **NUMBER OF BOSON SPECIES:** D for an SU(N) irrep of dimension D

- **EXPRESSION OF $\hat{S}_\nu^\mu$:** varies with each irrep

- **NUMBER OF MODES**

  ► Bipartite square in fully antisymmetric SU(N) irreps with $\frac{N}{2}$ particles per site:
  $\frac{N^2}{4}$ dispersive branches in the extended Brillouin zone,
  $\binom{N}{N/2} - 1 - \frac{N^2}{4}$ flat modes in the extended Brillouin zone.

  ► Bipartite chain in SU(3) adjoint irrep:
  6 dispersive branches in the reduced Brillouin zone,
  8 flat modes in the reduced Brillouin zone.

2. Mathur & Sen bosons

- **NUMBER OF BOSON SPECIES:** $2^N - 2$ for irreps of SU(N)

- **EXPRESSION OF $\hat{S}_\nu^\mu$:** $\hat{S}_\nu^\mu = a_\nu^\dagger a_\mu - b_\mu^\dagger b_\nu$
  up to a constant for SU(3), with $\mu, \nu \in \{A, B, C\}$

- **CONSTRAINTS FOR A GIVEN IRREP**

  ► For SU(3) irreps $[p, q]$:
  $$n_a = \sum_{\mu=A}^{C} n_{a,\mu} = p \quad \text{and} \quad n_b = \sum_{\mu=A}^{C} n_{b,\mu} = q$$

  ► Tracelessness condition
  $\delta_{\nu_a}^{\mu_a} v_{\nu_1 \dots \nu_q}^{\mu_1 \dots \mu_p} = 0$,
  where $a \in \{1, \dots, \min(p, q)\}$, and the coefficients v are given by
  $v_{\nu_1 \dots \nu_q}^{\mu_1 \dots \mu_p} a_{\mu_1}^\dagger \cdots a_{\mu_p}^\dagger b_{\nu_1}^\dagger \cdots b_{\nu_q}^\dagger |0\rangle = v_{\nu_1 \dots \nu_q}^{\mu_1 \dots \mu_p} \left| {\nu_1 \cdots \nu_q \atop \mu_1 \cdots \mu_p} \right\rangle$.

- **NUMBER OF MODES**

  ► Bipartite chain in SU(3) adjoint irrep:
  6 dispersive branches in the reduced Brillouin zone,
  2 flat modes in the reduced Brillouin zone.

3. Read & Sachdev bosons

- **NUMBER OF BOSON SPECIES:** Maximum $N(N-1)$ for irreps of SU(N)

- **EXPRESSION OF $\hat{S}_\nu^\mu$:** $\hat{S}_\nu^\mu = \sum_{a=1}^{m} d_{\nu a}^\dagger d_{\mu a}$
  up to a constant for SU(N) irreps with m rows in Young tableau

- **CONSTRAINTS FOR A GIVEN IRREP**

  ► For irreps with rectangular Young tableaux with m rows and n_c columns
  (a, b are row indices and μ is the colour index):
  $$\sum_{\mu=1}^{N} d_{\mu a}^\dagger d_{\mu b} = n_c \delta_{ab}$$

▶ For the SU(3) adjoint irrep ⊞ :

$$
\begin{cases}
\sum\limits_{\mu=1}^{3} d^{\dagger}_{\mu 1} d_{\mu 1} = 2n_c \\
\sum\limits_{\mu=1}^{3} d^{\dagger}_{\mu 2} d_{\mu 2} = n_c \\
\sum\limits_{\mu=1}^{3} d^{\dagger}_{\mu 1} d_{\mu 2} = 0
\end{cases}
\tag{5.1}
$$

• NUMBER OF MODES

▶ Bipartite square in fully antisymmetric SU(N) irreps with $\frac{N}{2}$ particles per site:
   $\frac{N^2}{4}$ dispersive branches in the extended Brillouin zone,
   No flat modes.

▶ Bipartite chain in SU(3) adjoint irrep:
   6 dispersive branches in the reduced Brillouin zone,
   2 flat modes in the reduced Brillouin zone.

We now turn our attention to a somewhat different subject in the next chapter.

VI Lifting the Line of Zero-Modes

Introduction: how to lift the accidental zero-modes?

Breaking with the continuity of the subject of the previous chapters, this chapter briefly presents the attempts made to lift the accidental zero-modes that are present in the dispersion relations of the AFM SU(3) Heisenberg model in the three-sublattice order in 2D with an infinitely large classical ground-state degeneracy. These accidental zero-modes are somewhat problematic when calculating the magnetisation of the system as it always diverges to $-\infty$, suggesting that the system is not ordered. However, this is an artifact originating from an extended ground-state degeneracy that can be parametrised by one parameter.

First, a method of establishing a self-consistent equation for the new dispersion relation using the perturbation theory and some physical assumptions will be presented. As the perturbation theory is in principle ill-defined when a line of zero-modes is present in the harmonic spectrum, this attempt will try to address this issue. Such an attempt yields a magnetisation value that is in reasonable agreement with the existing numerical results. However, there is a certain arbitrariness in establishing these self-consistent equations.

In the second part, we will present different calculation methods that yield the same result as the LFWT and pave a path for future investigations—establish the equations of motions of the system by correctly identifying the variables and their conjugate variables.

6.1 The line of zero-modes: the root of the problem

The model we are interested in is the AFM SU(3) nearest-neighbour Heisenberg model,

$$\mathcal{H} = J_1 \sum_{\langle i,j \rangle} \sum_{\mu,\nu} \hat{S}_\nu^\mu(i) \hat{S}_\mu^\nu(j), \tag{6.1}$$

on the 2D square lattice. Classically, the model possesses a huge number of ground states—the ground state degeneracy is, in fact, infinite. This can be seen easily by assuming a (normalised)
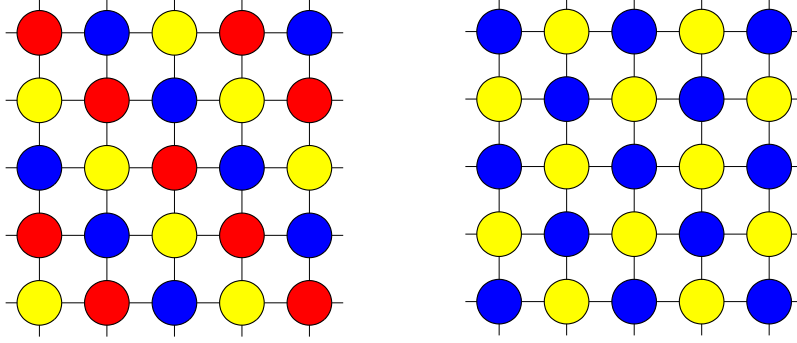
Figure 6.1 – The three-sublattice configuration that minimises the zero-point energy, and the two-sublattice configuration that yields the same energy classically.

wave function of the form

$$\left|\vec{\phi}_i\right\rangle := \sum_{\mu=A}^{C} \phi_i^{\mu}\left|\mu\right\rangle_i \tag{6.2}$$

for each site i of the system. The energy of a bond is then given by

$$E_{ij} = \left\langle \vec{\phi}_i \otimes \vec{\phi}_j \left| \mathcal{H}_{ij} \right| \vec{\phi}_i \otimes \vec{\phi}_j \right\rangle = J_1 \left| \vec{\phi}_i \cdot \vec{\phi}_j \right|^2. \tag{6.3}$$

It can be seen that the only condition for the ground state is then to have orthogonal states on adjacent sites. There are thus an infinite number of possibilities to achieve this: if we fix a colour A on one site, the adjacent site can take any linear combination of B and C, and this degree of freedom exists for every bond on the lattice. The Néel-like bipartite configuration or the diagonal-striped tripartite configuration depicted in Figure 6.1, which we already introduced in section 1.2, are notable examples of classical ground-state configurations of our system.

As seen in section 1.2, there is a line of zero-modes in the spectrum obtained with the LFWT calculations of this three-sublattice order.[12] Its existence suggests that there should exist a manifold of classical ground states with wave vectors corresponding to this line. Tóth et al. [53] indeed showed that one can parametrise this family of classical ground states with one parameter and that it connects continuously the Néel two-sublattice configuration and the three-sublattice configuration. In other words, there is a whole class of "helical" states that allows one to go from one configuration to the other continuously along a rotation parameter θ.[13] They also show that the three-sublattice order has the lowest zero-point energy $E_{\text{ZP}} = 2\sum_{\mathbf{k}} \frac{\omega_{\mathbf{k}}}{2}$ (the constant term of the harmonic oscillator term in (1.38))—in particular among

---

[12]It is worthwhile noting that the presence of lines of zero-modes depends on the nature of the ground-state manifold, which itself depends on the choice of the symmetry (irrep) of the system. As seen in section 3.2, Eq. (3.43), the classical ground state of the SU(3) adjoint model is the bipartite configuration whose dispersion relations do not feature any line of zero-modes.

[13]As with the SU(2) spin-wave theory, the LFWT can also be applied to such helical ground states as well by applying a rotation to the local frame. See Ref. [53] for an example of calculations on a helical state in SU(3).

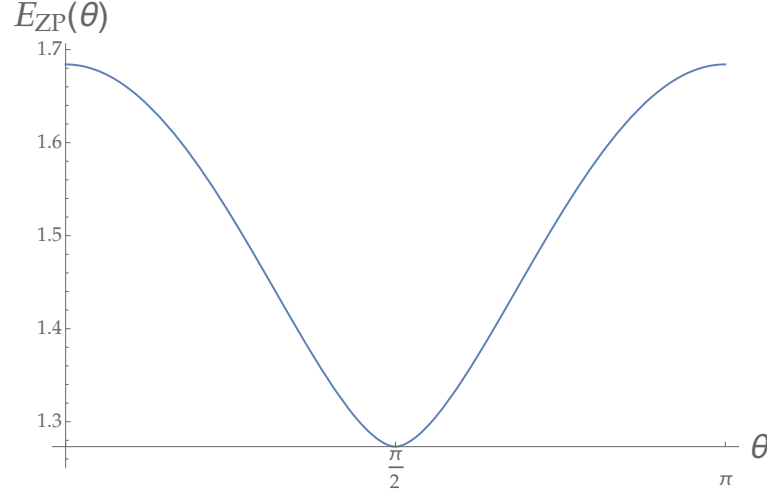the ground states parametrised by θ, see Figure 6.2— hence concluding that the quantum

Figure 6.2 – The zero point energy $E_{ZP}(\theta) = 2 \sum_{\mathbf{k}} \frac{\omega_{\mathbf{k}}(\theta)}{2}$ as a function of the helcal parameter θ. The calculations have first been done by Tóth et al. [53]. Here, $\theta = 0, \pi, \ldots$ correspond to the two-sublattice order whereas $\theta = \frac{\pi}{2}, \ldots$ correspond to the three-sublattice order. This shows that the tripartite configuration is the true quantum ground state.

fluctuations stabilise the three-sublattice order in this system. Since the tripartite configuration is confirmed as the true ground state, one could attempt to compute the magnetisation of this configuration using the LFWT to determine whether the colour-order survives the quantum fluctuations or not. However, as pointed out by Bauer et al. [31], the computation of the magnetisation involves calculating $\int \frac{1}{\omega_{\mathbf{k}}} d\mathbf{k}$, an ill-defined 2D integral in the presence of a line of zeros in the spectrum $\omega_{\mathbf{k}}$. This would in principle mean that quantum fluctuations would destroy the long-range order. However, the line of zero-modes are accidental in the sense that they come from a specific family of helical (classical) ground states, and since the true quantum ground state is selected by quantum fluctuations, we could expect that quantum fluctuations would lift the zero-modes in the true spectrum of the system, in which case the magnetisation could be finite and positive. Thus, what we ultimately aim to find is a method to obtain somehow the true (or renormalised) spectrum.

6.2 Self-consistent method

Since the LFWT with Holstein-Primakoff bosons yield an expansion in n_c, the perturbation theory naturally springs to mind when trying to obtain the renormalised spectrum. The perturbation theory, however, cannot be used in this situation due to the aforementioned problem related to the zero-modes. So if perturbation theory is not well-defined in this problem, what

can we try to solve it?

What we know is that there should be Goldstone modes in the spectrum, due to the spontaneous symmetry breaking, at pitch vectors $\mathbf{q}_0 \equiv 0$ and $\mathbf{q}_{\pm 1} \equiv \pm \left(\frac{2\pi}{3}, \frac{2\pi}{3} \right)$ related to our three-sublattice order. The final renormalised spectrum that we could expect, as shown qualitatively in Figure 6.3, is then to have the zero-modes lifted between these wave vectors $\mathbf{q}_i$ and to have a linear dispersion relation near $\mathbf{q}_i$ as required by the Goldstone modes for antiferromagnetic systems. We can thus use this information and take an educated guess for the renormalised
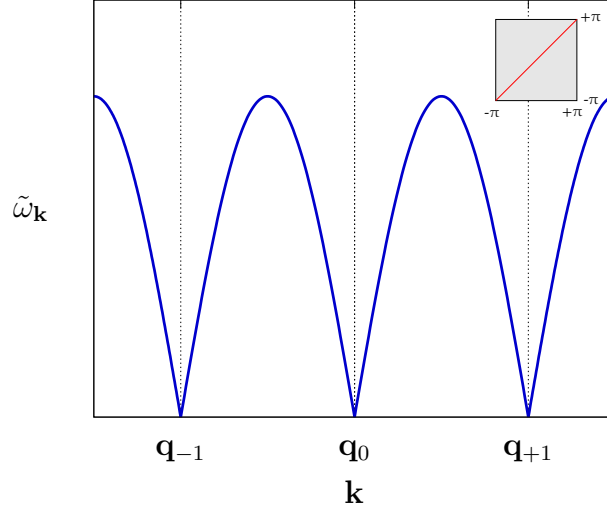

Figure 6.3 – An example of a qualitative behaviour of the expected renormalised spectrum $\tilde{\omega}$ of the AFM SU(3) tripartite configuration. The Goldstone modes are expected at $\mathbf{q}_0 = 0$ and $\mathbf{q}_{\pm 1} = \pm \left(\frac{2\pi}{3}, \frac{2\pi}{3} \right)$, and the other zero-modes along the diagonal of the Brillouin zone are expected to be lifted.

spectrum with some parameters. We can then equate this to the renormalised spectrum resulting from the perturbation theory applied on our original model (under the provisional assumption that the perturbation is well-defined), which will result in a self-consistent equations that have to be solved with respect to the initial parameters.

The easiest way to generate a spectrum with the properties (namely the Goldstone modes at q_i) that we wish to have is to incorporate one further-neighbour coupling,

$$\mathcal{H}_{J_1, J_n} = J_1 \sum_{\substack{\langle i,j \rangle \\ \mu, \nu}} \hat{S}_\nu^\mu(i) \hat{S}_\mu^\nu(j) + J_n \sum_{\substack{\langle \langle i,j' \rangle \rangle \\ \mu, \nu}} \hat{S}_\nu^\mu(i) \hat{S}_\mu^\nu(j'), \tag{6.4}$$

where J_n designates the nth-nearest-neighbour coupling and j' sums over the nth-nearest-neighbour sites with respect to the site i. In our subsequent calculations, we will be using three different couplings that accomodate our tripartite ground-state configuration: $J_3 > 0$, $J_6 < 0$ and anisotropic J_2. This additional term in the Hamiltonian lifts the classical degeneracy and leaves the Goldstone modes at $\mathbf{q}_i$ as the only zero-modes in the harmonic spectrum $\varepsilon_{J_n}(\mathbf{k})$ of the the tripartite configuration. With one further-neighbour coupling J_n, we get one parameter

for which the self-consistent equation needs to be solved. In principle, the equations from the Dyson equations without the on-shell approximation need to be solved for each point in the k-space, and the solutions depend on the integration involving the solution we are looking for. It is hence naive perhaps to establish a self-consistent equation with only one parameter. However, the hope is that this will already give a good approximation to the true solution, given the complicated nature of the equations involved (even in the case where the perturbation theory is well-defined). After all, the important physical features such as the Goldstone modes are qualitatively taken into account in the elaboration of our self-consistent equation. It should hence give a fairly good approximation to the renormalised spectrum.

The first step of the calculations is to come back to the original nearest-neighbour Heisenberg model and to calculate the perturbative terms using the Rayleigh-Schrödinger perturbation theory, ignoring the fact that the integrals are ill-defined. To simplify the perturbation calculations significantly, one can map the antiferromagnetic classical ground state to a ferromagnetic ground state before applying the LFWT, a procedure often used in SU(2) systems.

6.2.1 Mapping to the ferromagnetic state — rotation of local frames

The aim is choose the local basis for each site i such that the local colour $|A_i\rangle$ is the colour of the condensate on the site i. In other words, this means that we perform a local SU(3) rotation on the local frame such that the condensed flavour on each site is relabelled as A. For instance, on the sites of the sublattice Λ_B on which the condensate colour is B, the colour B will become the basis element $|A\rangle$.

This mapping of the AFM configuration to the ferromagnetic configuration[14] is given by

$$\mathscr{H} = J_1 n_c \sum_i \sum_{\substack{j \in \{i + \vec{e}_x, \\ i + \vec{e}_y\}}} \sum_{\mu,\nu} \hat{S}_\mu^\nu(i) \left(R^\dagger \hat{S}_\nu^\mu(i+1) R \right). \tag{6.5}$$

where the rotation R is given by

$$R = \begin{pmatrix} 0 & 0 & 1 \\ 1 & 0 & 0 \\ 0 & 1 & 0 \end{pmatrix}. \tag{6.6}$$

The site j will be the neighbouring site on the top and on the right of i, as it was the case in our original calculations in section 1.2 (we are supposed to sum over the bonds between two given sublattices). This will thus be the form of the Hamiltonian that will be used subsequently.

---

[14] Suppose that a SU(3) basis λ_i is given by a SU(3) rotation R on the reference (absolute) basis η. The action of this rotation R on the generators $\hat{S}_\nu^\mu(i)$ is given by the adjoint transformation (i.e., the conjugation). In other words, it is the adjoint representation of the group SU(3) (in the basis λ_i):

$$\mathrm{Ad}_R \hat{S}_\nu^\mu = R \hat{S}_\nu^\mu R^{-1}.$$

Ultimately, instead of having three bosons for each of the three sublattices — totalling nine bosons — the rotation of the local frames will result in three bosons only, in total.

6.2.2 Hamiltonian in the rotated frame

The subsequent computations are much simpler in the locally rotated frame. Now that our antiferromagnetic configuration is mapped into a ferromagnetic configuration, the only boson that is condensated is the boson b_A on each site. Hence, after the Holstein-Primakoff prescription, only b_B and b_C remain.

Up to order $\mathcal{O}(n_c^0)$, our nearest-neighbour Hamiltonian $\mathcal{H}$ is then given by

$$\mathcal{H} = \mathcal{H}^{(2)} + \mathcal{H}^{(3)} + \mathcal{H}^{(4)} + \mathcal{O}\left(\sqrt{\frac{1}{n_c}}\right) \qquad \text{where}$$

$$\mathcal{H}^{(2)} = J_1 n_c \sum_i \sum_{\substack{j \in \{i + \vec{e}_x, \\ i + \vec{e}_y\}}} \left[b_B^\dagger(i) b_B(i) + b_C^\dagger(j) b_C(j) + b_B^\dagger(i) b_C^\dagger(j) + b_B(i) b_C(j) \right],$$

$$\mathcal{H}^{(3)} = J_1 \sqrt{n_c} \sum_i \sum_{\substack{j \in \{i + \vec{e}_x, \\ i + \vec{e}_y\}}} \left[b_C^\dagger(i) b_B(i) b_B(j) + b_C^\dagger(i) b_C^\dagger(j) b_B(j) + b_B^\dagger(i) b_B^\dagger(j) b_C(i) + b_B^\dagger(j) b_C(i) b_C(j) \right],$$

$$\mathcal{H}^{(4)} = - J_1 \sum_i \sum_{\substack{j \in \{i + \vec{e}_x, \\ i + \vec{e}_y\}}} \frac{1}{2} \left[b_B^\dagger(i) b_B(i) b_B(i) b_C(j) + b_B^\dagger(i) b_C^\dagger(j) b_C^\dagger(j) b_C(j) + b_B^\dagger(i) b_C^\dagger(j) b_B^\dagger(j) b_B(j) \right.$$

$$+ b_B^\dagger(i) b_C^\dagger(j) b_C^\dagger(i) b_C(i) + b_C^\dagger(i) b_C^\dagger(j) b_C(i) b_C(j) + b_B^\dagger(i) b_B^\dagger(j) b_B(j) b_B(i)$$

$$\left. + 2 b_B^\dagger(i) b_C^\dagger(j) b_B(i) b_C(j) - b_C^\dagger(i) b_B^\dagger(j) b_C(i) b_B(j) + \text{h.c.} \right].$$

$$(6.7)$$

Notice the appearance of the cubic terms $\mathcal{H}^{(3)}$ unlike in the collinear antiferromagnetic $SU(2)$ models. The reason why the development of $\mathcal{H}$ was carried out to the quartic terms $\mathcal{H}^{(4)}$ is because the quartic terms in the first order of the perturbation theory will yield corrections to the harmonic spectrum which is of the order $\sim \frac{1}{n_c}$, just like the cubic terms $\mathcal{H}^{(3)}$ in the second order of the perturbation theory that will give corrections of the order $\sim \frac{\sqrt{n_c}^2}{n_c^2} = \frac{1}{n_c}$.

We first start by diagonalising $\mathcal{H}^{(2)}$ using the Bogoliubov transformation to obtain the harmonic energy spectrum $\varepsilon_{\mathbf{k}}$. The procedure here is very similar to the one in section 1.2 (it is in fact the same as the Bogoliubov transformation used for the sub-Hamiltonians $H_{\mu\nu}$ in section 1.2). Using the Fourier transform

$$b_\mu(l) = \sqrt{\frac{1}{N}} \sum_{\mathbf{k}} b_\mu(\mathbf{k}) e^{-i\mathbf{k}\mathbf{r}_l}, \tag{6.8}$$

with $\mu \in \{B, C\}$, we now denote the new Bogoliubov bosons by η_μ, which are given by

$$
\begin{cases}
b_C^\dagger(\mathbf{k}) = u_{\mathbf{k}}^* \eta_C^\dagger(\mathbf{k}) - v_{\mathbf{k}} \eta_B(-\mathbf{k}), \\
b_C(\mathbf{k}) = u_{\mathbf{k}} \eta_C(\mathbf{k}) - v_{\mathbf{k}} \eta_B^\dagger(-\mathbf{k}), \\
b_B^\dagger(\mathbf{k}) = -v_{\mathbf{k}} \eta_C(-\mathbf{k}) + u_{\mathbf{k}} \eta_B^\dagger(\mathbf{k}), \\
b_B(\mathbf{k}) = -v_{\mathbf{k}} \eta_C^\dagger(-\mathbf{k}) + u_{\mathbf{k}}^* \eta_B(\mathbf{k}).
\end{cases}
\tag{6.9}
$$

As in Appendix A, we have the following relations:

$$
\varepsilon_{\mathbf{k}} = \sqrt{\mathcal{A}^2 - |\mathcal{B}_{\mathbf{k}}|^2},
\tag{6.10a}
$$

$$
|u_{\mathbf{k}}|^2 + v_k^2 = \frac{\mathcal{A}}{\varepsilon_{\mathbf{k}}}, \qquad 2u_{\mathbf{k}} v_{\mathbf{k}} = \frac{\mathcal{B}_{\mathbf{k}}}{\varepsilon_{\mathbf{k}}},
\tag{6.10b}
$$

$$
u_{\mathbf{k}} = \sqrt{\frac{1}{2}\left(\frac{\mathcal{A}}{\varepsilon_{\mathbf{k}}} + 1\right)} e^{i \arg \mathcal{B}_{\mathbf{k}}} = \sqrt{\frac{1}{2}\left(\frac{\mathcal{A}}{\varepsilon_{\mathbf{k}}} + 1\right)} e^{i \arg \gamma_{\mathbf{k}}},
\tag{6.10c}
$$

$$
v_{\mathbf{k}} = \sqrt{\frac{1}{2}\left(\frac{\mathcal{A}}{\varepsilon_{\mathbf{k}}} - 1\right)},
\tag{6.10d}
$$

with

$$
\gamma_{\mathbf{k}} = \frac{1}{2}(e^{ik_x} + e^{ik_y}),
$$
$$
\mathcal{A} = 2J_1 n_c, \qquad \mathcal{B}_{\mathbf{k}} = 2J_1 n_c \gamma_{\mathbf{k}},
\tag{6.11}
$$

and the number $z = 2$ is the coordination number (the number of links) between two sublattices. The spectrum obtained here is identical to that in section 1.2 as it should. Note that we have the properties that

$$
u_{-\mathbf{k}} = u_{\mathbf{k}}^*, \qquad v_{-\mathbf{k}} = v_{\mathbf{k}},
\tag{6.12a}
$$

$$
\gamma_{-\mathbf{k}} = \gamma_{\mathbf{k}}^*, \qquad \omega_{-\mathbf{k}} = \omega_{\mathbf{k}}.
\tag{6.12b}
$$

We now look for the renormalised spectrum $\tilde{\varepsilon}_{\mathbf{k}}$, that will have the following form:

$$
\tilde{\varepsilon}(\mathbf{k}) = \varepsilon(\mathbf{k}) + \Sigma^{(3)}(\mathbf{k}) + \Sigma^{(4)}(\mathbf{k}).
\tag{6.13}
$$

This is in fact the Dyson equation. The self-energy $\Sigma^{(3)}(\mathbf{k})$ is the corrections coming from $\mathcal{H}^{(3)}$ and the self-energy $\Sigma^{(4)}(\mathbf{k})$ is the corrections coming from $\mathcal{H}^{(4)}$. Let us first look at the quartic contributions.

6.2.3 The corrections from $\mathcal{H}^{(4)}$

The quartic Hamiltonian can be written as $\mathcal{H}^{(4)} = \delta E^{(4)} + \delta\mathcal{H}^{(2)} + \tilde{\mathcal{H}}^{(4)}$. The uniform energy shift $\delta E^{(4)}$ can be ignored for our purpose, as well as the two-particle scattering process $\tilde{\mathcal{H}}^{(4)}$. The term $\delta\mathcal{H}^{(2)}$ is the term of our interest: it is the corrections to the harmonic spectrum that comes from the quartic term.

We perform the Wick decoupling to calculate the quadratic average in real-space to simplify the calculations, as done in Ref. [85] whose calculation method we will closely follow and adapt to our SU(3) calculations. The details of the calculations in this subsection can be consulted in Appendix C. As an example, let us show here the computation of one of the possible averages of a pair of bosons, $\left\langle b_B^\dagger(i) b_B(i) \right\rangle$. By using the ground state of $\mathcal{H}^{(2)}$ which is the Bogoliubov vacuum $|0\rangle$, we obtain

$$
\begin{aligned}
\left\langle b_B^\dagger(i) b_B(i) \right\rangle &= \frac{1}{N}\left\langle 0 \left| \sum_i b_B^\dagger(i) b_B(i) \right| 0 \right\rangle = \frac{1}{N}\left\langle 0 \left| \sum_\mathbf{k} b_B^\dagger(\mathbf{k}) b_B(\mathbf{k}) \right| 0 \right\rangle \\
&= \frac{1}{N}\left\langle 0 \left| \sum_\mathbf{k} \left(-v_\mathbf{k}\eta_C(-\mathbf{k}) + u_\mathbf{k}\eta_B^\dagger(\mathbf{k}) \right)\left(-v_\mathbf{k}\eta_C^\dagger(-\mathbf{k}) + u_\mathbf{k}^*\eta_B(\mathbf{k}) \right) \right| 0 \right\rangle \\
&= \frac{1}{N}\left\langle 0 \left| \sum_\mathbf{k} v_\mathbf{k}^2 \eta_{C,-\mathbf{k}} \eta_{C,-\mathbf{k}}^\dagger \right| 0 \right\rangle \\
&= \frac{1}{N}\sum_\mathbf{k} v_\mathbf{k}^2 \\
&\overset{(6.10)}{=} \frac{1}{N}\sum_\mathbf{k}\left[\frac{1}{2}\left(\frac{\mathcal{A}}{\omega_\mathbf{k}} - 1 \right) \right] \\
&=: n.
\end{aligned}
\tag{6.14}
$$

Similarly, we also obtain $\left\langle b_C^\dagger(j) b_C(j) \right\rangle = \left\langle b_B^\dagger(j) b_B(j) \right\rangle = \left\langle b_C^\dagger(i) b_C(i) \right\rangle = n$. The other non-zero possible Hartree-Fock average is given by

$$
\left\langle b_B^\dagger(i) b_C^\dagger(j) \right\rangle = \left\langle b_C^\dagger(j) b_B^\dagger(i) \right\rangle = \left\langle b_C(j) b_B(i) \right\rangle = \left\langle b_B(i) b_C(j) \right\rangle = -\frac{1}{N}\sum_\mathbf{k} |\gamma_\mathbf{k}| \frac{|\mathcal{B}_\mathbf{k}|}{2\omega_\mathbf{k}}
\tag{6.15}
$$
$$
=: \Delta_\gamma.
$$

We can now use them to compute $\delta\mathcal{H}^{(2)}$. The Wick theorem states that the term $\delta\mathcal{H}^{(2)}$ in which we are interested is the sum of the normal-ordered quartic terms $:\mathcal{H}^{(4)}:$ with one contraction (in all possible combinations). As an example, let us just take the first term of $\mathcal{H}^{(4)}$ in Eq. (6.7), $b_B^\dagger(i) b_B(i) b_B(i) b_C(j)$, without the numerical factor $-\frac{1}{2}$:

$$
\sum_i \sum_{\substack{j \in \{i+\vec{e}_x, \\ i+\vec{e}_y\}}} b_B^\dagger(i) b_B(i) b_B(i) b_C(j)
$$

$$\varepsilon_{\mathbf{k}}^{(4)}$$
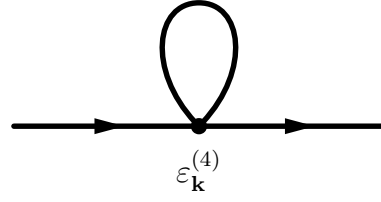
Figure 6.4 – The corrections $\varepsilon_{\mathbf{k}}^{(4)}$.

$$
\begin{aligned}
\longrightarrow \sum_{i} \sum_{\substack{j \in \{i+\vec{e}_x, \\ i+\vec{e}_y\}}} &\Big[:b_B^\dagger(i)b_B(i)b_B(i)b_C(j): + :b_B^\dagger(i)b_B(i)b_B(i)b_C(j): + :b_B^\dagger(i)b_B(i)b_B(i)b_C(j): \\
&+ :b_B^\dagger(i)b_B(i)b_B(i)b_C(j): + :b_B^\dagger(i)b_B(i)b_B(i)b_C(j): + :b_B^\dagger(i)b_B(i)b_B(i)b_C(j): \Big] \\
= z \sum_{\mathbf{k}} &\Big[n\gamma_{\mathbf{k}}^* :b_B(-\mathbf{k})b_C(\mathbf{k}): + n\gamma_{\mathbf{k}}^* :b_B(-\mathbf{k})b_C(\mathbf{k}): + 0 \\
&+ 0 + \Delta_\gamma^* :b_B^\dagger(-\mathbf{k})b_B(-\mathbf{k}): + \Delta_\gamma^* :b_B^\dagger(-\mathbf{k})b_B(-\mathbf{k}): \Big] \\
= z \sum_{\mathbf{k}} &\Big[2n\gamma_{\mathbf{k}}^* :b_B(-\mathbf{k})b_C(\mathbf{k}): + 2\Delta_\gamma^* :b_B^\dagger(-\mathbf{k})b_B(-\mathbf{k}): \Big].
\end{aligned}
\tag{6.16}
$$

By doing this with all the terms of the quartic Hamiltonian and by expressing them in terms of the Bogoliubov bosons $\eta_{\mathbf{k}}$, the term $\delta\mathcal{H}^{(2)}$ is then given by

$$
\begin{aligned}
\delta\mathcal{H}^{(2)} =& 2J \sum_{\mathbf{k}} \Big[\omega_{\mathbf{k}}^{(4)} \eta_{B,\mathbf{k}}^\dagger \eta_{B,\mathbf{k}} + \omega_{\mathbf{k}}^{(4)} \eta_{C,\mathbf{k}}^\dagger \eta_{C,\mathbf{k}} + B_{\mathbf{k}}^{(4)\,*} \eta_{B,-\mathbf{k}} \eta_{C,\mathbf{k}} + B_{\mathbf{k}}^{(4)} \eta_{B,-\mathbf{k}}^\dagger \eta_{C,\mathbf{k}}^\dagger \Big] \\
=& \sum_{\mathbf{k}} \Big[\varepsilon_{\mathbf{k}}^{(4)} \eta_{B,\mathbf{k}}^\dagger \eta_{B,\mathbf{k}} + \varepsilon_{\mathbf{k}}^{(4)} \eta_{C,\mathbf{k}}^\dagger \eta_{C,\mathbf{k}} + Jz \Big(B_{\mathbf{k}}^{(4)\,*} \eta_{B,-\mathbf{k}} \eta_{C,\mathbf{k}} + B_{\mathbf{k}}^{(4)} \eta_{B,-\mathbf{k}}^\dagger \eta_{C,\mathbf{k}}^\dagger \Big) \Big],
\end{aligned}
\tag{6.17}
$$

where

$$
\begin{aligned}
\delta A :=& -3 \left(n + \Delta_\gamma \right), \qquad \delta B_{\mathbf{k}} := -\gamma_{\mathbf{k}} \left(3n + 2\Delta_\gamma \right), \\
\omega_{\mathbf{k}}^{(4)} :=& \left(|u_{\mathbf{k}}|^2 + v_{\mathbf{k}}^2 \right) \delta A - 2\mathrm{Re}\left(u_{\mathbf{k}}^* v_{\mathbf{k}} \delta B_{\mathbf{k}} \right), \\
\varepsilon_{\mathbf{k}}^{(4)} :=& 2J_1 \omega_{\mathbf{k}}^{(4)}.
\end{aligned}
\tag{6.18}
$$

The two last terms involving $B_{\mathbf{k}}^{(4)}$, i.e., two-particle scattering process, can be ignored for the magnetisation calculations: we only keep track of $\epsilon_{\mathbf{k}}^{(4)}$ which corresponds to the first-order magnon energy correction, depicted in terms of the Feynmann diagram in Figure 6.4. The self-energy $\Sigma^{(4)}(\mathbf{k})$ that renormalises the harmonic spectrum is then simpliy given by $\epsilon_{\mathbf{k}}^{(4)}$:

$$
\Sigma^{(4)}(\mathbf{k}) \equiv \varepsilon_{\mathbf{k}}^{(4)}.
\tag{6.19}
$$

6.2.4 The corrections from $\mathcal{H}^{(3)}$

Let us now look at the cubic terms. After the Fourier transform and with the Bogoliubov bosons η, the cubic Hamiltonian $\mathcal{H}^{(3)}$ is given by

$$\mathcal{H}^{(3)} = 2J_1\sqrt{n_c}\sqrt{\frac{1}{N}}\sum_{\mathbf{k},\mathbf{q}}\Big[\tilde{\Gamma}_1^B(\mathbf{q},\mathbf{k}-\mathbf{q};\mathbf{k})\eta_{C,\mathbf{q}}^\dagger\eta_{C,\mathbf{k}-\mathbf{q}}^\dagger\eta_{B,\mathbf{k}} + \tilde{\Gamma}_2^B(\mathbf{q},-\mathbf{k}-\mathbf{q},\mathbf{k})\eta_{B,\mathbf{q}}^\dagger\eta_{B,-\mathbf{k}-\mathbf{q}}^\dagger\eta_{B,\mathbf{k}}^\dagger$$
$$+ \tilde{\Gamma}_1^C(\mathbf{q},\mathbf{k}-\mathbf{q};\mathbf{k})\eta_{B,\mathbf{q}}^\dagger\eta_{B,\mathbf{k}-\mathbf{q}}^\dagger\eta_{C,\mathbf{k}} + \tilde{\Gamma}_2^C(\mathbf{q},-\mathbf{k}-\mathbf{q},\mathbf{k})\eta_{C,\mathbf{q}}^\dagger\eta_{C,-\mathbf{k}-\mathbf{q}}^\dagger\eta_{C,\mathbf{k}}^\dagger + \text{h.c.}\Big] \tag{6.20}$$

with

$$\tilde{\Gamma}_1^B = \tilde{\Gamma}_1^C = -\gamma_{-\mathbf{k}}u_{\mathbf{q}}^* u_{-\mathbf{k}}v_{\mathbf{k}-\mathbf{q}} - \gamma_{\mathbf{q}}u_{\mathbf{k}-\mathbf{q}}^* u_{-\mathbf{k}}v_{\mathbf{q}} - \gamma_{\mathbf{q}}v_{-\mathbf{k}}v_{\mathbf{k}-\mathbf{q}}v_{\mathbf{q}}$$
$$+ \gamma_{\mathbf{q}-\mathbf{k}}u_{\mathbf{k}-\mathbf{q}}^* u_{\mathbf{q}}^* u_{-\mathbf{k}} + \gamma_{\mathbf{k}}u_{\mathbf{q}}^* v_{-\mathbf{k}}v_{\mathbf{k}-\mathbf{q}} + \gamma_{-\mathbf{q}}u_{\mathbf{q}}^* v_{-\mathbf{k}}v_{\mathbf{k}-\mathbf{q}},$$
$$\tilde{\Gamma}_2^B = \tilde{\Gamma}_2^C = \gamma_{\mathbf{q}}u_{\mathbf{k}}^* v_{-\mathbf{k}-\mathbf{q}}v_{\mathbf{q}} - \gamma_{-\mathbf{k}}u_{\mathbf{k}}^* u_{\mathbf{q}}^* v_{-\mathbf{k}-\mathbf{q}}. \tag{6.21}$$

These terms are symmetric in B and C. We now symmetrise $\tilde{\Gamma}_1(\mathbf{q},\mathbf{k}-\mathbf{q};\mathbf{k})$ with respect to $\mathbf{q}$ and $\mathbf{k}-\mathbf{q}$, and $\tilde{\Gamma}_2(\mathbf{q},\mathbf{k}-\mathbf{q},\mathbf{k})$ with respect to $\mathbf{q}$, $\mathbf{k}-\mathbf{q}$ and $\mathbf{k}$, as it is easier to apply the second-order perturbation theory with symmetrised terms. We finally obtain

$$\mathcal{H}^{(3)} = 2J_1\sqrt{n_c}\sqrt{\frac{1}{N}}\sum_{\mathbf{k},\mathbf{q}}\Big[\frac{1}{2!}\Gamma_1(\mathbf{q},\mathbf{k}-\mathbf{q};\mathbf{k})\eta_{C,\mathbf{q}}^\dagger\eta_{C,\mathbf{k}-\mathbf{q}}^\dagger\eta_{B,\mathbf{k}} + \frac{1}{3!}\Gamma_2(\mathbf{q},-\mathbf{k}-\mathbf{q},\mathbf{k})\eta_{B,\mathbf{q}}^\dagger\eta_{B,-\mathbf{k}-\mathbf{q}}^\dagger\eta_{B,\mathbf{k}}^\dagger$$
$$+ \frac{1}{2!}\Gamma_1(\mathbf{q},\mathbf{k}-\mathbf{q};\mathbf{k})\eta_{B,\mathbf{q}}^\dagger\eta_{B,\mathbf{k}-\mathbf{q}}^\dagger\eta_{C,\mathbf{k}} + \frac{1}{3!}\Gamma_2(\mathbf{q},-\mathbf{k}-\mathbf{q},\mathbf{k})\eta_{C,\mathbf{q}}^\dagger\eta_{C,-\mathbf{k}-\mathbf{q}}^\dagger\eta_{C,\mathbf{k}}^\dagger + \text{h.c.}\Big]. \tag{6.22}$$

The diagrammatic representation of the $\Gamma_{1,2}$ are depicted in Figure 6.5.

(a) Vertex Γ_1 in $\mathcal{H}^{(3)}$.

(b) Source vertex Γ_1 in $\mathcal{H}^{(3)}$.

(c) Normal self-energies from the 2nd-order perturbation theory with the cubic vertices $\Gamma_{1,2}$.
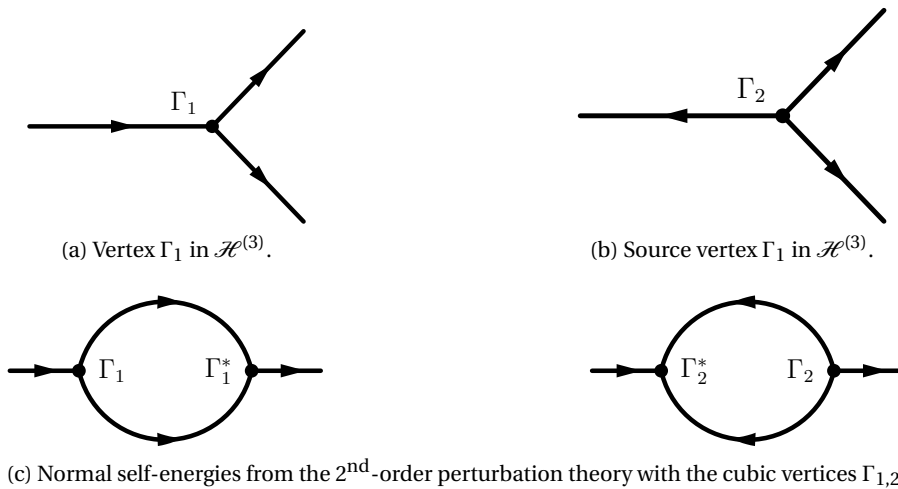
Figure 6.5 – Diagrammatic representation of the cubic vertices $\Gamma_{1,2}$ and their contribution to the renormalised spectrum $\Sigma^{(3)}$.

From this expression of $\mathscr{H}^{(3)}$, its contribution to the renormalised spectrum can be finally obtained with the second-order perturbation theory:

$$
\begin{aligned}
\Sigma^{(3)}(\mathbf{k}) = 2J_1 \Bigg(& \frac{1}{2} \frac{1}{\sigma_{\mathrm{BZ}}} \int\limits_{\mathrm{BZ}} \frac{\left|\Gamma_1(\mathbf{q};\mathbf{k})\right|^2}{\epsilon(\mathbf{k}) - \epsilon(\mathbf{q}) - \epsilon(\mathbf{k}-\mathbf{q})} \mathrm{d}\mathbf{q} \\
& - \frac{1}{2} \frac{1}{\sigma_{\mathrm{BZ}}} \int\limits_{\mathrm{BZ}} \frac{\left|\Gamma_2(\mathbf{q};\mathbf{k})\right|^2}{\epsilon(\mathbf{k}) + \epsilon(\mathbf{q}) + \epsilon(\mathbf{k}+\mathbf{q})} \mathrm{d}\mathbf{q} \Bigg).
\end{aligned}
\tag{6.23}
$$

The factor σ_{BZ} is the surface of the Brillouin zone. This expression also corresponds to the Dyson equation with the on-shell approximation. This completes the expression of the renormalised spectrum $\varepsilon_{\mathbf{k}}$ that we are looking for, $\tilde{\varepsilon}(\mathbf{k}) = \epsilon(\mathbf{k}) + \Sigma^{(3)}(\mathbf{k}) + \Sigma^{(4)}(\mathbf{k})$, with the self-energies $\Sigma^{(3)}(\mathbf{k})$ and $\Sigma^{(4)}(\mathbf{k})$.

As a side remark, we highlight the fact that Goldstone modes are preserved to all orders of the perturbation. If the harmonic spectrum ε has a Goldstone mode at $\bar{\mathbf{q}}$, then $\Sigma^{(3)}(\bar{\mathbf{q}}), \Sigma^{(4)}(\bar{\mathbf{q}})$ all diverge because $\varepsilon_{\bar{\mathbf{q}}} = 0$. However, the divergency of $\Sigma^{(3)}$ is exactly cancelled by $\Sigma^{(4)}$, yielding $\tilde{\varepsilon}(\bar{\mathbf{q}}) = 0$ as it should. This non-trivial cancellation could have been used as a small sanity check for our perturbation calculations if these calculations had been well-defined—this is of course not the case here. However, the AFM $J_1 - J_3$ model does not have any lines of zero-modes in the harmonic spectrum. This means that the perturbation calculations can be carried out without any problems, and we thus checked numerically that $\Sigma^{(3)}_{J_1, J_3}(\mathbf{k}) + \Sigma^{(4)}_{J_1, J_3}(\mathbf{k}) \to 0$ as $\mathbf{k} \to \bar{\mathbf{q}}$, as it should for this model. As the colour-configuration of the J_3-neighbours are similar to that of the J_1-neighbours, the perturbative terms $\mathscr{H}^{(3)}_{J_1, J_3}, \mathscr{H}^{(4)}_{J_1, J_3}$ in the real-space are nearly identical to those of the original J_1 model: only the sum over the third-nearest neighbors has to be added. In this sense, checking the preservation of the Goldstone modes with the $J_1 - J_3$ model can also serve as a small sanity check for the calculations of the perturbative terms of our J_1 model, to some degree. Albeit very indirectly.

6.2.5 Using J_n to get the renormalised spectrum

The expression that is sought after is $\tilde{\varepsilon}_{\mathbf{k}}$, i.e., the LHS of Eq. (6.13). However, as mentioned earlier, the RHS of this equation that we obtained is, in fact, infrared-divergent. Thus, the idea is to establish a self-consistent equation with it by using our physical knowledge that the authentic quantum spectrum would most certainly lift the line of zero-modes except at $\mathbf{q}_{0,\pm1}$ where the linear Goldstone modes are expected. As we expect that renormalised spectrum will qualitatively resemble the harmonic spectrum of the $J_1 - J_n$ model due to quantum fluctuations, we thus make the assumption that the renormalized spectrum on the LHS is given by the bare spectrum of the $J_1 - J_n$ model, $\tilde{\varepsilon}_{\mathbf{k}} \equiv \varepsilon_{J_1, J_n}$. We also replace all the bare spectra $\varepsilon(\mathbf{k})$ in the expressions of the self-energies $\Sigma^{(3)}, \Sigma^{(4)}$ on the RHS by $\varepsilon_{J_1, J_n}(\mathbf{k})$ which does not possess any line of zero-modes to treat the divergence problem. This yields a self-consistent

equation that can be solved for J_n for a specific value of $\mathbf{k}$:

$$
\begin{aligned}
\tilde{\varepsilon}(\mathbf{k}) &= \varepsilon(\mathbf{k}) + \Sigma^{(3)}(\mathbf{k}) + \Sigma^{(4)}(\mathbf{k}) \\
&\qquad\downarrow \\
\varepsilon_{J_1,J_n}(\mathbf{k};J_n) &\overset{!}{=} \varepsilon(\mathbf{k}) + \Sigma^{(3)}_{J_1,J_n}(\mathbf{k};J_n) + \Sigma^{(4)}_{J_1,J_n}(\mathbf{k};J_n) \\
&\equiv \tilde{\varepsilon}(\mathbf{k}).
\end{aligned}
\tag{6.24}
$$

We note that this replacement also applies to the expressions of $u_{\mathbf{k}}$ and $v_{\mathbf{k}}$ in the self-energies, as they also depend implicitly on $\varepsilon_{\mathbf{k}}$, see Eqs. (6.10):

$$
u_{\mathbf{k}} \quad\longrightarrow\quad u(\mathbf{k};J_n) = \sqrt{\frac{1}{2}\left(\frac{\mathcal{A}}{\varepsilon_{J_1,J_n}(\mathbf{k})} + 1\right)}\, e^{i\arg\mathcal{B}_{J_n}(\mathbf{k})},
\tag{6.25a}
$$

$$
v_{\mathbf{k}} \quad\longrightarrow\quad v(\mathbf{k};J_n) = \sqrt{\frac{1}{2}\left(\frac{\mathcal{A}}{\varepsilon_{J_1,J_n}(\mathbf{k})} - 1\right)}.
\tag{6.25b}
$$

All in all, the new self-consistent self energies on the RHS will be given by

$$
\begin{aligned}
\Sigma^{(3)}_{J_1,J_n}(\mathbf{k}) =2J_1 &\left(\frac{1}{2}\frac{1}{\sigma_{\mathrm{BZ}}}\int_{\mathrm{BZ}} \frac{\left|\Gamma_1\left(\mathbf{q};\mathbf{k};\varepsilon_{J_1,J_n}(\mathbf{k})\right)\right|^2}{\varepsilon_{J_1,J_n}(\mathbf{k}) - \varepsilon_{J_1,J_n}(\mathbf{q}) - \varepsilon_{J_1,J_n}(\mathbf{k}-\mathbf{q})}\mathrm{d}\mathbf{q} \right. \\
&\left. - \frac{1}{2}\frac{1}{\sigma_{\mathrm{BZ}}}\int_{\mathrm{BZ}} \frac{\left|\Gamma_2\left(\mathbf{q};\mathbf{k};\varepsilon_{J_1,J_n}(\mathbf{k})\right)\right|^2}{\varepsilon_{J_1,J_n}(\mathbf{k}) + \varepsilon_{J_1,J_n}(\mathbf{q}) + \varepsilon_{J_1,J_n}(\mathbf{k}+\mathbf{q})}\mathrm{d}\mathbf{q} \right), \\
\Sigma^{(4)}_{J_1,J_n}(\mathbf{k}) =2J_1 &\omega^{(4)}_{\mathbf{k}}\left(\varepsilon_{J_1,J_n}(\mathbf{k})\right),
\end{aligned}
\tag{6.26}
$$

where the dependence on $\varepsilon_{J_1,J_n}(\mathbf{k})$ of Γ_1, Γ_2 and $\omega^{(4)}_k$ come from their dependence on $u(\mathbf{k};J_n)$ and $v(\mathbf{k};J_n)$.

As there is only have one parameter J_n in this self-consistent equation, we cannot hope to obtain one universal solution J_n for all the values of $\mathbf{k}$. We will thus take one particular point in the Brillouin zone, $\bar{\mathbf{k}} = (\frac{\pi}{3},\frac{\pi}{3})$ to solve this equation. In this sense, it is a very crude approach. However, this has the advantage that the infrared divergency is eliminated and that it is very simple to solve. The reason for this particular choice of $\bar{\mathbf{k}}$ is because it is supposedly the point at which the gap is the largest, thus endowing it with a certain significance in our attempt of creating a gap in the spectrum. Furthermore, the self consistent equation not being an exact perturbation calculations, the cancellation of the divergencies is not achieved at the Goldstone points $\mathbf{q}_{0,\pm1}$, so it is desirable to solve the equation at the furthest possible point from the Goldstone points, which is precisely the point $\bar{\mathbf{k}}$.

With this in mind, we start with the calculations of the harmonic spectrum of the $J_1 - J_n$ models.[15]

---

[15]Note that the application of the LFWT to the further-neighbour coupling is identical to the nearest-neighbour Hamiltonian.

The $J_1 - J_3$ model

Let us first include the third-furthest-neighbour coupling J_3 (coupling between a site and its second-nearest horizontal/vertical neighbours). If $J_3 > 0$, it then stabilises the three-sublattice
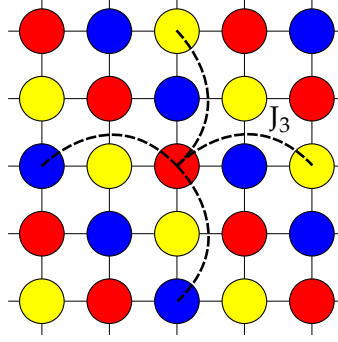

Figure 6.6 – The antiferromagnetic J_3-coupling with the three-sublattice order.

configuration. The colour configuration of the third-furthest neighbours is similar to the nearest-neighbours, only spatially inverted with respect to the reference site. Hence, the diagonalisation of $\mathcal{H}^{(2)}_{J_1,J_3}$ can be carried out in a similar fashion to that of $\mathcal{H}^{(2)}$ in subsection 6.2.2. The dispersion relation of $\mathcal{H}^{(2)}_{J_1,J_3}$ is then be given by

$$\varepsilon_{J_1,J_3}(\mathbf{k}) := n_c \sqrt{\mathcal{A}_{J_3}^2 - \left|\mathcal{B}_{J_3}(\mathbf{k})\right|^2}, \tag{6.27}$$

where

$$\begin{aligned} \mathcal{A}_{J_3} &= 4(J_1 + J_3), \\ \mathcal{B}_{J_3}(\mathbf{k}) &= 4(J_1\gamma_{\mathbf{k}} + J_3\gamma_{-2\mathbf{k}}). \end{aligned} \tag{6.28}$$

The $J_1 - J_6$ model

It is also possible to include the ferromagnetic sixth-nearest-neighbour coupling $J_6 < 0$ (or the third-nearest horizontal/vertical neighbours) to stabilise our tripartite configuration, see Figure 6.7: As we already have the quadratic Hamiltonian of the initial J_1-model, we only need to take care of the J_6-part of the $J_1 - J_6$ Hamiltonian. All the J_6-bonds connect one sublattice with itself, since the J_6-coupling is ferromagnetic. As we only derived the expression of the quadratic Hamiltonian for antiferromagnetic bonds until now, we need to derive the expression of the quadratic Hamiltonian for ferromagnetic bonds using the Holstein-Primakoff bosons by replacing $b_A(i)$ by $\sqrt{n_c}$. This is simply given by

$$\begin{aligned} \mathcal{H}^{(2)}_{J_6} = J_6 n_c \cdot \frac{1}{2} \sum_i \sum_{\langle\langle j'\rangle\rangle} \Big[&b_B(i)b_B^\dagger(j') + b_C(i)b_C^\dagger(j') + b_B^\dagger(i)b_B(j') + b_C^\dagger(i)b_C(j') \\ &- b_B^\dagger(i)b_B(i) - b_B^\dagger(j')b_B(j') - b_C^\dagger(i)b_C(i) - b_C^\dagger(j')b_C(j') \Big]. \end{aligned} \tag{6.29}$$

111
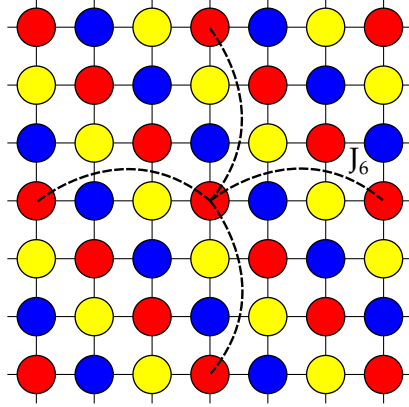
Figure 6.7 – The ferromagnetic J_6-coupling with the three-sublattice order.

The $\langle\langle j' \rangle\rangle$ refers to the sixth-nearest-neighbours of i. The Fourier transform yields

$$\mathcal{H}_{J_6}^{(2)} = J_6 n_c \sum_{\mathbf{k}} \left[\left(4\gamma_{J_6}(\mathbf{k}) - 4\right) b_B^\dagger(\mathbf{k}) b_B(\mathbf{k}) + \left(4\gamma_{J_6}(\mathbf{k}) - 4\right) b_C^\dagger(\mathbf{k}) b_C(\mathbf{k}) \right] + \text{cst}, \tag{6.30}$$

with

$$\gamma_{J_6}(\mathbf{k}) = \frac{1}{2}(\cos 3k_x + \cos 3k_y). \tag{6.31}$$

We can now add these terms with the terms from the J_1-Hamiltonian, Eq. (1.36), and perform the Bogoliubov transformation to obtain the dispersion relation of the $J_1 - J_6$ model. The resulting dispersion relation ε_{J_6} is given by

$$\varepsilon_{J_1, J_6}(\mathbf{k}) := n_c \sqrt{\mathcal{A}_{J_6}(\mathbf{k})^2 - \left|\mathcal{B}_{J_6}(\mathbf{k})\right|^2}, \tag{6.32}$$

with

$$\begin{aligned}
\mathcal{A}_{J_6}(\mathbf{k}) &= 2J_1 + 4J_6(\gamma_{J_6}(\mathbf{k}) - 1), \\
\mathcal{B}_{J_6}(\mathbf{k}) &= 2J_1 \gamma_{\mathbf{k}}.
\end{aligned} \tag{6.33}$$

The $J_1 - J_2$ model

The choice of the sign of the second-next-nearest-neighbour coupling J_2 should not be isotropic in the sense that the sign of the coupling must depend on the direction of the coupling to stabilise our tripartite configuration. Two of the diagonal couplings are ferromagnetic whereas the two other directions are antiferromagnetic: the north-west/south-east bonds should be ferromagnetic whereas the north-east/south-west bonds should be antiferromagnetic, see Figure 6.1. By convention, let us choose the value of J_2 to be positive. Using Eq. (1.36) for antiferromagnetic bonds and Eq. (6.29) for ferromagnetic bonds, it is straightfor-
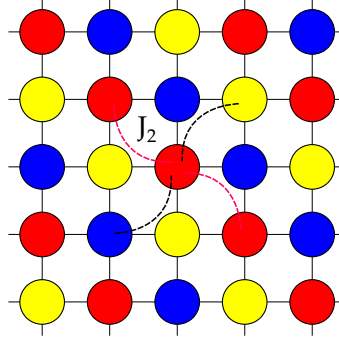
Figure 6.8 – The J_2-coupling with the three-sublattice order. The black dotted lines represent the antiferromagnetic bonds and the red dotted lines represent the ferromagnetic bonds.

ward to compute the dispersion relation. The result of the diagonalisation of the $J_1 - J_2$ model is given by

$$\varepsilon_{J_1,J_2}(\mathbf{k}) := n_c \sqrt{\mathcal{A}_{J_2}(\mathbf{k})^2 - \left|\mathcal{B}_{J_2}(\mathbf{k})\right|^2}, \tag{6.34}$$

with

$$\begin{aligned} \mathcal{A}_{J_2}(\mathbf{k}) &= 2J_1 + \left[J_2 - 2J_2\left(\cos(k_x - k_y) - 1\right)\right], \\ \mathcal{B}_{J_2}(\mathbf{k}) &= 2J_1\gamma_{\mathbf{k}} + J_2\gamma_{\mathbf{k}}^*. \end{aligned} \tag{6.35}$$

6.2.6 Magnetisation depending on the J_n

We now solve the equation $\varepsilon_{J_1,J_n}(\bar{\mathbf{k}};J_n) \overset{!}{=} \varepsilon(\bar{\mathbf{k}}) + \Sigma_{J_1,J_n}^{(3)}(\bar{\mathbf{k}};J_n) + \Sigma_{J_1,J_n}^{(4)}(\bar{\mathbf{k}};J_n)$ for J_n at the $\mathbf{k}$-point $\bar{\mathbf{k}} = \left(\pm\frac{\pi}{3}, \pm\frac{\pi}{3}\right)$ as mentioned before, where the gap is supposed to be the largest. For this, we set the value of the nearest-neighbour coupling $J_1 = 1$. For different J_n couplings, we obtain the solutions as follows:
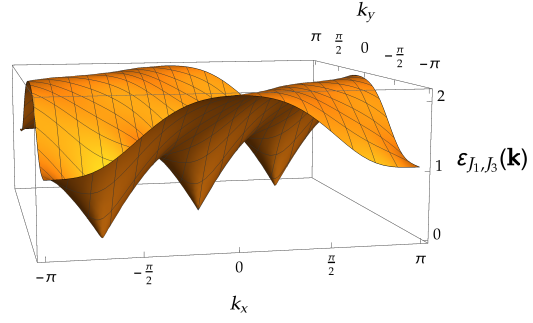
- $\tilde{\varepsilon} \equiv \varepsilon_{J_1,J_3} \quad \rightarrow \quad J_3 \approx 0.0689$
- $\tilde{\varepsilon} \equiv \varepsilon_{J_1,J_6} \quad \rightarrow \quad J_6 \approx -0.0324$ $\qquad$ (6.36)
- $\tilde{\varepsilon} \equiv \varepsilon_{J_1,J_2} \quad \rightarrow \quad J_2 \approx 0.1334$
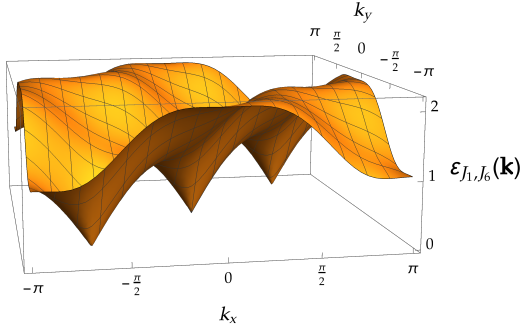
They are depicted in Figure 6.9 below.

Once we have the renormalised spectrum $\tilde{\varepsilon} \equiv \varepsilon_{J_1,J_n}$, we can compute the corrected value of the magnetisation $m \equiv m_{J_1,J_n}$ as in Ref. [31], but using the harmonic spectrum of the $J_1 - J_n$
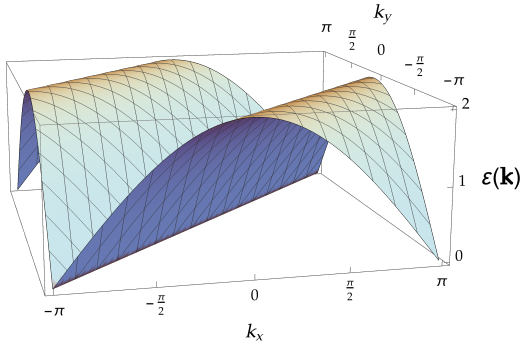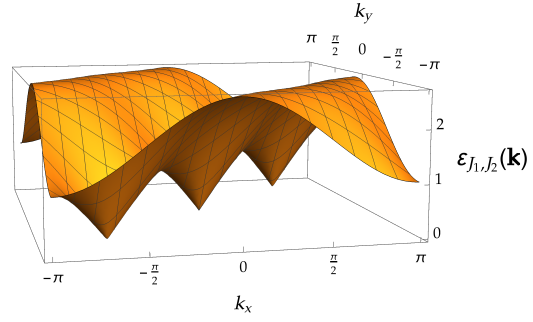
(a) Dispersion relation ε of the original J_1 model.

(b) Dispersion relation ε_{J_1,J_3} of the $J_1 - J_3$ model.

(c) Dispersion relation ε_{J_1,J_6} of the $J_1 - J_6$ model.

(d) Dispersion relation ε_{J_1,J_2} of the $J_1 - J_2$ model.

Figure 6.9 – The spectrum ε of the original J_1 model and the dispersion relations ε_{J_1,J_n} with the solutions J_n of the self-consistent equations. The spectra are all doubly degenerate in the extended Brillouin zone. We thus have 6 Goldstone modes in all the models.

model, as follows:

$$
\begin{aligned}
m &= \left\langle \hat{S}_A^A(i) \right\rangle \\
&= n_c - \left\langle b_B^{A\dagger}(i) b_B^A(i) + b_C^{A\dagger}(i) b_C^A(i) \right\rangle \\
&= n_c - 2 \left\langle v(\mathbf{k}; J_n)^2 \right\rangle .
\end{aligned}
\tag{6.37}
$$

The resulting results for the ordered moment are

- $\tilde{\varepsilon} \equiv \varepsilon_{J_1,J_3} \quad \rightarrow \quad m \approx 0.220$
- $\tilde{\varepsilon} \equiv \varepsilon_{J_1,J_6} \quad \rightarrow \quad m \approx 0.242$ $\qquad$ (6.38)
- $\tilde{\varepsilon} \equiv \varepsilon_{J_1,J_2} \quad \rightarrow \quad m \approx 0.301$

(a) ε_{J_1,J_3} and ε_{J_1,J_6}

(b) ε_{J_1,J_3} and ε_{J_1,J_2}
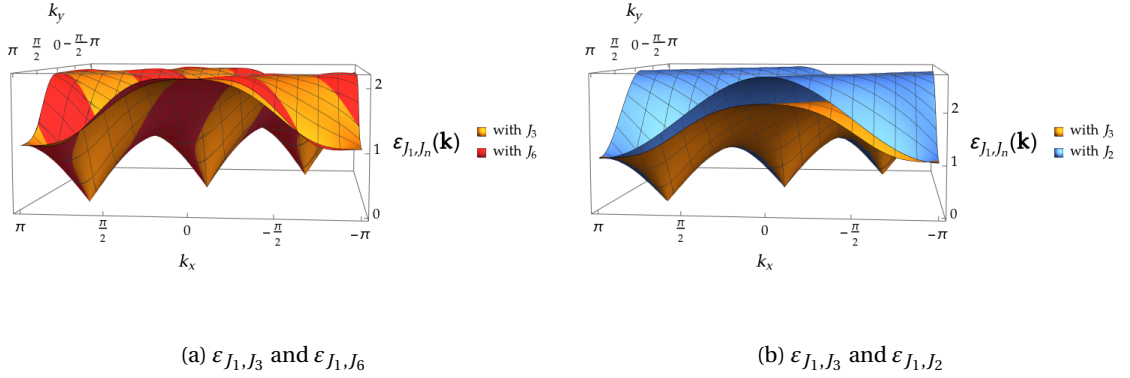
Figure 6.10 – Comparing the spectra ε_{J_1,J_3} with ε_{J_1,J_6} and ε_{J_1,J_2} with the solutions $J_3 \approx 0.0689$, $J_6 \approx -0.0324$, $J_2 \approx 0.1334$ of the respective self-consistent equations.

The value of m_{J_1,J_n} all vary, but they lie between $0.220 - 0.301$. They are all larger than zero, suggesting that the long-range colour-order would survive quantum fluctuations. These estimates of m are all within the numerical estimates $0.2 - 0.4$ suggested by the iPEPS and DMRG calculations in Ref. [31]. The linear fit of the largest system-size results of the iPEPS simulations seems to suggest the lower range of the estimate (0.2), so our estimates of m seem to be fairly consistent with these numerical results, given the rather basic nature of our calculations.

We would nonetheless point out the fact that the choice of J_n is very arbitrary, since any choice of J_n stabilising our tripartite configuration would be justified. Hence, it would be desirable to render these self-consistent equations more systematic in some way—perhaps by including more parameters. It could be conceivable to think that the true solution could be approached by adding more further-neighbour couplings. However, our attempt to solve the self-consistent equation based on the $J_1 - J_2 - J_3$ model in order to have two parameters has been hampered by numerical problems and has not been successful, probably due to the very crude nature of this self-consistent equation which makes it somewhat inconsistent with two such parameters.

It is however interesting to observe that the corrected magnetisation value is roughly similar between the three J_n that was used here, J_2, J_3, J_6. Indeed, it can be seen in Figure 6.10 that the dispersion relations of ε_{J_1,J_2}, ε_{J_1,J_3} and ε_{J_1,J_6} seem to be quite similar. More precisely, if we compare the velocity of the Goldstone modes of each of the ε_{J_1,J_n}, it can be seen that the velocities are similar. By denoting the velocity in the direction $k_x = k_y$ (i.e., in the direction of the line of zero-modes in the original model) by c_1 and the velocity of the orthogonal direction

$k_x = -k_y$ by c_2, we find that

- ε_{J_1, J_3} : $\quad c_1^{J_1, J_3} = 3\sqrt{2}\sqrt{J_1 J_3} = 1.114$ $\qquad c_2^{J_1, J_3} = \sqrt{2}\sqrt{J_1^2 + 5J_1 J_3 + 4J_3^2} = 1.651$

- ε_{J_1, J_3} : $\quad c_1^{J_1, J_6} = 6\sqrt{J_1 |J_6|} = 1.080$ $\qquad c_2^{J_1, J_6} = \sqrt{2}\sqrt{J_1^2 + 18J_1 |J_6|} = 1.779$ $\quad$ (6.39)

- ε_{J_1, J_3} : $\quad c_1^{J_1, J_2} = 3\sqrt{J_1 J_2} = 1.096$ $\qquad c_2^{J_1, J_2} = \sqrt{2J_1^2 + 9J_1 J_2 + 4J_2^2} = 1.809$

where we used $J_1 = 1$ and the solutions of J_n obtained in Eq. (6.36) for the values of J_n. The reduction of the magnetisation is proportional to $\int \frac{1}{\varepsilon_{J_1, J_n}} d\mathbf{k}$, thus the largest contribution to the magnetisation comes from the vicinity of the Goldstone modes. Since the velocities of the Goldstone modes are similar in all the three models, the magnetisation value m also turn out to be comparable in all three cases.

6.3 Different methods also show the line of zero-modes

As pointed out earlier, the line of zero-modes that appear in the quadratic spectrum of the SU(3) J_1-Hamiltonian in the three-sublattice configuration is due to the infinite classical ground-state degeneracy: it is not an artifact related to the LFWT method itself. To show this, we will derive the velocities of the Goldstone modes with two different calculations: first using the nonlinear sigma model (NLσM), and then by solving the quantum equations of motion of the generators $\hat{S}_\nu^\mu$, i.e., $\dot{\hat{S}}_\nu^\mu(i) = i\left[\mathcal{H}, \hat{S}_\nu^\mu(i)\right]$.

The equivalence of the velocity of the Goldstone modes obtained will all these methods is already known with the AFM SU(2) spin models. Indeed, the O(3) nonlinear sigma model [86] and the computation of the equations of motions of the spin operator $\mathbf{S}_i$ all yield the same velocity as the conventional spin-wave theory.[16] We will show here that it is also the case with our SU(3) model.

6.3.1 Non-linear σ model

The aim is to derive the velocities of the Goldstone modes from the action S in the continuum limit. For this, we closely follow the procedure used in [87, 12] for the SU(3) irreps with one row in the Young tableau (which includes the fundamental irrep we are considering).

The 2D SU(3) colour configuration considered here is the tripartite configuration. We first define the three-sublattice the unit cell as shown in Figure 6.11. With this in hand, we then define the primitive translation vectors

$$\mathbf{a_1} = (3,0)a \qquad \& \qquad \mathbf{a_2} = (-1,1)a \tag{6.40}$$

where a is the lattice spacing (that we will set to 1). From here onwards, we can write the

---

[16]Ref. [43] shows how to solve the equations of motions of the spin operator for the ferromagnetic case. The antiferromagnetic case can be consulted in the Appendix E.

position of a unit cell as a two-dimensional vector $(i, j) \in \mathbb{N}^2$ in the basis $\{\mathbf{a_1}, \mathbf{a_2}\}$. We now express the ground-state colour configuration of each of the three sites in the unit cell (i, j) with the three-dimensional complex vectors $\vec{\varphi}_1(i, j), \vec{\varphi}_2(i, j), \vec{\varphi}_3(i, j)$. Since the fields $\vec{\varphi}_{1,2,3}$
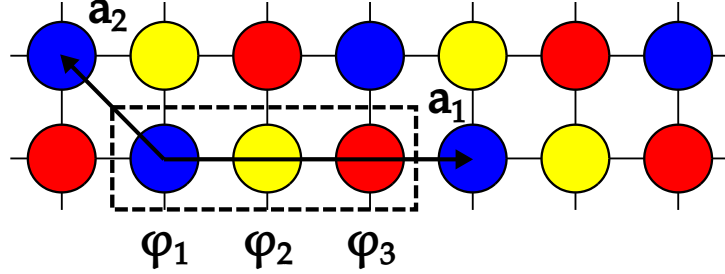

Figure 6.11 – The unit cell at the position (i, j) is depicted by the dashed box. The three orthogonal colours of the ground states $\vec{\phi}_1(i, j), \vec{\phi}_2(i, j)$ and $\vec{\phi}_3(i, j)$ are shown. The translation vectors $\mathbf{a_1}$ and $\mathbf{a_2}$ are shown by the arrows.

describe the ground-state configuration, they are all orthogonal to each other. In addition, in our ground-state configuration, there is a remaining U(1) × U(1) symmetry that has no effect on the energy of the bonds in the unit cell. Hence, the three vectors $\vec{\varphi}_{1,2,3}$ form together a matrix $U \in \mathrm{SU}(3) \setminus (\mathrm{U}(1) \times \mathrm{U}(1))$. This means that the matrix U can then be generated from the six non-diagonal Gell-Mann matrices[17] of SU(3) out of the eight Gell-Mann matrices that exist,

$$
\lambda_1 := \begin{pmatrix} 0 & 1 & 0 \\ 1 & 0 & 0 \\ 0 & 0 & 0 \end{pmatrix}, \qquad \lambda_2 := \begin{pmatrix} 0 & 0 & 1 \\ 0 & 0 & 0 \\ 1 & 0 & 0 \end{pmatrix}, \qquad \lambda_3 := \begin{pmatrix} 0 & 0 & 0 \\ 0 & 0 & 1 \\ 0 & 1 & 0 \end{pmatrix},
$$
$$
\lambda_4 := \begin{pmatrix} 0 & -i & 0 \\ i & 0 & 0 \\ 0 & 0 & 0 \end{pmatrix}, \qquad \lambda_5 := \begin{pmatrix} 0 & 0 & -i \\ 0 & 0 & 0 \\ i & 0 & 0 \end{pmatrix}, \qquad \lambda_6 := \begin{pmatrix} 0 & 0 & 0 \\ 0 & 0 & -i \\ 0 & i & 0 \end{pmatrix}, \tag{6.41}
$$
$$
\lambda_7 := \begin{pmatrix} 1 & 0 & 0 \\ 0 & -1 & 0 \\ 0 & 0 & 0 \end{pmatrix}, \qquad \lambda_8 := \frac{1}{\sqrt{3}} \begin{pmatrix} 1 & 0 & 0 \\ 0 & 1 & 0 \\ 0 & 0 & -2 \end{pmatrix},
$$

since the two diagonal matrices $\lambda_{7,8}$ are related to the remaining U(1) × U(1) symmetry. We thus conclude that

$$
U := \exp\left(i \sum_{k=1}^{6} \theta_k(i, j, \tau) \lambda_k \right) \tag{6.42}
$$

---

[17]Note that the numbering order of the Gell-Mann matrices are different from the one used in subsection 1.1.2 for practical purposes.

117

and

$$^{\mathrm{t}}\vec{\varphi}_i(i,j,\tau) = {}^{\mathrm{t}}\vec{e}_i\, U(i,j,\tau). \tag{6.43}$$

Note here that the symmetry of our system is reduced to $H := \mathrm{U}(1) \times \mathrm{U}(1)$ in our tripartite configuration from the initial $G := \mathrm{SU}(3)$ symmetry.[18] The number of Goldstone modes is then given by

$$\begin{aligned}
\dim\!\Big(G \setminus H\Big) &= \dim(G) - \dim(H) \\
&= \dim\!\Big(\mathrm{SU}(3)\Big) - \dim\!\Big(\mathrm{U}(1) \times \mathrm{U}(1)\Big) = 8 - 2 \\
&= 6.
\end{aligned} \tag{6.44}$$

This indeed corresponds to the number of Goldstone modes that we expect in the case where the accidental zero-modes are lifted, see Figure 6.9.

To allow the fluctuations from our ground-state configuration, we define the L matrices

$$L_1 := \begin{pmatrix} \cos l_1 & \sin l_1 & 0 \\ \sin l_1 & \cos l_1 & 0 \\ 0 & 0 & 1 \end{pmatrix}, \quad L_2 := \begin{pmatrix} \cos l_2 & 0 & \sin l_2 \\ 0 & 1 & 0 \\ \sin l_2 & 0 & \cos l_2 \end{pmatrix}, \quad L_3 := \begin{pmatrix} 1 & 0 & 0 \\ 0 & \cos l_3 & \sin l_3 \\ 0 & \sin l_3 & \cos l_3 \end{pmatrix},$$

$$L_4 := \begin{pmatrix} \cos l_4 & i\sin l_4 & 0 \\ -i\sin l_4 & \cos l_4 & 0 \\ 0 & 0 & 1 \end{pmatrix}, \quad L_5 := \begin{pmatrix} \cos l_5 & 0 & -i\sin l_5 \\ 0 & 1 & 0 \\ i\sin l_5 & 0 & \cos l_5 \end{pmatrix}, \quad L_6 := \begin{pmatrix} 1 & 0 & 0 \\ 0 & \cos l_6 & i\sin l_6 \\ 0 & -i\sin l_6 & \cos l_6 \end{pmatrix}.$$

$$\tag{6.45}$$

We can then generate a general fluctuation matrix L by multiplying all the L_k together. Before doing this, let us first attach the factor $\frac{a}{p}$ to the l_k to explicitly make the fluctuations small, where p is the number of horizontal boxes of the Young tableaux $\square, \square\square, \square\square\square \ldots$ which corresponds to our expansion parameter that allows us to reach the classical limit, $p \to \infty$ (p will be set to 1 at the end of our calculations). To the order $\frac{a^2}{p^2}$, L is then given by

$$\begin{aligned}
L(\vec{l}) &= \prod_{k=1}^{6} L_k(l_k) \\
&=: \begin{pmatrix} \sqrt{1 - \frac{a^2}{p^2}\left(|L_{12}|^2 + |L_{13}|^2\right)} & \frac{a}{p}L_{12} & \frac{a}{p}L_{13} \\ \frac{a}{p}L_{12}^{*} & \sqrt{1 - \frac{a^2}{p^2}\left(|L_{12}|^2 + |L_{23}|^2\right)} & \frac{a}{p}L_{23} \\ \frac{a}{p}L_{13}^{*} & \frac{a}{p}L_{23}^{*} & \sqrt{1 - \frac{a^2}{p^2}\left(|L_{13}|^2 + |L_{23}|^2\right)} \end{pmatrix} \\
&=: L(L_{12}, L_{23}, L_{13}),
\end{aligned} \tag{6.46}$$

where we now parametrise L with its matrix elements defined by $L_{12} := l_1 + l_4$, $L_{23} := l_3 + l_6$

---

[18]The remaining symmetry group H is what is known as the little group in physics. In algebraic mathematics, it is called a stabiliser.

and $L_{13} := l_2^* + l_5^*$ to simplify the subsequent calculations. This matrix skews any pair of axes out of the three axes in the three dimensional complex space. Hence, it allows us to generate states departing from the ground state. A state ϕ_i from an arbitrary configuration is then given by

$$^{\mathrm{t}}\vec{\phi}_i(i,j,\tau) = {}^{\mathrm{t}}\vec{e}_i \, LU(i,j,\tau). \tag{6.47}$$

We are now ready to write down the action S of our system. With appropriately defined spin coherent states and the Haas measure, whose details can be found in Ref. [87, 12], the imaginary-time partition function can be given as

$$\mathrm{Tr}\left(e^{-\beta\mathcal{H}}\right) = \int \mathscr{D}[\vec{\phi}] \exp\left\{-\int_0^\beta d\tau \left[\left(\bigotimes_{i,j}\langle\rangle\vec{\phi}(i,j;\tau)|\right)\mathcal{H}\left(\bigotimes_{i,j}|\vec{\phi}(i,j;\tau)\rangle\right) + \sum_{i,j} p\vec{\phi}^*(i,j;\tau)\partial_\tau\vec{\phi}(i,j;\tau)\right]\right\}$$

$$= \int \mathscr{D}[\vec{\phi}]e^{-S[\vec{\phi}]} \tag{6.48}$$

using the standard field-theoretical calculation techniques with the Lie-Trotter decomposition. The last term is the Berry phase. The SU(3) Hamiltonian that will be considered here is the $J_1 - J_3$ Hamiltonian,

$$\mathcal{H} = J_1 \sum_{\substack{\langle i,j\rangle \\ \mu,\nu}} S_\nu^\mu(i)S_\mu^\nu(j) + J_3 \sum_{\substack{\langle\langle i,j'\rangle\rangle \\ \mu,\nu}} S_\nu^\mu(i)S_\mu^\nu(j'). \tag{6.49}$$

This will allow us to derive the velocity of the Goldstone modes of the $J_1 - J_3$ model as well as the J_1 model in which we are interested. The action S of our discrete 2D lattice model with the $J_1 - J_3$ couplings is then given by

$$S = \int_0^\beta \sum_{i,j\in\mathbb{N}} \left\{ p^2 J_1 \left[\left|\vec{\phi}_1^*(i,j)\cdot\vec{\phi}_2(i,j)\right|^2 + \left|\vec{\phi}_2^*(i,j)\cdot\vec{\phi}_3(i,j)\right|^2 + \left|\vec{\phi}_3^*(i,j)\cdot\vec{\phi}_1(i+1,j)\right|^2 \right.\right.$$

$$\left. + \left|\vec{\phi}_1^*(i,j)\cdot\vec{\phi}_2(i,j+1)\right|^2 + \left|\vec{\phi}_2^*(i,j)\cdot\vec{\phi}_3(i,j+1)\right|^2 + \left|\vec{\phi}_3^*(i,j)\cdot\vec{\phi}_1(i+1,j+1)\right|^2 \right]$$

$$+ p^2 J_3 \left[\left|\vec{\phi}_1^*(i,j)\cdot\vec{\phi}_3(i,j)\right|^2 + \left|\vec{\phi}_2^*(i,j)\cdot\vec{\phi}_1(i+1,j)\right|^2 + \left|\vec{\phi}_3^*(i,j)\cdot\vec{\phi}_2(i+1,j)\right|^2 \right.$$

$$\left. + \left|\vec{\phi}_1^*(i,j)\cdot\vec{\phi}_3(i,j+2)\right|^2 + \left|\vec{\phi}_2^*(i,j)\cdot\vec{\phi}_1(i+1,j+2)\right|^2 + \left|\vec{\phi}_3^*(i,j)\cdot\vec{\phi}_2(i+1,j+2)\right|^2 \right]$$

$$\left. + p \sum_{n=1}^3 \vec{\phi}_n^*(i,j)\cdot\partial_\tau\vec{\phi}_n(i,j) \right\} d\tau, \tag{6.50}$$

where the τ-dependency is implicit and the individual terms come from each bond of the unit cell. In the continuum limit, the fluctuations L_{12}, L_{23}, L_{13} can be integrated out, after

which the fields $\vec{\varphi}$ can be linearised in θ_k—remember that $U := \exp\left(i \sum\limits_{k=1}^{6} \theta_k(i,j,\tau)\lambda_k\right)$—such that we can obtain the low-energy behaviour of our system. Furthermore, we now consider a coordinate basis $\{x', y'\}$ rotated by $\frac{\pi}{2}$ such that we can conveniently calculate the velocities of the Goldstone modes in the direction of the line of zero-modes in the Brillouin zone ($k_x = k_y$) and in its orthogonal direction $k_x = -k_y$. The details of all these calculations can be found in Appendix D. All in all, the linearised action $S_0[\theta]$ is given by

$$S_0[\theta] = \int dx' dy' d\tau \mathscr{L} = \int dx' dy' d\tau \sum_{i=1}^{6} \left(\chi |\partial_\tau \theta_i|^2 + \rho_1 |\partial_1 \theta_i|^2 + \rho_2 |\partial_2 \theta_i|^2\right) \tag{6.51}$$

with $\partial_1 = \frac{\partial}{\partial x'}$, $\partial_2 = \frac{\partial}{\partial y'}$ and

$$\chi := \frac{1}{2(J_1 + J_3)}, \qquad \rho_1 := 9a^2 p^2 \left(-\frac{J_3}{J_1 + J_3} + J_3\right), \qquad \rho_2 := a^2 p^2 (J_1 + 4J_3). \tag{6.52}$$

We will now set $a = 1$ and $p = 1$. The Euler-Lagrange equations of our action $S_0[\theta]$ yield the equations of motion,

$$\partial_\mu \left(\frac{\partial \mathscr{L}}{\partial(\partial_\mu \theta_k)}\right) - \frac{\delta \mathscr{L}}{\delta \theta_i} = 0 \qquad \Longrightarrow \qquad \left(\chi \partial_\tau^2 + \rho_1 \partial_1^2 + \rho_2 \partial_2^2\right) = 0, \tag{6.53}$$

with $\mu \in \{x', y', \tau\}$. They can be solved with the ansatz $\theta_i = C_i \left(e^{i\mathbf{k}\cdot\mathbf{r} + \omega_{i,\mathbf{k}}\tau} + c.c.\right)$, yielding the solution for $\omega_{i,\mathbf{k}}$:

$$\Longrightarrow \quad \omega_{i,\mathbf{k}} = \sqrt{\frac{\rho_1}{\chi} k_{x'}^2 + \frac{\rho_2}{\chi} k_{y'}^2}$$

$$=: \sqrt{c_1^2 k_{x'}^2 + c_2^2 k_{y'}^2}, \tag{6.54}$$

where $i \in \{1, \ldots, 6\}$. The velocities of the Goldstone modes $c_1^{J_1, J_3}$ and $c_2^{J_1, J_3}$ are then given by

$$c_1^{J_1, J_3} = \sqrt{\frac{\rho_1}{\chi}} = ap3\sqrt{2}\sqrt{J_1 J_3},$$

$$c_2^{J_1, J_3} = \sqrt{\frac{\rho_2}{\chi}} = ap\sqrt{2}\sqrt{J_1^2 + 5J_1 J_3 + 4J_3^2} \tag{6.55}$$

for each of the 6 modes ω_i. We thus obtain 6 Goldstone modes related the broken rotational symmetries $\lambda_{1,\ldots,6}$. The $c_1^{J_1, J_3}$ and $c_2^{J_1, J_3}$ indeed correspond to the velocities of the $J_1 - J_3$ model obtained with the LFWT in Eq. (6.39) in section 6.1. In particular, the velocity of the J_1 model (i.e., $J_3 = 0$) in the $k_{x'}$ direction is 0 as it should according to the LFWT:

$$c_1^{J_1} = 0, \qquad c_2^{J_1} = \sqrt{2}J_1. \tag{6.56}$$

We also note that (6.54) is reminiscent of the hydrodynamic investigation of the magnetic spin

systems where the spin-wave velocity c is indeed given by $c = \sqrt{\frac{\rho}{\chi}}$ [88, 89, 90, 91] in isotropic Goldstone modes, with ρ being the stiffness constant and χ the magnetic susceptibility.

6.3.2 The Liouville equation

Let us now compute the velocities of the Goldstone modes using the quantum version of the Liouville equation. It yields a system of differential equations (equations of motion) to solve. It can be instructive to first perform these calculations for the conventional AFM SU(2) spins on the square lattice—details of which can be found in the Appendix E. Here, we start with our usual SU(3) Hamiltonian

$$\mathcal{H} = J \sum_{\langle i,j \rangle} \sum_{\mu,\nu} \hat{S}_\nu^\mu(i) \hat{S}_\mu^\nu(j), \tag{6.57}$$

where μ, ν are the colour indices. One should note that the Hamiltonian is written using 9 generators instead of 8 generators (i.e., they are not all independent) and that they are written in terms of ladder operators.

For ease of readability, we will exceptionally use the numbers $1, 2, 3$ instead of the letters A, B, C to designate the three SU(3) colours in this subsection, and we will also omit the hat symbol $\hat{}$ from the operators $\hat{S}_\nu^\mu$. The sites in each of the three sublattices of our ground-state configuration will be denoted by $i \in \Lambda_1$, $j \in \Lambda_2$, $k \in \Lambda_3$. Furthermore, the colour indices will be denoted by $\alpha, \beta, \mu, \nu \in \{1, 2, 3\}$.

Using the SU(3) commutation relations, let us calculate the Liouville equation for $S_\beta^\alpha(i)$ for any $\alpha, \beta \in \{1, 2, 3\}$ and $i \in \Lambda_1$:

$$
\begin{aligned}
\dot{S}_\beta^\alpha(i) =& i \left[\mathcal{H}, S_\beta^\alpha(i) \right] \\
=& iJ \sum_{\langle j \in \{\mathbf{e}_x, \mathbf{e}_y\} \rangle} \sum_{\mu,\nu=1}^{3} \left[S_\nu^\mu(i), S_\beta^\alpha(i) \right] S_\mu^\nu(j) + iJ \sum_{\langle k \in \{-\mathbf{e}_x, -\mathbf{e}_y\} \rangle} \sum_{\mu,\nu=1}^{3} S_\nu^\mu(k) \left[S_\mu^\nu(i), S_\beta^\alpha(i) \right] \\
=& iJ \sum_{\mu,\nu=1}^{3} \left\{ \sum_{\langle j \rangle} \left(\delta_\beta^\mu S_\nu^\alpha(i) - \delta_\nu^\alpha S_\beta^\mu(i) \right) S_\mu^\nu(j) + \sum_{\langle k \rangle} S_\nu^\mu(k) \left(\delta_\beta^\nu S_\mu^\alpha(i) - \delta_\mu^\alpha S_\beta^\nu(i) \right) \right\} \\
=& iJ \sum_{\mu=1}^{3} \left\{ \sum_{\langle j \rangle} \left(S_\mu^\alpha(i) S_\beta^\mu(j) - S_\beta^\mu(i) S_\mu^\alpha(j) \right) + \sum_{\langle k \rangle} \left(S_\beta^\mu(k) S_\mu^\alpha(i) - S_\mu^\alpha(k) S_\beta^\mu(i) \right) \right\}.
\end{aligned}
\tag{6.58}
$$

Due to the symmetry of the order we consider, the Liouville equations for $S_\beta^\alpha(j)$ and $S_\beta^\alpha(k)$ are identical to (6.58) up to a cyclic rotation of the site indices i, j, k.

We now consider the colours on each site to be $\mathbb{C}^3$ vectors with length n_c (just as we would assume that the spin has length S in the SU(2) calculations). Given a $\mathbb{C}^3$ basis $\{\mathbf{e}_1, \mathbf{e}_2, \mathbf{e}_3\}$, we can assume that the colour of the sublattice Λ_α is given by $n_c \mathbf{e}_\alpha$ with $\alpha \in \{1, 2, 3\}$. Taking into account the action of the generators on these vectors, we can conclude that the generators

121

can be approximated by

$$
\begin{aligned}
S_\beta^\alpha(i;t) &= n_c \delta_1^\alpha \delta_\beta^1 + \delta S_\beta^\alpha(i;t), \\
S_\beta^\alpha(j;t) &= n_c \delta_2^\alpha \delta_\beta^2 + \delta S_\beta^\alpha(j;t), \\
S_\beta^\alpha(k;t) &= n_c \delta_3^\alpha \delta_\beta^3 + \delta S_\beta^\alpha(k;t).
\end{aligned}
\tag{6.59}
$$

Plugging this approximation into Eq. (6.58) yields

$$
\begin{cases}
\delta \dot{S}_\beta^\alpha(i) = & i J n_c \left\{ \sum\limits_{\langle j \rangle} \left[\delta_\beta^2\, \delta S_2^\alpha(i) + \delta_1^\alpha\, \delta S_\beta^1(j) - \delta_2^\alpha\, \delta S_\beta^2(i) - \delta_\beta^1\, \delta S_1^\alpha(j) \right] \right. \\
& \left. + \sum\limits_{\langle k \rangle} \left[\delta_1^\alpha\, \delta S_\beta^1(k) + \delta_\beta^3\, \delta S_3^\alpha(i) - \delta_\beta^1\, \delta S_1^\alpha(k) - \delta_3^\alpha\, \delta S_\beta^3(i) \right] \right\}, \\
\delta \dot{S}_\beta^\alpha(j) = & i J n_c \left\{ \sum\limits_{\langle k \rangle} \left[\delta_\beta^3\, \delta S_3^\alpha(j) + \delta_2^\alpha\, \delta S_\beta^2(k) - \delta_3^\alpha\, \delta S_\beta^3(j) - \delta_\beta^2\, \delta S_2^\alpha(k) \right] \right. \\
& \left. + \sum\limits_{\langle i \rangle} \left[\delta_2^\alpha\, \delta S_\beta^2(i) + \delta_\beta^1\, \delta S_1^\alpha(j) - \delta_\beta^2\, \delta S_2^\alpha(i) - \delta_1^\alpha\, \delta S_\beta^1(j) \right] \right\}, \\
\delta \dot{S}_\beta^\alpha(k) = & i J n_c \left\{ \sum\limits_{\langle i \rangle} \left[\delta_\beta^1\, \delta S_1^\alpha(k) + \delta_3^\alpha\, \delta S_\beta^3(i) - \delta_1^\alpha\, \delta S_\beta^1(k) - \delta_\beta^3\, \delta S_3^\alpha(i) \right] \right. \\
& \left. + \sum\limits_{\langle j \rangle} \left[\delta_3^\alpha\, \delta S_\beta^3(j) + \delta_\beta^2\, \delta S_2^\alpha(k) - \delta_\beta^3\, \delta S_3^\alpha(j) - \delta_2^\alpha\, \delta S_\beta^2(k) \right] \right\},
\end{cases}
\tag{6.60}
$$

up to order $\mathcal{O}(\delta S^2)$. The time dependence is implicit in these equations as a matter of convenience.

Taking advantage of the periodicity of the order, we can go to the Fourier space to help to solve the equations. Let us define the Fourier transform

$$
\delta S_{\beta,l}^\alpha(\mathbf{p}) = \sqrt{\frac{3}{N}} \sum_{l \in \Lambda_l} \delta S_\beta^\alpha(l) e^{-i\mathbf{p} \cdot \mathbf{R}_l},
\tag{6.61}
$$

and the coordination number between two sublattices $z = 2$ as well as the geometrical factor

$$
\gamma_{\mathbf{k}} = \frac{1}{2} \left(e^{ik_x} + e^{ik_y} \right).
\tag{6.62}
$$

Then, the equations (6.60) become[19]

$$
\begin{cases}
\delta \dot{S}^{\alpha}_{\alpha,l,\mathbf{p}}(t) = \delta \dot{S}^{2}_{3,i,\mathbf{p}}(t) = \delta \dot{S}^{3}_{2,i,\mathbf{p}}(t) = \delta \dot{S}^{3}_{1,j,\mathbf{p}}(t) = \delta \dot{S}^{1}_{3,j,\mathbf{p}}(t) = \delta \dot{S}^{1}_{2,k,\mathbf{p}}(t) = \delta \dot{S}^{2}_{1,k,\mathbf{p}}(t) = 0, \\
\delta \dot{S}^{1}_{2,i,\mathbf{p}}(t) = +iJn_c z \left[\delta S^{1}_{2,i,\mathbf{p}}(t) + \gamma_{\mathbf{p}} \, \delta S^{1}_{2,j,\mathbf{p}}(t) + \gamma^{*}_{\mathbf{p}} \, \delta S^{1}_{2,k,\mathbf{p}}(t) \right], \\
\delta \dot{S}^{2}_{1,i,\mathbf{p}}(t) = -iJn_c z \left[\delta S^{2}_{1,i,\mathbf{p}}(t) + \gamma_{\mathbf{p}} \, \delta S^{2}_{1,j,\mathbf{p}}(t) + \gamma^{*}_{\mathbf{p}} \, \delta S^{2}_{1,k,\mathbf{p}}(t) \right], \\
\delta \dot{S}^{1}_{3,i,\mathbf{p}}(t) = +iJn_c z \left[\delta S^{1}_{3,i,\mathbf{p}}(t) + \gamma_{\mathbf{p}} \, \delta S^{1}_{3,j,\mathbf{p}}(t) + \gamma^{*}_{\mathbf{p}} \, \delta S^{1}_{3,k,\mathbf{p}}(t) \right], \\
\delta \dot{S}^{3}_{1,i,\mathbf{p}}(t) = -iJn_c z \left[\delta S^{3}_{1,i,\mathbf{p}}(t) + \gamma_{\mathbf{p}} \, \delta S^{3}_{1,j,\mathbf{p}}(t) + \gamma^{*}_{\mathbf{p}} \, \delta S^{3}_{1,k,\mathbf{p}}(t) \right], \\
\delta \dot{S}^{2}_{3,j,\mathbf{p}}(t) = +iJn_c z \left[\delta S^{2}_{3,j,\mathbf{p}}(t) + \gamma_{\mathbf{p}} \, \delta S^{2}_{3,k,\mathbf{p}}(t) + \gamma^{*}_{\mathbf{p}} \, \delta S^{2}_{3,i,\mathbf{p}}(t) \right], \\
\delta \dot{S}^{3}_{2,j,\mathbf{p}}(t) = -iJn_c z \left[\delta S^{3}_{2,j,\mathbf{p}}(t) + \gamma_{\mathbf{p}} \, \delta S^{3}_{2,k,\mathbf{p}}(t) + \gamma^{*}_{\mathbf{p}} \, \delta S^{3}_{2,i,\mathbf{p}}(t) \right], \\
\delta \dot{S}^{2}_{1,j,\mathbf{p}}(t) = +iJn_c z \left[\delta S^{2}_{1,j,\mathbf{p}}(t) + \gamma_{\mathbf{p}} \, \delta S^{2}_{1,k,\mathbf{p}}(t) + \gamma^{*}_{\mathbf{p}} \, \delta S^{2}_{1,i,\mathbf{p}}(t) \right], \\
\delta \dot{S}^{1}_{2,j,\mathbf{p}}(t) = -iJn_c z \left[\delta S^{1}_{2,j,\mathbf{p}}(t) + \gamma_{\mathbf{p}} \, \delta S^{1}_{2,k,\mathbf{p}}(t) + \gamma^{*}_{\mathbf{p}} \, \delta S^{1}_{2,i,\mathbf{p}}(t) \right], \\
\delta \dot{S}^{3}_{1,k,\mathbf{p}}(t) = +iJn_c z \left[\delta S^{3}_{1,k,\mathbf{p}}(t) + \gamma_{\mathbf{p}} \, \delta S^{3}_{1,i,\mathbf{p}}(t) + \gamma^{*}_{\mathbf{p}} \, \delta S^{3}_{1,j,\mathbf{p}}(t) \right], \\
\delta \dot{S}^{1}_{3,k,\mathbf{p}}(t) = -iJn_c z \left[\delta S^{1}_{3,k,\mathbf{p}}(t) + \gamma_{\mathbf{p}} \, \delta S^{1}_{3,i,\mathbf{p}}(t) + \gamma^{*}_{\mathbf{p}} \, \delta S^{1}_{3,j,\mathbf{p}}(t) \right], \\
\delta \dot{S}^{3}_{2,k,\mathbf{p}}(t) = +iJn_c z \left[\delta S^{3}_{2,k,\mathbf{p}}(t) + \gamma_{\mathbf{p}} \, \delta S^{3}_{2,i,\mathbf{p}}(t) + \gamma^{*}_{\mathbf{p}} \, \delta S^{3}_{2,j,\mathbf{p}}(t) \right], \\
\delta \dot{S}^{2}_{3,k,\mathbf{p}}(t) = -iJn_c z \left[\delta S^{2}_{3,k,\mathbf{p}}(t) + \gamma_{\mathbf{p}} \, \delta S^{2}_{3,i,\mathbf{p}}(t) + \gamma^{*}_{\mathbf{p}} \, \delta S^{2}_{3,j,\mathbf{p}}(t) \right].
\end{cases}
$$

$$(6.63)$$

We will use a compacter notation $\delta S^{\alpha\beta\pm}_{l,\mathbf{p}}$ for $\delta S^{\alpha}_{\beta,l}(\mathbf{p})$ and $\delta S^{\beta}_{\alpha,l}(\mathbf{p})$ whose expressions have opposite signs. The notation $\delta S^{\alpha\beta\pm}_{l,\mathbf{p}}$ thus designates two equations. We may, however, drop the superscript $\pm$ in certain equations for ease of notation.

We now proceed to solving the equations to obtain the frequency ω. The structure of the differential equations are not exactly the same as in the SU(2) case in Appendix E due to the more complex structure of SU(3). For instance, one can observe that $\delta S^{12}_{i,\mathbf{p}}$ is coupled to $\delta S^{12}_{j,\mathbf{p}}$ and $\delta S^{12}_{k,\mathbf{p}}$ unlike in the SU(2) calculations. However, the most important fact here is that the first line in Eq. (6.63) implies that $\delta S^{12}_{k,\mathbf{p}}$ is a constant in time. We thus have a system of

---

[19]The fact that

$$
\delta \dot{S}^{2}_{3,i,\mathbf{p}}(t) = \delta \dot{S}^{3}_{2,i,\mathbf{p}}(t) = \delta \dot{S}^{3}_{1,j,\mathbf{p}}(t) = \delta \dot{S}^{1}_{3,j,\mathbf{p}}(t) = \delta \dot{S}^{1}_{2,k,\mathbf{p}}(t) = \delta \dot{S}^{2}_{1,k,\mathbf{p}}(t) = 0
$$

are zero is reminiscent of the fact that the exponential map of the SU(3) manifold—which is a first-order approximation—considers geodesics along the "longitudinal lines" of the manifold starting from the origin. The "latitudinal lines" are not described by the first-order terms of the exponential map.

inhomogeneous differential equations to solve, and the Ansätze[20]

$$
\begin{aligned}
\delta S_{i,\mathbf{p}}^{12\,\pm}(t) &= \delta S_{i,\mathbf{p}}^{12\,\pm}\, e^{i\omega_{\mathbf{p}}^{\alpha\beta\pm}t} + C_{i,\mathbf{p}}^{\alpha\beta\pm}, \\
\delta S_{j,\mathbf{p}}^{12\,\pm}(t) &= \delta S_{j,\mathbf{p}}^{12\,\pm}\, e^{i\omega_{\mathbf{p}}^{\alpha\beta\pm}t} + C_{j,\mathbf{p}}^{\alpha\beta\pm}, \\
\delta S_{k,\mathbf{p}}^{12\,\pm}(t) &= \delta S_{k,\mathbf{p}}^{12\,\pm},
\end{aligned}
\tag{6.64}
$$

can be used. This then yields

$$
\begin{cases}
\begin{cases}
i\omega_{\mathbf{p}}^{12}\delta\dot{S}_{i,\mathbf{p}}^{12}e^{i\omega_{\mathbf{p}}^{12}t} = \pm iJn_c z\left\{\left[\delta S_{i,\mathbf{p}}^{12} + \gamma_{\mathbf{p}}\,\delta S_{j,\mathbf{p}}^{12}\right]e^{i\omega_{\mathbf{p}}^{12}t} + \left[C_{i,\mathbf{p}}^{12} + \gamma_{\mathbf{p}}C_{j,\mathbf{p}}^{12} + \gamma_{\mathbf{p}}^*\,\delta S_{k,\mathbf{p}}^{12}\right]\right\}, \\
i\omega_{\mathbf{p}}^{12}\delta\dot{S}_{j,\mathbf{p}}^{12}e^{i\omega_{\mathbf{p}}^{12}t} = \mp iJn_c z\left\{\left[\delta S_{j,\mathbf{p}}^{12} + \gamma_{\mathbf{p}}^*\,\delta S_{i,\mathbf{p}}^{12}\right]e^{i\omega_{\mathbf{p}}^{12}t} + \left[C_{j,\mathbf{p}}^{12} + \gamma_{\mathbf{p}}C_{i,\mathbf{p}}^{12} + \gamma_{\mathbf{p}}\,\delta S_{k,\mathbf{p}}^{12}\right]\right\}, \\
\end{cases} \\
\begin{cases}
i\omega_{\mathbf{p}}^{13}\delta\dot{S}_{i,\mathbf{p}}^{13}e^{i\omega_{\mathbf{p}}^{12}t} = \pm iJn_c z\left\{\left[\delta S_{i,\mathbf{p}}^{13} + \gamma_{\mathbf{p}}^*\,\delta S_{k,\mathbf{p}}^{13}\right]e^{i\omega_{\mathbf{p}}^{13}t} + \left[C_{i,\mathbf{p}}^{13} + \gamma_{\mathbf{p}}C_{k,\mathbf{p}}^{13} + \gamma_{\mathbf{p}}\,\delta S_{p,\mathbf{p}}^{13}\right]\right\}, \\
i\omega_{\mathbf{p}}^{13}\delta\dot{S}_{k,\mathbf{p}}^{13}e^{i\omega_{\mathbf{p}}^{12}t} = \mp iJn_c z\left\{\left[\delta S_{k,\mathbf{p}}^{13} + \gamma_{\mathbf{p}}\,\delta S_{i,\mathbf{p}}^{13}\right]e^{i\omega_{\mathbf{p}}^{13}t} + \left[C_{k,\mathbf{p}}^{13} + \gamma_{\mathbf{p}}C_{i,\mathbf{p}}^{13} + \gamma_{\mathbf{p}}^*\,\delta S_{j,\mathbf{p}}^{13}\right]\right\}, \\
\end{cases} \\
\begin{cases}
i\omega_{\mathbf{p}}^{23}\delta\dot{S}_{j,\mathbf{p}}^{23}e^{i\omega_{\mathbf{p}}^{23}t} = \pm iJn_c z\left\{\left[\delta S_{j,\mathbf{p}}^{23} + \gamma_{\mathbf{p}}\,\delta S_{k,\mathbf{p}}^{23}\right]e^{i\omega_{\mathbf{p}}^{23}t} + \left[C_{j,\mathbf{p}}^{23} + \gamma_{\mathbf{p}}C_{k,\mathbf{p}}^{23} + \gamma_{\mathbf{p}}^*\,\delta S_{i,\mathbf{p}}^{23}\right]\right\}, \\
i\omega_{\mathbf{p}}^{23}\delta\dot{S}_{k,\mathbf{p}}^{23}e^{i\omega_{\mathbf{p}}^{12}t} = \mp iJn_c z\left\{\left[\delta S_{k,\mathbf{p}}^{23} + \gamma_{\mathbf{p}}^*\,\delta S_{j,\mathbf{p}}^{23}\right]e^{i\omega_{\mathbf{p}}^{23}t} + \left[C_{k,\mathbf{p}}^{23} + \gamma_{\mathbf{p}}C_{j,\mathbf{p}}^{23} + \gamma_{\mathbf{p}}\,\delta S_{i,\mathbf{p}}^{23}\right]\right\}, \\
\end{cases}
\end{cases}
\tag{6.65}
$$

i.e., a system of 12 equations in subsets of 2 equations. The inhomogeneous parts and the homogeneous parts are to be solved separately. The solutions of the inhomogeneous parts can be found in the Appendix E. Here, we only concentrate on the time-dependent homogeneous part that will yield $\omega_{\mathbf{p}}$. Looking at the first subset of (6.65), we have

$$
\omega_{\mathbf{p}}^{12\pm}\begin{pmatrix}\delta S_{i,\mathbf{p}}^{12\,\pm} \\ \delta S_{j,\mathbf{p}}^{12\,\pm}\end{pmatrix} = \pm Jn_c z\begin{pmatrix}1 & \gamma_{\mathbf{p}} \\ -\gamma_{\mathbf{p}}^* & -1\end{pmatrix}\begin{pmatrix}\delta S_{i,\mathbf{p}}^{12\,\pm} \\ \delta S_{j,\mathbf{p}}^{12\,\pm}\end{pmatrix}
\tag{6.66}
$$

$$
\begin{aligned}
\Leftrightarrow\quad & \begin{pmatrix}\pm Jn_c z - \omega_{\mathbf{p}}^{12\pm} & \pm Jn_c z\gamma_{\mathbf{p}} \\ \mp Jn_c z\gamma_{\mathbf{p}}^* & \mp Jn_c z - \omega_{\mathbf{p}}^{12\pm}\end{pmatrix} = 0 \\
\Rightarrow\quad & (Jn_c z - \omega_{\mathbf{p}}^{12\pm})(-Jn_c z - \omega_{\mathbf{p}}^{12\pm}) + \left|\gamma_{\mathbf{p}}\right|^2 = 0 \\
\Rightarrow\quad & \omega_{\mathbf{p}}^{12\pm} = Jn_c z\sqrt{1 - \left|\gamma_{\mathbf{p}}\right|^2}
\end{aligned}
$$

The other subsets of equations are similar and yield the same characteristic polynomial. We hence obtain the following 6 degenerate modes:

$$
\boxed{\omega_2^1(\mathbf{p}) = \omega_1^2(\mathbf{p}) = \omega_3^2(\mathbf{p}) = \omega_2^3(\mathbf{p}) = \omega_1^3(\mathbf{p}) = \omega_3^1(\mathbf{p}) = Jn_c z\sqrt{1 - \left|\gamma_{\mathbf{p}}\right|^2}}.
\tag{6.67}
$$

The dispersion relation obtained here is indeed identical to those calculated with the LFWT, see Eq. (1.39). In both methods, we obtain 6 degenerate modes that come from the exchange of two neighbouring colours, as suggested by the indices ω_β^α used here (with $\alpha \neq \beta$). From this

---

[20]Note that the solution of a simple inhomogeneous differential equation $a\frac{df(x)}{dx} + bf(x) + c = 0$ is given by $f(x) = Ae^{-\frac{b}{a}x} - \frac{c}{b}$.

expression of ω_β^α we have obtained here, we finally find that

$$c_1^{J_1} = 0, \qquad c_2^{J_1} = \sqrt{2}J_1 \tag{6.68}$$

along the diagonal lines of the Brillouin zone, again in agreement with the LFWT.

This concludes our comparison of different calculation methods for finding the velocity of the Goldstone modes. We indeed see that all of the methods show that the velocity is indeed zero along the diagonal line of the Brillouin zone. The accidental zeros related to the infinite ground-state degeneracy are not an artifact related to a method.

6.4 The path forward

A different way of generating a finite velocity must be found to circumvent the accidental zero-modes in the system. Rau et al. [92] recently showed that the accidental degeneracies can be lifted by computing the curvature of the classical and quantum zero-point energy manifolds in the variable θ that parametrises the classically degenerate manifold and its conjugate variable ϕ, and the resulting spectrum is in agreement with the renormalised spectrum obtained with the perturbation theory. Unfortunately, this cannot be applied in our case as numerical calculations of $E_{\mathrm{ZP}}(\theta)$ (see Figure 6.2) of our system suggest that $\frac{\partial^2 E_{\mathrm{ZP}}}{\partial \theta^2}$ seems to be ill-defined at the three-sublattice configuration point $\theta = \frac{\pi}{2}$.[21] However, by correctly identifying and defining the variables θ and ϕ in our three-sublattice configuration of the SU(3) model, it could pave the way to establishing a set of equations of motion in a similar fashion to Ref. [93], whose solutions would correctly generate the true Goldstone velocity.

---

[21]We note that this is also the case with the SU(2) $J_1 - J_2$ model at $J_2 = \frac{J_1}{2}$ with the variable θ that parametrises a family of helical ground states, connecting notably the Néel configuration (the true quantum minimum) and the spin-columnar configuration. At the minimum of E_{ZP}, its second derivative with respect to θ is ill-defined.

VII Conclusion

This concludes our investigation of the LFWT on AFM SU(N) Heisenberg models with long-range colour-ordered ground states. As the recent progress in experimental techniques of ultra-cold atomic gas manipulations in optical lattices make it possible to realise SU(N)-symmetric models, it is crucial to have a simple yet useful analytical method such as the LFWT to investigate the low-energy properties of such models.

First, the multiboson method of LFWT has been introduced in chapter II. This method introduces one bosonic species for each state in a given irrep. This allows to perform the Holstein-Primakoff expansion with ease as in the SU(2) spin-wave theory, yielding the low-energy spectra of the Heisenberg Hamiltonian and allowing the computation of the ordered moment of the system. The method yields the dispersive energy modes containing the Goldstone modes which are linear in **k** in the low-energy limit in the absence of frustration, and it also yields multipolar energy modes that appear as flat modes in the harmonic order of the Hamiltonian expansion. The method was applied on the square/honeycomb/triangular lattices in the bipartite/tripartite colour configuration for various SU(N) particles with $m > 1$ particle per site in completely antisymmetric irreps. It was found that the LFWT supports the long-range colour order for only one model, namely the AFM SU(4) Heisenberg model on the square lattice with two particles per site, for which the quantum corrections to the ordered moment is already large ($\sim$ 79%) with respect to the classical value. For $N > 4$ and $m > 2$, and for other lattice geometries, the quantum fluctuations become large as N or m increases, thus destroying the long-range colour order. The multiboson method was also used to derive the energy spectra of the AFM SU(3) Heisenberg chain in the adjoint irrep and in a bipartite configuration. It showed that the model yields Goldstone modes with two different velocities, a feature inherited from the algebraic group structure of SU(3).

The Mathur & Sen bosons were then introduced in chapter III for SU(3). Two sets of boson triplets were introduced: one for the fundamental irrep and one for its conjugate irrep. These bosons also allow us to apply the Holstein-Primakoff prescription consistently, and we have found for the AFM SU(3) Heisenberg chain in the adjoint irrep that they yield identical dispersive modes to those obtained with the multiboson method in chapter II. This method also

yields multipolar flat modes, whose nature is slightly different from the ones with the multi-boson method: the flat modes obtained here come only from the states that are degenerate in the weight-diagram, and their nature is not completely clear. The Mathur & Sen bosonic method can easily generalise the adjoint irrep model to any arbitrary irrep $[p, q]$ of SU(3). Consequently, it was found that the energy spectra of the model in non-self-conjugate irreps show linear and quadratic behaviour in small **k**, exhibiting ferromagnetic and antiferromagnetic behaviour simultaneously as in SU(2) ferrimagnetic models.

We also included one last bosonic representation in chapter IV: the Read & Sachdev bosons. In this bosonic representation, there is one boson per colour and per row of the Young tableau. The semi-classical expansion of the condensate bosons is not straightforward in this case, but the computation of the energy modes is easier than with the other methods for general irreps of SU(N). The models in chapter II and chapter III were treated using the Read & Sachdev bosons, and the resulting dispersive energy modes were identical to those found with the two previous methods. They also yield flat modes whose nature is similar to the flat modes of the Mathur & Sen bosonic method.

We briefly mention here that only the boson representations have been used in this work, as we were interested in studying the low-energy excitation spectra of long-range colour-ordered states, in which case the bosons are well adapted to the study the flavour waves with a large condensate as it is the case with the SU(2) spin waves. However, it is worth noting that the fermion representations can be more adapted for other types of ground states, such as the valence cluster states (VCS) comprising of singlets formed across multiple sites [69] or disordered states such as SU(N) chiral spin liquids (CSL) for which the fermion representation works well [69, 94]. It is also interesting to know that Read & Sachdev [8] indeed introduced a fermion representation for SU(N) generators already for the $\frac{1}{N}$ expansion they perform by taking $N \to \infty$ with $m \propto N$ and n_c fixed. They point out that the boson representation is more useful when taking the other large-N limit where $n_c \propto N$ and m fixed as in Ref. [95], and that the properties of the Hamiltonian does not depend on the choice of bosonic or fermionic operators.

The chapter VI was dedicated to the attempt of lifting the accidental zero-modes that exist in the harmonic spectrum of the SU(3) Heisenberg model on the square lattice with one particle per site and in a tripartite configuration. The line of zero-modes in the spectrum is related to an infinite number of ground-states that are related by a helical rotation, and such accidental modes can also be found in SU(2) models such as the $J_1 - J_2$ model. We showed that the accidental zero modes are not an artifact related to the LFWT, as field-theoretical calculations and quantum equations of motion also show the same feature. Such lines of zero modes in the harmonic spectrum lead to computations showing an absence of long-range colour order, but such conclusions can be premature as the zero modes are accidental. We thus established self-consistent equations using qualitative physical arguments that allowed us to estimate the ordered moment of the system, and the resulting magnetisation was in line with existing numerical simulations. Our approximation method is however very simple and needs to be

more systematic. As a further perspective to solve this problem of accidental zero modes, one could possibly try to set up a different way of establishing the set of equations of motions in the SU(3) manifold in the vein of Refs. [92, 93].

A The Bogoliubov transformation

1.1 The Bogoliubov transformation with two bosons

Let us take the following Hamiltonian $\mathscr{H}_{AB}$ in section 1.2 as an example on which we will perform the Bogoliubov transformation:

$$\mathscr{H}_{AB} = zJn_c \sum_{\mathbf{k}\in\text{RBZ}} \left[b^{B\dagger}_{A,\mathbf{k}} b^{B}_{A,\mathbf{k}} + b^{A\dagger}_{B,-\mathbf{k}} b^{A}_{B,-\mathbf{k}} + \gamma_{\mathbf{k}} b^{A\dagger}_{B,-\mathbf{k}} b^{B\dagger}_{A,\mathbf{k}} + \gamma^{*}_{\mathbf{k}} b^{A}_{B,-\mathbf{k}} b^{B}_{A,\mathbf{k}} \right]. \tag{1.1}$$

The factor $z = 2$ is the coordination number between two sublattices, i.e., the number of bonds connecting a site from the sublattice Λ_A to the sites from the sublattice Λ_B. In addition, the geometrical factor $\gamma_{\mathbf{k}}$ is given by

$$\gamma_{\mathbf{k}} = \frac{1}{2} \left(e^{ik_x} + e^{ik_y} \right). \tag{1.2}$$

The Bogoliubov transformation is given by

$$\begin{pmatrix} \tilde{b}^{B\dagger}_{A,\mathbf{k}} \\ \tilde{b}^{A}_{B,-\mathbf{k}} \end{pmatrix} = \underbrace{\begin{pmatrix} u_{\mathbf{k}} & v_{\mathbf{k}} \\ v_{\mathbf{k}} & u^{*}_{\mathbf{k}} \end{pmatrix}}_{=:M} \begin{pmatrix} b^{B\dagger}_{A,\mathbf{k}} \\ b^{A}_{B,-\mathbf{k}} \end{pmatrix}, \tag{1.3}$$

We now define the inverse Bogoliubov transformation:

$$\begin{pmatrix} b^{B\dagger}_{A,\mathbf{k}} \\ b^{A}_{B,-\mathbf{k}} \end{pmatrix} = \underbrace{\begin{pmatrix} u^{*}_{\mathbf{k}} & -v_{\mathbf{k}} \\ -v_{\mathbf{k}} & u_{\mathbf{k}} \end{pmatrix}}_{=M^{-1}} \begin{pmatrix} \tilde{b}^{B\dagger}_{A,\mathbf{k}} \\ \tilde{b}^{A}_{B,-\mathbf{k}} \end{pmatrix}. \tag{1.4}$$

Since $M^{-1}M = \left(|u|^2 - |v|^2 \right) \mathbb{1} \overset{!}{=} \mathbb{1}$, it follows that we can write $u_{\mathbf{k}} = |u_{\mathbf{k}}| e^{it} = \cosh\theta_{\mathbf{k}} e^{it}$ and $v_{\mathbf{k}} = \sinh\theta_{\mathbf{k}}$, i.e. $u_{\mathbf{k}} \in \mathbb{C}$, $v_{\mathbf{k}} \in \mathbb{R}$. The phase e^{it} will turn out to be equal to the phase of $\gamma(\mathbf{k})$ ($e^{i\arg\gamma_{\mathbf{k}}}$).

Appendix A. The Bogoliubov transformation

We can now diagonalise $\mathcal{H}_{AB}$. Let and $\mathcal{A} := 1$, $\mathcal{B}_{\mathbf{k}} := \gamma_k$. Then

$$
\begin{aligned}
\mathcal{H}_{AB} &= zJn_c \sum_{\mathbf{k} \in \text{RBZ}} \left[\begin{pmatrix} b_{A,\mathbf{k}}^B & b_{B,-\mathbf{k}}^{A\dagger} \end{pmatrix} \begin{pmatrix} 1 & \gamma_{\mathbf{k}}^* \\ \gamma_{\mathbf{k}} & 1 \end{pmatrix} \begin{pmatrix} b_{A,\mathbf{k}}^{B\dagger} \\ b_{B,-\mathbf{k}}^A \end{pmatrix} - 1 \right] \\
&= zJn_c \sum_{\mathbf{k} \in \text{RBZ}} \begin{pmatrix} b_{A,\mathbf{k}}^B & b_{B,-\mathbf{k}}^{A\dagger} \end{pmatrix} \begin{pmatrix} \mathcal{A} & \mathcal{B}_{\mathbf{k}}^* \\ \mathcal{B}_{\mathbf{k}} & \mathcal{A} \end{pmatrix} \begin{pmatrix} b_{A,\mathbf{k}}^{B\dagger} \\ b_{B,-\mathbf{k}}^A \end{pmatrix} - zJn_c \frac{N}{3} \\
&= zJn_c \sum_{\mathbf{k} \in \text{RBZ}} \begin{pmatrix} \tilde{b}_{A,\mathbf{k}}^B & \tilde{b}_{B,-\mathbf{k}}^{A\dagger} \end{pmatrix} \underbrace{(M^{-1})^\dagger \begin{pmatrix} \mathcal{A} & \mathcal{B}_{\mathbf{k}}^* \\ \mathcal{B}_{\mathbf{k}} & \mathcal{A} \end{pmatrix} M^{-1}}_{=: \begin{pmatrix} D & O \\ O^* & D \end{pmatrix}} \begin{pmatrix} \tilde{b}_{A,\mathbf{k}}^{B\dagger} \\ \tilde{b}_{B,-\mathbf{k}}^A \end{pmatrix} - 2Jn_c \frac{N}{3} \\
&= zJn_c \sum_{\mathbf{k} \in \text{RBZ}} \begin{pmatrix} \tilde{b}_{A,\mathbf{k}}^B & \tilde{b}_{B,-\mathbf{k}}^{A\dagger} \end{pmatrix} \begin{pmatrix} D & O \\ O^* & D \end{pmatrix} \begin{pmatrix} \tilde{b}_{A,\mathbf{k}}^{B\dagger} \\ \tilde{b}_{B,-\mathbf{k}}^A \end{pmatrix} - zJn_c \frac{N}{3},
\end{aligned}
\tag{1.5}
$$

where

$$
\begin{aligned}
D &:= \mathcal{A}(|u|^2 + v^2) - 2|\mathcal{B}| |u| v, \\
O &:= e^{it}[-2\mathcal{A} |u| v + \mathcal{B}(|u|^2 + v^2)],
\end{aligned}
$$

From the requirement that $O \overset{!}{=} 0$ and $D \overset{!}{=} \omega_{\mathbf{k}}$, we obtain

$$
\begin{aligned}
& D = \omega_{\mathbf{k}} \\
& \implies \begin{cases} |u_{\mathbf{k}}|^2 + v_k^2 = \frac{\mathcal{A}}{\omega_{\mathbf{k}}} \\ 2|u_{\mathbf{k}}| v_{\mathbf{k}} = \frac{|\mathcal{B}|}{\omega_{\mathbf{k}}} \end{cases} \\
& \implies \omega_{\mathbf{k}} = \sqrt{\mathcal{A}^2 - |\mathcal{B}_{\mathbf{k}}|^2},
\end{aligned}
\tag{1.6}
$$

leading us finally to

$$
\begin{aligned}
\mathcal{H}_{AB} &= zJn_c \sum_{\mathbf{k} \in \text{RBZ}} \begin{pmatrix} \tilde{b}_{A,\mathbf{k}}^B & \tilde{b}_{B,-\mathbf{k}}^{A\dagger} \end{pmatrix} \begin{pmatrix} \omega_{\mathbf{k}} & 0 \\ 0 & \omega_{-\mathbf{k}} \end{pmatrix} \begin{pmatrix} \tilde{b}_{A,\mathbf{k}}^{B\dagger} \\ \tilde{b}_{B,-\mathbf{k}}^A \end{pmatrix} - zJn_c \frac{N}{3} \\
&= \sum_{\mathbf{k} \in \text{RBZ}} \omega_{\mathbf{k}} \left(\tilde{b}_{A,\mathbf{k}}^{B\dagger} \tilde{b}_{A,\mathbf{k}}^B + \tilde{b}_{B,\mathbf{k}}^{A\dagger} \tilde{b}_{B,\mathbf{k}}^A + 1 \right) - zJn_c \frac{N}{3} \\
&= zJn_c \sum_{\mathbf{k} \in \text{RBZ}} \sum_{\mu \in \{A,B\}} \sum_{\nu \neq \mu} \omega_{\mathbf{k}} \left(\tilde{b}_{\mu,\mathbf{k}}^{\nu\dagger} \tilde{b}_{\mu,\mathbf{k}}^\nu + \frac{1}{2} \right) - zJn_c \frac{N}{3}.
\end{aligned}
\tag{1.7}
$$

The Bogoliubov transformation can also be achieved by demanding that

$$
\left[\mathcal{H}, \tilde{b}_B(-\mathbf{k}) \right] \overset{!}{=} -zJn_c \omega(-\mathbf{k}) \tilde{b}_B(-\mathbf{k}).
\tag{1.8}
$$

Since

$$
\left[\mathcal{H}, b_B(-\mathbf{k})\right] = zJn_c\left(-\mathcal{A}\,b_B(-\mathbf{k}) - \mathcal{B}_{\mathbf{k}}\,b_A^\dagger(\mathbf{k})\right),
$$
$$
\left[\mathcal{H}, b_A^\dagger(\mathbf{k})\right] = zJn_c\left(\mathcal{A}\,b_B^\dagger(\mathbf{k}) + \mathcal{B}_{\mathbf{k}}^*\,b_B(-\mathbf{k})\right),
\tag{1.9}
$$

we conclude that

$$
\begin{aligned}
\left[\mathcal{H}, \tilde{b}_B(-\mathbf{k})\right] &= \left[\mathcal{H}, v_{\mathbf{k}}^* b_A^\dagger(\mathbf{k}) + u_{\mathbf{k}}^* b_B(-\mathbf{k})\right] \\
&= \left(\mathcal{A}\,v_{\mathbf{k}}^* - \mathcal{B}_{\mathbf{k}} u_{\mathbf{k}}^*\right) b_A^\dagger(\mathbf{k}) + \left(\mathcal{B}_{\mathbf{k}}^* v_{\mathbf{k}}^* - \mathcal{A}\,u_{\mathbf{k}}^*\right) b_B(-\mathbf{k}) \\
&\overset{!}{=} -zJn_c\omega(-\mathbf{k})\tilde{b}_B(-\mathbf{k}) = -zJn_c\omega(-\mathbf{k})\left(v_{\mathbf{k}}^* b_A^\dagger(\mathbf{k}) + u_{\mathbf{k}}^* b_B(-\mathbf{k})\right).
\end{aligned}
\tag{1.10}
$$

By comparing the coefficients of the bosons $b_A^\dagger(\mathbf{k})$ and $b_B(-\mathbf{k})$, we finally obtain the same spectrum as in (1.6):

$$
\begin{cases}
-v_{\mathbf{k}}^*\omega(-\mathbf{k}) = \mathcal{A}\,v_{\mathbf{k}}^* - \mathcal{B}_{\mathbf{k}} u_{\mathbf{k}}^* \\
-u_{\mathbf{k}}^*\omega(-\mathbf{k}) = -\mathcal{A}\,u_{\mathbf{k}}^* + \mathcal{B}_{\mathbf{k}}^* v_{\mathbf{k}}^*
\end{cases}
\implies
\begin{pmatrix} -\mathcal{A} & \mathcal{B}_{\mathbf{k}}^* \\ -\mathcal{B}_{\mathbf{k}} & \mathcal{A} \end{pmatrix}
\begin{pmatrix} u_{\mathbf{k}}^* \\ v_{\mathbf{k}}^* \end{pmatrix}
= -\omega(-\mathbf{k})
\begin{pmatrix} u_{\mathbf{k}}^* \\ v_{\mathbf{k}}^* \end{pmatrix}
\tag{1.11}
$$

$$
\implies \quad \omega_{\mathbf{k}} = \sqrt{\mathcal{A}^2 - |\mathcal{B}_{\mathbf{k}}|^2}.
\tag{1.12}
$$

Note that from the first equation of (1.11), namely $v_{\mathbf{k}}(\mathcal{A} + \omega_{-\mathbf{k}}) = \gamma_{\mathbf{k}} u_{\mathbf{k}}^*$, we infer that

$$
u_{\mathbf{k}} = \sqrt{\frac{1}{2}\left(\frac{\mathcal{A}}{\omega_{\mathbf{k}}} + 1\right)}\, e^{i\arg\gamma_{\mathbf{k}}},
\tag{1.13a}
$$

$$
v_{\mathbf{k}} = \sqrt{\frac{1}{2}\left(\frac{\mathcal{A}}{\omega_{\mathbf{k}}} - 1\right)}.
\tag{1.13b}
$$

1.2 The generalised Bogoliubov transformation

When having more than two bosons, the method commonly known as the generalised Bogoliubov transformation can be used, the details of which can be found in Ref. [96]. A generic Hamiltonian can be written as

$$
\mathcal{H}^{(2)} = \sum_{\mathbf{k}} \sum_{\mu,\nu=1}^{N} \left[A_{\mathbf{k}}^{\mu\nu} d_{\mu,\mathbf{k}}^\dagger d_{\nu,\mathbf{k}} + \left(B_{\mathbf{k}}^{\mu\nu} d_{\mu,\mathbf{k}}^\dagger d_{\nu,-\mathbf{k}}^\dagger + B_{\mathbf{k}}^{\mu\nu*} d_{\mu,\mathbf{k}} d_{\nu,-\mathbf{k}} \right) \right],
\tag{1.14}
$$

in which there are n boson species and the indices μ,ν label the boson species. We will write it in a more suitable form for the transformation by doubling the number of bosons in the grading of the matrix $M_{\mathbf{k}}$:

$$
\mathcal{H}^{(2)} = \sum_{\mathbf{k}} \left(\mathbf{d}_{\mathbf{k}}^\dagger, \mathbf{d}_{-\mathbf{k}} \right) \frac{1}{2} M_{\mathbf{k}} \begin{pmatrix} {}^{\mathrm{t}}\mathbf{d}_{\mathbf{k}} \\ {}^{\mathrm{t}}\mathbf{d}_{-\mathbf{k}}^\dagger \end{pmatrix},
\tag{1.15}
$$

133

where

$$\mathbf{d}_{\mathbf{k}}^{\dagger} = {}^{t}\Big(d_{1}^{\dagger}(\mathbf{k}), \ldots, d_{\mu}^{\dagger}(\mathbf{k})\Big), \qquad\qquad \mathbf{d}_{-\mathbf{k}} = {}^{t}\Big(d_{1}(-\mathbf{k}), \ldots, d_{\mu}(-\mathbf{k})\Big),$$

$$M_{\mathbf{k}} := \begin{pmatrix} \mathcal{A}_{\mathbf{k}} & \mathcal{B}_{\mathbf{k}} \\ \mathcal{B}_{\mathbf{k}}^{\dagger} & \mathcal{A}_{-\mathbf{k}}^{T} \end{pmatrix} = \begin{pmatrix} \mathcal{A}_{\mathbf{k}} & \mathcal{B}_{\mathbf{k}} \\ \mathcal{B}_{-\mathbf{k}}^{*} & \mathcal{A}_{-\mathbf{k}}^{*} \end{pmatrix}. \tag{1.16}$$

Note that the equalities

$$\mathcal{A}_{\mathbf{k}}^{T} = \mathcal{A}_{\mathbf{k}}^{*}, \qquad \mathcal{B}_{\mathbf{k}}^{\dagger} = \mathcal{B}_{-\mathbf{k}}^{*} \tag{1.17}$$

hold in general. The dispersion relations of such a Hamiltonian is then given by the diagonalisation of

$$Y M_{\mathbf{k}} := \begin{pmatrix} \mathbb{1} & 0 \\ 0 & -\mathbb{1} \end{pmatrix} \begin{pmatrix} A_{\mathbf{k}} & B_{\mathbf{k}} \\ B_{\mathbf{k}}^{\dagger} & A_{-\mathbf{k}}^{T} \end{pmatrix} = \begin{pmatrix} A_{\mathbf{k}} & B_{\mathbf{k}} \\ -B_{\mathbf{k}}^{\dagger} & -A_{-\mathbf{k}}^{T} \end{pmatrix} \tag{1.18}$$

as we shall see.

The aim is to find a transformation $U_{\mathbf{k}}$ for the bosons $\mathbf{d}_{\mathbf{k}}$ that would diagonalise $M_{\mathbf{k}}$. Let us consider new bosons $\tilde{d}_{\mu}$ that satisfy

$$\tilde{\mathbf{d}}_{\mathbf{k}} = U_{1,\mathbf{k}}\mathbf{d}_{\mathbf{k}} + U_{2,\mathbf{k}}{}^{t}\mathbf{d}_{-\mathbf{k}}^{\dagger}$$

$$\Longrightarrow \tilde{\mathbf{d}}_{-\mathbf{k}}^{\dagger} = {}^{t}U_{1,-\mathbf{k}}^{\dagger}\mathbf{d}_{-\mathbf{k}}^{\dagger} + {}^{t}U_{2,-\mathbf{k}}^{\dagger}\mathbf{d}_{\mathbf{k}}$$

$$\Longrightarrow \begin{pmatrix} \tilde{\mathbf{d}}_{\mathbf{k}} \\ \tilde{\mathbf{d}}_{-\mathbf{k}}^{\dagger} \end{pmatrix} = \underbrace{\begin{pmatrix} U_{1,\mathbf{k}} & U_{2,\mathbf{k}} \\ U_{2,-\mathbf{k}}^{*} & U_{1,-\mathbf{k}}^{*} \end{pmatrix}}_{=:T^{-1}} \begin{pmatrix} \mathbf{d}_{\mathbf{k}} \\ \mathbf{d}_{-\mathbf{k}}^{\dagger} \end{pmatrix}, \tag{1.19}$$

in which we have defined

$$T_{\mathbf{k}}^{-1} := \begin{pmatrix} U_{1,\mathbf{k}} & U_{2,\mathbf{k}} \\ U_{2,-\mathbf{k}}^{*} & U_{1,-\mathbf{k}}^{*} \end{pmatrix}. \tag{1.20}$$

They also have to satisfy

$$\left[\tilde{d}_{\mu,\mathbf{k}}, \tilde{d}_{\nu,\mathbf{p}}^{\dagger}\right] = \delta_{\mu\nu}\delta_{\mathbf{kp}}, \qquad \left[\tilde{d}_{\mu,\mathbf{k}}, \tilde{d}_{\nu,\mathbf{p}}\right] = \left[\tilde{d}_{\mu,\mathbf{k}}^{\dagger}, \tilde{d}_{\nu,\mathbf{p}}^{\dagger}\right] = 0. \tag{1.21}$$

Using the Einstein summation convention without distinguishing between the covariant and

contravariant indices, we note that Eqs. (1.21) imply

$$
\begin{aligned}
\left[\tilde{d}_{\mu,\mathbf{k}}, \tilde{d}_{\nu,\mathbf{p}}^\dagger\right] &= \left[[U_{1,\mathbf{k}}]_{\mu\rho} d_{\rho,\mathbf{k}} + [U_{2,\mathbf{k}}]_{\mu\rho} d_{\rho,-\mathbf{k}}^\dagger, [U_{1,\mathbf{p}}^*]_{\nu\sigma} d_{\sigma,\mathbf{p}}^\dagger + [U_{2,\mathbf{p}}^*]_{\nu\sigma} d_{\sigma,-\mathbf{p}}\right] \\
&= [U_{1,\mathbf{k}}]_{\mu\rho} [U_{1,\mathbf{p}}^*]_{\nu\sigma} \underbrace{\left[d_{\rho,\mathbf{k}}, d_{\sigma,\mathbf{p}}^\dagger\right]}_{=\delta_{\rho\sigma}\delta_{\mathbf{kp}}} + [U_{2,\mathbf{k}}]_{\mu\rho} [U_{2,\mathbf{p}}^*]_{\nu\sigma} \underbrace{\left[d_{\rho,-\mathbf{k}}^\dagger, d_{\sigma,-\mathbf{p}}\right]}_{=-\delta_{\rho\sigma}\delta_{\mathbf{kp}}} \\
&= [U_{1,\mathbf{k}}]_{\mu\rho} \underbrace{[U_{1,\mathbf{p}}^*]_{\nu\rho}}_{{}^t[U_{1,\mathbf{p}}^*]_{\rho\nu}} \delta_{\mathbf{kp}} - [U_{2,\mathbf{k}}]_{\mu\rho} \underbrace{[U_{2,\mathbf{p}}^*]_{\nu\rho}}_{{}^t[U_{2,\mathbf{p}}^*]_{\rho\nu}} \delta_{\mathbf{kp}} \\
&= \left\{[U_{1,\mathbf{k}} U_{1,\mathbf{p}}^\dagger]_{\mu\nu} - [U_{2,\mathbf{k}} U_{2,\mathbf{p}}^\dagger]_{\mu\nu}\right\} \delta_{\mathbf{kp}} \\
&\overset{!}{=} \delta_{\mu\nu}\delta_{\mathbf{kp}} \\
\implies\quad & U_{1,\mathbf{k}} U_{1,\mathbf{k}}^\dagger - U_{2,\mathbf{k}} U_{2,\mathbf{k}}^\dagger = \mathbb{1},
\end{aligned}
\tag{1.22}
$$

as well as

$$
\begin{aligned}
\left[\tilde{d}_{i,\mathbf{k}}, \tilde{d}_{j,\mathbf{p}}\right] &= \left[\tilde{d}_{i,\mathbf{k}}^\dagger, \tilde{d}_{j,\mathbf{p}}^\dagger\right] = 0 \\
\implies\quad & U_{1,\mathbf{k}}{}^t U_{2,\mathbf{p}} - U_{2,\mathbf{k}}{}^t U_{1,\mathbf{p}} = 0 \qquad \forall \mathbf{k}, \forall \mathbf{p}, \\
\implies\quad & U_{1,\mathbf{k}}{}^t U_{2,-\mathbf{k}} - U_{2,\mathbf{k}}{}^t U_{1,-\mathbf{k}} = 0.
\end{aligned}
\tag{1.23}
$$

After the introduction of the matrix Y,

$$
Y := \begin{pmatrix} \mathbb{1} & 0 \\ 0 & -\mathbb{1} \end{pmatrix},
\tag{1.24}
$$

Eqs. (1.22) and (1.23) can be written compactly as follows:

$$
Y T_{\mathbf{k}}^{-1} Y (T_{\mathbf{k}}^{-1})^\dagger = \mathbb{1} \quad \Leftrightarrow \quad Y T_{\mathbf{k}}^\dagger Y T_{\mathbf{k}} = \mathbb{1}.
\tag{1.25}
$$

This finally results in

$$
T_{\mathbf{k}}^\dagger = Y T_{\mathbf{k}}^{-1} Y.
\tag{1.26}
$$

Let us now apply all the results on the Hamiltonian in Eq. (1.15):

$$
\begin{aligned}
\mathcal{H}^{(2)} &= \frac{1}{2} \sum_{\mathbf{k}} \left(\mathbf{d}_{\mathbf{k}}^\dagger, \mathbf{d}_{-\mathbf{k}}\right) M_{\mathbf{k}} \begin{pmatrix} {}^t\mathbf{d}_{\mathbf{k}} \\ {}^t\mathbf{d}_{-\mathbf{k}}^\dagger \end{pmatrix} \\
&\overset{(1.19)}{=} \frac{1}{2} \sum_{\mathbf{k}} \left(\tilde{\mathbf{d}}_{\mathbf{k}}^\dagger, \tilde{\mathbf{d}}_{-\mathbf{k}}\right) T_{\mathbf{k}}^\dagger M_{\mathbf{k}} T_{\mathbf{k}} \begin{pmatrix} {}^t\tilde{\mathbf{d}}_{\mathbf{k}} \\ {}^t\tilde{\mathbf{d}}_{-\mathbf{k}}^\dagger \end{pmatrix} \\
&\overset{(1.26)}{=} \frac{1}{2} \sum_{\mathbf{k}} \left(\tilde{\mathbf{d}}_{\mathbf{k}}^\dagger, \tilde{\mathbf{d}}_{-\mathbf{k}}\right) Y \underbrace{[T_{\mathbf{k}}^{-1} (Y M_{\mathbf{k}}) T_{\mathbf{k}}]}_{=:D_{\mathbf{k}}} \begin{pmatrix} {}^t\tilde{\mathbf{d}}_{\mathbf{k}} \\ {}^t\tilde{\mathbf{d}}_{-\mathbf{k}}^\dagger \end{pmatrix}.
\end{aligned}
\tag{1.27}
$$

To this end, $T_\mathbf{k}$ must be the matrix that diagonalise $YM_\mathbf{k}$. Without loss of generality, let $T_\mathbf{k}^{-1} :=$ $\begin{pmatrix} U_{1,\mathbf{k}} & U_{2,\mathbf{k}} \\ U_{2,-\mathbf{k}}^* & U_{1,-\mathbf{k}}^* \end{pmatrix}$ be a $2n \times 2n$ matrix, and write it as follows:

$$T_\mathbf{k} = \begin{pmatrix} \mathbf{X}_{1,\mathbf{k}} & \cdots & \mathbf{X}_{n,\mathbf{k}} & \mathbf{X}_{n+1,\mathbf{k}} & \cdots & \mathbf{X}_{2n,\mathbf{k}} \\ \mathbf{Y}_{1,\mathbf{k}} & \cdots & \mathbf{Y}_{n,\mathbf{k}} & \mathbf{Y}_{n+1,\mathbf{k}} & \cdots & \mathbf{Y}_{2n,\mathbf{k}} \end{pmatrix}. \tag{1.28}$$

Then $\mathbf{v}_{\mu,\mathbf{k}} = \begin{pmatrix} \mathbf{X}_{\mu,\mathbf{k}} \\ \mathbf{Y}_{\mu,\mathbf{k}} \end{pmatrix}$ is an eigenvector of $YM_\mathbf{k}$ with eigenvalue $\tilde{\omega}_{i,\mathbf{k}}$, where $i \in \{1, \dots, 2n\}$. Then it follows that

$$YM_\mathbf{k}\mathbf{v}_{i,\mathbf{k}} = \tilde{\omega}_{i,\mathbf{k}}\mathbf{v}_{i,\mathbf{k}} \quad \Leftrightarrow \quad \begin{cases} A_\mathbf{k}\mathbf{X}_{i,\mathbf{k}} + B_\mathbf{k}\mathbf{Y}_{i,\mathbf{k}} = \tilde{\omega}_{i,\mathbf{k}}\mathbf{X}_{\mathbf{i},\mathbf{k}} \\ -B_\mathbf{k}^\dagger\mathbf{X}_{i,\mathbf{k}} - A_{-\mathbf{k}}^T\mathbf{Y}_{i,\mathbf{k}} = \tilde{\omega}_{i,\mathbf{k}}\mathbf{Y}_{i,\mathbf{k}} \end{cases} \tag{1.29}$$

The conjugation of the latter (along with the properties (1.17)) gives

$$\begin{cases} A_\mathbf{k}^*\mathbf{X}_{i,\mathbf{k}}^* + B_\mathbf{k}^*\mathbf{Y}_{i,\mathbf{k}}^* = \tilde{\omega}_{i,\mathbf{k}}^*\mathbf{X}_{\mathbf{i},\mathbf{k}}^* \\ B_{-\mathbf{k}}\mathbf{X}_{i,\mathbf{k}}^* + A_{-\mathbf{k}}\mathbf{Y}_{i,\mathbf{k}}^* = -\tilde{\omega}_{i,\mathbf{k}}^*\mathbf{Y}_{\mathbf{i},\mathbf{k}}^* \end{cases} \Rightarrow \begin{cases} A_\mathbf{k}^*\mathbf{X}_{i,-\mathbf{k}}^* + B_{-\mathbf{k}}^*\mathbf{Y}_{i,-\mathbf{k}}^* = \tilde{\omega}_{i,-\mathbf{k}}^*\mathbf{X}_{\mathbf{i},-\mathbf{k}}^* \\ B_\mathbf{k}\mathbf{X}_{i,-\mathbf{k}}^* + A_\mathbf{k}\mathbf{Y}_{i,-\mathbf{k}}^* = -\tilde{\omega}_{i,-\mathbf{k}}^*\mathbf{Y}_{\mathbf{i},-\mathbf{k}}^* \end{cases} \tag{1.30}$$

Finally, by defining

$$\begin{aligned} \mathbf{X}'_{i,\mathbf{k}} &:= \mathbf{Y}_{i,-\mathbf{k}}^*, & \mathbf{Y}'_{i,\mathbf{k}} &:= \mathbf{X}_{i,-\mathbf{k}}^*, \\ \tilde{\omega}'_{i,\mathbf{k}} &:= -\tilde{\omega}_{i,-\mathbf{k}}^*, \end{aligned} \tag{1.31}$$

we obtain

$$\implies \begin{cases} A_\mathbf{k}\mathbf{X}'_{i,\mathbf{k}} + B_\mathbf{k}\mathbf{Y}'_{i,\mathbf{k}} = \tilde{\omega}'_{i,\mathbf{k}}\mathbf{X}'_{\mathbf{i},\mathbf{k}} \\ B_\mathbf{k}^*\mathbf{X}'_{i,\mathbf{k}} + A_\mathbf{k}^*\mathbf{Y}'_{i,\mathbf{k}} = -\tilde{\omega}'_{i,\mathbf{k}}\mathbf{Y}'_{\mathbf{i},\mathbf{k}} \end{cases} \tag{1.32}$$

Hence, we can immediately infer that the vector $\begin{pmatrix} \mathbf{X}'_{i,\mathbf{k}} \\ \mathbf{Y}'_{i,\mathbf{k}} \end{pmatrix} = \begin{pmatrix} \mathbf{Y}_{i,-\mathbf{k}}^* \\ \mathbf{X}_{i,-\mathbf{k}}^* \end{pmatrix}$ is also an eigenvector of $YM_\mathbf{k}$ with eigenvalue $-\tilde{\omega}_{i,-\mathbf{k}}^*$ by comparing Eq. (1.30) and Eq. (1.31). The eigenvectors and

eigenvalues of $Y M_{\mathbf{k}}$ are finally given by

$$T_{\mathbf{k}} = \begin{pmatrix} \mathbf{X}_{1,\mathbf{k}} & \cdots & \mathbf{X}_{n,\mathbf{k}} & \mathbf{Y}_{1,-\mathbf{k}}^* & \cdots & \mathbf{Y}_{n,-\mathbf{k}}^* \\ \mathbf{Y}_{1,\mathbf{k}} & \cdots & \mathbf{Y}_{n,\mathbf{k}} & \mathbf{X}_{1,-\mathbf{k}}^* & \cdots & \mathbf{X}_{n,-\mathbf{k}}^* \end{pmatrix},$$

$$D_{\mathbf{k}} = \begin{pmatrix} \tilde{\omega}_{1,\mathbf{k}} & & & & & \\ & \ddots & & & & \\ & & \tilde{\omega}_{n,\mathbf{k}} & & & \\ & & & -\tilde{\omega}_{1,-\mathbf{k}}^* & & \\ & & & & \ddots & \\ & & & & & -\tilde{\omega}_{n,-\mathbf{k}}^* \end{pmatrix}. \tag{1.33}$$

Ultimately, the Hamiltonian will then have the following form:

$$\begin{aligned} \mathcal{H}^{(2)} &= \frac{1}{2} \sum_{\mathbf{k}} \left(\tilde{\mathbf{d}}_{\mathbf{k}}^\dagger, \tilde{\mathbf{d}}_{-\mathbf{k}} \right) Y D_{\mathbf{k}} \begin{pmatrix} {}^{\mathrm{t}}\tilde{\mathbf{d}}_{\mathbf{k}} \\ {}^{\mathrm{t}}\tilde{\mathbf{d}}_{-\mathbf{k}}^\dagger \end{pmatrix} \\ &= \frac{1}{2} \sum_{\mathbf{k}} \sum_{i=1}^{n} \left[\tilde{\omega}_{i,\mathbf{k}} \tilde{d}_i^\dagger(\mathbf{k}) \tilde{d}_i(\mathbf{k}) + \tilde{\omega}_{i,-\mathbf{k}}^* \tilde{d}_i(-\mathbf{k}) \tilde{d}_i^\dagger(-\mathbf{k}) \right] \\ &= \frac{1}{2} \sum_{\mathbf{k}} \sum_{i=1}^{n} \left[2 \underbrace{\mathrm{Re}(\tilde{\omega}_{i,\mathbf{k}})}_{=:\omega_{i,\mathbf{k}}} \tilde{d}_i^\dagger(\mathbf{k}) \tilde{d}_i(\mathbf{k}) + \tilde{\omega}_{i,-\mathbf{k}}^* \right] \\ &= \sum_{\mathbf{k}} \sum_{i=1}^{n} \left[\underbrace{\mathrm{Re}(\tilde{\omega}_{i,\mathbf{k}})}_{=:\omega_{i,\mathbf{k}}} \tilde{d}_i^\dagger(\mathbf{k}) \tilde{d}_i(\mathbf{k}) + \tilde{\omega}_{i,-\mathbf{k}}^* \right]. \end{aligned} \tag{1.34}$$

The semi-positivity of the eigenvalues and the existence of matrix $T_{\mathbf{k}}$ are guaranteed by the fact that $M_{\mathbf{k}}$ is positive definite when $\gamma_{\mathbf{k}} \neq 0$, and by the fact that it is semi-positive definite when $\gamma_{\mathbf{k}} = 0$ (which is the consequence of the Goldstone-symmetry breaking).

B The expectation values with Read and Sachdev bosons

2.1 Case of $SU(4)$ $m = 2$ irrep

We consider the square lattice and its ordered state in subsection 4.1.1. Let us assume that color A and B sit on the sublattice Λ_{AB} and the color C and D on the sublattice Λ_{CD} of the square lattice (we are considering the irrep with $m = 2$). We have deliberately broken the symmetry by choosing specific colors for the sublattice. Then the ground-state can be expressed as

$$\tilde{C} \prod_{\substack{i,j \\ i \in \Lambda_1 \\ j \in \Lambda_2}} A^\dagger_{AB}(i) A^\dagger_{CD}(j) \,|0\rangle, \tag{2.1}$$

where $\tilde{C}$ is a normalisation constant. When assuming a condensate of colors A and B on site i by taking the semi-classical limit (i.e. by taking the limit $M \to \infty$), the ground-state is then written as

$$|gs\rangle = C \prod_{\substack{i,j \\ i \in \Lambda_1 \\ j \in \Lambda_2}} \left(A^\dagger_{AB}(i) A^\dagger_{CD}(j) \right)^{n_c} |0\rangle, \tag{2.2}$$

with N being the number of sites and C another normalisation factor.

We first observe that

$$\begin{aligned}
|gs(i)\rangle &:= \tilde{C} \left(A^\dagger_{AB} \right)^{n_c} |0\rangle \\
&= \tilde{C} \left(d^\dagger_{A1} d^\dagger_{B2} - d^\dagger_{B1} d^\dagger_{A2} \right)^{n_c} |0\rangle \\
&= \tilde{C} \sum_{k=0}^{n_c} \binom{M}{k} \left(d^\dagger_{A1} d^\dagger_{B2} \right)^{n_c - k} \left(-d^\dagger_{B1} d^\dagger_{A2} \right)^k |0\rangle,
\end{aligned} \tag{2.3}$$

where $\tilde{C} = \frac{1}{(n_c!)^2(1+n_c)}$ is the normalisation factor. Then it follows that

$$\implies \quad \left\langle gs(i) \left| d_{A2}^\dagger d_{A2} \right| gs(i) \right\rangle = \frac{1}{(n_c!)^2(1+n_c)} (n_c!)^2 \underbrace{\sum_{k=1}^{n_c} k}_{=(1+n_c)\frac{n_c}{2}}$$

$$= \frac{n_c}{2}. \tag{2.4}$$

Hence, we conclude that

$$\left\langle d_{\mu a}^\dagger(i) d_{\mu a}(i) \right\rangle = \left\langle gs \left| d_{\mu a}^\dagger(i) d_{\mu a}(i) \right| gs \right\rangle = \frac{M}{2},$$
$$\left\langle d_{\nu a}^\dagger(j) d_{\nu a}(j) \right\rangle = \left\langle gs \left| d_{\nu a}^\dagger(j) d_{\nu a}(j) \right| gs \right\rangle = \frac{M}{2}, \tag{2.5}$$

with $\forall i \in \Lambda_{AB}$, $\forall j \in \Lambda_{CD}$ and $\mu \in \{A, B\}$, $\nu \in \{C, D\}$, $a \in \{1, 2\}$. Other quadratic combinations of bosons yield zero.

2.2 Case of $SU(3)$ adjoint irrep

We refer here to subsection 4.2.2. We now assume that there is a large condensate of the ground state $\epsilon^{ab} d_{Aa}^\dagger d_{Cb}^\dagger d_{A1}^\dagger |0\rangle$ on Λ_1 and a large condensate of $\epsilon^{ab} d_{Ba}^\dagger d_{Cb}^\dagger d_{B1}^\dagger |0\rangle$ on Λ_2, i.e., we consider

$$\left| gs(i) \right\rangle := \tilde{C} \left[\epsilon^{ab} d_{Aa}^\dagger(i) d_{Cb}^\dagger(i) d_{A1}^\dagger(i) \right]^{n_c} |0\rangle,$$
$$\left| gs(j) \right\rangle := \tilde{C} \left[\epsilon^{ab} d_{Ba}^\dagger(j) d_{Cb}^\dagger(j) d_{B1}^\dagger(j) \right]^{n_c} |0\rangle, \tag{2.6}$$

for any $i \in \Lambda_1$, $j \in \Lambda_2$ and $a \in \{1, 2\}$, with $\tilde{C}$ being the normalisation constant and n_c being the control parameter such that $n_c \to \infty$. We will concentrate on the sublattice Λ_1 from hereon as the argument will be identical for the sublattice Λ_2.

Let us first state two identities will be useful for our subsequent calculations:

$$\sum_{k=0}^{n_c} \frac{(cn_c - k)!}{(n_c - k)!} = \frac{(cn_C + 1)(cn_c)!}{n_c! [(c-1)n_c + 1]}$$
$$= \frac{(cn_c + 1)!}{n_c! [(c-1)n_c + 1]}$$
$$\sum_{k=0}^{n_c} \frac{(cn_c - k)!}{(n_c - k)!} k = \frac{cn_c(cn_c + 1)(cn_c - 1)!}{(n_c - 1)! [(c-1)n_c + 1] [(c-1)n_c + 2]}$$
$$= \frac{(cn_c + 1)!}{(n_c - 1)! [(c-1)n_c + 1] [(c-1)n_c + 2]}. \tag{2.7}$$

These equations are true for any non-zero integer c.

Let us now determine the renormalisation constant $\tilde{C}$:

$$
\begin{aligned}
\tilde{C} \left| gs(i) \right\rangle &= \left(\epsilon^{ab} d^\dagger_{Aa} d^\dagger_{Cb} d^\dagger_{A1} \right)^{n_c} \left| 0 \right\rangle \\
&= \left(d^\dagger_{A1} d^\dagger_{C2} d^\dagger_{A1} - d^\dagger_{C1} d^\dagger_{A2} d^\dagger_{A1} \right)^{n_c} \left| 0 \right\rangle \\
&= \sum_{k=0}^{n_c} \binom{n_c}{k} \left(d^\dagger_{A1} d^\dagger_{C2} d^\dagger_{A1} \right)^{n_c-k} \left(-d^\dagger_{C1} d^\dagger_{A2} d^\dagger_{A1} \right)^{k} \left| 0 \right\rangle \\
&= \sum_{k=0}^{n_c} \frac{n_c!}{(n_c-k)!k!} (-1)^k \left(d^\dagger_{A1} \right)^{2(n_c-k)+k} \left(d^\dagger_{C1} \right)^{k} \left(d^\dagger_{A2} \right)^{k} \left(d^\dagger_{C2} \right)^{n_c-k} \left| 0 \right\rangle \\
&= \sum_{k=0}^{n_c} \frac{n_c!}{(n_c-k)!k!} (-1)^k \sqrt{(2n_c-k)!} \sqrt{k!} \sqrt{k!} \sqrt{(n_c-k)!} \left| (2n_c-k)_{A1}, (k)_{C1}, (k)_{A2}, (n_c-k)_{C2} \right\rangle \\
&= n_c! \sum_{k=0}^{n_c} (-1)^k \frac{\sqrt{(2n_c-k)!}}{\sqrt{(n_c-k)!}} \left| (2n_c-k)_{A1}, (k)_{C1}, (k)_{A2}, (n_c-k)_{C2} \right\rangle .
\end{aligned}
\tag{2.8}
$$

$$
\begin{aligned}
\implies \quad & \left\langle gs(i) \middle| gs(i) \right\rangle = \tilde{C}^2 (n_c!)^2 \sum_{k=0}^{n_c} \frac{(2n_c-k)!}{(n_c-k)!} \overset{!}{=} 1 \\
\implies \quad & \tilde{C}^2 = \left[(n_c!)^2 \sum_{k=0}^{n_c} \frac{(2n_c-k)!}{(n_c-k)!} \right]^{-1} .
\end{aligned}
\tag{2.9}
$$

From Eq. (2.8), it is easy to see that

$$
\left\langle gs(i) \middle| d^\dagger_{A1} d_{A2} \middle| gs(i) \right\rangle = 0, \qquad \left\langle gs(i) \middle| d^\dagger_{C1} d_{C2} \middle| gs(i) \right\rangle = 0,
\tag{2.10}
$$

and we also trivially obtain

$$
\left\langle gs(i) \middle| d^\dagger_{Ba} d_{Ba} \middle| gs(i) \right\rangle = 0, \qquad \left\langle gs(i) \middle| d^\dagger_{Da} d_{Da} \middle| gs(i) \right\rangle = 0,
\tag{2.11}
$$

for $a \in \{1, 2\}$. The number expectation value of $\langle n_{A1} \rangle$ is given by

$$
\begin{aligned}
\left\langle gs(i) \middle| d^\dagger_{A1} d_{A1} \middle| gs(i) \right\rangle &= \tilde{C}^2 (n_c!)^2 \sum_{k=0}^{n_c} \frac{(2n_c-k)!}{(n_c-k)!} (2n_c-k) \\
&= 2n_c - \frac{\sum_{k=0}^{n_c} \frac{(2n_c-k)!}{(n_c-k)!} k}{\sum_{k=0}^{n_c} \frac{(2n_c-k)!}{(n_c-k)!}} \\
&\overset{(2.7)}{=} \frac{2n_c+3}{n_c+2} n_c .
\end{aligned}
\tag{2.12}
$$

Similarly, we obtain

$$
\left\langle gs(i)\left|d_{C2}^{\dagger}d_{C2}\right|gs(i)\right\rangle = \tilde{C}^2(n_c!)^2 \sum_{k=0}^{n_c} \frac{(2n_c-k)!}{(n_c-k)!}(n_c-k) = n_c - \frac{\sum_{k=0}^{n_c}\frac{(2n_c-k)!}{(n_c-k)!}k}{\sum_{k=0}^{n_c}\frac{(2n_c-k)!}{(n_c-k)!}}
$$

$$
\overset{(2.7)}{=} \frac{n_c+1}{n_c+2}n_c,
$$

$$
\left\langle gs(i)\left|d_{C1}^{\dagger}d_{C1}\right|gs(i)\right\rangle = \tilde{C}^2(n_c!)^2 \sum_{k=0}^{n_c} \frac{(2n_c-k)!}{(n_c-k)!}k = \frac{\sum_{k=0}^{n_c}\frac{(2n_c-k)!}{(n_c-k)!}k}{\sum_{k=0}^{n_c}\frac{(2n_c-k)!}{(n_c-k)!}} \tag{2.13}
$$

$$
\overset{(2.7)}{=} \frac{1}{n_c+2}n_c,
$$

$$
\left\langle gs(i)\left|d_{A2}^{\dagger}d_{A2}\right|gs(i)\right\rangle = \tilde{C}^2(n_c!)^2 \sum_{k=0}^{n_c} \frac{(2n_c-k)!}{(n_c-k)!}k
$$

$$
\overset{(2.7)}{=} \frac{1}{n_c+2}n_c.
$$

However, what we are really interested in is these number expectation values in the limit $n_c \to \infty$:

$$
\lim_{n_c\to\infty}\frac{1}{n_c}\left\langle d_{A1}^{\dagger}d_{A1}\right\rangle = \lim_{n_c\to\infty}\frac{2n_c+3}{n_c+2} = 2,
$$

$$
\lim_{n_c\to\infty}\frac{1}{n_c}\left\langle d_{C2}^{\dagger}d_{C2}\right\rangle = \lim_{n_c\to\infty}\frac{n_c+1}{n_c+2} = 1,
$$

$$
\lim_{n_c\to\infty}\frac{1}{n_c}\left\langle d_{C1}^{\dagger}d_{C1}\right\rangle = \lim_{n_c\to\infty}\frac{1}{n_c+2} = 0, \tag{2.14}
$$

$$
\lim_{n_c\to\infty}\frac{1}{n_c}\left\langle d_{A2}^{\dagger}d_{A2}\right\rangle = \lim_{n_c\to\infty}\frac{1}{n_c+2} = 0.
$$

Hence, all these expectation values indeed justify the Holstein-Primakoff approach in Eq. (4.55):

$$
b_{A1}^{\dagger}(i), b_{A1}(i) \quad \longrightarrow \quad \sqrt{2n_c - \sum_{\mu\neq A} d_{\mu1}^{\dagger}(i)d_{\mu1}(i)} \approx \sqrt{2n_c} - \frac{1}{2\sqrt{2n_c}}\sum_{\mu\neq A} d_{\mu1}^{\dagger}(i)d_{\mu1}(i),
$$

$$
b_{C2}^{\dagger}(i), b_{C2}(i) \quad \longrightarrow \quad \sqrt{n_c - \sum_{\mu\neq C} b_{\mu2}^{\dagger}(i)b_{\mu2}(i)} \approx \sqrt{n_c} - \frac{1}{2\sqrt{n_c}}\sum_{\mu\neq C} b_{\mu2}^{\dagger}(i)b_{\mu2}(i). \tag{2.15}
$$

Furthermore, they show that the expectation values of the LHS of the constraints respect the

constraints (4.47) in the limit $n_c \to \infty$:

$$
\begin{cases}
\left\langle \sum_{\alpha=1}^{3} d_{\alpha 1}^{\dagger}(l) d_{\alpha 1}(l) \right\rangle = 2 n_c, \\
\left\langle \sum_{\alpha=1}^{3} d_{\alpha 2}^{\dagger}(l) d_{\alpha 2}(l) \right\rangle = n_c, \\
\left\langle \sum_{\alpha=1}^{3} d_{\alpha 1}^{\dagger}(l) d_{\alpha 2}(l) \right\rangle = 0.
\end{cases}
\tag{2.16}
$$

C The corrections from the $\mathrm{SU}(3)$ quartic terms $\mathscr{H}^{(4)}$

3.1 Wick decoupling/Hartree-Fock average of the quartic terms

As explained in subsection 6.2.3, the quartic Hamiltonian can be written as $\mathscr{H}^{(4)} = \delta E^{(4)} + \delta \mathscr{H}^{(2)} + \tilde{\mathscr{H}}^{(4)}$, where $\delta \mathscr{H}^{(2)}$ is the term of our interest: it is the renormalisation of the spectrum that comes from the quartic term. Following the procedure in Ref. [85], we perform the Wick decoupling to calculate the quadratic average in real-space to simplify. With the coordination number between two sublattices $z = 2$, the possible Hartree-Fock averages in $\mathscr{H}^{(4)}$ are given as follows:

(i)

$$
\begin{aligned}
\left\langle b_B^\dagger(i) b_B(i) \right\rangle &= \frac{1}{N} \left\langle 0 \left| \sum_i b_B^\dagger(i) b_B(i) \right| 0 \right\rangle = \frac{1}{N} \left\langle 0 \left| \sum_{\mathbf{k}} b_B^\dagger(\mathbf{k}) b_B(\mathbf{k}) \right| 0 \right\rangle \\
&= \frac{1}{N} \left\langle 0 \left| \sum_{\mathbf{k}} \left(-v_{\mathbf{k}} \eta_C(-\mathbf{k}) + u_{\mathbf{k}} \eta_B^\dagger(\mathbf{k}) \right) \left(-v_{\mathbf{k}} \eta_C^\dagger(-\mathbf{k}) + u_{\mathbf{k}}^* \eta_B(\mathbf{k}) \right) \right| 0 \right\rangle \\
&= \frac{1}{N} \left\langle 0 \left| \sum_{\mathbf{k}} v_{\mathbf{k}}^2 \eta_{C,-\mathbf{k}} \eta_{C,-\mathbf{k}}^\dagger \right| 0 \right\rangle = \frac{1}{N} \sum_{\mathbf{k}} v_{\mathbf{k}}^2 \qquad (3.1) \\
&\overset{(6.10)}{=} \frac{1}{N} \sum_{\mathbf{k}} \left[\frac{1}{2} \left(\frac{\mathcal{A}}{\omega_{\mathbf{k}}} - 1 \right) \right] \\
&=: n,
\end{aligned}
$$

and similarly, $\left\langle b_C^\dagger(j) b_C(j) \right\rangle = \left\langle b_B^\dagger(j) b_B(j) \right\rangle = \left\langle b_C^\dagger(i) b_C(i) \right\rangle = n.$

Appendix C. The corrections from the SU(3) quartic terms $\mathcal{H}^{(4)}$

(ii)

$$
\begin{aligned}
\left\langle b_B^\dagger(i) b_B(j) \right\rangle &= \frac{1}{N} \left\langle 0 \left| \sum_i \frac{1}{2} \sum_{\substack{j \in \{i+\vec{e}_x, \\ i+\vec{e}_y\}}} b_B^\dagger(i) b_B(j) \right| 0 \right\rangle \\
&= \frac{1}{N} \left\langle 0 \left| \sum_{\mathbf{k}} \frac{1}{2} (e^{-ik_x} + e^{-ik_y}) b_B^\dagger(\mathbf{k}) b_B(\mathbf{k}) \right| 0 \right\rangle \\
&= \frac{1}{N} \left\langle 0 \left| \sum_{\mathbf{k}} \gamma_{\mathbf{k}}^* b_B^\dagger(\mathbf{k}) b_B(\mathbf{k}) \right| 0 \right\rangle \\
&= \frac{1}{N} \left\langle 0 \left| \sum_{\mathbf{k}} \gamma_{\mathbf{k}}^* v_{\mathbf{k}}^2 \eta_{C,-\mathbf{k}} \eta_{C,-\mathbf{k}}^\dagger \right| 0 \right\rangle = \frac{1}{N} \sum_{\mathbf{k}} \gamma_{\mathbf{k}}^* v_{\mathbf{k}}^2 \\
&\stackrel{(6.10)}{=} \frac{1}{N} \sum_{\mathbf{k}} \gamma_{\mathbf{k}}^* \left[\frac{1}{2} \left(\frac{\mathcal{A}}{\omega_{\mathbf{k}}} - 1 \right) \right] \\
&=: n_C^* \\
&= 0 \qquad \text{because } \int_{\text{BZ}} \gamma_{\mathbf{k}} d\mathbf{k} = 0, \text{ and } v_{\mathbf{k}} \text{ is even in BZ,}
\end{aligned}
$$

$$(3.2)$$

and similarly, $\left\langle b_B^\dagger(j) b_B(i) \right\rangle = \left\langle b_C^\dagger(j) b_C(i) \right\rangle = \left\langle b_C^\dagger(i) b_C(j) \right\rangle = 0.$

(iii)

$$
\begin{aligned}
\left\langle b_B^\dagger(i) b_C^\dagger(j) \right\rangle &= \frac{1}{N} \left\langle 0 \left| \sum_i \frac{1}{2} \sum_{\substack{j \in \{i+\vec{e}_x, \\ i+\vec{e}_y\}}} b_B^\dagger(i) b_C^\dagger(j) \right| 0 \right\rangle \\
&= \frac{1}{N} \left\langle 0 \left| \sum_{\mathbf{k}} \frac{1}{2} (e^{ik_x} + e^{ik_y}) b_B^\dagger(-\mathbf{k}) b_C^\dagger(\mathbf{k}) \right| 0 \right\rangle \\
&= \frac{1}{N} \left\langle 0 \left| \sum_{\mathbf{k}} \gamma_{\mathbf{k}} \left(-v_{\mathbf{k}} \eta_C(\mathbf{k}) + u_{\mathbf{k}}^* \eta_B^\dagger(-\mathbf{k}) \right) \left(u_{\mathbf{k}}^* \eta_C^\dagger(\mathbf{k}) - v_{\mathbf{k}} \eta_B(-\mathbf{k}) \right) \right| 0 \right\rangle \\
&= \frac{1}{N} \left\langle 0 \left| \sum_{\mathbf{k}} (-\gamma_{\mathbf{k}} u_{\mathbf{k}}^* v_{\mathbf{k}}) \eta_{C,\mathbf{k}} \eta_{C,\mathbf{k}}^\dagger \right| 0 \right\rangle = -\frac{1}{N} \sum_{\mathbf{k}} \gamma_{\mathbf{k}} u_{\mathbf{k}}^* v_{\mathbf{k}} \\
&\stackrel{(6.10)}{=} -\frac{1}{N} \sum_{\mathbf{k}} \gamma_{\mathbf{k}} \frac{\mathcal{B}_{\mathbf{k}}^*}{2\omega_{\mathbf{k}}} \\
&=: \Delta_\gamma,
\end{aligned}
$$

$$(3.3)$$

and similarly, $\left\langle b_C^\dagger(j) b_B^\dagger(i) \right\rangle = \Delta_\gamma,$

$$\left\langle b_C(j) b_B(i) \right\rangle = \left\langle b_B(i) b_C(j) \right\rangle = \Delta_\gamma^*,$$

where it is worth noting that

$$\left\langle b_B^\dagger(i) b_C^\dagger(j) \right\rangle = -\frac{1}{N} \sum_{\mathbf{k}} \gamma_{\mathbf{k}} u_{\mathbf{k}}^* v_{\mathbf{k}} \overset{(6.10)}{=} -\frac{1}{N} \sum_{\mathbf{k}} |\gamma_{\mathbf{k}}| |u_{\mathbf{k}}| v_{\mathbf{k}}$$

$$\overset{(6.10)}{=} -\frac{1}{N} \sum_{\mathbf{k}} |\gamma_{\mathbf{k}}| \frac{|\mathcal{B}_{\mathbf{k}}|}{2\omega_{\mathbf{k}}} \tag{3.4}$$

$$\implies \quad \Delta_\gamma = \Delta_\gamma^*.$$

(iv)

$$\begin{aligned}
\left\langle b_C^\dagger(i) b_B^\dagger(j) \right\rangle &= \frac{1}{N} \left\langle 0 \left| \sum_i \frac{1}{2} \sum_{\substack{j \in \{i+\vec{e}_x, \\ i+\vec{e}_y\}}} b_C^\dagger(i) b_B^\dagger(j) \right| 0 \right\rangle \\
&= \frac{1}{N} \left\langle 0 \left| \sum_{\mathbf{k}} \frac{1}{2} (e^{-ik_x} + e^{-ik_y}) b_C^\dagger(\mathbf{k}) b_B^\dagger(-\mathbf{k}) \right| 0 \right\rangle \\
&= \frac{1}{N} \left\langle 0 \left| \sum_{\mathbf{k}} \gamma_{\mathbf{k}}^* \left(u_{\mathbf{k}}^* \eta_C^\dagger(\mathbf{k}) - v_{\mathbf{k}} \eta_B(-\mathbf{k}) \right) \left(-v_{\mathbf{k}} \eta_C(\mathbf{k}) + u_{\mathbf{k}}^* \eta_B^\dagger(-\mathbf{k}) \right) \right| 0 \right\rangle \\
&= \frac{1}{N} \left\langle 0 \left| \sum_{\mathbf{k}} (-\gamma_{\mathbf{k}}^* u_{\mathbf{k}}^* v_{\mathbf{k}}) \eta_{B,-\mathbf{k}} \eta_{B,-\mathbf{k}}^\dagger \right| 0 \right\rangle \\
&= -\frac{1}{N} \sum_{\mathbf{k}} \gamma_{\mathbf{k}}^* u_{\mathbf{k}}^* v_{\mathbf{k}} \\
&= 0 \qquad \text{because } \int_{\text{BZ}} \gamma_{\mathbf{k}}^* \mathrm{d}\mathbf{k} = 0,
\end{aligned} \tag{3.5}$$

and similarly, $\left\langle b_B(j) b_C(i) \right\rangle = \left\langle b_B^\dagger(j) b_C^\dagger(i) \right\rangle = \left\langle b_C(i) b_B(j) \right\rangle = 0$.

(v)

$$\left\langle b_B^\dagger(i) b_C^\dagger(i) \right\rangle = \frac{1}{N} \left\langle 0 \left| \sum_i b_B^\dagger(i) b_C^\dagger(i) \right| 0 \right\rangle = \frac{1}{N} \left\langle 0 \left| \sum_{\mathbf{k}} b_B^\dagger(-\mathbf{k}) b_C^\dagger(\mathbf{k}) \right| 0 \right\rangle$$

$$= \frac{1}{N} \left\langle 0 \left| \sum_{\mathbf{k}} \left(-v_{\mathbf{k}} \eta_C(\mathbf{k}) + u_{\mathbf{k}}^* \eta_B^\dagger(-\mathbf{k}) \right) \left(u_{\mathbf{k}}^* \eta_C^\dagger(\mathbf{k}) - v_{\mathbf{k}} \eta_B(-\mathbf{k}) \right) \right| 0 \right\rangle$$

$$= \frac{1}{N} \left\langle 0 \left| \sum_{\mathbf{k}} (-u_{\mathbf{k}}^* v_{\mathbf{k}}) \eta_{C,\mathbf{k}} \eta_{C,\mathbf{k}}^\dagger \right| 0 \right\rangle = -\frac{1}{N} \sum_{\mathbf{k}} u_{\mathbf{k}}^* v_{\mathbf{k}}$$

$$\overset{(6.10)}{=} -\frac{1}{N} \sum_{\mathbf{k}} \frac{\mathcal{B}_{\mathbf{k}}^*}{2\omega_{\mathbf{k}}} \tag{3.6}$$

$$\overset{(6.10)}{=} -\frac{1}{N} \sum_{\mathbf{k}} \frac{z J_1 n_c \gamma_{\mathbf{k}}}{2\omega_{\mathbf{k}}}$$

$$=: \Delta$$

$$= 0 \qquad \text{because } \int_{BZ} \gamma_{\mathbf{k}} d\mathbf{k} = 0, \text{ and } \omega_{\mathbf{k}} \text{ is even in BZ,}$$

and similarly, $\left\langle b_C(i) b_B(i) \right\rangle = 0$.

(vi)

$$\left\langle b_B^\dagger(i) b_C(j) \right\rangle = \frac{1}{N} \left\langle 0 \left| \sum_i \frac{1}{2} \sum_{\substack{j \in \{i + \vec{e}_x, \\ i + \vec{e}_y\}}} b_B^\dagger(i) b_C(j) \right| 0 \right\rangle$$

$$= \frac{1}{N} \left\langle 0 \left| \sum_{\mathbf{k}} \frac{1}{2} (e^{-i k_x} + e^{-i k_y}) b_B^\dagger(-\mathbf{k}) b_C(\mathbf{k}) \right| 0 \right\rangle \tag{3.7}$$

$$= \frac{1}{N} \left\langle 0 \left| \sum_{\mathbf{k}} \gamma_{-\mathbf{k}} \left(-v_{\mathbf{k}} \eta_C(\mathbf{k}) + u_{\mathbf{k}}^* \eta_B^\dagger(-\mathbf{k}) \right) \left(u_{\mathbf{k}} \eta_C(\mathbf{k}) - v_{\mathbf{k}} \eta_B^\dagger(-\mathbf{k}) \right) \right| 0 \right\rangle$$

$$= 0,$$

and similarly, $\left\langle b_C^\dagger(i) b_B(j) \right\rangle = \left\langle b_B^\dagger(i) b_C(i) \right\rangle = 0$.

(vii)

$$\langle b_B(i)b_B(j)\rangle = \frac{1}{N}\left\langle 0 \left| \sum_i \frac{1}{2} \sum_{\substack{j\in\{i+\vec{e}_x, \\ i+\vec{e}_y\}}} b_B(i)b_B(j) \right| 0 \right\rangle$$

$$= \frac{1}{N}\left\langle 0 \left| \sum_{\mathbf{k}} \frac{1}{2}(e^{-ik_x}+e^{-ik_y})b_B(\mathbf{k})b_B(\mathbf{k}) \right| 0 \right\rangle$$

$$= \frac{1}{N}\left\langle 0 \left| \sum_{\mathbf{k}} \gamma_{-\mathbf{k}}\left(-v_{\mathbf{k}}\eta_C^\dagger(-\mathbf{k})+u_{\mathbf{k}}^*\eta_B(\mathbf{k})\right)\left(-v_{\mathbf{k}}\eta_C^\dagger(-\mathbf{k})+u_{\mathbf{k}}^*\eta_B(\mathbf{k})\right) \right| 0 \right\rangle$$

$$= 0,$$

and similarly, $\left\langle b_B^\dagger(i)b_B^\dagger(j)\right\rangle = \left\langle b_B(i)b_B(i)\right\rangle = \left\langle b_B^\dagger(i)b_B^\dagger(i)\right\rangle = 0,$

$$\left\langle b_C^\dagger(i)b_C^\dagger(j)\right\rangle = \left\langle b_C(i)b_C(i)\right\rangle = \left\langle b_C^\dagger(i)b_C^\dagger(i)\right\rangle = 0.$$

(3.8)

The Wick theorem can now be used. The term $\delta\mathcal{H}^{(2)}$ we are looking for is the sum of the normal-ordered quartic terms $:\mathcal{H}^{(4)}:$ containing one contraction in all possible combinations. For each of the quartic terms in $\mathcal{H}^{(4)}$ in Eq. (6.7), we obtain the following:

(i)

$$\sum_i \sum_{\substack{j\in\{i+\vec{e}_x, \\ i+\vec{e}_y\}}} b_B^\dagger(i)b_B(i)b_B(i)b_C(j)$$

$$\longrightarrow \sum_i \sum_{\substack{j\in\{i+\vec{e}_x, \\ i+\vec{e}_y\}}} \Big[:b_B^\dagger(i)b_B(i)b_B(i)b_C(j): + :b_B^\dagger(i)b_B(i)b_B(i)b_C(j): + :b_B^\dagger(i)b_B(i)b_B(i)b_C(j):$$

$$+ :b_B^\dagger(i)b_B(i)b_B(i)b_C(j): + :b_B^\dagger(i)b_B(i)b_B(i)b_C(j): + :b_B^\dagger(i)b_B(i)b_B(i)b_C(j): \Big]$$

$$= z\sum_{\mathbf{k}}\Big[nC_{\mathbf{k}}^* :b_B(-\mathbf{k})b_C(\mathbf{k}): + nC_{\mathbf{k}}^* :b_B(-\mathbf{k})b_C(\mathbf{k}): + 0$$

$$+ 0 + \Delta_C^* :b_B^\dagger(-\mathbf{k})b_B(-\mathbf{k}): + \Delta_C^* :b_B^\dagger(-\mathbf{k})b_B(-\mathbf{k}): \Big]$$

$$= z\sum_{\mathbf{k}}\Big[2nC_{\mathbf{k}}^* :b_B(-\mathbf{k})b_C(\mathbf{k}): + 2\Delta_C^* :b_B^\dagger(-\mathbf{k})b_B(-\mathbf{k}): \Big].$$

(3.9)

(ii)

$$\sum_i \sum_{\substack{j\in\{i+\vec{e}_x, \\ i+\vec{e}_y\}}} b_B^\dagger(i)b_C^\dagger(j)b_C^\dagger(j)b_C(j)$$

$$\longrightarrow \sum_i \sum_{\substack{j\in\{i+\vec{e}_x,\\ i+\vec{e}_y\}}} \Big[:b_B^\dagger(i)b_C^\dagger(j)b_C^\dagger(j)b_C(j): + :b_B^\dagger(i)b_C^\dagger(j)b_C^\dagger(j)b_C(j): + :b_B^\dagger(i)b_C^\dagger(j)b_C^\dagger(j)b_C(j):$$

$$+ :b_B^\dagger(i)b_C^\dagger(j)b_C^\dagger(j)b_C(j): + :b_B^\dagger(i)b_C^\dagger(j)b_C^\dagger(j)b_C(j): + :b_B^\dagger(i)b_C^\dagger(j)b_C^\dagger(j)b_C(j):$$

$$= z\sum_{\mathbf{k}} \Big[\Delta_\gamma :b_C^\dagger(\mathbf{k})b_C(\mathbf{k}): + \Delta_\gamma :b_C^\dagger(\mathbf{k})b_C(\mathbf{k}): + 0$$

$$+ 0 + nC_{\mathbf{k}} :b_B^\dagger(-\mathbf{k})b_C^\dagger(\mathbf{k}): + nC_{\mathbf{k}} :b_B^\dagger(-\mathbf{k})b_C^\dagger(\mathbf{k}): \Big]$$

$$= z\sum_{\mathbf{k}} \Big[2\Delta_\gamma :b_C^\dagger(\mathbf{k})b_C(\mathbf{k}): + 2nC_{\mathbf{k}} :b_B^\dagger(-\mathbf{k})b_C^\dagger(\mathbf{k}): \Big],$$

$$(3.10)$$

(iii)

$$\sum_i \sum_{\substack{j\in\{i+\vec{e}_x,\\ i+\vec{e}_y\}}} b_B^\dagger(i)b_C^\dagger(j)b_B^\dagger(j)b_B(j)$$

$$\longrightarrow \sum_i \sum_{\substack{j\in\{i+\vec{e}_x,\\ i+\vec{e}_y\}}} \Big[:b_B^\dagger(i)b_C^\dagger(j)b_B^\dagger(j)b_B(j): + :b_B^\dagger(i)b_C^\dagger(j)b_B^\dagger(j)b_B(j): + :b_B^\dagger(i)b_C^\dagger(j)b_B^\dagger(j)b_B(j):$$

$$+ :b_B^\dagger(i)b_C^\dagger(j)b_B^\dagger(j)b_B(j): + :b_B^\dagger(i)b_C^\dagger(j)b_B^\dagger(j)b_B(j): + :b_B^\dagger(i)b_C^\dagger(j)b_B^\dagger(j)b_B(j):$$

$$= z\sum_{\mathbf{k}} \Big[\Delta_\gamma :b_B^\dagger(-\mathbf{k})b_B(-\mathbf{k}): + 0 + 0$$

$$+ 0 + 0 + nC_{\mathbf{k}} :b_B^\dagger(-\mathbf{k})b_C^\dagger(\mathbf{k}): \Big]$$

$$= z\sum_{\mathbf{k}} \Big[\Delta_\gamma :b_B^\dagger(-\mathbf{k})b_B(-\mathbf{k}): + nC_{\mathbf{k}} :b_B^\dagger(-\mathbf{k})b_C^\dagger(\mathbf{k}): \Big],$$

$$(3.11)$$

(vi)

$$\sum_i \sum_{\substack{j\in\{i+\vec{e}_x,\\ i+\vec{e}_y\}}} b_B^\dagger(i)b_C^\dagger(j)b_C^\dagger(i)b_C(i)$$

$$\longrightarrow \sum_i \sum_{\substack{j \in \{i+\vec{e}_x, \\ i+\vec{e}_y\}}} \Big[:b_B^\dagger(i)\underline{b_C^\dagger(j)b_C^\dagger(i)}b_C(i): + :b_B^\dagger(i)\underline{b_C^\dagger(j)b_C^\dagger(i)b_C(i)}: + :b_B^\dagger(i)b_C^\dagger(j)\underline{b_C^\dagger(i)b_C(i)}:$$

$$+ :b_B^\dagger(i)\underline{b_C^\dagger(j)b_C^\dagger(i)}b_C(i): + :b_B^\dagger(i)\underline{b_C^\dagger(j)b_C^\dagger(i)b_C(i)}: + :b_B^\dagger(i)b_C^\dagger(j)\underline{b_C^\dagger(i)b_C(i)}:$$

$$= z \sum_{\mathbf{k}} \Big[\Delta_\gamma :b_C^\dagger(\mathbf{k})b_C(\mathbf{k}): + 0 + 0$$

$$+ 0 + 0 + n\gamma_{\mathbf{k}} :b_B^\dagger(-\mathbf{k})b_C^\dagger(\mathbf{k}): \Big]$$

$$= z \sum_{\mathbf{k}} \Big[\Delta_\gamma :b_C^\dagger(\mathbf{k})b_C(\mathbf{k}): + n\gamma_{\mathbf{k}} :b_B^\dagger(-\mathbf{k})b_C^\dagger(\mathbf{k}): \Big],$$

$$\tag{3.12}$$

(v)

$$\sum_i \sum_{\substack{j \in \{i+\vec{e}_x, \\ i+\vec{e}_y\}}} b_C^\dagger(i)b_C^\dagger(j)b_C(i)b_C(j)$$

$$\longrightarrow \sum_i \sum_{\substack{j \in \{i+\vec{e}_x, \\ i+\vec{e}_y\}}} \Big[:\underline{b_C^\dagger(i)b_C^\dagger(j)}b_C(i)b_C(j): + :\underline{b_C^\dagger(i)b_C^\dagger(j)b_C(i)}b_C(j): + :b_C^\dagger(i)\underline{b_C^\dagger(j)b_C(i)}b_C(j):$$

$$+ :b_C^\dagger(i)\underline{b_C^\dagger(j)b_C(i)b_C(j)}: + :b_C^\dagger(i)b_C^\dagger(j)\underline{b_C(i)b_C(j)}: + :b_C^\dagger(i)b_C^\dagger(j)b_C(i)b_C(j):$$

$$= z \sum_{\mathbf{k}} \Big[0 + n :b_C^\dagger(\mathbf{k})b_C(\mathbf{k}): + 0$$

$$+ 0 + n :b_C^\dagger(\mathbf{k})b_C(\mathbf{k}): + 0 \Big]$$

$$= z \sum_{\mathbf{k}} 2n :b_C^\dagger(\mathbf{k})b_C(\mathbf{k}):,$$

$$\tag{3.13}$$

(vi)

$$\sum_i \sum_{\substack{j \in \{i+\vec{e}_x, \\ i+\vec{e}_y\}}} b_B^\dagger(i)b_B^\dagger(j)b_B(j)b_B(i)$$

$$
\longrightarrow \sum_i \sum_{\substack{j \in \{i+\vec{e}_x, \\ i+\vec{e}_y\}}} \Big[:b_B^\dagger(i)b_B^\dagger(j)b_B(j)b_B(i): + :b_B^\dagger(i)b_B^\dagger(j)b_B(j)b_B(i): + :b_B^\dagger(i)b_B^\dagger(j)b_B(j)b_B(i):
$$

$$
+ :b_B^\dagger(i)b_B^\dagger(j)b_B(j)b_B(i): + :b_B^\dagger(i)b_B^\dagger(j)b_B(j)b_B(i): + :b_B^\dagger(i)b_B^\dagger(j)b_B(j)b_B(i):
$$

$$
= z \sum_{\mathbf{k}} \Big[0 + 0 + n :b_B^\dagger(-\mathbf{k})b_B(-\mathbf{k}):
$$

$$
+ n :b_B^\dagger(-\mathbf{k})b_B(-\mathbf{k}): \Big]
$$

$$
= z \sum_{\mathbf{k}} 2n :b_B^\dagger(-\mathbf{k})b_B(-\mathbf{k}):,
$$

$$
\tag{3.14}
$$

(vii)

$$
\sum_i \sum_{\substack{j \in \{i+\vec{e}_x, \\ i+\vec{e}_y\}}} b_B^\dagger(i)b_C^\dagger(j)b_C(j)b_B(i)
$$

$$
\longrightarrow \sum_i \sum_{\substack{j \in \{i+\vec{e}_x, \\ i+\vec{e}_y\}}} \Big[:b_B^\dagger(i)b_C^\dagger(j)b_C(j)b_B(i): + :b_B^\dagger(i)b_C^\dagger(j)b_C(j)b_B(i): + :b_B^\dagger(i)b_C^\dagger(j)b_C(j)b_B(i):
$$

$$
+ :b_B^\dagger(i)b_C^\dagger(j)b_C(j)b_B(i): + :b_B^\dagger(i)b_C^\dagger(j)b_C(j)b_B(i): + :b_B^\dagger(i)b_C^\dagger(j)b_C(j)b_B(i):
$$

$$
= z \sum_{\mathbf{k}} \Big[\Delta_\gamma C_{\mathbf{k}}^* :b_C(\mathbf{k})b_B(-\mathbf{k}): + 0 + n :b_C^\dagger(\mathbf{k})b_C(\mathbf{k}):
$$

$$
+ n :b_B^\dagger(-\mathbf{k})b_B(-\mathbf{k}): + 0 + \Delta_C^* C_{\mathbf{k}} :b_C^\dagger(\mathbf{k})b_B^\dagger(\mathbf{k}): \Big]
$$

$$
= z \sum_{\mathbf{k}} \Big[n :b_C^\dagger(\mathbf{k})b_C(\mathbf{k}): + n :b_B^\dagger(-\mathbf{k})b_B(-\mathbf{k}): + \Delta_\gamma C_{\mathbf{k}}^* :b_C(\mathbf{k})b_B(-\mathbf{k}): + \Delta_C^* C_{\mathbf{k}} :b_C^\dagger(\mathbf{k})b_B^\dagger(-\mathbf{k}): \Big].
$$

$$
\tag{3.15}
$$

(viii)

$$
-\sum_i \sum_{\substack{j \in \{i+\vec{e}_x, \\ i+\vec{e}_y\}}} b_C^\dagger(i)b_B^\dagger(j)b_C(i)b_B(j)
$$

$$\longrightarrow -\sum_{i}\sum_{\substack{j\in\{i+\vec{e}_x,\\i+\vec{e}_y\}}} \Big[:b_C^\dagger(i)b_B^\dagger(j)b_C(i)b_B(j): + :b_C^\dagger(i)b_B^\dagger(j)b_C(i)b_B(j): + :b_C^\dagger(i)b_B^\dagger(j)b_C(i)b_B(j):$$

$$+ :b_C^\dagger(i)b_B^\dagger(j)b_C(i)b_B(j): + :b_C^\dagger(i)b_B^\dagger(j)b_C(i)b_B(j): + :b_C^\dagger(i)b_B^\dagger(j)b_C(i)b_B(j):$$

$$= -z\sum_{\mathbf{k}}\Big[\Delta_\gamma C_{\mathbf{k}}^* :b_C(\mathbf{k})b_B(-\mathbf{k}): + n:b_B^\dagger(-\mathbf{k})b_B(-\mathbf{k}): + 0$$

$$+ 0 + n:b_C^\dagger(\mathbf{k})b_C(\mathbf{k}): + \Delta_C^* C_{\mathbf{k}} :b_C^\dagger(\mathbf{k})b_B^\dagger(-\mathbf{k}):\Big]$$

$$= -z\sum_{\mathbf{k}}\Big[n:b_C^\dagger(\mathbf{k})b_C(\mathbf{k}): + n:b_B^\dagger(-\mathbf{k})b_B(-\mathbf{k}): + \Delta_\gamma C_{\mathbf{k}}^* :b_C(\mathbf{k})b_B(-\mathbf{k}): + \Delta_C^* C_{\mathbf{k}} :b_C^\dagger(\mathbf{k})b_B^\dagger(-\mathbf{k}):\Big].$$

(3.16)

By regrouping all these terms and their Hermitian conjugate as well as the overall factor $-\frac{1}{2}$ from Eq. (6.7), the term $\delta\mathcal{H}^{(2)}$ is then given by

$$\delta\mathcal{H}^{(2)} = Jz\sum_{\mathbf{k}}\Big[\delta A_{-\mathbf{k}}^B :b_{B,-\mathbf{k}}^\dagger b_{B,-\mathbf{k}}: + \delta A_{\mathbf{k}}^C :b_{C,\mathbf{k}}^\dagger b_{C,\mathbf{k}}: + \delta B_{\mathbf{k}}^* :b_{B,-\mathbf{k}}b_{C,\mathbf{k}}: + \delta B_{\mathbf{k}} :b_{B,-\mathbf{k}}^\dagger b_{C,\mathbf{k}}^\dagger:\Big],\quad (3.17)$$

where

$$\delta A_{-\mathbf{k}}^B = -\frac{1}{2}\left(3n + 3\Delta_\gamma + \text{h.c.}\right) = -\text{Re}\left(3n + 3\Delta_\gamma\right)$$

$$= -3\left[n + \text{Re}\left(\Delta_\gamma\right)\right]$$

$$=:\delta A,$$

$$\delta A_{\mathbf{k}}^C = -\frac{1}{2}\left(3n + 3\Delta_\gamma + \text{h.c.}\right)$$

$$= \delta A,$$

$$\delta B_{\mathbf{k}} = -\frac{1}{2}\left(6n\gamma_{\mathbf{k}} + 4\Delta_\gamma^*\gamma_{\mathbf{k}}\right)$$

$$= -\gamma_{\mathbf{k}}\left(3n + 2\Delta_\gamma^*\right).$$

(3.18)

Appendix C. The corrections from the $SU(3)$ quartic terms $\mathcal{H}^{(4)}$

We will now write $\delta\mathcal{H}^{(2)}$ in terms of the Bogoliubov bosons $\eta_{\mathbf{k}}$ by using

$$
\begin{aligned}
:b_{B,-\mathbf{k}}^{\dagger}b_{B,-\mathbf{k}}: &=:(-v_{\mathbf{k}}\eta_{C,\mathbf{k}}+u_{\mathbf{k}}^{*}\eta_{B,-\mathbf{k}}^{\dagger})(-v_{\mathbf{k}}\eta_{C,\mathbf{k}}^{\dagger}+u_{\mathbf{k}}\eta_{B,-\mathbf{k}}):\\
&=v_{\mathbf{k}}^{2}\eta_{C,\mathbf{k}}^{\dagger}\eta_{C,\mathbf{k}}+|u_{\mathbf{k}}|^{2}\eta_{B,-\mathbf{k}}^{\dagger}\eta_{B,-\mathbf{k}}-u_{\mathbf{k}}v_{\mathbf{k}}\eta_{C,\mathbf{k}}\eta_{B,-\mathbf{k}}-u_{\mathbf{k}}^{*}v_{\mathbf{k}}\eta_{B,-\mathbf{k}}^{\dagger}\eta_{C,\mathbf{k}}^{\dagger},\\
:b_{C,\mathbf{k}}^{\dagger}b_{C,\mathbf{k}}: &=:(u_{\mathbf{k}}^{*}\eta_{C,\mathbf{k}}^{\dagger}-v_{\mathbf{k}}\eta_{B,-\mathbf{k}})(u_{\mathbf{k}}\eta_{C,\mathbf{k}}-v_{\mathbf{k}}\eta_{B,-\mathbf{k}}^{\dagger}):\\
&=|u_{\mathbf{k}}|^{2}\eta_{C,\mathbf{k}}^{\dagger}\eta_{C,\mathbf{k}}+v_{\mathbf{k}}^{2}\eta_{B,-\mathbf{k}}^{\dagger}\eta_{B,-\mathbf{k}}-u_{\mathbf{k}}v_{\mathbf{k}}\eta_{B,-\mathbf{k}}\eta_{C,\mathbf{k}}-u_{\mathbf{k}}^{*}v_{\mathbf{k}}\eta_{C,\mathbf{k}}^{\dagger}\eta_{B,-\mathbf{k}}^{\dagger},\\
:b_{B,-\mathbf{k}}b_{C,\mathbf{k}}: &=:(-v_{\mathbf{k}}\eta_{C,\mathbf{k}}^{\dagger}+u_{\mathbf{k}}\eta_{B,-\mathbf{k}})(u_{\mathbf{k}}\eta_{C,\mathbf{k}}-v_{\mathbf{k}}\eta_{B,-\mathbf{k}}^{\dagger}):\\
&=-u_{\mathbf{k}}v_{\mathbf{k}}\eta_{C,\mathbf{k}}^{\dagger}\eta_{C,\mathbf{k}}-u_{\mathbf{k}}v_{\mathbf{k}}\eta_{B,-\mathbf{k}}^{\dagger}\eta_{B,-\mathbf{k}}+v_{\mathbf{k}}^{2}\eta_{C,\mathbf{k}}^{\dagger}\eta_{B,-\mathbf{k}}^{\dagger}+u_{\mathbf{k}}^{2}\eta_{B,-\mathbf{k}}\eta_{C,\mathbf{k}},\\
:b_{C,\mathbf{k}}^{\dagger}b_{B,-\mathbf{k}}^{\dagger}: &=:(u_{\mathbf{k}}^{*}\eta_{C,\mathbf{k}}^{\dagger}-v_{\mathbf{k}}\eta_{B,-\mathbf{k}})(-v_{\mathbf{k}}\eta_{C,\mathbf{k}}+u_{\mathbf{k}}^{*}\eta_{B,-\mathbf{k}}^{\dagger}):\\
&=-u_{\mathbf{k}}^{*}v_{\mathbf{k}}\eta_{C,\mathbf{k}}^{\dagger}\eta_{C,\mathbf{k}}-u_{\mathbf{k}}^{*}v_{\mathbf{k}}\eta_{B,-\mathbf{k}}^{\dagger}\eta_{B,-\mathbf{k}}+u_{\mathbf{k}}^{*2}\eta_{C,\mathbf{k}}^{\dagger}\eta_{B,-\mathbf{k}}^{\dagger}+v_{\mathbf{k}}^{2}\eta_{B,-\mathbf{k}}\eta_{C,\mathbf{k}}
\end{aligned}
\tag{3.19}
$$

We thus obtain

$$
\delta\mathcal{H}^{(2)}=Jz\sum_{\mathbf{k}}\left[\delta A_{-\mathbf{k}}^{B}:b_{B,-\mathbf{k}}^{\dagger}b_{B,-\mathbf{k}}:+\delta A_{\mathbf{k}}^{C}:b_{C,\mathbf{k}}^{\dagger}b_{C,\mathbf{k}}:+\delta B_{\mathbf{k}}^{*}:b_{B,-\mathbf{k}}b_{C,\mathbf{k}}:+\delta B_{\mathbf{k}}:b_{B,-\mathbf{k}}^{\dagger}b_{C,\mathbf{k}}^{\dagger}:\right]
\tag{3.20}
$$

$$
=Jz\sum_{\mathbf{k}}\left[\omega_{-\mathbf{k}}^{B(4)}\eta_{B,-\mathbf{k}}^{\dagger}\eta_{B,-\mathbf{k}}+\omega_{\mathbf{k}}^{C(4)}\eta_{C,\mathbf{k}}^{\dagger}\eta_{C,\mathbf{k}}+B_{\mathbf{k}}^{(4)\,*}\eta_{B,-\mathbf{k}}\eta_{C,\mathbf{k}}+B_{\mathbf{k}}^{(4)}\eta_{B,-\mathbf{k}}^{\dagger}\eta_{C,\mathbf{k}}^{\dagger}\right],
\tag{3.21}
$$

with

$$
\begin{aligned}
\omega_{-\mathbf{k}}^{B(4)} &=|u_{\mathbf{k}}|^{2}\delta A_{-\mathbf{k}}^{B}+v_{\mathbf{k}}^{2}\delta A_{\mathbf{k}}^{C}-u_{\mathbf{k}}v_{\mathbf{k}}\delta B_{\mathbf{k}}^{*}-u_{\mathbf{k}}^{*}v_{\mathbf{k}}\delta B_{\mathbf{k}}\\
&=\left(|u_{\mathbf{k}}|^{2}+v_{\mathbf{k}}^{2}\right)\delta A-2\mathrm{Re}\left(u_{\mathbf{k}}^{*}v_{\mathbf{k}}\delta B_{\mathbf{k}}\right)\\
&=\frac{A}{\omega_{\mathbf{k}}}\delta A-2\mathrm{Re}\left(\frac{B_{k}^{*}}{2\omega_{\mathbf{k}}}\delta B_{\mathbf{k}}\right)\\
&=:\omega_{-\mathbf{k}}^{(4)}\\
&=\omega_{\mathbf{k}}^{(4)},\\
\omega_{\mathbf{k}}^{C(4)} &=v_{\mathbf{k}}^{2}\delta A_{-\mathbf{k}}^{B}+|u_{\mathbf{k}}|^{2}\delta A_{\mathbf{k}}^{C}-u_{\mathbf{k}}v_{\mathbf{k}}\delta B_{\mathbf{k}}^{*}-u_{\mathbf{k}}^{*}v_{\mathbf{k}}\delta B_{\mathbf{k}}\\
&=\left(|u_{\mathbf{k}}|^{2}+v_{\mathbf{k}}^{2}\right)\delta A-2\mathrm{Re}\left(u_{\mathbf{k}}^{*}v_{\mathbf{k}}\delta B_{\mathbf{k}}\right)\\
&=\omega_{\mathbf{k}}^{(4)}.
\end{aligned}
\tag{3.22}
$$

All in all, we obtain

$$
\delta\mathcal{H}^{(2)}=\sum_{\mathbf{k}}\left[\varepsilon_{\mathbf{k}}^{(4)}\eta_{B,\mathbf{k}}^{\dagger}\eta_{B,\mathbf{k}}+\varepsilon_{\mathbf{k}}^{(4)}\eta_{C,\mathbf{k}}^{\dagger}\eta_{C,\mathbf{k}}+Jz\left(B_{\mathbf{k}}^{(4)\,*}\eta_{B,-\mathbf{k}}\eta_{C,\mathbf{k}}+B_{\mathbf{k}}^{(4)}\eta_{B,-\mathbf{k}}^{\dagger}\eta_{C,\mathbf{k}}^{\dagger}\right)\right],
\tag{3.23}
$$

where we defined

$$
\varepsilon_{\mathbf{k}}^{(4)}:=Jz\omega_{\mathbf{k}}^{(4)}.
\tag{3.24}
$$

154

D The nonlinear sigma model of SU(3) \ (U(1) × U(1))

From [subsection 6.3.1](#), the action S of the discrete 2D lattice model of the SU(3) $J_1 - J_3$ Hamiltonian is given by

$$
S = \int_0^\beta \sum_{i,j\in\mathbb{N}} \left\{ p^2 J_1 \left[\left|\vec{\phi}_1^*(i,j)\cdot\vec{\phi}_2(i,j)\right|^2 + \left|\vec{\phi}_2^*(i,j)\cdot\vec{\phi}_3(i,j)\right|^2 + \left|\vec{\phi}_3^*(i,j)\cdot\vec{\phi}_1(i+1,j)\right|^2 \right. \right.
$$
$$
\left. + \left|\vec{\phi}_1^*(i,j)\cdot\vec{\phi}_2(i,j+1)\right|^2 + \left|\vec{\phi}_2^*(i,j)\cdot\vec{\phi}_3(i,j+1)\right|^2 + \left|\vec{\phi}_3^*(i,j)\cdot\vec{\phi}_1(i+1,j+1)\right|^2 \right]
$$
$$
+ p^2 J_3 \left[\left|\vec{\phi}_1^*(i,j)\cdot\vec{\phi}_3(i,j)\right|^2 + \left|\vec{\phi}_2^*(i,j)\cdot\vec{\phi}_1(i+1,j)\right|^2 + \left|\vec{\phi}_3^*(i,j)\cdot\vec{\phi}_2(i+1,j)\right|^2 \right.
$$
$$
\left. + \left|\vec{\phi}_1^*(i,j)\cdot\vec{\phi}_3(i,j+2)\right|^2 + \left|\vec{\phi}_2^*(i,j)\cdot\vec{\phi}_1(i+1,j+2)\right|^2 + \left|\vec{\phi}_3^*(i,j)\cdot\vec{\phi}_2(i+1,j+2)\right|^2 \right]
$$
$$
\left. + p \sum_{n=1}^3 \vec{\phi}_n^*(i,j)\cdot\partial_\tau\vec{\phi}_n(i,j) \right\} d\tau,
$$

(4.1)

where the τ-dependency is implicit. We now go to the continuum limit by using the Riemann sum

$$
\lim_{N\to\infty} \Delta A \sum_{i,j=0}^{N-1} f(i,j) \longrightarrow \int f(x,y)\,dx\,dy, \tag{4.2}
$$

in which $f(x,y)$ represents the expression of the Taylor expansion of $f(i,j)$ in x and y, and $\Delta A = 3a^2$ is the volume of the unit cell. In this case,

$$
\begin{aligned}
U(i\pm 1,j) &\longrightarrow U(x,y) \pm 3a\partial_x U(x,y) + \mathcal{O}(a^2),\\
U(i,j\pm 1) &\longrightarrow U(x,y) \pm a[-\partial_x U(x,y) + \partial_y U(x,y)] + \mathcal{O}(a^2),\\
U(i,j+2) &\longrightarrow U(x,y) + 2a[-\partial_x U(x,y) + \partial_y U(x,y)] + \mathcal{O}(a^2),\\
U(i+1,j+1) &\longrightarrow U(x,y) \pm a[2\partial_x U(x,y) + \partial_y U(x,y)] + \mathcal{O}(a^2),\\
U(i+1,j+2) &\longrightarrow U(x,y) \pm a[\partial_x U(x,y) + 2\partial_y U(x,y)] + \mathcal{O}(a^2).
\end{aligned} \tag{4.3}
$$

Appendix D. The nonlinear sigma model of $SU(3) \setminus (U(1) \times U(1))$

This gradient expansion can be used on the terms in Eq. (4.1). For instance, the second term is given by

$$
\begin{aligned}
p^2 \left| \vec{\phi}_2^*(i,j) \cdot \vec{\phi}_3(i,j) \right|^2 &= p^2 \left| (\vec{e}_2^\top LU)^* (\vec{e}_3^\top LU)^\top \right|^2 \\
&= p^2 \left(\frac{a^2}{p^2} L_{12} L_{13}^* + 2\frac{a}{p} L_{23}^* \right) \left(\frac{a^2}{p^2} L_{12}^* L_{13} + 2\frac{a}{p} L_{23} \right) \mathcal{O}(a^5) \\
&= 4a^2 |L_{23}|^2 + \mathcal{O}(a^3)
\end{aligned}
\tag{4.4}
$$

up to a^2. Performing this gradient expansion on on the action S (4.1) up to the the order a^2, and with the help of the Λ_n matrices defined by

$$
\Lambda_1 = \begin{pmatrix} 1 & 0 & 0 \\ 0 & 0 & 0 \\ 0 & 0 & 0 \end{pmatrix}, \quad
\Lambda_2 = \begin{pmatrix} 0 & 0 & 0 \\ 0 & 1 & 0 \\ 0 & 0 & 0 \end{pmatrix}, \quad
\Lambda_3 = \begin{pmatrix} 0 & 0 & 0 \\ 0 & 0 & 0 \\ 0 & 0 & 1 \end{pmatrix},
\tag{4.5}
$$

we obtain the action $S[U, L]$ (remember that U contains the fields $\vec{\varphi}$) in the continuum limit:

$$
S[U, L] = \frac{1}{3a^2} \int dx\, dy\, d\tau \left(\mathcal{L}_{12}[U, L_{12}] + \mathcal{L}_{23}[U, L_{23}] + \mathcal{L}_{13}[U, L_{13}] + \mathcal{L}_U[U] \right),
\tag{4.6}
$$

with

$$
\begin{aligned}
\mathcal{L}_{12}[U, L_{12}] :={}& a \left[2L_{12}(\partial_\tau UU^\dagger)_{21} + 2L_{12}^*(\partial_\tau UU^\dagger)_{12} \right] + a^2 \left[8(J_1 + J_3) |L_{12}|^2 \right] \\
&+ a^2 p L_{12} \left\{ J_1 \left[-2(\partial_x UU^\dagger)_{21} + 2(\partial_y UU^\dagger)_{21} \right] + J_3 \left[-8(\partial_x UU^\dagger)_{21} - 4(\partial_y UU^\dagger)_{21} \right] \right\} \\
&+ a^2 p L_{12}^* \left\{ J_1 \left[-2(U\partial_x U^\dagger)_{12} + 2(U\partial_y U^\dagger)_{12} \right] + J_3 \left[-8(U\partial_x U^\dagger)_{12} - 4(U\partial_y U^\dagger)_{12} \right] \right\},
\end{aligned}
\tag{4.7a}
$$

$$
\begin{aligned}
\mathcal{L}_{23}[U, L_{23}] :={}& a \left[2L_{23}(\partial_\tau UU^\dagger)_{32} + 2L_{23}^*(\partial_\tau UU^\dagger)_{23} \right] + a^2 \left[8(J_1 + J_3) |L_{23}|^2 \right] \\
&+ a^2 p L_{23} \left\{ J_1 \left[-2(\partial_x UU^\dagger)_{32} + 2(\partial_y UU^\dagger)_{32} \right] + J_3 \left[-8(\partial_x UU^\dagger)_{32} - 4(\partial_y UU^\dagger)_{32} \right] \right\} \\
&+ a^2 p L_{23}^* \left\{ J_1 \left[-2(U\partial_x U^\dagger)_{23} + 2(U\partial_y U^\dagger)_{23} \right] + J_3 \left[-8(U\partial_x U^\dagger)_{23} - 4(U\partial_y U^\dagger)_{23} \right] \right\},
\end{aligned}
\tag{4.7b}
$$

$$
\begin{aligned}
\mathcal{L}_{13}[U, L_{13}] :={}& a \left[2L_{13}(\partial_\tau UU^\dagger)_{31} + 2L_{13}^*(\partial_\tau UU^\dagger)_{13} \right] + a^2 \left[8(J_1 + J_3) |L_{13}|^2 \right] \\
&+ a^2 p L_{13}^* \left\{ J_1 \left[10(\partial_x UU^\dagger)_{13} + 2(\partial_y UU^\dagger)_{13} \right] + J_3 \left[4(\partial_x UU^\dagger)_{13} - 4(\partial_y UU^\dagger)_{13} \right] \right\} \\
&+ a^2 p L_{13} \left\{ J_1 \left[10(U\partial_x U^\dagger)_{31} + 2(U\partial_y U^\dagger)_{31} \right] + J_3 \left[4(U\partial_x U^\dagger)_{31} - 4(U\partial_y U^\dagger)_{31} \right] \right\},
\end{aligned}
\tag{4.7c}
$$

$$\mathcal{L}_U[U] := a^2 p^2 \left\{ J_1 \left[\sum_{r \in \{x,y\}} \sum_{n=1}^{3} \text{Tr}[\Lambda_{n-1}(U\partial_r U^\dagger)\Lambda_n(\partial_r UU^\dagger)] \right. \right.$$

$$- \sum_{n=1}^{3} \left(\text{Tr}[\Lambda_{n-1}(U\partial_x U^\dagger)\Lambda_n(\partial_y UU^\dagger)] + \text{Tr}[\Lambda_{n-1}(U\partial_y U^\dagger)\Lambda_n(\partial_x UU^\dagger)] \right)$$

$$+ 12\,\text{Tr}[\Lambda_3(U\partial_x U^\dagger)\Lambda_1(\partial_x UU^\dagger)]$$

$$\left. + 3\left(\text{Tr}[\Lambda_3(U\partial_x U^\dagger)\Lambda_1(\partial_y UU^\dagger)] + \text{Tr}[\Lambda_3(U\partial_y U^\dagger)\Lambda_1(\partial_x UU^\dagger)] \right) \right]$$

$$+ J_3 \left[\sum_{n=1}^{3} \left(10\,\text{Tr}[\Lambda_{n-1}(U\partial_x U^\dagger)\Lambda_n(\partial_x UU^\dagger)] + 4\,\text{Tr}[\Lambda_{n-1}(U\partial_y U^\dagger)\Lambda_n(\partial_y UU^\dagger)] \right) \right.$$

$$+ 2\sum_{n=1}^{3} \left(\text{Tr}[\Lambda_{n-1}(U\partial_x U^\dagger)\Lambda_n(\partial_y UU^\dagger)] + \text{Tr}[\Lambda_{n-1}(U\partial_y U^\dagger)\Lambda_n(\partial_x UU^\dagger)] \right)$$

$$- 6\,\text{Tr}[\Lambda_3(U\partial_x U^\dagger)\Lambda_1(\partial_x UU^\dagger)]$$

$$\left. \left. - 6\left(\text{Tr}[\Lambda_3(U\partial_x U^\dagger)\Lambda_1(\partial_y UU^\dagger)] + \text{Tr}[\Lambda_3(U\partial_y U^\dagger)\Lambda_1(\partial_x UU^\dagger)] \right) \right] \right\}.$$

(4.7d)

The shorthand notation $A_{\mu\nu}^n := \text{Tr}\left[\Lambda_{n-1}\left(U\partial_\mu U^\dagger\right)\Lambda_n\left(\partial_\nu UU^\dagger\right)\right]$ will be used in the subsequent calculations for the ease of notation, with $n \in \{1,2,3\}$[22]. The L fields describing the fluctuations can now be integrated out by using

$$\int dz^* dz\, e^{-z^*\omega z + u^* z + v z^*} = \frac{\pi}{\omega} e^{\frac{u^* v}{\omega}}, \tag{4.8}$$

which yields the action $S[U]$:

$$S[U] = \int dx\,dy\,d\tau \left\{ \sum_{n=1}^{3} \left\{ \frac{1}{a^2} \frac{1}{6(J_1+J_3)} A_{\tau\tau}^n \right. \right.$$

$$p^2 + A_{xx}^n \left[\frac{1}{6(J_1+J_3)}\left(-J_1^2 - 8J_1J_3 - 16J_3^2\right) + \frac{1}{3}J_1 + J_3\frac{10}{3} \right]$$

$$p^2 + A_{yy}^n \left[\frac{1}{6(J_1+J_3)}\left(-J_1^2 + 4J_1J_3 - 4J_3^2\right) + \frac{1}{3}J_1 + J_3\frac{4}{3} \right]$$

$$+ p^2(A_{xy}^n + A_{yx}^n)\left[\frac{1}{6(J_1+J_3)}\left(J_1^2 + 2J_1J_3 - 8J_3^2\right) - \frac{1}{3}J_1 + J_3\frac{2}{3} \right]$$

$$\left. + \frac{p}{a}\frac{1}{6(J_1+J_3)}\left[(A_{x\tau}^n - A_{\tau x}^n) + (A_{\tau y}^n - A_{y\tau}^n)\right](J_1 + 4J_3) \right\}$$

$$+ p^2 A_{xx}^1 \left[\frac{2}{J_1+J_3}\left(-2J_1^2 - J_1J_3 + J_3^2\right) + 4J_1 - 2J_3 \right]$$

$$+ p^2(A_{xy}^1 + A_{yx}^1)\left[\frac{1}{J_1+J_3}\left(-J_1^2 + \frac{4}{3}J_1J_3 + 2J_3^2\right) + J_1 - 2J_3 \right]$$

$$\left. + \frac{p}{a}(A_{x\tau}^1 - A_{\tau x}^1) \right\}. \tag{4.9}$$

[22]When $n = 0$, it corresponds to $n = 3$.

Appendix D. The nonlinear sigma model of SU(3) \ (U(1) × U(1))

As we are looking for the velocity of the Goldstone modes to compare it with the velocity obtained with the LFWT along the diagonal of the Brillouin zone ($k_x = k_y$) along which there is a line of zero-modes in the J_1 model, we consider a new (rotated) coordinate basis $\{x', y'\}$:

$$
\begin{cases} x' = \frac{1}{\sqrt{2}}(x+y) \\ y' = \frac{1}{\sqrt{2}}(-x+y) \end{cases}
\implies
\begin{cases}
\dfrac{\partial}{\partial x} = \dfrac{\partial x'}{\partial x}\dfrac{\partial}{\partial x'} + \dfrac{\partial x'}{\partial x}\dfrac{\partial}{\partial x'} = \dfrac{1}{\sqrt{2}}\left(\dfrac{\partial}{\partial x'} - \dfrac{\partial}{\partial y'}\right) \\
\qquad =: \dfrac{1}{\sqrt{2}}(\partial_1 - \partial_2) \\
\dfrac{\partial}{\partial y} = \dfrac{1}{\sqrt{2}}\left(\dfrac{\partial}{\partial x'} + \dfrac{\partial}{\partial y'}\right) \\
\qquad =: \dfrac{1}{\sqrt{2}}(\partial_1 + \partial_2)
\end{cases}
\tag{4.10}
$$

In this rotated basis, the action $S[U]$ in Eq. (4.9) becomes

$$
\begin{aligned}
S[U] = &\int dx'dy'd\tau \sum_{n=1}^{3}\left[\frac{1}{2(J_1+J_3)}A_{\tau\tau}^n + 9a^2p^2 A_{11}^n\left(-\frac{J_3^2}{J_1+J_3}+J_3\right)+a^2p^2 A_{22}^n(J_1+4J_3)\right] \\
&+\int dx'dy'd\tau\left\{\sum_{n=1}^{3}\left[ap(A_{1\tau}^n - A_{\tau1}^n)\frac{J_3}{J_1+J_3}\frac{3\sqrt{2}}{2}+ap(A_{\tau2}^n - A_{2\tau}^n)\frac{\sqrt{2}}{3}\right]\right. \\
&\left.-ap(A_{1\tau}^1 - A_{\tau1}^1)\frac{3\sqrt{2}}{2}-ap(A_{\tau2}^1 - A_{2\tau}^1)\frac{3\sqrt{2}}{2}\right\}.
\end{aligned}
\tag{4.11}
$$

As we are looking for the low-energy behaviour of our system, we now linearise U (or the fields $\vec{\varphi}$) by truncating the exponential in Eq. (6.42) at the linear order of $\theta_k(x', y', \tau)$:

$$
U[\theta] = \exp\left(i\sum_{k=1}^{6}\theta_k\lambda_k\right) \approx \begin{pmatrix} 1 & \theta_1 + i\theta_4 & -\theta_2 + i\theta_5 \\ -\theta_1 + i\theta_4 & 1 & \theta_3 + i\theta_6 \\ \theta_2 + i\theta_5 & -\theta_3 + i\theta_6 & 1 \end{pmatrix}, \quad \text{or}
$$

$$
\vec{\varphi}_1 \approx \begin{pmatrix} 1 \\ \theta_1 + i\theta_4 \\ -\theta_2 + i\theta_5 \end{pmatrix}, \qquad
\vec{\varphi}_2 \approx \begin{pmatrix} -\theta_1 + i\theta_4 \\ 1 \\ \theta_3 + i\theta_6 \end{pmatrix}, \qquad
\vec{\varphi}_3 \approx \begin{pmatrix} \theta_2 + i\theta_5 \\ -\theta_3 + i\theta_6 \\ 1 \end{pmatrix}.
\tag{4.12}
$$

After this linearisation, the action $S[U]$ in Eq. (4.11) finally simplies into the linearised action $S_0[\theta]$:

$$
S_0[\theta] = \int dx'dy'd\tau\,\mathscr{L} = \int dx'dy'd\tau \sum_{k=1}^{6}\left(\chi|\partial_\tau\theta_k|^2 + \rho_1|\partial_1\theta_k|^2 + \rho_2|\partial_2\theta_k|^2\right)
\tag{4.13}
$$

with

$$
\chi := \frac{1}{2(J_1+J_3)}, \qquad \rho_1 := 9a^2p^2\left(-\frac{J_3}{J_1+J_3}+J_3\right), \qquad \rho_2 := a^2p^2(J_1+4J_3).
\tag{4.14}
$$

158

E The quantum Liouville equations

5.1 The antiferromagnetic $SU(2)$ model

We start with the Hamiltonian

$$\mathcal{H} = J \sum_{\langle i,j \rangle} \mathbf{S}_i \cdot \mathbf{S}_j = J \sum_i {}' \sum_{\langle j \rangle} \mathbf{S}_i \cdot \mathbf{S}_j, \tag{5.1}$$

where the reduced sum $\sum_{\langle i \rangle} {}'$ indicates that the sum is taken over one sublattice only, and $\langle j \rangle$ indicates the sum over the nearest neighbors of i.

Let us denote the two sublattices by Λ_i and Λ_j. From hereon, the sites that belong to Λ_i will be denoted by i, and the sites belonging to Λ_j will be denoted by j. What we are interested in is the equation of motion of the operator $\mathbf{S}_i$ where $i \in \Lambda_i$. To this end, we will use the commutation relation of the spin operators,

$$\left[S_l^\alpha, S_l^\beta \right] = i\epsilon_{\alpha\beta\gamma} S^\gamma \quad \Leftrightarrow \quad \mathbf{S}_l \times \mathbf{S}_l = i\hbar\mathbf{S}, \tag{5.2}$$

where $\alpha, \beta, \gamma \in \{x, y, z\}$ and $l \in \{i, j\}$.

We are now ready to calculate the equation of motion of $\mathbf{S}_i$. According to the quantum Liouville's theorem, we derive

$$\begin{aligned}
\frac{d\mathbf{S}_i}{dt} &= \frac{i}{\hbar} [\mathcal{H}, \mathbf{S}_i] \\
&= i \begin{pmatrix} [\mathcal{H}, S_i^x] \\ [\mathcal{H}, S_i^y] \\ [\mathcal{H}, S_i^z] \end{pmatrix} = \frac{iJ}{\hbar} \sum_{\langle j \rangle} \begin{pmatrix} [S_i^y, S_i^x] S_j^y + [S_i^z, S_i^x] S_j^z \\ [S_i^x, S_i^y] S_j^x + [S_i^z, S_i^y] S_j^z \\ [S_i^x, S_i^z] S_j^x + [S_i^y, S_i^z] S_j^y \end{pmatrix} = -J \sum_{\langle j \rangle} \begin{pmatrix} -S_i^z S_j^y + S_i^y S_j^z \\ S_i^z S_j^x - S_i^x S_j^z \\ -S_i^y S_j^x + S_i^x S_j^y \end{pmatrix} \\
&= J \sum_{\langle j \rangle} \mathbf{S}_j \times \mathbf{S}_i.
\end{aligned} \tag{5.3}$$

159

Appendix E. The quantum Liouville equations

Similarly, for $j \in \Lambda_j$, we obtain

$$\frac{d\mathbf{S}_j}{dt} = i\left[\mathcal{H}, \mathbf{S}_j\right] = J\sum_{\langle i \rangle}\mathbf{S}_i \times \mathbf{S}_j, \tag{5.4}$$

leading us finally to a set of equations

$$\begin{cases} \frac{d\mathbf{S}_i}{dt} & = J\sum_{\langle j \rangle}\mathbf{S}_j \times \mathbf{S}_i, \\ \frac{d\mathbf{S}_j}{dt} & = J\sum_{\langle i \rangle}\mathbf{S}_i \times \mathbf{S}_j. \end{cases} \tag{5.5}$$

We will work in natural units from hereon so that $\hbar = 1$.

Let us assume that the spins are classical in the three-dimensional space, aligned along the z-axis ($\mathbf{S} = S\mathbf{e_z}$). With the further assumption that the fluctuations are small, we can write

$$\mathbf{S}_i(t) = \mathbf{S} + \delta\mathbf{S}_i(t), \qquad \mathbf{S}_j(t) = -\mathbf{S} + \delta\mathbf{S}_j(t). \tag{5.6}$$

The equations of motion (5.5) then become

$$\begin{cases} \delta\dot{\mathbf{S}}_i = & J\sum_{\langle j \rangle}\left[(-\mathbf{S} \times \delta\mathbf{S}_i) + (\delta\mathbf{S}_j \times \mathbf{S})\right] \\ \delta\dot{\mathbf{S}}_j = & J\sum_{\langle i \rangle}\left[(\mathbf{S} \times \delta\mathbf{S}_j) + (\delta\mathbf{S}_i \times -\mathbf{S})\right] \end{cases} \tag{5.7}$$

up to order $\mathcal{O}(\delta S^2)$. The time dependence has been omitted to simplify the notation. We now perform the Fourier transform

$$\delta\mathbf{S}_{i,\mathbf{k}} = \sqrt{\frac{2}{N}}\sum_{i\in\Lambda_i}{}' \delta\mathbf{S}_i e^{-i\mathbf{k}\cdot\mathbf{R}_i}, \qquad \delta\mathbf{S}_{j,\mathbf{k}} = \sqrt{\frac{2}{N}}\sum_{j\in\Lambda_j}{}' \delta\mathbf{S}_j e^{-i\mathbf{k}\cdot\mathbf{R}_j}, \tag{5.8}$$

to obtain

$$\begin{cases} d\dot{\mathbf{S}}_{i,\mathbf{k}} & = zJ\left[(-\mathbf{S} \times \delta\mathbf{S}_{i,\mathbf{k}}) + \gamma_\mathbf{k}(\delta\mathbf{S}_{j,\mathbf{k}} \times \mathbf{S})\right] \\ d\dot{\mathbf{S}}_{j,\mathbf{k}} & = zJ\left[(\mathbf{S} \times \delta\mathbf{S}_{j,\mathbf{k}}) + \gamma_\mathbf{k}(\delta\mathbf{S}_{i,\mathbf{k}} \times -\mathbf{S})\right] \end{cases} \Leftrightarrow \begin{cases} d\dot{S}^x_{i,\mathbf{k}} & = zJS\left(\delta S^y_{i,\mathbf{k}} + \gamma_\mathbf{k}\delta S^y_{j,\mathbf{k}}\right) \\ d\dot{S}^y_{i,\mathbf{k}} & = -zJS\left(\delta S^x_{i,\mathbf{k}} + \gamma_\mathbf{k}\delta S^x_{j,\mathbf{k}}\right) \\ d\dot{S}^z_{i,\mathbf{k}} & = 0 \\ d\dot{S}^x_{j,\mathbf{k}} & = -zJS\left(\delta S^y_{j,\mathbf{k}} + \gamma_\mathbf{k}\delta S^y_{i,\mathbf{k}}\right) \\ d\dot{S}^y_{j,\mathbf{k}} & = zJS\left(\delta S^x_{j,\mathbf{k}} + \gamma_\mathbf{k}\delta S^x_{i,\mathbf{k}}\right) \\ d\dot{S}^z_{j,\mathbf{k}} & = 0 \end{cases} \tag{5.9}$$

where $z = 4$ is the coordination number and $\gamma_\mathbf{k} = \frac{1}{2}\left(\cos k_x + \cos k_y\right)$ is the geometrical factor.

Let us now reexpress the spin operators $\mathbf{S}^\alpha$ in the spherical basis (i.e., in terms of ladder

operators) $S^\pm$, as we will work in the ladder-operator basis for the SU(3) case. By defining

$$\delta S^\pm_{l,\mathbf{k}} = \delta S^x_{l,\mathbf{k}} \pm i \delta S^y_{l,\mathbf{k}}, \tag{5.10}$$

the equations (5.9) become

$$\begin{cases} d\dot{S}^\pm_{i,\mathbf{k}} &= \mp i z J S \left(\delta S^\pm_{i,\mathbf{k}} + \gamma_{\mathbf{k}} \delta S^\pm_{j,\mathbf{k}} \right) \\ d\dot{S}^z_{i,\mathbf{k}} &= 0 \\ d\dot{S}^\pm_{j,\mathbf{k}} &= \pm i z J S \left(\delta S^\pm_{j,\mathbf{k}} + \gamma_{\mathbf{k}} \delta S^\pm_{i,\mathbf{k}} \right) \\ d\dot{S}^z_{j,\mathbf{k}} &= 0. \end{cases} \tag{5.11}$$

We can ignore the trivial equations, thus being left with four equations to solve:

$$\begin{cases} d\dot{S}^\pm_{i,\mathbf{k}} &= \mp i z J S \left(\delta S^\pm_{i,\mathbf{k}} + \gamma_{\mathbf{k}} \delta S^\pm_{j,\mathbf{k}} \right) \\ d\dot{S}^\pm_{j,\mathbf{k}} &= \pm i z J S \left(\delta S^\pm_{j,\mathbf{k}} + \gamma_{\mathbf{k}} \delta S^\pm_{i,\mathbf{k}} \right). \end{cases} \tag{5.12}$$

The equations can now be solved in time. We observe that $\delta S^+_{i,\mathbf{k}}$ is coupled to $\delta S^+_{j,\mathbf{k}}$ and that $\delta S^-_{i,\mathbf{k}}$ is coupled to $\delta S^-_{i,\mathbf{k}}$. This allows us to make the ansatz

$$\delta S^\pm_{l,\mathbf{k}}(t) \propto \delta S^\pm_{l,\mathbf{k}} e^{i\omega^\pm_{\mathbf{k}} t}, \tag{5.13}$$

i.e., there is one frequency $\omega^+_{\mathbf{k}}$ for $\delta S^+_{i,\mathbf{k}}$ and $\delta S^+_{j,\mathbf{k}}$. The same applies to their negative counterparts. The equations (5.12) are then given by

$$\begin{cases} i\omega^\pm_{\mathbf{k}} d\dot{S}^\pm_{i,\mathbf{k}} e^{i\omega^\pm_{\mathbf{k}} t} &= \mp i z J S \left(\delta S^\pm_{i,\mathbf{k}} + \gamma_{\mathbf{k}} \delta S^\pm_{j,\mathbf{k}} \right) e^{i\omega^\pm_{\mathbf{k}} t} \\ i\omega^\pm_{\mathbf{k}} d\dot{S}^\pm_{j,\mathbf{k}} e^{i\omega^\pm_{\mathbf{k}} t} &= \pm i z J S \left(\delta S^\pm_{j,\mathbf{k}} + \gamma_{\mathbf{k}} \delta S^\pm_{i,\mathbf{k}} \right) e^{i\omega^\pm_{\mathbf{k}} t} \end{cases} \tag{5.14}$$

$$\Leftrightarrow \quad \omega^\pm_{\mathbf{k}} \begin{pmatrix} S^\pm_{i,\mathbf{k}} \\ S^\pm_{j,\mathbf{k}} \end{pmatrix} = \mp \begin{pmatrix} zJS & zJS\gamma_{\mathbf{k}} \\ -zJS\gamma_{\mathbf{k}} & -zJS\gamma \end{pmatrix} \begin{pmatrix} S^\pm_{i,\mathbf{k}} \\ S^\pm_{j,\mathbf{k}} \end{pmatrix} = 0$$

$$\Leftrightarrow \quad \left[\mp \begin{pmatrix} zJS & zJS\gamma_{\mathbf{k}} \\ -zJS\gamma_{\mathbf{k}} & -zJS\gamma \end{pmatrix} - \omega^\pm_{\mathbf{k}} \mathbb{1} \right] \begin{pmatrix} S^\pm_{i,\mathbf{k}} \\ S^\pm_{j,\mathbf{k}} \end{pmatrix} = 0.$$

The determinant of the matrix on the LHS finally yields the solutions:

$$\Rightarrow \quad \omega^{\pm 2}_{\mathbf{k}} - (zJS)^2 (1 - \gamma^2_k) = 0$$

$$\Rightarrow \quad \omega^\pm_{\mathbf{k}} = zJS\sqrt{1 - \gamma^2_{\mathbf{k}}}.$$

Hence, we obtain two spectra that are identical to that of the spin-wave theory with Holstein-

Primakoff transformation:

$$\boxed{\begin{aligned} \omega_{\mathbf{k}}^+ &= zJS\sqrt{1-\gamma_{\mathbf{k}}^2} \\ \omega_{\mathbf{k}}^- &= zJS\sqrt{1-\gamma_{\mathbf{k}}^2} \end{aligned}} \tag{5.15}$$

5.2   The inhomogeneous solutions of the AFM $SU(3)$ model

We first consider the inhomogeneous part of the equations in subsection 6.3.2. We want them to be equal to zero in order to be able to solve the homogeneous part. Let us consider the first subset of (6.63) only as the other subsets have similar structures:

$$\begin{cases} \pm\left(C_{i,\mathbf{p}}^{12} + \gamma_{\mathbf{p}}C_{j,\mathbf{p}}^{12} + \gamma_{\mathbf{p}}^*\,\delta S_{k,\mathbf{p}}^{12}\right) = 0 \\ \mp\left(C_{j,\mathbf{p}}^{12} + \gamma_{\mathbf{p}}C_{i,\mathbf{p}}^{12} + \gamma_{\mathbf{p}}\,\delta S_{k,\mathbf{p}}^{12}\right) = 0 \end{cases} \Leftrightarrow \pm\begin{pmatrix} 1 & \gamma_{\mathbf{p}} \\ -\gamma_{\mathbf{p}} & -1 \end{pmatrix}\begin{pmatrix} C_{i,\mathbf{p}}^{12} \\ C_{j,\mathbf{p}}^{12} \end{pmatrix} = \begin{pmatrix} -\gamma_{\mathbf{p}}^* \\ +\gamma_{\mathbf{p}} \end{pmatrix}\delta S_{k,\mathbf{p}}^{12} \tag{5.16}$$

$$\Rightarrow \begin{pmatrix} C_{i,\mathbf{p}}^{12} \\ C_{j,\mathbf{p}}^{12} \end{pmatrix} = \pm\begin{pmatrix} 1 & \gamma_{\mathbf{p}} \\ -\gamma_{\mathbf{p}} & -1 \end{pmatrix}^{-1}\begin{pmatrix} -\gamma_{\mathbf{p}}^* \\ +\gamma_{\mathbf{p}} \end{pmatrix}\delta S_{k,\mathbf{p}}^{12}$$

$$\Rightarrow \begin{pmatrix} C_{i,\mathbf{p}}^{12} \\ C_{j,\mathbf{p}}^{12} \end{pmatrix} = \pm\frac{1}{1-\gamma_p^2}\begin{pmatrix} 1 & \gamma_{\mathbf{p}} \\ -\gamma_{\mathbf{p}} & -1 \end{pmatrix}\begin{pmatrix} -\gamma_{\mathbf{p}}^* \\ +\gamma_{\mathbf{p}} \end{pmatrix}\delta S_{k,\mathbf{p}}^{12}$$

$$\Rightarrow \boxed{\begin{cases} C_{i,\mathbf{p}}^{12\,\pm} = \pm\delta S_{k,\mathbf{p}}^{12} \pm \frac{1}{1-\gamma_{\mathbf{p}}^2}\left(\gamma_{\mathbf{p}}^2 - \gamma_{\mathbf{p}}^*\right) \\ C_{j,\mathbf{p}}^{12\,\pm} = \pm\delta S_{k,\mathbf{p}}^{12} \pm \frac{1}{1-\gamma_{\mathbf{p}}^2}\left(|\gamma_{\mathbf{p}}|^2 - \gamma_{\mathbf{p}}\right) \end{cases}} \tag{5.17}$$

Similarly, the remaining constants from the other subsets

$$\boxed{\begin{cases} \begin{cases} C_{i,\mathbf{p}}^{13\,\pm} = \pm\delta S_{j,\mathbf{p}}^{13} \pm \frac{1}{1-\gamma_{\mathbf{p}}^2}\left(|\gamma_{\mathbf{p}}|^2 - \gamma_{\mathbf{p}}\right) \\ C_{k,\mathbf{p}}^{13\,\pm} = \pm\delta S_{j,\mathbf{p}}^{13} \pm \frac{1}{1-\gamma_{\mathbf{p}}^2}\left(\gamma_{\mathbf{p}}^2 - \gamma_{\mathbf{p}}^*\right) \end{cases} \\ \begin{cases} C_{j,\mathbf{p}}^{23\,\pm} = \pm\delta S_{i,\mathbf{p}}^{23} \pm \frac{1}{1-\gamma_{\mathbf{p}}^2}\left(\gamma_{\mathbf{p}}^2 - \gamma_{\mathbf{p}}^*\right) \\ C_{k,\mathbf{p}}^{23\,\pm} = \pm\delta S_{i,\mathbf{p}}^{23} \pm \frac{1}{1-\gamma_{\mathbf{p}}^2}\left(|\gamma_{\mathbf{p}}|^2 - \gamma_{\mathbf{p}}\right) \end{cases} \end{cases}} \tag{5.18}$$

can be obtained. These (time-)constants are, however, not of interest for us.

If we consider the equations up to order $\mathcal{O}(\delta S^2)$ as we did here, we could in fact physically argue that the (time-)constants

$$\delta S_{3,i}^2(\mathbf{p}) = \delta S_{2,i}^3(\mathbf{p}) = \delta S_{1,j}^3(\mathbf{p}) = \delta S_{3,j}^1(\mathbf{p}) = \delta S_{2,k}^1(\mathbf{p}) = \delta S_{1,k}^2(\mathbf{p}) = 0$$

can be set to zero, as they are second-order colour transitions. This is something that we

had also observed in the LFWT: in the harmonic order, only the colours of the condensate are involved. This assumption would yield homogeneous equations as in the SU(2) case which are easier to solve (and lead to the same homogeneous solutions for SU(3) obtained in subsection 6.3.2). However, our treatment of these constants here is, of course, more general.

Bibliography

[1] P. W. Anderson. More Is Different. *Science*, 177(4047):393–396, 1972. ISSN 0036-8075. URL https://www.jstor.org/stable/1734697.

[2] Bill Sutherland. Model for a multicomponent quantum system. *Physical Review B*, 12 (9):3795–3805, November 1975. doi:10.1103/PhysRevB.12.3795. URL http://link.aps.org/doi/10.1103/PhysRevB.12.3795.

[3] Ian Affleck. Exact critical exponents for quantum spin chains, non-linear σ-models at $\theta=\pi$ and the quantum hall effect. *Nuclear Physics B*, 265(3):409–447, March 1986. ISSN 0550-3213. doi:10.1016/0550-3213(86)90167-7. URL http://www.sciencedirect.com/science/article/pii/0550321386901677.

[4] Ian Affleck. Critical behaviour of SU(n) quantum chains and topological non-linear σ-models. *Nuclear Physics B*, 305(4):582–596, December 1988. ISSN 0550-3213. doi:10.1016/0550-3213(88)90117-4. URL http://www.sciencedirect.com/science/article/pii/0550321388901174.

[5] Ian Affleck and J. Brad Marston. Large-n limit of the Heisenberg-Hubbard model: Implications for high-T_c superconductors. *Physical Review B*, 37(7):3774–3777, March 1988. doi:10.1103/PhysRevB.37.3774. URL https://link.aps.org/doi/10.1103/PhysRevB.37.3774.

[6] J. Brad Marston and Ian Affleck. Large-n limit of the Hubbard-Heisenberg model. *Physical Review B*, 39(16):11538–11558, June 1989. doi:10.1103/PhysRevB.39.11538. URL https://link.aps.org/doi/10.1103/PhysRevB.39.11538.

[7] N. Read and Subir Sachdev. Valence-bond and spin-Peierls ground states of low-dimensional quantum antiferromagnets. *Physical Review Letters*, 62(14):1694–1697, April 1989. doi:10.1103/PhysRevLett.62.1694. URL https://link.aps.org/doi/10.1103/PhysRevLett.62.1694.

[8] N. Read and Subir Sachdev. Some features of the phase diagram of the square lattice SU(N) antiferromagnet. *Nuclear Physics B*, 316(3):609–640, April 1989. ISSN 0550-3213. doi:10.1016/0550-3213(89)90061-8. URL http://www.sciencedirect.com/science/article/pii/0550321389900618.

Bibliography

[9] N. Read and Subir Sachdev. Spin-Peierls, valence-bond solid, and Néel ground states of low-dimensional quantum antiferromagnets. *Physical Review B*, 42(7):4568–4589, September 1990. doi:10.1103/PhysRevB.42.4568. URL https://link.aps.org/doi/10.1103/PhysRevB.42.4568.

[10] N. Read and Subir Sachdev. Large-N expansion for frustrated quantum antiferromagnets. *Physical Review Letters*, 66(13):1773–1776, April 1991. doi:10.1103/PhysRevLett.66.1773. URL http://link.aps.org/doi/10.1103/PhysRevLett.66.1773.

[11] Ian Affleck, D. P. Arovas, J. B. Marston, and D. A. Rabson. SU(2n) quantum antiferromagnets with exact C-breaking ground states. *Nuclear Physics B*, 366(3):467–506, December 1991. ISSN 0550-3213. doi:10.1016/0550-3213(91)90027-U. URL http://www.sciencedirect.com/science/article/pii/055032139190027U.

[12] Miklós Lajkó, Kyle Wamer, Frédéric Mila, and Ian Affleck. Generalization of the Haldane conjecture to SU(3) chains. *Nuclear Physics B*, 924:508–577, November 2017. ISSN 0550-3213. doi:10.1016/j.nuclphysb.2017.09.015. URL http://www.sciencedirect.com/science/article/pii/S0550321317303097.

[13] Pierre Nataf and Frédéric Mila. Exact Diagonalization of Heisenberg SU(N) Models. *Physical Review Letters*, 113(12):127204, September 2014. doi:10.1103/PhysRevLett.113.127204. URL https://link.aps.org/doi/10.1103/PhysRevLett.113.127204.

[14] Pierre Nataf and Frédéric Mila. Exact diagonalization of Heisenberg SU(N) chains in the fully symmetric and antisymmetric representations. *Physical Review B*, 93(15), April 2016. ISSN 2469-9950, 2469-9969. doi:10.1103/PhysRevB.93.155134. URL http://link.aps.org/doi/10.1103/PhysRevB.93.155134.

[15] Beat Frischmuth, Frédéric Mila, and Matthias Troyer. Thermodynamics of the One-Dimensional SU(4) Symmetric Spin-Orbital Model. *Physical Review Letters*, 82(4):835–838, January 1999. doi:10.1103/PhysRevLett.82.835. URL http://link.aps.org/doi/10.1103/PhysRevLett.82.835.

[16] F. F. Assaad. Phase diagram of the half-filled two-dimensional SU(N) Hubbard-Heisenberg model: A quantum Monte Carlo study. *Physical Review B*, 71(7):075103, February 2005. doi:10.1103/PhysRevB.71.075103. URL https://link.aps.org/doi/10.1103/PhysRevB.71.075103.

[17] K. S. D. Beach, Fabien Alet, Matthieu Mambrini, and Sylvain Capponi. SU(N) Heisenberg model on the square lattice: A continuous-N quantum Monte Carlo study. *Physical Review B*, 80(18):184401, November 2009. doi:10.1103/PhysRevB.80.184401. URL http://link.aps.org/doi/10.1103/PhysRevB.80.184401.

[18] Laura Messio and Frédéric Mila. Entropy Dependence of Correlations in One-Dimensional SU(N) Antiferromagnets. *Physical Review Letters*, 109(20):205306, November 2012. doi:10.1103/PhysRevLett.109.205306. URL http://link.aps.org/doi/10.1103/PhysRevLett.109.205306.

166

[19] Lars Bonnes, Kaden R. A. Hazzard, Salvatore R. Manmana, Ana Maria Rey, and Stefan Wessel. Adiabatic Loading of One-Dimensional SU(N) Alkaline-Earth-Atom Fermions in Optical Lattices. *Physical Review Letters*, 109(20):205305, November 2012. doi:10.1103/PhysRevLett.109.205305. URL http://link.aps.org/doi/10.1103/PhysRevLett.109.205305.

[20] Zi Cai, Hsiang-Hsuan Hung, Lei Wang, and Congjun Wu. Quantum magnetic properties of the SU(2N) Hubbard model in the square lattice: A quantum Monte Carlo study. *Physical Review B*, 88(12):125108, September 2013. doi:10.1103/PhysRevB.88.125108. URL http://link.aps.org/doi/10.1103/PhysRevB.88.125108.

[21] Thomas C. Lang, Zi Yang Meng, Alejandro Muramatsu, Stefan Wessel, and Fakher F. Assaad. Dimerized Solids and Resonating Plaquette Order in SU(N)-Dirac Fermions. *Physical Review Letters*, 111(6):066401, August 2013. doi:10.1103/PhysRevLett.111.066401. URL https://link.aps.org/doi/10.1103/PhysRevLett.111.066401.

[22] Da Wang, Yi Li, Zi Cai, Zhichao Zhou, Yu Wang, and Congjun Wu. Competing Orders in the 2d Half-Filled SU(2N) Hubbard Model through the Pinning-Field Quantum Monte Carlo Simulations. *Physical Review Letters*, 112(15):156403, April 2014. doi:10.1103/PhysRevLett.112.156403. URL http://link.aps.org/doi/10.1103/PhysRevLett.112.156403.

[23] Arun Paramekanti and J. B. Marston. SU(N) quantum spin models: a variational wavefunction study. *Journal of Physics: Condensed Matter*, 19(12):125215, 2007. ISSN 0953-8984. doi:10.1088/0953-8984/19/12/125215. URL http://stacks.iop.org/0953-8984/19/i=12/a=125215.

[24] Fa Wang and Ashvin Vishwanath. Z_2 spin-orbital liquid state in the square lattice Kugel-Khomskii model. *Physical Review B*, 80(6):064413, August 2009. doi:10.1103/PhysRevB.80.064413. URL https://link.aps.org/doi/10.1103/PhysRevB.80.064413.

[25] Miklós Lajkó and Karlo Penc. Tetramerization in a SU(4) Heisenberg model on the honeycomb lattice. *Physical Review B*, 87(22):224428, June 2013. doi:10.1103/PhysRevB.87.224428. URL https://link.aps.org/doi/10.1103/PhysRevB.87.224428.

[26] Jérôme Dufour, Pierre Nataf, and Frédéric Mila. Variational Monte Carlo investigation of SU(N) Heisenberg chains. *Physical Review B*, 91(17), May 2015. ISSN 1098-0121, 1550-235X. doi:10.1103/PhysRevB.91.174427. URL http://link.aps.org/doi/10.1103/PhysRevB.91.174427.

[27] Jérôme Dufour and Frédéric Mila. Stabilization of the chiral phase of the SU(6m) Heisenberg model on the honeycomb lattice with m particles per site for m larger than 1. *Physical Review A*, 94(3):033617, September 2016. doi:10.1103/PhysRevA.94.033617. URL http://link.aps.org/doi/10.1103/PhysRevA.94.033617.

Bibliography

[28] Philippe Corboz, Andreas M. Läuchli, Karlo Penc, Matthias Troyer, and Frédéric Mila. Simultaneous Dimerization and SU(4) Symmetry Breaking of 4-Color Fermions on the Square Lattice. *Physical Review Letters*, 107(21), November 2011. ISSN 0031-9007, 1079-7114. doi:10.1103/PhysRevLett.107.215301. URL http://link.aps.org/doi/10.1103/PhysRevLett.107.215301.

[29] Philippe Corboz, Miklós Lajkó, Andreas M. Läuchli, Karlo Penc, and Frédéric Mila. Spin-Orbital Quantum Liquid on the Honeycomb Lattice. *Physical Review X*, 2(4), November 2012. ISSN 2160-3308. doi:10.1103/PhysRevX.2.041013. URL http://link.aps.org/doi/10.1103/PhysRevX.2.041013.

[30] Philippe Corboz, Karlo Penc, Frédéric Mila, and Andreas M. Läuchli. Simplex solids in SU(N) Heisenberg models on the kagome and checkerboard lattices. *Physical Review B*, 86(4):041106, July 2012. doi:10.1103/PhysRevB.86.041106. URL https://link.aps.org/doi/10.1103/PhysRevB.86.041106.

[31] Bela Bauer, Philippe Corboz, Andreas M. Läuchli, Laura Messio, Karlo Penc, Matthias Troyer, and Frédéric Mila. Three-sublattice order in the SU(3) Heisenberg model on the square and triangular lattice. *Physical Review B*, 85(12), March 2012. ISSN 1098-0121, 1550-235X. doi:10.1103/PhysRevB.85.125116. URL http://link.aps.org/doi/10.1103/PhysRevB.85.125116.

[32] Pierre Nataf and Frédéric Mila. Density matrix renormalization group simulations of SU(N) Heisenberg chains using standard Young tableaus: Fundamental representation and comparison with a finite-size Bethe ansatz. *Physical Review B*, 97(13):134420, April 2018. doi:10.1103/PhysRevB.97.134420. URL https://link.aps.org/doi/10.1103/PhysRevB.97.134420.

[33] D. Jaksch and P. Zoller. The cold atom Hubbard toolbox. *Annals of Physics*, 315(1):52–79, January 2005. ISSN 0003-4916. doi:10.1016/j.aop.2004.09.010. URL http://www.sciencedirect.com/science/article/pii/S0003491604001782.

[34] M. A. Cazalilla, A. F. Ho, and M. Ueda. Ultracold gases of ytterbium: ferromagnetism and Mott states in an SU(6) Fermi system. *New Journal of Physics*, 11(10):103033, 2009. ISSN 1367-2630. doi:10.1088/1367-2630/11/10/103033. URL http://stacks.iop.org/1367-2630/11/i=10/a=103033.

[35] A. V. Gorshkov, M. Hermele, V. Gurarie, C. Xu, P. S. Julienne, J. Ye, P. Zoller, E. Demler, M. D. Lukin, and A. M. Rey. Two-orbital SU(N) magnetism with ultracold alkaline-earth atoms. *Nature Physics*, 6(4):289–295, April 2010. ISSN 1745-2473, 1745-2481. doi:10.1038/nphys1535. URL http://www.nature.com/doifinder/10.1038/nphys1535.

[36] Shintaro Taie, Rekishu Yamazaki, Seiji Sugawa, and Yoshiro Takahashi. An SU(6) Mott insulator of an atomic Fermi gas realized by large-spin Pomeranchuk cooling. *Nature Physics*, 8(11):825–830, November 2012. ISSN 1745-2481. doi:10.1038/nphys2430. URL https://www.nature.com/articles/nphys2430.

[37] F. Scazza, C. Hofrichter, M. Höfer, P. C. De Groot, I. Bloch, and S. Fölling. Observation of two-orbital spin-exchange interactions with ultracold SU(N)-symmetric fermions. *Nature Physics*, 10(10):779–784, October 2014. ISSN 1745-2481. doi:10.1038/nphys3061. URL https://www.nature.com/articles/nphys3061.

[38] X. Zhang, M. Bishof, S. L. Bromley, C. V. Kraus, M. S. Safronova, P. Zoller, A. M. Rey, and J. Ye. Spectroscopic observation of SU(N)-symmetric interactions in Sr orbital magnetism. *Science*, 345(6203):1467–1473, September 2014. ISSN 0036-8075, 1095-9203. doi:10.1126/science.1254978. URL https://science.sciencemag.org/content/345/6203/1467.

[39] Miguel A. Cazalilla and Ana Maria Rey. Ultracold Fermi gases with emergent SU(N) symmetry. *Reports on Progress in Physics*, 77(12):124401, November 2014. ISSN 0034-4885. doi:10.1088/0034-4885/77/12/124401. URL https://doi.org/10.1088%2F0034-4885%2F77%2F12%2F124401.

[40] Guido Pagano, Marco Mancini, Giacomo Cappellini, Pietro Lombardi, Florian Schäfer, Hui Hu, Xia-Ji Liu, Jacopo Catani, Carlo Sias, Massimo Inguscio, and Leonardo Fallani. A one-dimensional liquid of fermions with tunable spin. *Nature Physics*, 10(3):198–201, March 2014. ISSN 1745-2481. doi:10.1038/nphys2878. URL https://www.nature.com/articles/nphys2878.

[41] Christian Hofrichter, Luis Riegger, Francesco Scazza, Moritz Höfer, Diogo Rio Fernandes, Immanuel Bloch, and Simon Fölling. Direct Probing of the Mott Crossover in the SU(N) Fermi-Hubbard Model. *Physical Review X*, 6(2):021030, June 2016. doi:10.1103/PhysRevX.6.021030. URL https://link.aps.org/doi/10.1103/PhysRevX.6.021030.

[42] S. Capponi, P. Lecheminant, and K. Totsuka. Phases of one-dimensional SU(N) cold atomic Fermi gases—From molecular Luttinger liquids to topological phases. *Annals of Physics*, 367:50–95, April 2016. ISSN 0003-4916. doi:10.1016/j.aop.2016.01.011. URL http://www.sciencedirect.com/science/article/pii/S0003491616000130.

[43] C. Kittel. *Introduction to Solid State Physics*. Wiley series on the science and technology of materials. Wiley, 1953. URL https://books.google.ch/books?id=Ag5RAAAAMAAJ.

[44] A. Auerbach. *Interacting Electrons and Quantum Magnetism*. Graduate Texts in Contemporary Physics. Springer New York, 2012. ISBN 9781461208693. URL https://books.google.ch/books?id=d-sHCAAAQBAJ.

[45] P. W. Anderson. An Approximate Quantum Theory of the Antiferromagnetic Ground State. *Physical Review*, 86(5):694–701, June 1952. doi:10.1103/PhysRev.86.694. URL https://link.aps.org/doi/10.1103/PhysRev.86.694.

[46] Ryogo Kubo. The Spin-Wave Theory of Antiferromagnetics. *Physical Review*, 87(4):568–580, August 1952. doi:10.1103/PhysRev.87.568. URL https://link.aps.org/doi/10.1103/PhysRev.87.568.

Bibliography

[47] Efstratios Manousakis. The spin-1/2 Heisenberg antiferromagnet on a square lattice and its application to the cuprous oxides. *Reviews of Modern Physics*, 63(1):1, 1991. URL http://journals.aps.org/rmp/abstract/10.1103/RevModPhys.63.1.

[48] M. Louis Néel. Propriétés magnétiques des ferrites ; ferrimagnétisme et antiferro-magnétisme. *Annales de Physique*, 12(3):137–198, 1948. ISSN 0003-4169, 1286-4838. doi:10.1051/anphys/194812030137. URL https://www.annphys.org/articles/anphys/abs/1948/03/anphys19481203p137/anphys19481203p137.html.

[49] N. Papanicolaou. Pseudospin approach for planar ferromagnets. *Nuclear Physics B*, 240 (3):281–311, October 1984. ISSN 0550-3213. doi:10.1016/0550-3213(84)90268-2. URL http://www.sciencedirect.com/science/article/pii/0550321384902682.

[50] N. Papanicolaou. Unusual phases in quantum spin-1 systems. *Nuclear Physics B*, 305 (3):367–395, November 1988. ISSN 0550-3213. doi:10.1016/0550-3213(88)90073-9. URL http://www.sciencedirect.com/science/article/pii/0550321388900739.

[51] A. V. Chubukov. Fluctuations in spin nematics. *Journal of Physics: Condensed Matter*, 2 (6):1593, 1990. ISSN 0953-8984. doi:10.1088/0953-8984/2/6/018. URL http://stacks.iop.org/0953-8984/2/i=6/a=018.

[52] A. Joshi, M. Ma, F. Mila, D. N. Shi, and F. C. Zhang. Elementary excitations in magnetically ordered systems with orbital degeneracy. *Physical Review B*, 60(9):6584–6587, September 1999. doi:10.1103/PhysRevB.60.6584. URL https://link.aps.org/doi/10.1103/PhysRevB.60.6584.

[53] Tamás A. Tóth, Andreas M. Läuchli, Frédéric Mila, and Karlo Penc. Three-Sublattice Ordering of the SU(3) Heisenberg Model of Three-Flavor Fermions on the Square and Cubic Lattices. *Physical Review Letters*, 105(26), December 2010. ISSN 0031-9007, 1079-7114. doi:10.1103/PhysRevLett.105.265301. URL http://link.aps.org/doi/10.1103/PhysRevLett.105.265301.

[54] N. D. Mermin and H. Wagner. Absence of Ferromagnetism or Antiferromagnetism in One- or Two-Dimensional Isotropic Heisenberg Models. *Physical Review Letters*, 17(22): 1133–1136, November 1966. doi:10.1103/PhysRevLett.17.1133. URL https://link.aps.org/doi/10.1103/PhysRevLett.17.1133.

[55] Sidney Coleman. There are no Goldstone bosons in two dimensions. *Communications in Mathematical Physics*, 31(4):259–264, December 1973. ISSN 1432-0916. doi:10.1007/BF01646487. URL https://doi.org/10.1007/BF01646487.

[56] Alfred Young. On quantitative substitutional analysis. *Proceedings of the London Mathematical Society*, 2(1):304–368, 1934.

[57] Murray Gell-Mann. M. gell-mann, phys. rev. 125, 1067 (1962). *Phys. Rev.*, 125:1067, 1962.

[58] M. Hamermesh. *Group Theory and Its Application to Physical Problems.* Elsevier Science & Technology, 1962. ISBN 9780080096261. URL https://books.google.ch/books?id=qPuAAQAACAAJ.

[59] H. Georgi. *Lie Algebras In Particle Physics: from Isospin To Unified Theories.* Frontiers in Physics. Avalon Publishing, 1999. ISBN 9780813346113. URL https://books.google.ch/books?id=dhY5DgAAQBAJ.

[60] W. Pfeifer. *The Lie Algebras su(N): An Introduction.* Birkhäuser Basel, 2003. ISBN 9783764324186. URL https://books.google.ch/books?id=xoHWEPENKNEC.

[61] Rok Žitko. Sneg – mathematica package for symbolic calculations with second-quantization-operator expressions. *Computer Physics Communications*, 182(10):2259 – 2264, 2011. ISSN 0010-4655. doi:https://doi.org/10.1016/j.cpc.2011.05.013. URL http://www.sciencedirect.com/science/article/pii/S0010465511001792.

[62] Francisco H. Kim, Karlo Penc, Pierre Nataf, and Frédéric Mila. Linear flavor-wave theory for fully antisymmetric SU(N) irreducible representations. *Physical Review B*, 96(20):205142, November 2017. doi:10.1103/PhysRevB.96.205142. URL https://link.aps.org/doi/10.1103/PhysRevB.96.205142.

[63] N. Papanicolaou. On the phase structure of spin-1 planar magnetic chains. *Zeitschrift für Physik B Condensed Matter*, 61(2):159–166, June 1985. ISSN 1431-584X. doi:10.1007/BF01307771. URL https://doi.org/10.1007/BF01307771.

[64] FP Onufrieva. Zh. é ksp. teor. fiz. 89, 2270 1985 sov. phys. *JETP*, 62:1311, 1985.

[65] Matsumoto Masashige, Kuroe Haruhiko, Sekine Tomoyuki, and Masuda Takatsugu. Transverse and Longitudinal Excitation Modes in Interacting Multispin Systems. *Journal of the Physical Society of Japan*, 79(8):084703, July 2010. ISSN 0031-9015. doi:10.1143/JPSJ.79.084703. URL http://journals.jps.jp/doi/10.1143/JPSJ.79.084703.

[66] Judit Romhányi and Karlo Penc. Multiboson spin-wave theory for $Ba_2CoGe_2O_7$: A spin-3/2 easy-plane Néel antiferromagnet with strong single-ion anisotropy. *Physical Review B*, 86(17):174428, November 2012. doi:10.1103/PhysRevB.86.174428. URL https://link.aps.org/doi/10.1103/PhysRevB.86.174428.

[67] K. Penc, J. Romhányi, T. Rõõm, U. Nagel, Á. Antal, T. Fehér, A. Jánossy, H. Engelkamp, H. Murakawa, Y. Tokura, D. Szaller, S. Bordács, and I. Kézsmárki. Spin-Stretching Modes in Anisotropic Magnets: Spin-Wave Excitations in the Multiferroic $Ba_2CoGe_2O_7$. *Physical Review Letters*, 108(25):257203, June 2012. doi:10.1103/PhysRevLett.108.257203. URL https://link.aps.org/doi/10.1103/PhysRevLett.108.257203.

[68] Michael Hermele, Victor Gurarie, and Ana Maria Rey. Mott Insulators of Ultracold Fermionic Alkaline Earth Atoms: Underconstrained Magnetism and Chiral Spin Liquid. *Physical Review Letters*, 103(13):135301, September 2009.

doi:10.1103/PhysRevLett.103.135301. URL https://link.aps.org/doi/10.1103/PhysRevLett.103.135301.

[69] Michael Hermele and Victor Gurarie. Topological liquids and valence cluster states in two-dimensional SU(N) magnets. *Physical Review B*, 84(17), November 2011. ISSN 1098-0121, 1550-235X. doi:10.1103/PhysRevB.84.174441. URL http://link.aps.org/doi/10.1103/PhysRevB.84.174441.

[70] Hirokazu Tsunetsugu and Mitsuhiro Arikawa. Spin Nematic Phase in S=1 Triangular Antiferromagnets. *Journal of the Physical Society of Japan*, 75(8):083701, July 2006. ISSN 0031-9015. doi:10.1143/JPSJ.75.083701. URL http://journals.jps.jp/doi/10.1143/JPSJ.75.083701.

[71] Andreas Läuchli, Frédéric Mila, and Karlo Penc. Quadrupolar Phases of the S=1 Bilinear-Biquadratic Heisenberg Model on the Triangular Lattice. *Physical Review Letters*, 97(8):087205, August 2006. doi:10.1103/PhysRevLett.97.087205. URL https://link.aps.org/doi/10.1103/PhysRevLett.97.087205.

[72] Cheng Luo, Trinanjan Datta, and Dao-Xin Yao. Spin and quadrupolar orders in the spin-1 bilinear-biquadratic model for iron-based superconductors. *Physical Review B*, 93(23):235148, June 2016. doi:10.1103/PhysRevB.93.235148. URL https://link.aps.org/doi/10.1103/PhysRevB.93.235148.

[73] A. V. Onufriev and J. B. Marston. Enlarged symmetry and coherence in arrays of quantum dots. *Physical Review B*, 59(19):12573–12578, May 1999. doi:10.1103/PhysRevB.59.12573. URL https://link.aps.org/doi/10.1103/PhysRevB.59.12573.

[74] Francisco H. Kim, Fakher F. Assaad, Karlo Penc, and Frédéric Mila. Dimensional crossover in the SU(4) Heisenberg model in the six-dimensional antisymmetric self-conjugate representation: Quantum Monte Carlo versus linear flavor-wave theory. *arXiv:1906.06938 [cond-mat]*, June 2019. URL http://arxiv.org/abs/1906.06938. arXiv: 1906.06938.

[75] Zheng Weihong, J. Oitmaa, and C. J. Hamer. Second-order spin-wave results for the quantum XXZ and XY models with anisotropy. *Physical Review B*, 44(21):11869, 1991. URL http://journals.aps.org/prb/abstract/10.1103/PhysRevB.44.11869.

[76] Kyle Wamer, Francisco H. Kim, Miklós Lajkó, Frédéric Mila, and Ian Affleck. Self-conjugate representation SU(3) chains. *arXiv:1906.08817 [cond-mat]*, June 2019. URL http://arxiv.org/abs/1906.08817. arXiv: 1906.08817.

[77] Manu Mathur and Diptiman Sen. Coherent states for SU(3). *Journal of Mathematical Physics*, 42(9):4181–4196, August 2001. ISSN 0022-2488. doi:10.1063/1.1385563. URL https://aip.scitation.org/doi/abs/10.1063/1.1385563.

[78] Manu Mathur and H. S. Mani. SU(N) coherent states. *Journal of Mathematical Physics*, 43(11):5351–5364, October 2002. ISSN 0022-2488. doi:10.1063/1.1513651. URL https://aip.scitation.org/doi/abs/10.1063/1.1513651.

[79] Ramesh Anishetty, Manu Mathur, and Indrakshi Raychowdhury. Irreducible SU(3) Schwinger bosons. *Journal of Mathematical Physics*, 50(5):053503, May 2009. ISSN 0022-2488. doi:10.1063/1.3122666. URL https://aip.scitation.org/doi/10.1063/1.3122666.

[80] Manu Mathur, Indrakshi Raychowdhury, and Ramesh Anishetty. SU(N) irreducible Schwinger bosons. *Journal of Mathematical Physics*, 51(9):093504, September 2010. ISSN 0022-2488. doi:10.1063/1.3464267. URL https://aip.scitation.org/doi/abs/10.1063/1.3464267.

[81] S. Brehmer, H.-J. Mikeska, and Shoji Yamamoto. Low-temperature properties of quantum antiferromagnetic chains with alternating spins S=1 and S=1/2. *Journal of Physics: Condensed Matter*, 9(19):3921, 1997. ISSN 0953-8984. doi:10.1088/0953-8984/9/19/012. URL http://stacks.iop.org/0953-8984/9/i=19/a=012.

[82] Shoji Yamamoto, S. Brehmer, and H.-J. Mikeska. Elementary excitations of Heisenberg ferrimagnetic spin chains. *Physical Review B*, 57(21):13610–13616, June 1998. doi:10.1103/PhysRevB.57.13610. URL https://link.aps.org/doi/10.1103/PhysRevB.57.13610.

[83] E. Solano-Carrillo, R. Franco, and J. Silva-Valencia. Interacting spin-wave dispersion relations of ferrimagnetic Heisenberg chains with crystal-field anisotropy. *Solid State Communications*, 150(41):2061–2064, November 2010. ISSN 0038-1098. doi:10.1016/j.ssc.2010.08.003. URL http://www.sciencedirect.com/science/article/pii/S0038109810004746.

[84] N Bogoliubov. On the theory of superfluidity. *J. Phys*, 11(1):23, 1947.

[85] A. L. Chernyshev and M. E. Zhitomirsky. Spin waves in a triangular lattice antiferromagnet: Decays, spectrum renormalization, and singularities. *Physical Review B*, 79(14), April 2009. ISSN 1098-0121, 1550-235X. doi:10.1103/PhysRevB.79.144416. URL http://link.aps.org/doi/10.1103/PhysRevB.79.144416.

[86] F. D. M. Haldane. Continuum dynamics of the 1-D Heisenberg antiferromagnet: Identification with the O(3) nonlinear sigma model. *Physics Letters A*, 93(9):464–468, February 1983. ISSN 0375-9601. doi:10.1016/0375-9601(83)90631-X. URL http://www.sciencedirect.com/science/article/pii/037596018390631X.

[87] Andrew Smerald. *Theory of the Nuclear Magnetic $1/T_1$ Relaxation Rate in Conventional and Unconventional Magnets*. Springer Science & Business Media, August 2013. ISBN 978-3-319-00434-1. Google-Books-ID: yVO6BAAAQBAJ.

[88] B. I. HALPERIN and P. C. HOHENBERG. Hydrodynamic Theory of Spin Waves. *Physical Review*, 188(2):898–918, December 1969. doi:10.1103/PhysRev.188.898. URL https://link.aps.org/doi/10.1103/PhysRev.188.898.

[89] Rajiv R. P. Singh and David A. Huse. Microscopic calculation of the spin-stiffness constant for the spin-1/2 square-lattice Heisenberg antiferromagnet. *Physical Review B*, 40(10):

7247–7251, October 1989. doi:10.1103/PhysRevB.40.7247. URL https://link.aps.org/doi/10.1103/PhysRevB.40.7247.

[90] C. J. Hamer, Zheng Weihong, and J. Oitmaa. Spin-wave stiffness of the Heisenberg antiferromagnet at zero temperature. *Physical Review B*, 50(10):6877–6888, September 1994. doi:10.1103/PhysRevB.50.6877. URL https://link.aps.org/doi/10.1103/PhysRevB.50.6877.

[91] P.M. Chaikin and T.C. Lubensky. *Principles of Condensed Matter Physics*. Cambridge University Press, 2000. ISBN 9780521794503. URL https://books.google.ch/books?id=P9YjNjzr9OIC.

[92] Jeffrey G. Rau, Paul A. McClarty, and Roderich Moessner. Pseudo-Goldstone gaps and order-by-quantum-disorder in frustrated magnets. *arXiv:1805.00947 [cond-mat]*, May 2018. URL http://arxiv.org/abs/1805.00947. arXiv: 1805.00947.

[93] B. Douçot and P. Simon. A semiclassical analysis of order from disorder. *Journal of Physics A: Mathematical and General*, 31(28):5855, 1998. ISSN 0305-4470. doi:10.1088/0305-4470/31/28/005. URL http://stacks.iop.org/0305-4470/31/i=28/a=005.

[94] Pierre Nataf, Miklós Lajkó, Alexander Wietek, Karlo Penc, Frédéric Mila, and Andreas M. Läuchli. Chiral Spin Liquids in Triangular-Lattice SU(N) Fermionic Mott Insulators with Artificial Gauge Fields. *Physical Review Letters*, 117(16):167202, October 2016. doi:10.1103/PhysRevLett.117.167202. URL https://link.aps.org/doi/10.1103/PhysRevLett.117.167202.

[95] Daniel P. Arovas and Assa Auerbach. Functional integral theories of low-dimensional quantum Heisenberg models. *Physical Review B*, 38(1):316, 1988. URL http://journals.aps.org/prb/abstract/10.1103/PhysRevB.38.316.

[96] S.R.P.G. Ripka, J.P. Blaizot, and G. Ripka. *Quantum Theory of Finite Systems*. Cambridge, MA, 1986. ISBN 9780262022149. URL https://books.google.ch/books?id=s_xlQgAACAAJ.

List of publications

[1] Francisco H. Kim, Karlo Penc, Pierre Nataf and Frédéric Mila.

Linear flavor-wave theory for fully antisymmetric SU(N) *irreducible representations,*

Physical Review B, 96(20): 205142, November 2017. doi: 10.1103/PhysRevB.96.205142.

[2] Kyle Wamer, Francisco H. Kim, Miklós Lajkó, Frédéric Mila and Ian Affleck.

Self-conjugate representation SU(3) *chains*

arXiv:1906.08817 [cond-mat], June 2019.

[3] Francisco H. Kim, Fakher F. Assaad, Karlo Penc and Frédéric Mila.

Dimensional crossover in the SU(4) *Heisenberg model in the six-dimensional antisymmetric self-conjugate representation: Quantum Monte Carlo versus linear flavor-wave theory,*

arXiv:1906.06938 [cond-mat], June 2019.
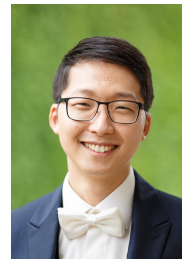
Francisco Hyunkyu Kim

✉ francisco.kim@epfl.ch
in Francisco Kim

Nationality: Swiss
Age: 30
Married

French – English – German

- *Mathematical/analytical ability*
- *Good knowledge of Linux*
- *Key understanding of programming languages*

Education

2015–2019	**PhD in Theoretical Physics, EPFL**.
	Thesis in condensed matter physics on the **Linear Flavour-Wave Theory of SU(N) Lattice Models with Arbitrary Irreducible Representations**
2012–2014	**Master of Science in Physics, ETH Zürich**.
	Thesis based on classical field-theoretical & group-theoretical methods, numerical calculations with $C++$: **Ginzburg-Landau theory of d-soliton in spin-triplet superconductor with tetragonal crystal symmetry**
	Emphasis on theoretical physics, computational physics and mathematics.
2008–2012	**Bachelor of Science in Physics, ETH Zürich**.
	Diploma presentation on the reduced density matrix: **Classical/Quantum Margins in the context of Quantum Information Theory**
2004–2008	**Maturité gymnasiale, Collège Sismondi**, *(Geneva, CH)*.
	Diploma work on String theory: **String Theory, the "Theory of Everything"?**

Other notable experience

Teaching experience	In charge of various theoretical physics exercise sessions & exams during the PhD; approximately 490 hours of experience between 2015–2018. Supervision of Master students during their Master theses. Teaching German and Mathematics to high school students from low-income families in 2007-2008.
Library	Worked in the ETHZ Physics Library (Dec–Avr 2014).
Internships in hospital sector	Auxiliary nurse Swiss Red Cross. Worked in various hospitals & nursing home for the elderly (CHUV, HFR, HNE, EMS La Clairière) as a nurse during the military service in the Swiss Army for a cumulative duration of 7 weeks. Training on various injection techniques and cardiopulmonary resuscitation.
Military service	Compulsory military service (245 days) expected to be accomplished in 2019.

Languages

French	First language	
Korean	Native language	
English	C1/C2	*Lived in the UK, aged 3 to 6; attended Manor First School in Portsmouth*
German	C1	*Fluent; studied in Zurich*
Italian/Spanish	A1	*Basic knowledge*

Other interests

Musicology (Music theory, history of music), piano, various sports, reading

Quelque chose en vous grandit et détache les amarres, jusqu'au jour où,
pas trop sûr de soi, on s'en va pour de bon. Un voyage se passe de motifs.
Il ne tarde pas à prouver qu'il se suffit à lui-même. On croit qu'on va faire
un voyage, mais bientôt c'est le voyage qui vous fait, ou vous défait.

Nicolas Bouvier,
L'usage du monde

On dirait encore une de ces robes étranges de danseuses, où une gaze
transparente et sombre laisse entrevoir les splendeurs amorties d'une jupe
éclatante, comme sous le noir présent transperce le délicieux passé ; et les
étoiles vacillantes d'or et d'argent, dont elle est semée, représentent ces feux
de la fantaisie qui ne s'allument bien que sous le deuil profond de la Nuit.

Charles Baudelaire,
Le Crépuscule du soir, Le Spleen de Paris

Il n'y a sans doute rien de plus émouvant dans la vie d'un homme
que la découverte fortuite de la perversion à laquelle il est voué.

Michel Tournier,
Le Roi des aulnes